CHAPTER 6

APPENDIX A

ANALYSIS OF DOE-OWNED FUELS

98Φ918ΦΦ67
Part 3

CONTENTS

A-1. SOURCE TERM FOR DOE SNF A6-1

A-1.1 WASTE FORM CATEGORIES A6-1

A-1.2 RADIONUCLIDE INVENTORIES A6-1

A-1.3 WASTE PACKAGE TYPES AND LOADING A6-3

A-1.4 PHYSICAL PROPERTIES OF DOE SNF A6-4

A-1.5 WASTE FORM DISSOLUTION MODELS A6-6

A-1.5.1 Metallic Spent Fuel A6-6
A-1.5.2 Silicon Carbide Spent Fuel A6-6
A-1.5.3 Ceramic A6-7
A-1.5.4 Oxide (Commercial) Spent Fuel A6-8
A-1.5.5 High-Level Waste Glass A6-8

A-2. DOSE TO HUMANS FROM DOE SNF A6-9

A-2.1 DOSE ATTRIBUTED TO EACH WASTE FORM A6-9

A-2.1.1 Uranium Metal Spent Fuel (Category 1) A6-9
A-2.1.2 Uranium-Zirconium Alloy Spent Fuel (Category 2) A6-10
A-2.1.3 Uranium-Molybdenum Alloy Spent Fuel (Category 3) A6-10
A-2.1.4 Uranium Oxide Spent Fuel (Category 4) A6-10
A-2.1.5 Uranium Oxide-Disrupted Clad Spent Fuel (Category 5) A6-11
A-2.1.6 Uranium-Aluminum Alloy Spent Fuel (Category 6) A6-11
A-2.1.7 Uranium Silicide Spent Fuel (Category 7) A6-11
A-2.1.8 High-Integrity Uranium-Thorium Carbide Spent Fuel (Category 8) A6-11
A-2.1.9 Low-Integrity Uranium-Thorium Carbide Spent Fuel (Category 9) A6-12
A-2.1.10 Uranium and Uranium-Plutonium Carbide Spent Fuel (Category 10) A6-12
A-2.1.11 Mixed Oxide Spent Fuel (Category 11) A6-12
A-2.1.12 Uranium-Thorium Oxide Spent Fuel (Category 12) A6-12
A-2.1.13 Uranium-Zirconium Hydride Spent Fuel (Category 13) A6-12
A-2.1.14 Navy Spent Fuel (Category 15) A6-13
A-2.1.15 Miscellaneous Spent Fuel (Category 16) A6-13
A-2.1.16 Summary of Results A6-14

A-2.2 2.2 DOSE ATTRIBUTED TO COMBINED WASTE FORMS A6-14

A-2.2.1 HLW Used for Co-Disposal for Different MTHM Algorithms A6-14

A-2.2.2 DOE SNF A6-15
A-2.2.3 Commercial Spent Fuel A6-15

A-2.3 COMPARISON OF RESULTS A6-15

A-2.3.1 Categories that Contribute Significantly to Total Dose A6-15
A-2.3.2 Comparison among Repository Loading Scenarios A6-16

A-3. EVALUATION OF SENSITIVITY AND UNCERTAINTY A6-17

A-3.1 UNSATURATED ZONE WATER FLUX A6-17

A-3.2 FUEL ALTERATION AT TIME OF WASTE PACKAGE PAILURE A6-18

A-3.3 CLADDING A6-18

A-3.4 WASTE FORM DISSOLUTION MODEL A6-19

A-3.5 WASTE FORM DISSOLUTION RATE AND SURFACE AREA A6-19

A-3.6 DOSE FROM CATEGORIES 2 AND 10 ..... A6-20

A-3.7 NUMBER OF WASTE PACKAGES A6-20

A-3.8 REPOSITORY REGION A6-20

A-3.9 SUMMARY OF RESULTS A6-21

A-4. CONCLUSIONS A6-23

A-5. REFERENCES A6-25

FIGURES

Figure 6A-1. Comparison of dissolution rates for high-level waste and oxide, metallic, carbide, and ceramic spent fuel. A6-29
Figure 6A-2. Expected-Value Dose History at 20 Kilometers Over 100,000 Years from Category 1 Spent Fuel and HLW. A6-30
Figure 6A-3. Expected-Value Dose History at 20 Kilometers Over 100,000 years from Category 1 Spent Fuel. A6-31
Figure 6A-4. Expected-Value Dose History at 20 Kilometers Over 100,000 Years from Commercial Spent Fuel Equivalent to Category 1 Spent Fuel. A6-32
Figure 6A-5. Expected-Value Dose History at 20 Kilometers Over 100,000 Years from Category 3 Spent Fuel and HLW. A6-33
Figure 6A-6. Expected-Value Dose History at 20 Kilometers Over 100,000 Years from Category 3 Spent Fuel. A6-34
Figure 6A-7. Expected-Value Dose History at 20 Kilometers Over 100,000 Years from Commercial Spent Fuel Equivalent to Category 3 Spent Fuel. A6-35
Figure 6A-8. Expected-Value Dose History at 20 Kilometers Over 100,000 Years from Category 4 Spent Fuel and HLW. A6-36
Figure 6A-9. Expected-Value Dose History at 20 Kilometers Over 100,000 Years from Category 4 Spent Fuel. A6-37
Figure 6A-10. Expected-Value Dose History at 20 Kilometers Over 100,000 Years from Commercial Spent Fuel Equivalent to Category 4 Spent Fuel. A6-38
Figure 6A-11. Expected-Value Dose History at 20 Kilometers Over 100,000 Years from Category 5 Spent Fuel and HLW. A6-39
Figure 6A-12. Expected-Value Dose History at 20 Kilometers Over 100,000 Years from Category 5 Spent Fuel. A6-40
Figure 6A-13. Expected-Value Dose History at 20 Kilometers Over 100,000 Years from Commercial Spent Fuel Equivalent to Category 5 Spent Fuel. A6-41
Figure 6A-14. Expected-Value Dose History at 20 Kilometers Over 100,000 Years from Category 6 Spent Fuel and HLW. A6-42
Figure 6A-15. Expected-Value Dose History at 20 Kilometers Over 100,000 Years from Category 6 Spent Fuel. A6-43
Figure 6A-16. Expected-Value Dose History at 20 Kilometers Over 100,000 Years from Commercial Spent Fuel Equivalent to Category 6 Spent Fuel. A6-44
Figure 6A-17. Expected-Value Dose History at 20 Kilometers Over 100,000 Years from Category 7 Spent Fuel and HLW. A6-45
Figure 6A-18. Expected-Value Dose History at 20 Kilometers Over 100,000 Years from Category 7 Spent Fuel. A6-46
Figure 6A-19. Expected-Value Dose History at 20 Kilometers Over 100,000 Years from Commercial Spent Fuel Equivalent to Category 7 Spent Fuel. A6-47
Figure 6A-20. Expected-Value Dose History at 20 Kilometers Over 100,000 Years from Category 8 Spent Fuel and HLW. A6-48
Figure 6A-21. Expected-Value Dose History at 20 Kilometers Over 100,000 Years from Category 8 Spent Fuel. A6-49
Figure 6A-22. Expected-Value Dose History at 20 Kilometers Over 100,000 Years from Commercial Spent Fuel Equivalent to Category 8 Spent Fuel. A6-50

Figure 6A-23. Expected-Value Dose History at 20 Kilometers Over 100,000 Years from Category 9 Spent Fuel and HLW. A6-51
Figure 6A-24. Expected-Value Dose History at 20 Kilometers Over 100,000 Years from Category 9 Spent Fuel. A6-52
Figure 6A-25. Expected-Value Dose History at 20 Kilometers Over 100,000 Years from Commercial Spent Fuel Equivalent to Category 9 Spent Fuel. A6-53
Figure 6A-26. Expected-Value Dose History at 20 Kilometers Over 100,000 Years from Category 11 Spent Fuel and HLW. A6-54
Figure 6A-27. Expected-Value Dose History at 20 Kilometers Over 100,000 Years from Category 11 Spent Fuel. A6-55
Figure 6A-28. Expected-Value Dose History at 20 Kilometers Over 100,000 Years from Commercial Spent Fuel Equivalent to Category 11 Spent Fuel. A6-56
Figure 6A-29. Expected-Value Dose History at 20 Kilometers Over 100,000 Years from Category 12 Spent Fuel and HLW. A6-57
Figure 6A-30. Expected-Value Dose History at 20 Kilometers Over 100,000 Years from Category 12 Spent Fuel. A6-58
Figure 6A-31. Expected-Value Dose History at 20 Kilometers Over 100,000 Years from Commercial Spent Fuel Equivalent to Category 12 Spent Fuel. A6-59
Figure 6A-32. Expected-Value Dose History at 20 Kilometers Over 100,000 Years from Category 13 Spent Fuel and HLW. A6-60
Figure 6A-33. Expected-Value Dose History at 20 Kilometers Over 100,000 Years from Category 13 Spent Fuel. A6-61
Figure 6A-34. Expected-Value Dose History at 20 Kilometers Over 100,000 Years from Commercial Spent Fuel Equivalent to Category 13 Spent Fuel. A6-62
Figure 6A-35. Expected-Value Dose History at 20 Kilometers Over 100,000 Years from Category 15 Spent Fuel. A6-63
Figure 6A-36. Expected-Value Dose History at 20 Kilometers Over 100,000 Years from Commercial Spent Fuel Equivalent to Category 15 Spent Fuel. A6-64
Figure 6A-37. Expected-Value Dose History at 20 Kilometers Over 100,000 Years from Category 16 Spent Fuel and HLW. A6-65
Figure 6A-38. Expected-Value Dose History at 20 Kilometers Over 100,000 Years from Category 16 Spent Fuel. A6-66
Figure 6A-39. Expected-Value Dose History at 20 Kilometers Over 100,000 Years from Commercial Spent Fuel Equivalent to Category 16 Spent Fuel. A6-67
Figure 6A-40. Expected-Value Total Dose History at 20 Kilometers Over 100,000 Years from all of Categories 1 through 7 DOE SNF. A6-68
Figure 6A-41. Expected-Value Total Dose History at 20 Kilometers Over 100,000 Years from all of Categories 8 through 13, 15, and 16 DOE SNF. A6-69
Figure 6A-42. Expected-Value Dose History at 20 Kilometers Over 100,000 Years from 9,334 Canisters of HLW. A6-70
Figure 6A-43. Expected-Value Dose History at 20 Kilometers Over 100,000 Years from 400 and 18,994 Canisters of HLW. A6-71
Figure 6A-44. Expected-Value Dose History at 20 Kilometers Over 100,000 Years from 2,496 MTHM of DOE SNF and from 2,496 MTHM of Commercial Spent Fuel. A6-72

Figure 6A-45. Expected-Value Dose History at 20 Kilometers Over 100,000 Years from 2,333 MTHM of DOE SNF, from 2,333 MTHM of the Surrogate DOE SNF used in the Base case, and from 2,333 MTHM of Commercial Spent Fuel.... A6-73
Figure 6A-46. Expected-Value Dose History at 20 Kilometers Over 100,000 Years from 63,000 MTHM of Commercial Spent Fuel.... A6-74
Figure 6A-47. Expected-Value Total Dose History at 20 Kilometers Over 100,000 Years from the Base Case Repository, 2,333 MTHM of DOE SNF, and 9,334 Canisters of HLW.... A6-75
Figure 6A-48. Expected-Value Total Dose History at 20 Kilometers Over 100,000 Years from 63,000 MTHM of Commercial Spent Fuel, 2,333 MTHM of DOE SNF, 2,496 MTHM of DOE SNF.... A6-76
Figure 6A-49. Expected-Value Total Dose History at 20 Kilometers Over 100,000 Years from 400 Canisters of HLW, 9,334 Canisters of HLW, and 18,994 Canisters of HLW.... A6-77
Figure 6A-50. Effects of Climatic Conditions on the Dose from the Surrogate DOE SNF used in the Base Case.... A6-78
Figure 6A-51. Effects of Climatic Conditions on the Dose from Category 1 Spent Fuel.... A6-79
Figure 6A-52. Effects of Climatic Conditions on the Dose from Category 6 Spent Fuel.... A6-80
Figure 6A-53. Effects of Time of Waste Package Failure for Category 1 Spent Fuel.... A6-81
Figure 6A-54. Comparison of Cladding and No Cladding for 2,333 MTHM of Commercial Spent Fuel.... A6-82
Figure 6A-55. Comparison of 50% Cladding and No Cladding for Category 1 Spent Fuel.... A6-83
Figure 6A-56. Comparison of Dissolution Rates for HLW, Metallic Spent Fuel, Oxide Spent Fuel, Carbide Spent Fuel, and Ceramic Spent Fuel.... A6-84
Figure 6A-57. Comparison of Using Ten-Times the Metallic Dissolution Model to Using the Carbide Dissolution Model For Category 9 Spent Fuel.... A6-85
Figure 6A-58. Comparison of Using the Ceramic Dissolution Model for Category 12 Spent Fuel to Using the Congruent Dissolution of Thorium-Uranium Oxide.... A6-86
Figure 6A-59. Comparison of Dose from Category 1 Spent Fuel for Different Dissolution Rates for the Base Case Climate.... A6-87
Figure 6A-60. Comparison of Dose from Category 1 Spent Fuel for Different Dissolution Rates for Long Term Average Climate for 100,000 Years Base.... A6-88
Figure 6A-61. Comparison of Dose from Category 1 Spent Fuel for Different Surface Areas for the Base Case Climate.... A6-89
Figure 6A-62. Comparison of Dose from Category 1 Spent Fuel for Different Surface Areas for Long Term Average Climate for 100,000 Years Base.... A6-90
Figure 6A-63. Comparison of Dose from Category 13 Spent Fuel for Different Dissolution Rates for the Base Case Climate.... A6-91

Figure 6A-64. Comparison of Dose from One Failed Package of Category 2 Spent Fuel to One Failed Package of Commercial Spent Fuel. A6-92
Figure 6A-65. Comparison of Dose from One Failed Package of Category 10 Spent Fuel to One Failed Package of Commercial Spent Fuel. A6-93
Figure 6A-66. Dose from Category 13 Spent Fuel for Different Numbers of Waste Packages. A6-94
Figure 6A-67. Dose from Category 1 Spent Fuel for Different Numbers of Waste Packages. A6-95
Figure 6A-68. Comparison of Disposal of 2,333 MTHM of Commercial Spent Fuel in One Region to Disposal in Six Regions. A6-96
Figure 6A-69. Comparison of Disposal of Category 1 Spent Fuel in Region Six to Disposal of it in Region Two. A6-97

TABLES

Table 6A-1. DOE spent fuel categories for total system performance assessment (TSPA) (modified from Stroupe 1997). A6-99

Table 6A-2. Categories of DOE SNF and Typical Members of Each Category. A6-102

Table 6A-3. Metric Tons Heavy Metal for Each Category of DOE SNF for the Total (2,496 MTHM) and Modified Inventories (2,333 MTHM). A6-103

Table 6A-4. ORIGEN2 Analyses Conducted to Obtain Radionuclide Inventories for DOE SNF. A6-104

Table 6A-5. Radionuclide Inventory for DOE SNF.[1] A6-105

Table 6A-6. Radionuclide Inventory for Commercial Spent Nuclear Fuel (CSNF), Surrogate DOE SNF, and High-Level Waste (HLW) and Used in the TSPA-VA Base Case- A6-107

Table 6A-7. Release Source Term at the Boundary of a Failed Waste Package for Category 15 (Navy) Spent Fuel.[1] A6-108

Table 6A-8. Number and Type of Waste Packages for the Total Inventory of DOE SNF (2,496 MTHM) by Category.* A6-112

Table 6A-9. Number of Waste Packages and HLW Canisters for Disposal of the Total Inventory of DOE Spent Fuel (2,496 MTHM). A6-113

Table 6A-10. Number and Type of Waste Packages for the Modified Inventory of DOE SNF (2,333 MTHM) by Category.* A6-114

Table 6A-11. Number of Waste Packages and HLW Canisters for Disposal of the Modified Inventory of DOE Spent Fuel (2,333 MTHM). A6-115

Table 6A-12. Physical Characteristics of DOE SNF.[1] A6-116

APPENDIX A
ANALYSIS OF DOE-OWNED FUELS

A-1. SOURCE TERM FOR DOE SNF

A-1.1 WASTE FORM CATEGORIES

The U.S. Department of Energy (DOE) has categorized all of its spent fuel into performance assessment categories that were developed based on fuel composition and characteristics (Stroupe 1997). The primary concern in grouping the spent fuels was assigning every fuel to a category and making certain that all of the spent fuels fit into a specific category. The grouping of spent fuels into categories is dependent on the analyses that will be preformed using a representative spent fuel from that category. For example, the spent fuels are grouped differently for conducting a Total System Performance Assessment (TSPA) than they are for conducting criticality analyses because different attributes of the fuel are important in performing different analyses. The DOE Spent Nuclear Fuel (SNF) categories for TSPA are shown in Table 6A-1. Category 14, Sodium-bonded spent fuel was not analyzed because treatment is expected for this category of spent fuel.

The physical properties of a spent fuel category are assumed to be bounded by the properties of a specific spent fuel or combination of several spent fuels in that category depending on the type of analyses that are being performed using these data (i.e., performance assessment or criticality). Table 6A-2 shows the 15 categories of DOE spent fuel that were analyzed and the typical fuel that was used to bound the physical properties of that category.

The data for the Categories of DOE SNF, except for Category 15, were provided by the National Spent Nuclear Fuel Program (Stroupe 1998). These data consisted of the amount of spent fuel, the radionuclide inventory, packaging, and physical properties for each category of DOE SNF. The total amount of DOE SNF in the 15 categories is approximately 2,496 metric tons having metal (MTHM) (Table 6A-2). About 85% of this spent fuel is represented by Category 1, with the majority of the metallic fuel in the category being from N reactor. Table 6A-3 also shows the amount of fuel in each category for the modified inventory of DOE SNF. For the modified inventory the total amount is reduced by approximately 7% to reduce the inventory to 2,333 MTHM. Data for Category 15 spent fuel were provided by Bettis Atomic Power Laboratory (Beckett 1998).

A-1.2 RADIONUCLIDE INVENTORIES

The analyses of the performance of DOE SNF require the determination of the radionuclide inventory for each category of fuel that is placed in the repository. In this section ORIGEN2 is referenced only to provide the method that the National Spent Nuclear Fuel Program used to analyze the radionuclide inventories for the categories of DOE spent fuel that were provided in Stroupe 1998. These data (Stroupe 1998) were not obtained under the OCRWM Quality Assurance Program. The computer code ORIGEN2 (Oak Ridge Isotope Generation) is widely accepted for calculating spent fuel radionuclide inventories (ORNL no date). An ORIGEN2 run requires detailed input of data for the fuel core composition, the power history of the reactor, and

the operating conditions of the reactor. In particular, the nuclear-cross section libraries for each fuel type are required for the particular reactor, and this library development is a lengthy and involved task. With rigorous library development and comparison of calculated results to measured values, the ORIGEN2 model is capable of accuracy sufficient for nuclear reactor operational support. Such carefully developed nuclear cross-section libraries were not available for all fuels evaluated in this performance assessment, and some of the input data for the ORIGEN2 runs had to be estimated.

A conservative approach for the use of ORIGEN2 was adopted to estimate the radionuclide inventory for each spent fuel category. For categories that contain large amounts of spent fuel (i.e., Category 1 represented by N Reactor spent fuel), an effort was made to minimize the degree of conservatism. Minimizing the degree of conservatism for categories containing small amounts of spent fuel is less important because it is easier to accept the "penalty" of an overestimate of radionuclides. The dose the overestimate produces is relatively small as compared to the dose from larger amounts of spent fuel in other categories.

The radionuclides included in the performance assessment are based on screening that was conducted for TSPA-1993 (Andrews et. al. 1994). The screening was done in two ways. First, radionuclides were screened using the ratio of their inventory to EPA Table 1 release limits (EPA 1985). The ratio of the weighted average inventories of specific radionuclides were determined for spent commercial fuel corresponding to the EPA Table 1 values for 1,000, 10,000, 100,000, and 1,000,000 years. The fractional contribution of each isotope to release at a time of 1,000, 10,000, 100,000, and 1,000,000 years was calculated assuming a combination of delay due to waste package lifetime and retarded transport of 1,000 to 1,000,000 years. Isotopes which contributed at least a fraction (0.01%) of the EPA release limit at any of the selected times passed this screening. The entire decay chain for daughters that contributed greater than 10^{-5} of the EPA release limit at anytime were also included (Andrews et al. 1994).

Second, the screening was also conducted using dose for the same time periods. The waste form was assumed to alter at a rate of 10^{-5} of the total inventory per year. The isotopes were assumed to dissolve, as they were made available by the assumed waste form alteration rate, at the maximum solubility according to the National Research Council (NAS) (1983), Electric Power Research Institute (EPRI) (1992), and Barnard et al. (1992). The advective, downward flux in groundwater moving through the unsaturated zone was assumed to occur at 0.1 mm/yr over the footprint of the repository. On arrival at the saturated zone, the isotopes were assumed to mix in the saturated zone with a flow rate of 10,000 m^3/yr. Ingestion of 700 liters/year by a person using this groundwater was assumed. The ingested dose was calculated using the maximum effective (whole body) dose conversion factor from DOE (1988), Nuclear Regulatory Commission (NRC) (1981), or EPA (1988). The fractional contribution of each isotope to total dose at times of 1,000, 10,000, 100,000, and 1,000,000 years was determined. For radionuclides with two or more isotopes present in the waste, the solubility limit was set for the element (i.e., all isotopes) and then proportioned between the individual isotopes by the mass fraction present at the corresponding time. All isotopes contributing less than 10^{-5} of total dose at any time period were eliminated from the inventory unless they were in the decay chain for daughters that contributed 10^{-5} of total dose at any time. This process yields 39 radionuclides. The process of using the maximum dose conversion factor is sufficiently conservative that a change in flux would not yield additional radionuclides to the 39 being considered.

In order to estimate the 39 radionuclides needed as input to the performance assessment, ORIGEN2 was used to model the fuel types in a given category of spent fuel (in the National Spent Fuel Data Base). The ORIGEN2 analyses that were conducted to obtain the radionuclide inventory for each DOE SNF category are presented in Table 6A-4. Spreadsheets were prepared to merge the results (radionuclide concentrations) from the ORIGEN2 runs into a composite radionuclide inventory for each category. For each fuel entry selected in the category, a representative ORIGEN2 run was made. The inventory was then calculated as a scaled amount based on Uranium content of each fuel type in the category. Totals were then calculated for each of the 39 radionuclides.

The packaging of the fuel was calculated separately, as described in Section A1.3. The cumulative curie count for each category was divided by the total packages in the category to arrive at the mean inventory for each package. The fuel inventories used in this study were based on the National Spent Fuel Data Base (DOE 1996), which was used as the authority to resolve any discrepancies in other data.

Composite spreadsheet totals of the curies in a particular category were apportioned equally across the total number of canisters in that category. This results in a mean value per canister, but does not consider that canisters within a category are of different size. For instance, no distinction in curie inventory was made between the different diameter fuel canisters, or for different canister lengths.

The analyses resulted in the radionuclide inventories that are presented in Table 6A-5 (as mentioned previously, data presented in this table was supplied by the National Spent Nuclear Program in Stroupe, 1998, and was not obtained under the OCRWM Quality Assurance Program). The radionuclide inventory for each category of DOE spent fuel is presented in the units of Ci/MTHM for ease in comparison of radionuclide content among categories. The radionuclide inventory for Navy spent fuel is not presented because that information is classified. The radionuclide inventory for commercial spent fuel, the surrogate DOE SNF, and HLW used in the TSPA-VA base case is presented in Table 6A-6. The release term for Category 15 (Navy) spent fuel at the boundary of a failed waste package is presented in Table 6A-7.

A-1.3 WASTE PACKAGE TYPES AND LOADING

The fuel loading configurations for the analyses of DOE SNF are based on the co-disposal approach for high-and medium-enriched fuels prevalent in the DOE spent fuel inventory. In the absence of complete, definitive criticality analyses for each fuel type, the amount of U-235 for high-enriched fuel (i.e., enrichment greater than 20 percent U-235) was restricted to approximately 14.4 kg per package (Research Reactor Spent Nuclear Fuel Task Team, 1996). A maximum fissile content of 14.4 kilograms per package of U-235 or equivalent was assumed for the high-enriched spent fuel and 44 kilograms per package of U-235 or equivalent was assumed for medium enriched spent fuel. However in most cases, the volume of the spent fuel dictates the amount that can be placed in a package. These assumptions were made to reduce the potential for criticality by limiting the fissile mass content of each package based on its enrichment. In the co-disposal packages high-level waste glass canisters are considered to be emplaced in the same package with the spent fuel. The co-disposed spent fuel is assumed to be in four canister high-level waste (HLW) packages and co-disposal packages.

The DOE SNF is assumed to be contained in 432 mm (17 inch) and 632 mm (24 inch) diameter canisters (Duguid et. al. 1997). Co-disposal in a HLW package is achieved by substitution of a canister of spent fuel for one of the canisters of HLW glass (a 3 × 1 package). In the package nomenclature used in this report, the first number refers to the number of HLW canisters and the second number refers to the number of spent fuel canisters in the package (i.e., a 3 × 1 package would contain three canisters of HLW and one canister of spent fuel). The co-disposal package contains five canisters of HLW and a central 432-mm (17-inch) canister of spent fuel. Hence, using the waste package nomenclature, a co-disposal package is a 5 × 1 package (Stroupe, 1998).

Low-enriched spent fuel (N Reactor), is assumed to be disposed in four canister HLW package with no canisters of HLW, and are referred to as 0 × 4 packages. The N Reactor spent fuel is being treated and packaged in a Multi-Canister Overpack (MCO) for interim storage. The MCO has an external diameter of 25.31 inch (about 643 mm), and is assumed to fit into a HLW canister position. The Savannah River spent fuel (Categories 6 and 7) is being placed in 432-mm (17-inch) canisters and it is assumed to be disposed in co-disposal packages. The Idaho National Engineering and Environmental Laboratory (INEEL) spent fuel dimensions and fissile content allows most of the fuels to be contained in 432-mm (17-inch) canisters. For the INEEL spent fuels, the 610-mm (24-inch) canister was used for fuel of large dimensions (Stroupe, 1998).

Table 6A-8 shows the waste package configurations for each category of spent fuel for the total inventory of DOE SNF. Based on Table 6A-8, the number of HLW canisters needed for co-disposal of the high- and medium-enriched DOE SNF are shown in Table 6A-9. Co-disposal of high- and medium-enriched spent fuel in the total inventory of DOE SNF (2496 MTHM) requires 7,240 short canisters (3.05 m or 10 feet) and 7,836 long canisters (4.57 m or 15 feet) of HLW. This is equivalent to 18,994 short canisters of HLW. Assuming that each short canister of HLW contains 0.5 MTHM, it takes 9,497 MTHM of HLW to co-dispose the high- and medium-enriched DOE SNF.

Table 6A-10 shows the number and types of waste packages needed to dispose of the modified inventory of DOE SNF (2,333 MTHM). This packaging information was used to develop the number of HLW canisters needed to co-dispose the modified inventory of DOE SNF (Table 6A-11). The number of equivalent short HLW canisters necessary to co-dispose the high- and medium enriched spent fuel in the modified inventory is 17,796. Thus, co-disposal of the high- and medium-enriched spent fuel in the modified inventory, under the current packaging assumptions, would require 8,898 MTHM of HLW.

A-1.4 PHYSICAL PROPERTIES OF DOE SNF

Fuel properties were determined by the judgement of those personnel most familiar with the fuel inventory, and a consensus on the values was gained by review among the local spent fuel programs at the DOE sites (Cresap 1997). The grouping of fuel into categories, based on chemical fuel form, aided in assigning common properties to each of the categories. The physical properties that are used in the performance assessment are presented in Table 6A-12 for each category of DOE spent fuel.

The prior performance assessments (i.e., TSPA-1995) have compiled the physical properties for commercial spent fuel, and these values were adopted or used as a beginning point for estimating

values for the DOE spent fuel categories. For instance, some fuel categories use the same value for dissolution rate as commercial fuel, others use the commercial rate scaled by an appropriate factor, and still others use entirely different models. Using existing models wherever possible simplified the approach for both data generation by the National Spent Nuclear Fuel Program and modeling done in this performance assessment. The effect of a range of physical properties of the fuels on performance is examined in Section A-3, Evaluation of Sensitivity and Uncertainty.

Table 6A-12 provides estimates of fuel dissolution rate, surface area, cladding failure, free radionuclide inventory, gap radionuclide inventory, fuel area, and fuel volume. The fuel area and volume are the current fuel meat area perpendicular to ground-water flux and the current fuel meat volume.

The dissolution under wet oxic conditions is taken from the dissolution models that are described in Section A-1.5 or as some fraction of the results of these dissolution models. For dry oxic conditions, the dissolution rate is assumed to be zero, as in the case for commercial spent fuel. Surface area for DOE fuels was based on the area and weight of the fuel meat (unclad fuel) itself. Calculations were simplified by the fact that the chemical form of the fuel meat within each category was the same. Where different geometry's or dimensions contributed to the same category, a dominant type was selected or average values were used. Conservative estimates were made of the fraction of fuel cladding that has failed. These numbers are typically high, reflecting the approach that little, if any, credit is claimed for fuel cladding as a barrier to releases from DOE SNF. The value given is an estimate of the initial condition at the time of waste package failure, and normal corrosion processes would proceed after that time. In the analyses reported in this document, no credit is taken for the cladding of DOE SNF and the results are compared to equivalent amounts of unclad commercial spent fuel. The assumption of unclad commercial spent fuel was made to determine if it could serve as a conservative bound for the DOE SNF.

Two columns of Table 6A-12 provide the free and gap radionuclide inventory that has been released from the fuel, but is still contained in the disposal package until the time the package is breached. It is then available for immediate release. Since the fuel in most cases has been stored a long time prior to repository package emplacement, most of the inventory available for immediate release would already be gone prior to sealed containment in a canister. After the canister is sealed for repository disposal, conditions in it are benign, and not likely to facilitate degradation of the fuel. For these reasons, the free fraction of the inventory is low. The gap referred to in the gap inventory is between the fuel meat and the cladding. The inventory is the fraction of radionuclides that has migrated from the fuel meat to the gap and is available for immediate release when the cladding is penetrated. This inventory may be specified separately for different isotopes (i.e., C-14). Some of the DOE spent fuels are physically constructed so as to eliminate a gap that could accumulate radionuclides. For example, the N Reactor fuel meat is co-extruded with the cladding that eliminates the presence of a gap. Thus it has no gap inventory (Table 6A-12).

A-1.5 WASTE FORM DISSOLUTION MODELS

Dissolution models for metallic, carbide, ceramic, and oxide (commercial) spent fuel and for HLW glass are presented below. The metallic and carbide models were taken from the analyses of DOE SNF conducted by Sandia National Laboratories (Rechard, 1995), the models for commercial spent fuel and HLW were used in TSPA-1995 (Andrews et al., 1995), and the ceramic model was used in the evaluation of plutonium waste forms (Duguid et al., 1996). These dissolution models were also used in the assessment of the performance of INEEL spent fuels (INEEL Task Team on Spent Nuclear Fuel, 1997). A comparison of the glass and spent fuel dissolution models that are described below is presented in Figure 6A-1. This figure indicates that the largest dissolution rate over time is for metallic spent fuel and the slowest is for carbide spent fuel. The dissolution rates in order from fastest to slowest are metallic spent fuel under wit oxic conditions, metallic spent fuel under humid oxic conditions, oxide spent fuel, HLW glass, ceramic, and carbide spent fuel. The change in rate over time is caused by the build up of corrosion products on the surface of the waste form, which slows the rate of dissolution. Initially there are about seven orders of magnitude difference between the fastest and the slowest waste form dissolution rate (i.e., metallic and carbide), and after 100,000 years there are about five orders of magnitude difference in dissolution rate between these models.

A-1.5.1 Metallic Spent Fuel

See Section 6.3.2.1.1.

A-1.5.2 Silicon Carbide Spent Fuel

The model for silicon carbide spent fuel was taken from the 1994 performance assessment of DOE SNF (Rechard 1995). The 1994 assessment used a dissolution model that is based on the following equation:

$$M = Ae^{-B/T}(t_2^C - t_1^C)\,(D \times E \times M_{layer})$$

For fuel particles with silicon carbide coatings,

M	=	mass of layer corroded in a time step (kg),
A	=	3×10^{-12} / sec,
B	=	0,
C	=	1,
T	=	time (sec),
D	=	1 which is assumed to be conservative,
E	=	0.2, and
M_{layer}	=	the mass of the layer at time zero.

This equation can be used to calculate the mass of corroded silicone carbide fuel at any time step. In order to obtain the dissolution rate, the mass of the layer at time zero and the surface area must be known. For silicone carbide spent fuel, the surface area of the silicone carbide is assumed to

be 1325 m^2 and the mass of the layer (M_{layer}) is assumed to be 126 kg. The surface area is not used to evaluate the mass release, but was used to estimate the initial mass of the coatings. This dissolution model only applies to carbide fuel that has silicone carbide coatings on the carbide fuel particles (Category 8, high integrity Uranium-Thorium carbide spent fuel), and does not represent the dissolution of the fuel itself. Once the coating has failed the fuel reacts rapidly with water releasing the radionuclide inventory of the fuel particles. This is the reason for using the metallic dissolution for Categories 9 and 10 and applying a factor of ten and one hundred to the dissolution rate, respectively (Table 6A-10). Categories 9 and 10 are both low integrity carbide fuels that are expected to dissolve rapidly in the presence of water (they do not have silicone carbide coated fuel particles).

A-1.5.3 Ceramic

The dissolution model for ceramic was taken from Lappa (1995). The composition of the ceramic was assumed by Lappa to be similar to that of Synroc-C, a titanate ceramic. Reeve et al. (1989) proposed that the cumulative release from Synroc to be:

$$Q = Q_0 + \theta + SFt/A$$

where

Q	=	release rate per unit surface area (g/m^2),
Q_0	=	instantaneous release from grain boundaries and metastable phases (g/m^2),
θ	=	is a kinetic function that accounts for ionic diffusion, selective matrix attack, etc (g/m^2),
S	=	solubility of the matrix (g/m^2),
F	=	groundwater flow rate (m^3/ day),
A	=	is the surface area (m^2), and
T	=	time (days).

Lappa states that it is likely that the long-term release from the Synroc is controlled by the third term of the equation. Existing data indicate that S is less than or equal to 0.007 g/m^3 based on a long-term leaching rate of less than or equal to 10^{-4} g/m^2/day when SA/C is 10 m^{-1} at 70 degrees Centigrade in deionized water (Lappa 1995). The leaching rate also increases with increasing temperature (Ringwood et al. 1988). This temperature effect is described by:

$$R = \alpha\ 10^{-\beta(1000/T)}$$

where

R	=	leaching rate (g/m^2 day),
T	=	temperature in degrees K, and
α and β	=	are constants.

Based on the Synroc data of Ringwood et al (1988), $\beta \approx 1.0$ and $\alpha \approx 0.082$ g/m^2/day when SA/C is 10 m^{-1} at 70 degrees Centigrade. These are the same conditions that were assumed in TSPA 1995 for HLW glass. The release rate can be calculated by multiplying R by the surface area (S) and the elapsed time (t). The radionuclides are released from the waste form based on its alteration rate, and are then transported at a rate dependant on whether they are alteration controlled or solubility-limited radionuclides.

The alteration/dissolution rate presented above is for a monolithic form, and if the monolith is cracked the release rate could be significantly different. The release rate should be measured in the ongoing research and development program to provide a more valid release in the repository environment. However, the ceramic model is only used for Category 12 spent fuel that is less than 2% of the total amount of DOE SNF on an MTHM basis.

A-1.5.4 Oxide (Commercial) Spent Fuel

See Section 6.3.1.3.2.

A-1.5.5 High-Level Waste Glass

See Section 6.3.3.3).

A-2. DOSE TO HUMANS FROM DOE SNF

The Individual categories of DOE SNF were analyzed by placing them, one at a time, in the environment of the TSPA-VA base case and calculating the expected-value dose history attributed to that waste form for an individual using water from a well 20 kilometers down gradient from the repository. Each category of DOE SNF or equivalent amount of unclad commercial spent fuel was assumed to be placed in the TSPA-VA base case environment (i.e., added to the inventory) and the resulting dose from the DOE SNF or equivalent amount of unclad commercial spent fuel was analyzed. The dose to an individual from all sources was analyzed: ingestion of food and water, inhalation, and exposure to contaminated areas and water. The analyses in this chapter, except where specified, are for the total amount of DOE SNF (2,496 MTHM). This was done to determine the full impact of all of the DOE SNF and co-disposed HLW in each category. These results are presented in Section 2.1. The results from the total amount of DOE SNF are compared to the 2,333 MTHM of DOE SNF and 4,667 MTHM of HLW in Sections 2.2 and 2.3.

A-2.1 DOSE ATTRIBUTED TO EACH WASTE FORM

A total of 15 categories of DOE SNF were analyzed. These are Categories 1 through 13, Category 15, and Category 16. Category 14, sodium-bonded spent fuel, was not analyzed because it will be treated. All of the categories, except Category 15, contain some high- and medium-enriched spent fuel that is assumed to be co-disposed. For this reason, the analyses of dose are presented for the HLW included and excluded in the dose history. The analysis of the fuel in each category (excluding the co-disposed HLW) is compared to an equivalent amount of unclad commercial spent fuel (equivalent on an MTHM basis). For these comparisons, the assumption was that the commercial spent fuel is packaged in the same number of packages as the DOE SNF in category. Also, for conservatism, the DOE SNF was assumed to be disposed in Region 6 of the repository. Region 6 has the highest unsaturated-zone flux through the repository.

The Navy spent fuel, Category 15, is not co-disposed, and because it is classified, it is handled differently than the other categories of DOE SNF. For this category, data on thermal conditions and waste package failure rate were furnished to Bettis Atomic Power Laboratory (Duguid 1998), and their staff used these data to calculate an unclassified release rate at the boundary of the waste package (Beckett 1998). This release rate was then used in the TSPA-VA model (RIP) to analyze the dose 20-kilometer from the repository. The analyses of Navy spent fuel are discussed in Section 2.1-14.

A-2.1.1 Uranium Metal Spent Fuel (Category 1)

The expected-value dose history at 20 kilometer from the repository for Category 1 spent fuel and co-disposed HLW is presented in Figure 6A-2. The analysis indicates that of the 107 packages disposed, only six packages are expected to fail over the first 100,000 years. The package failures are shown as spikes in dose from Tc-99, I-129, and C-14 that are observed on Figure 6A-2. The release of these three radionuclides is alteration controlled, and when a waste package fails they are rapidly released from it (over a few thousand years as indicated by the

width of the spikes). For the solubility-controlled radionuclides, such as Np-237, the dose curves are smoother because of the slower release from the failed waste package. Figure 6A-3 shows the dose attributed only to the Category 1 spent fuel. A comparison for Figures 6A-2 and 6A-3 shows little change due to removal of the HLW. This is because much of the spent fuel in this category is low enriched N Reactor spent fuel contained in 101 packages that do not contain HLW. There are only six co-disposal packages in the category (see Table 6A-8), and removal of this small amount of HLW does not significantly affect the dose. Figure 6A-4 shows the dose history for an equivalent amount of unclad commercial spent fuel (2122.26 MTHM, see Table 6A-3) contained in 107 waste packages. The results are similar to the results from Category 1 SNF except the doses are somewhat higher (i.e., Tc-99, I-129, and Np-237).

A-2.1.2 Uranium-Zirconium Alloy Spent Fuel (Category 2)

The spent fuel of Category 2 is disposed in eight co-disposal packages (see Table 6A-9). Because of the small number of waste packages in this category, none are expected to fail in the first 100,000 years. Consequently, no results for Category 2 are shown. In the sensitivity analyses of Chapter 5, failure of a single package of Category 2 spent fuel will be assumed and the results will be compared to failure of an equivalent amount of commercial spent.

A-2.1.3 Uranium-Molybdenum Alloy Spent Fuel (Category 3)

Figure 6A-5 shows the dose attributed to disposal of 3.77 MTHM of Category 3 spent fuel in 70 co-disposal packages along with that from the co-disposed HLW. Of the 70 packages it is expected that four fail over the first 100,000 years. A waste package failure is shown as a peak of dose from I-129 on Figure 6A-5. Figure 6A-6 shows the dose attributed only to the Category 3 spent fuel. The nearly two-order of magnitude decrease in dose is because of the removal of the relatively large amount of HLW from the analysis. To dispose of 3.77 MTHM of Category 3 spent fuel, it requires 350 canisters of HLW (see Table 6A-9). If it is assumed that there is 0.5 MTHM per 10-foot canister of HLW, the disposal of 3.77 MTHM of spent fuel requires 175 MTHM of HLW. Figure 6A-7 shows the dose from disposal of 3.77 MTHM of commercial spent fuel in 70 waste packages. The dose from the commercial spent fuel is nearly the same as that from co-disposal of Category 3 spent fuel and HLW (see Figure 6A-5), and is more than two orders of magnitude higher than that from the Category 3 spent fuel alone.

A-2.1.4 Uranium Oxide Spent Fuel (Category 4)

Figure 6A-8 shows the expected-value dose history from Category 4 spent fuel and co-disposed HLW in 214 waste packages, of which 193 are co-disposal packages. The dose shown in Figure 6A-8 is somewhat higher (about a factor of two) than the dose from only the Category 4 spent fuel (Figure 6A-9). The dose from Category 4 spent fuel (Figure 6A-9) is nearly identical to that from an equivalent amount of commercial spent fuel (98.68 MTHM) shown in Figure 6A-10. The dose from Category 4 spent fuel being nearly identical to that from commercial spent fuel is not surprising, because much of the category is made up of commercial oxide spent fuel.

A-2.1.5 Uranium Oxide-Disrupted Clad Spent Fuel (Category 5)

Figure 6A-11 shows the expected-value dose history from Category 5 spent fuel and HLW disposed in 686 packages, all of which are co-disposal packages. The dose from the spent fuel and HLW is nearly an order of magnitude above that of the spent fuel alone (Figure 6A-12). The difference is caused by the relatively large amount of HLW because all of the waste packages are co-disposal packages. When this result is compared to the equivalent amount of commercial spent fuel (87.02 MTHM) in Figure 6A-13 it is seen that the dose from Category 5 spent fuel is nearly an order of magnitude below that from the commercial spent fuel. The lower dose is attributed to the Three Mile Island fuel being at lower burnup than average commercial spent fuel at the time of the accident.

A-2.1.6 Uranium-Aluminum Alloy Spent Fuel (Category 6)

Figure 6A-14 shows the expected-value dose history for Category 6 spent fuel and co-disposed HLW. The 8.75 MTHM of spent fuel is co-disposed in 706 packages that contain about 1806 MTHM of HLW. Because of the relatively large amount of HLW the dose is reduced significantly when the effects of the HLW are removed (Figure 6A-15). Comparison of the spent fuel in Category 6 (see Figure 6A-15) with an equivalent amount of commercial spent fuel (Figure 6A-16) shows that dose from the DOE spent fuel is somewhat higher (less than a factor of two) than that from commercial spent fuel for the first 60,000 years. The dose during this time period is largely from Tc-99 and I-129. After about 60,000 years, the dose from commercial spent is somewhat larger than that from Category 2 spent fuel (Figures 6A-15 and 6A-16). The dose during this later period is largely from Np-237.

A-2.1.7 Uranium Silicide Spent Fuel (Category 7)

The expected-value dose history from Category 7 spent fuel and co-disposed HLW is shown in Figure 6A-17. There are 11.55 MTHM of Category 7 spent fuel that is co-disposed in 250 packages with 600 MTHM of HLW. The peak dose from the spent fuel of this category (Figure 6A-18) is about the same as that from an equivalent amount of commercial spent fuel (Figure 6A-19). As stated earlier, comparisons between DOE SNF and commercial spent fuel are always made using the same number of packages of each spent fuel type. This is done to ensure that there is the same number of waste package failures of the DOE SNF and commercial spent fuel.

A-2.1.8 High-Integrity Uranium-Thorium Carbide Spent Fuel (Category 8)

The 24.67 MTHM of Category 8 SNF is disposed in 503 co-disposal packages with about 1886 MTHM of HLW. The expected-value dose history from these packages is shown in Figure 6A-20 The dose attributed to only the Category 8 spent fuel is more than two orders of magnitude lower (Figure 6A-21). The dose from an equivalent amount of commercial spent fuel is shown in Figure 6A-22, and is about the same as that from the combined Category 8 spent fuel and HLW (see Figure 6A-20). The lower dose from Category 8 spent fuel is attributed to two factors, a lower radionuclide inventory (Table 6A-5) and a slower leach rate of the silicon carbide spent fuel as compared to oxide spent fuel (Figure 6A-1).

A-2.1.9 Low-Integrity Uranium-Thorium Carbide Spent Fuel (Category 9)

There are 1.66 MTHM of Category 9 spent fuel that are co-disposed in 60 waste packages with 225 MTHM of HLW. The expected-value dose history for the combined waste is shown in Figure 6A-23. The dose from the combined waste is somewhat (about half an order of magnitude) higher than that from only the Category 9 spent fuel (compare Figure 6A-23 with Figure 6A-24). The dose from an equivalent amount of commercial spent fuel is about the same (Figure 6A-25) as that from the combined Category 9 spent fuel and co-disposed HLW (Figure 6A-23).

A-2.1.10 Uranium and Uranium-Plutonium Carbide Spent Fuel (Category 10)

The spent fuel of Category 10 is co-disposed in five waste packages. Because of the small number of packages in this category, none are expected to fail in the first 100,000 years. Consequently no results for Category 10 are shown. In the sensitivity analyses of Chapter 5, failure of a single package of Category 10 spent fuel will be assumed and the results will be compared to failure of an equivalent amount of commercial spent fuel.

A-2.1.11 Mixed Oxide Spent Fuel (Category 11)

The 12.32 MTHM of mixed oxide (MOX) spent fuel in Category 11 is packaged in 367 co-disposal packages along with about 1329 MTHM of HLW. The expected-value dose history for the combined spent fuel and HLW is shown in Figure 6A-26, and the dose attributed to only the MOX spent fuel is shown in Figure 6A-27. The dose from only the MOX spent fuel is more than an order of magnitude below that of the combined spent fuel and HLW. This is because of the relatively large amount of HLW co-disposed with the spent fuel (i.e., all of the packages contain one canister of spent fuel and five canisters of HLW. Figure 6A-28 shows the dose from an equivalent amount of commercial spent fuel. The dose from the commercial spent fuel is nearly the same as that from the combined MOX spent fuel and HLW (compare Figures 6A-26 and 6A-28).

A-2.1.12 Uranium-Thorium Oxide Spent Fuel (Category 12)

Figure 6A-29 shows the expected-value dose history from 49.63 MTHM of Category 12 spent fuel and co-disposed HLW (177 MTHM) disposed in 71 waste packages. Twenty-four of these packages are co-disposal packages and the remainder (47) are 3 x 1 packages (they contain 3 canisters of HLW and 1 canister of spent fuel). Figure 6A-30 and Figure 6A-31 show the dose attributed to the Category 12 spent fuel and an equivalent amount of commercial spent fuel, respectively. The difference between the two results, about two orders of magnitude, is because of differences in radionuclide inventory and the slower dissolution rate of the ceramic fuel (Category 12).

A-2.1.13 Uranium-Zirconium Hydride Spent Fuel (Category 13)

The dose history attributed to 2.03 MTHM of Category 13 spent fuel and co-disposed HLW (260 MTHM) is shown in Figure 6A-32. Category 13 spent fuel is contained in 100 co-disposal packages (5 x 1 packages). The dose from only the spent fuel (Figure 6A-33) is more than an

order of magnitude below that from combined spent fuel and HLW (Figure 6A-32). Figure 6A-34 shows the dose from an equivalent amount of commercial spent fuel. The dose from the commercial spent fuel is nearly the same as that from the combined Category 13 spent fuel and HLW (see Figure 6A-32).

A-2.1.14 Navy Spent Fuel (Category 15)

The analyses of Navy spent fuel were conducted differently than other categories of DOE SNF to avoid having to have security clearances for the Performance Assessment staff so that they could work with the classified data for Navy spent fuel. Instead of having a radionuclide inventory for the Navy spent fuel, a dissolution model, and a packaging scenario, the analyses of the Navy fuel were done based on a source term at the boundary of the waste package. To obtain this source term data that consisted of waste package surface temperatures and waste package failure rates for the six regions of the base case repository were transferred to Bettis Atomic Power Laboratory (Duguid 1998), and their staff developed the source term. Bettis staff assumed that the current dry climate prevailed for the first 5,000 years and then switched to the long-term average climate. This climate is the same as used for the expected-value analyses of the other categories of DOE SNF. They also used the waste package failure for the northeast region of the repository and assumed that waste form degradation and release began at the first breach of the waste package. Bettis staff used these data and assumptions to estimate the radionuclide release from the failed waste packages, and their analyses showed that the Zircaloy spent fuel cladding would not be breached in the first one million years. They found that only a small amount of radionuclides that buildup on the cladding during operation (crud) is released. The release rate through time provided by Bettis (Beckett 1998) was used in RIP to analyze the expected-value dose from the Navy Spent fuel.

Figure 6-35 shows the dose history for Category 15 spent fuel over 100,000 years using the release source term provided by Bettis (Beckett 1998). The total dose is from 300 packages of Navy spent fuel that is disposed in spent fuel packages. The dose is from crud that forms on the outside of the Zircaloy cladding. The Zircaloy cladding of the Navy spent fuel is not expected to fail in the first million years, and the dose is from crud that forms on the outside of the fuel (Beckett 1998). Figure 6A-36 shows the dose from an equivalent amount of unclad commercial spent fuel. The dose from the commercial spent fuel is about two orders of magnitude higher than that from the Navy fuel. However, had the commercial spent fuel been assumed to be clad the difference between the Navy and commercial spent fuel would have been less (See Figure 6A-54).

A-2.1.15 Miscellaneous Spent Fuel (Category 16)

Figure 6A-37 shows the expected-value dose history from 10.73 MTHM of Category 16 spent fuel and 135 MTHM of HLW packaged in 44 co-disposal packages. The dose from the combined spent fuel and HLW is somewhat higher than that attributed to the spent fuel alone (Figure 6A-38). The dose from Category 16 spent fuel is also somewhat higher than that from an equivalent amount of commercial spent fuel (Figure 6A-39).

A-2.1.16 Summary of Results

The expected-value total dose history from the spent fuel in Categories 1 through 7 is plotted on Figure 6A-40. Categories 1 and 6 contribute the highest dose from these seven categories. Category 2 does not contribute because there are expected to be no package failures in the first 100,000 years. Category 3 has a dose history that is about three orders of magnitude below that of the other spent fuels shown on Figure 6A-40. The dose history for Categories 8 through 13, and 16 are shown in Figure 6A-41. Category 10 has no dose history because no packages are expected to fail in the first 100,000 years. Comparing Figures 6A-40 and 6A-41 it appears that Category 1, 4, 5, 6, 7, 8, 11, and 16 will contribute significantly to the dose from all DOE spent fuel. The analyses conducted in 1997 (Duguid, et. al. 1996) found that categories 1, 4, 5, 6, 8, and 11 contributed significantly to the dose from a composite of the first 13 categories of DOE SNF. The current analyses indicate that Category 7 has been added to the group of fuels that contribute significantly to the dose from all DOE spent fuels. The reason for this increase is that the radionuclide inventory for Category 7 was increased because of additional ORIGEN analyses for this category. Category 16 is also added to the group, but it had not been previously analyzed.

A-2.2 DOSE ATTRIBUTED TO COMBINED WASTE FORMS

A-2.2.1 HLW Used for Co-Disposal for Different MTHM Algorithms

The HLW used in the base case is assumed to be 4,667 MTHM that is disposed in 1,663 co-disposal packages. If it is assumed that a 10-foot canister of HLW is 0.5 MTHM, then 4,667 MTHM is the same as 9,334 canisters of HLW. The expected–value dose history from disposal of 9,334 canisters of HLW in 1,663 packages is shown in Figure 6A-42. The dose from 4,667 MTHM of HLW reaches about one mrem/yr at 100,000 years with the dose being from Np-237 after about 45,000 years. Prior to 45,000 years, the dose is primarily from Tc-99.

Two additional algorithms for estimating the MTHM of HLW have been considered: the first is based on a strict interpretation of the Nuclear Waste Policy Act and a second is based on the toxicity of the HLW. The first algorithm the HLW waste is equivalent to the fuel from which it was produced would yield about 400 canisters as being equivalent to 4,667 MTHM of HLW. The second, the toxicity basis, would allow co-disposal of all of the high- and medium-enriched spent fuel and still remain below the 4,667 MTHM. The HLW waste necessary for co-disposal of all of the DOE SNF is 7,240 10-foot canisters and 7,836 15-foot canisters of HLW (see Table 6A-9). This is equivalent to 18,994 or approximately 19,000 10-foot canisters of HLW. The HLW for both of these algorithms is assumed to be disposed in co-disposal packages and the results are shown in Figure 6A-43. The results indicate that the dose from 18,994 canisters is only somewhat higher then the dose from 9,334 canisters of HLW (compare Figures 6A-42 and 6A-43). The dose for the 400-canister case is more than two orders of magnitude below that from 18,994 canisters. Here it should be observed that the results do not scale from one case to another. This is because the peak dose is from Np-237 and its release from the engineered barrier system is solubility controlled (i.e., the peak is related to the number of failed waste packages that are releasing Np-237 at its solubility limit).

A-2.2.2 DOE SNF

Figure 6A-44 shows the expected-value total dose history from all of the DOE SNF (2,496 MTHM) compared to an equivalent amount of commercial spent fuel. The analysis of commercial spent fuel is for unclad fuel disposed in Region 6. Both are packaged in the same number of waste packages (3,156, see Table 6A-8). The reason for the difference in roughness is because of how the two curves were derived. The commercial spent fuel curve is from 3,156 packages that contain an equal amount of spent fuel in each package, and with this large number of packages there are enough package failures so that the curve is smooth. The curve for DOE SNF is a composite of the categories that contribute significantly to the dose from all DOE SNF. Several of the categories have few enough packages that package failures appear as spikes in Tc-99 and I-129 dose, and the roughness of the DOE SNF curve results from these spikes (i.e., Category 1).

Figure 6A-45 shows a comparison among 2,333 MTHM of unclad commercial spent fuel, 2,333 MTHM of the metallic surrogate spent fuel used in the base case, and 2,333 MTHM of DOE SNF. For the analyses of both the surrogate and the commercial, the waste packages are disposed in Region 6. This figure indicates that the surrogate metallic spent fuel is a good average for the DOE SNF. The surrogate curve appears as a best-fit curve through the spikes of the DOE SNF curve, but at a later time, it bounds the spikes (after about 70,000 years). The 2,333 MTHM of unclad commercial appears to be a good bound for the DOE SNF; it is above all of the spikes on the DOE SNF curve that are created by individual waste package failures (see Figure 6A-45).

A-2.2.3 Commercial Spent Fuel

Figure 6A-46 shows the expected-value dose history attributed to 63,000 MTHM of commercial spent fuel of the TSPA-VA base case. The spent fuel is assumed to be Zircaloy clad and is distributed across the six regions of the repository. Comparison of the dose from 63,000 MTHM of spent fuel with 4,667 MTHM of HLW (see Figure 6A-42) shows that the total dose from the spent fuel is an approximation of the dose from the entire repository. This is because adding in the dose from HLW (see Figure6A-42) and the dose from DOE SNF (see Figure 6A-45) would only change the dose by a relatively small factor.

A-2.3 COMPARISON OF RESULTS

A-2.3.1 Categories that Contribute Significantly to Total Dose

The categories that contribute significantly to the total dose from all categories of DOE SNF can be observed on Figures6A-40 and 6A-41. Categories 1, 4, 5, 6, 7, and 16 contribute significantly to the total dose from all DOE SNF. Categories 8, 9, and 11 are below a dose of 1×10^{-2} mrem/yr and are not considered to be significant, but are the next three highest categories. Categories 1, 4, 5, 6, 8, and 11 were previously found to contribute significantly to the dose from all DOE SNF (Duguid et. al. 1996), and Categories 1 and 6 were found to be the largest contributors. The current analyses also show that Categories 1 and 6 are the largest contributors (see Figure 6A-40 and 6A-41). It would appear that the dose from Category 7 has increased somewhat, and this increase is due to increased radionuclide inventory based on new ORIGEN

analyses. Category 9 has also increased somewhat because the metallic dissolution model is now thought to be a better representation. Prior analyses (Duguid et. al. 1996) assumed the carbide dissolution model for this category.

A-2.3.2 Comparison among Repository Loading Scenarios

Figure 6A-47 shows the expected-value dose history for the base case repository, 2,333 MTHM of DOE SNF, and 9,334 canisters (4,667 MTHM) of HLW. The reason for the roughness of the curve for DOE SNF on Figure 6A-47 is because of the way was constructed. It is a composite of the individual categories of DOE SNF, and this causes some of the spikes form individual package failures to be higher than curve for the base case. The base case contains a surrogate DOE SNF in 2,546 packages and this produces a smoother curve because of the larger number of package failures (Figure 6A-45). Figure 6A-48 shows the comparison of 63,000 MTHM of clad commercial spent fuel with 2,333 MTHM of DOE SNF, and 2,496 MTHM of DOE SNF. Here it should be observed that the peak dose from 63,000 MTHM of clad commercial spent fuel is nearly the same as that from the base case repository (compare Figures 6A-48 and 6A-47). At early times, the DOE spent fuel curve is somewhat lower than that of the base case repository, and the peak dose from 63,000 MTHM of clad commercial fuel is higher than that from the unclad DOE SNF (by less than a factor of five). It can also be observed that the expected value dose history from 2,333 MTHM of DOE SNF is nearly the same as that from 2,496 MTHM of DOE SNF (see Figure 6A-48). Here the primary difference between the two loading scenarios stems from the number of waste packages in each. The 2,496 MTHM dose curve is somewhat higher, and has somewhat different waste package failures because it has more waste packages.

Figure 6A-49 shows the expected-value total dose curves for 400, 9,334, and 18,996 canisters of HLW. Here it should be noted that the 400 and 9,334 canister cases do not have a very significant dose contribution to the entire repository. The 18,996 canister does affect the dose from the entire repository because of the early contribution from Tc-99 at about 30,000 years and by a lessor amount due to Np-237 at later times. The 18,996 canisters of HLW is the amount that is needed to co-dispose the high- and medium-enriched spent fuel in all (2,496 MTHM) of the DOE SNF.

A-3. EVALUATION OF SENSITIVITY AND UNCERTAINTY

A considerable amount of uncertainty exists both in the long-term repository environment and in the physical characteristics of DOE SNF. The primary natural system parameter that is uncertain over the long-term is the percolation flux through the repository, and consequently, the sensitivity of dose to it will be examined. Other fuel properties that are uncertain are effects of fuel cladding, choice of dissolution model, dissolution rate, and surface area. In addition, because of criticality considerations, the number of packages of spent fuel for some categories is also uncertain. The effects of all of these uncertainties on dose are analyzed in this Chapter.

A-3.1 UNSATURATED ZONE WATER FLUX

The results of prior assessments such as TSPA 1995 (Andrews, et. al. 1995) have shown that dose is sensitive to percolation flux through the repository. However, because of the coupled nature of the TSPA-VA model, this parameter should not be varied independent of other coupled parameters. For the TSPA-VA, the model has been properly coupled for three different fluxes that relate to climate change. These fluxes are the current dry climate, the long-term average climate, and the super pluvial climate. Changes in flux would be expected to have the largest effect on metallic spent fuel because of their faster dissolution rate. For this reason, the metallic surrogate spent fuel used in the base case, Category 1 spent fuel, and Category 6 spent fuel, are analyzed. As discussed earlier, Categories 1 and 6 are the largest contributors to dose from all DOE SNF.

Figure 6A-50 shows the effects on dose from the surrogate spent fuel for the three sets of climatic conditions. The dose peaks at about 40,000 when the current dry conditions are assumed over 100,000 years, and is still increasing at 100,000 years for the two increased flux conditions (long-term average and super pluvial). The dose from the three sets of conditions are about half an order of magnitude apart at 100,000 years, and the dose from the super pluvial conditions is about on a factor of five above that of the surrogate under the base case conditions (see Figure 6A-50 and 6A-45). The same number of failed packages was used for the super pluvial climate as was used for the long-term average climate. Because of this the additional water from the super pluvial produces a dilution effect for the first 50,000 years (until enough ^{237}Np is flushed from the failed waste packages to increase the dose above the extended dry conditions). Also, because there is little dilution for the extended dry conditions the dose from 20,000 to 50,000 is higher than for either the long-term average climate or the super pluvial.

Figure 6A-51 shows the effects of the three climatic conditions on Category 1 spent fuel. Here the peak dose for the three climate conditions is about the same, with the peaks being sharper for wetter conditions because of the more rapid flushing of alteration-controlled radionuclides from the waste package under these conditions. The peaks under super pluvial climate are somewhat lower because of dilution of alteration-controlled radionuclides in the increased flux. Both the long-term average climate and the super pluvial climate produce a dilution effect and yield doses that are lower than those from the extended dry climate (Figure 6A-51). This effect is similar to that from the surrogate DOE spent fuel at early time when few waste packages have failed (Figure 6A-50, between 20,000 and 40,000 years).

Figure 6A-52 shows the effects of the three climate conditions on dose from Category 6 spent fuel. Here it is interesting to note the dose at about 80,000 years from the long-term average climate is higher than that from the super pluvial climate. Using the same waste package failure rate for both climates causes this difference in dose. The larger groundwater flow during the super pluvial begins to deplete the ^{237}Np from the waste packages that fail early (because of the small amount of spent fuel that they contain), and the dose drops below that from the long-term average climate. At earlier time when few packages have failed (Figure 6A-50 and 6A-51) dilution causes the highest dose to be from the extended dry climate (Figure 6A-52).

A-3.2 FUEL ALTERATION AT TIME OF WASTE PACKAGE PAILURE

The TSPA-VA model does not track individual waste packages within the repository. Consequently, the alteration of the spent fuel in a waste package cannot be initiated at the time of waste package failure. For metallic spent fuel this conservatism could have a significant effect on peak dose. To test this, a single package was assumed to fail at 1,000 years and the results are compared to those from a single package that fails at 40,000 years (Figure 6A-53). To avoid the influence of the change of climate at 5,000 years both results were analyzed for the long-term average climate for the entire 100,000-year period. Figure 6A-53 shows two separate analyses plotted on the same figure, one for a single package failure at 1,000 years and the other for a single package failure at 40,000 years. The spike in Tc-99 and I-129 is lower for the package that fails earlier than for the package that fails later. The lower peak is due to the fewer number of corrosion patches present on a failed package at 1,000 years than at 40,000 years (i.e., there would be a few pits through which diffusion occurs at 1,000 years and there would likely be flux through the package at 40,000 years). A more likely explanation of the Tc-99 and I-129 spikes that occur at waste package failure (Figure 6A-3) is that they caused by the rapid dissolution of the metallic spent fuel (i.e., the fuel dissolves within one model time step).

A-3.3 CLADDING

The effects of cladding were found to be significant for commercial spent fuel in the base case. Figure 6A-54 shows the effects of cladding of commercial spent fuel as modeled in the base case for 2,333 MTHM of commercial spent fuel. Here the cladding makes a difference of about two orders of magnitude between about 10,000 and 40,000 years (Figure 6A-54). As the cladding fails, the two dose curves are similar after about 70,000 years.

Category 1 spent fuel was originally clad with Zircaloy, but much of the cladding has failed during pool storage of the spent fuel. Figure 6A-55 shows the effects of assuming 50% intact cladding for Category 1 fuel. Here the peak dose is reduced somewhat (about a factor of two) because of the cladding. The 50% cladding changes the dose from Tc-99 and I-129 by a factor of two because they are alteration-controlled radionuclides, and little affect on Np-237 because it is solubility controlled. It would appear a significant fraction of the cladding on Category 1 spent fuel would have to be in tact to substantially change the dose spikes from Tc-99 and I-129.

A-3.4 WASTE FORM DISSOLUTION MODEL

For the analyses of disposal, DOE SNF dissolution models are used for oxide, metallic, carbide, and ceramic spent fuel and for HLW glass. A comparison of these dissolution models is presented in Figure 6A-56. The dissolution rates in descending order of rate are metallic spent fuel, oxide spent fuel, HLW glass, ceramic, and carbide spent fuel. After about 20,000 years the range of dissolution rate is more than four orders of magnitude

The dissolution model for some of the DOE SNF is uncertain to the point that different dissolution models could be assumed for the spent fuel. For example, for Category 9, low integrity carbide, ten times the metallic dissolution model, was used in the analyses instead of using the carbide dissolution model. The carbide model only applied to the silicon carbide coated fuel; (the high integrity carbide spent fuel Category 8). A comparison of using ten times the metallic dissolution model and the carbide dissolution model for Category 9 spent fuel is shown in Figure 6A-57. This comparison shows that the choice of dissolution model has little effect on dose because the release from the waste package is being controlled by diffusion/advection rather than dissolution rate.

The ceramic dissolution model used in these analyses was developed based on studies Synroc and may not be applicable to the ceramic spent fuel of Category 12. To analyze the effect of assuming the ceramic dissolution model, the results are compared to assuming dissolution of the fuel congruent with Thorium-Uranium oxide (Figure 6A-58). The assumption of congruent dissolution model reduces the peak dose from Category 12 spent fuel by more than a factor of five. However, this reduction would not effect the dose from a composite of all categories of DOE spent fuel because Category 12 does not contribute significantly to the total dose.

A-3.5 WASTE FORM DISSOLUTION RATE AND SURFACE AREA

The dissolution rate and surface area of many of the DOE spent fuels are uncertain because few test data are available. As guidance to the spent fuel testing the sensitivity of dose to these parameters was examined for selected categories of DOE spent fuel. Figure 6A-59 shows the effects of increasing and decreasing the dissolution rate of Category 1 spent fuel by three orders of magnitude. The increase in dissolution has no effect on the dose because radionuclides are dissolved that can be transported from the waste package (see Figure 6A-59). However, the decrease in dissolution rate by three orders of magnitude significantly effects the dose peaks (by as much as two orders of magnitude). The same effect is observed at the higher flux through the repository that would exist when the long-term average climate is applied over the 100,000-year period (Figure 6A-60). A similar, but less dramatic, effect of a range of surface areas on the dose from Category 1 spent fuel is observed (Figure 6A-61). Increased surface area has little effect on dose, but a decrease in surface area of a factor of ten produces a decrease in dose of about a factor of five. This indicates that being overly conservative in the assumption of metallic spent fuel surface area can have a significant effect on dose (i.e., assuming a larger than actual surface area will increase dose). A similar effect is observed at the higher flux through the repository created by the assumption of long-term average climate (Figure 6A-62).

Figure 6A-63 shows the effect of dissolution rate on Category 13 spent fuel. This category was selected because, as mentioned previously, the dissolution model for this fuel is uncertain. An increase of three orders of magnitude in rate increases the peak dose by about two orders of magnitude at early time, to more than a factor of five at later time. A similar decrease in rate decreases the dose by about three orders of magnitude (Figure 6A-63).

A-3.6 DOSE FROM CATEGORIES 2 AND 10

Because no waste package failures are expected over the first 100,000 years for Categories 2 and 10 the dose attributed to these spent fuels could not be compared to an equivalent amount of commercial spent fuel. Figure 6A-64 shows the comparison of the dose from failing one package of Category 2 spent fuel at 40,000 years and failing an equivalent amount of commercial spent fuel at the same time. The peak dose from commercial spent fuel is about a two orders of magnitude higher than that from Category 2 spent fuel. Similar results were obtained when one package of Category 10 fuel was failed at 40,000 years and the results were compared to an equivalent amount of commercial spent fuel (Figure 6A-65). In this case the peak dose from the commercial spent fuel is only about a factor of five higher than that of Category 10 spent fuel.

A-3.7 NUMBER OF WASTE PACKAGES

The number of waste packages has two effects on the dose from the same amount of waste, more waste packages means there will be more waste package failures and more failed packages means that there will be more release of solubility limited radionuclides (such as Np-237). These effects were analyzed for Category 13 spent fuel where the number of waste packages is uncertain because of criticality. Figure 6A-66 shows the results for a factor of five or ten increase in the number of packages for Category 13 spent fuel. This category was assumed to be packaged in 100 waste packages. The primary radionuclide that contributes to the long-term dose from the category is Np-237 (see Figure 6A-32). An increase in the number of waste packages by a factor of five has about an order of magnitude effect on the dose (i.e., packages fail earlier and there are more waste packages releasing Np-237 at its solubility limit). The number of failed packages is represented by the number of dose spikes on each curve. Another factor of two increase in the number of waste packages produces about a factor of two increase in dose (see Figure 6A-66).

The effects of increasing the number of waste packages for Category 1 spent fuel was also investigated, even though the number of waste is not uncertain (Figure 6A-67). Here the dose peaks from Tc-99 and I-129 changes little even though there are more waste package failures, but the best fit curve through the results show an increase in dose that is attributed to Np-237. The lack of change in the peak dose from Tc-99 and I-129 is because they are alteration-controlled radionuclides that are flushed from the waste package relatively rapidly because of their high solubility.

A-3.8 REPOSITORY REGION

The footprint of the repository is dived into six regions that have somewhat different flux. Region 6 has the highest flux and Region 2 has the lowest. For conservatism, the DOE spent

fuels were analyzed individually in Region 6 and compared to an equivalent amount of commercial spent fuel that was also in Region 6. The composite of DOE spent fuel was compared to the surrogate and to an equivalent amount of commercial spent fuel that were Region 6, when in fact the surrogate in the base case would have been distributed evenly over all six regions. The results are shown in Figure 6A-68 for 2,333 MTHM of commercial spent fuel in Region 6 as compared to being evenly distributed over the six repository regions. The dose is higher when the spent fuel is in Region because of the higher flux and the curve is rougher when the waste packages are distributed evenly over six regions because of differences in transport length.

In order to evaluate the conservatism of placing the spent fuel in Region 6, a comparison of the results of placing Category spent fuel in Region 6 and Region 2 is presented in Figure 6A-69. Region 6 has the highest flux through the repository and Region 2 has the lowest. The difference in peak height is due to the difference in flux and the lag of one peak behind the other is due to the difference in transport path length for the two regions. This result differs from that described in Section 3.1 where the effects of different climates were compared, and dilution caused the dose from higher flux to be lower. Here the higher flux causes higher dose because the higher flux is part of the same flow system (i.e., a different location in the unsaturated zone, but the same saturated-zone flux).

A-3.9 SUMMARY OF RESULTS

Increased flux through the repository increases the long-term dose from Np-237 significantly even though the same number of waste package failures are assumed. In reality, there should be increased waste package failures with increased flux and the increase in dose would be expected to be even greater. For Category 6 spent fuel, when the flux for the super pluvial is assumed for the entire 100,000-year period, while not realistic, begins to deplete the Np-237 so that the dose curve drops below that attributed to long-term average climate over the entire period. The depletion of Np-237 was not observed for Category 1 spent fuel because there is more fuel in these waste packages than for Category 6.

The assumption that alteration of the spent fuel in a waste begins at time zero rather than at waste package failure may have a significant affect on the height of the dose spike from Tc-99 and I-129 for metallic spent fuel. This is because the metallic spent fuels alter rapidly and there could be a significant amount of altered fuel in the package at the time of waste package failure. The effects of this assumption should be investigated further, especially in regard to Category 1 spent fuel (i.e., for this category the dose spikes have a significant effect on the dose from all DOE SNF).

The effect of cladding on dose diminishes with time as the cladding fails and the presence of cladding tends to smooth out the dose curve. Assuming 50% cladding for Category 1 spent fuel has a factor of two in the dose spikes from Tc-99 and I-129 as would be expected for these alteration-controlled radionuclides. It appears that there would have to be significantly more in tact cladding to produce a significant effect on dose from Category 1 spent fuel.

Reduced dissolution rate and surface area can have a significant effect on the dose from DOE SNF. For Category 1 spent fuel, a reduction in dissolution rate reduces the dose spikes from

Tc-99 and I-129 significantly while a reduction in surface area has a lessor corresponding reduction. For Category 13 spent fuel a change in dissolution rate effects both the alteration-controlled radionuclides (Tc-99 and I-129) and the solubility-controlled radionuclide Np-237.

The dose from Category 2 and 10 DOE SNF is less than that from an equivalent amount of unclad commercial spent fuel. Because of the small number of waste packages in Categories 2 and 10 (8 and 5, respectively), no packages are expected to fail over 100,000 years.

An increased number of waste packages that contain the same total amount of spent fuel increases the total dose. The increase does not affect the dose from alteration-controlled radionuclides, but does increase the dose from the solubility-controlled radionuclide Np-237. This is because with a greater number of packages there are more failed packages releasing Np-237 at its solubility limit.

A-4. CONCLUSIONS

- The dose from a composite of all categories of DOE SNF can be bounded by an equivalent amount, on an MTHM basis, of unclad commercial spent fuel.

- The largest contributor to dose from all DOE SNF is Category 1 that is composed primarily of N Reactor spent fuel.

- The metallic surrogate spent fuel that represented the DOE SNF in the TSPA-VA base case appears to be an appropriate average of the composite of the categories of DOE SNF. Some of the dose spikes from Tc-99 and I-129 caused by individual package failures of Category 1 spent fuel are higher than the dose from the surrogate; but overall the surrogate dose curve is higher including the peak dose that occurs at 100,000 years.

- The spikes in dose from Tc-99 and I-129 caused by individual package failures of Category 1 spent fuel are sensitive to changes in dissolution rate and surface area. They do not increase as dissolution rate is increased, but are nearly eliminated when dissolution rate is reduced by three orders of magnitude. For surface area, the spikes remain the same for increased surface area and are decreased as surface area is decreased. These results indicate the importance of reducing any conservatism that may exist in the assumed values of dissolution rate and surface area through Laboratory testing.

- Categories 1, 4, 5, 6, and 7 are the largest contributors to dose from all DOE SNF, and Categories 1 and 6 are the largest contributors. All other Categories (2, 3, 8, 9, 10, 11, 12, 13, 14, 15, and 16) produce dose that is more than two orders of magnitude below that from all DOE SNF. Of the lower dose-producing categories, Categories 8, 9, and 11 are highest.

- The dose from Category 15, Navy spent fuel, is more than two orders of magnitude below that from all DOE spent fuel. Category 15 dose is also more than two orders of magnitude below that of an equivalent amount of commercial spent fuel. The reasons for the low dose from Navy spent fuel are that the dose is from crud on the outside of the Zircaloy clad, and that the robust clad is not expected to fail for over a million years.

- The spikes in dose from Tc-99 and I-129 caused by individual package failures of Category 1 spent fuel are caused by rapid dissolution of the metallic fuel once the waste package has failed. Similar results are found for unclad commercial spent fuel.

- The dose from approximately 19,000 canisters of HLW that would be needed to co-dispose the high- and medium-enriched spent fuel in all or the DOE SNF is less than a factor of five higher than the 4,667 MTHM of HLW in the TSPA-VA base case (9334 canisters).

- The dose from spent fuel disposed in regions of the repository where there is less unsaturated zone flux is lower. If the dose spikes from Category 1 spent fuel were to be viewed as being undesirable they could be lowered by disposing Category 1 spent fuel in regions of lower flux.

A-5. REFERENCES

Andrews, R., T. Dale, and J. McNeish, 1994. *Total System Performance Assessment-1993: An Evaluation of the Potential Yucca Mountain Repository*, B00000000-01717-2200-00099-Rev. 01, Civilian Radioactive Waste Management System, Management and Operating Contractor, Vienna, Virginia.

Andrews, R. W., J. E. Atkins, J. O. Duguid, B. E. Dunlap, J. E. Houseworth, L. R. Kennedy, J. H. Lee, S. Lingineni, J. A. McNeish, S. Mishra, M. Reeves, D. C. Sassani, S. D. Sevougian, F. Tsai, V. Vallikat, Q. L. Wang, and Y. Xiang, November, 1995. *Total System Performance Assessment - 1995: An Evaluation of the Potential Yucca Mountain Repository*, B00000000-01717-2200-00136, Rev. 01, Civilian Radioactive Waste Management System, Management and Operating Contractor, Las Vegas, Nevada.

Barnard, R. W., M. L. Wilson, H. A. Dockery, J. H. Gauthier, P. G. Kaplan, R. R. Eaton, F. W. Bingham, and T. H. Robey, 1992. *TSPA 1991: An Initial Total-System Performance Assessment for Yucca Mountain*, SAND91-2795, Sandia National Laboratories, Albuquerque, New Mexico.

Beckett, T. H., 1998. Letter to J. Russell Dyer, Yucca Mountain Site Characterization Office, Las Vegas, NV from Department of the Navy, Arlington, Virginia, May 8, 1998.

Cresap, D., 1997. *Results of Sensitivity Studies on Parameters for INEEL Spent Fuel*, Idaho National Engineering and Environmental Laboratory, National Spent Fuel Program, Idaho Falls, Idaho, (Draft).

DOE (U.S. Department of Energy), 1988. *Internal Dose Conversion Factors for Calculation of Dose to the Public*, DOE/EH-0071, Office of Environment and Health, Washington, D.C.

DOE (U. S. Department of Energy), 1996. *Spent Fuel Database SFD-96*, Office of Spent Fuel Management, Idaho Falls, Idaho, Database Available on Internet, Contact William Hurt, (208)-526-7338.

Duguid, J. O., J. A. McNeish, V. Vallikat, D. Cresap, and N. Erb, "Total System Performance Assessment Sensitivity Studies of U. S. Department of Energy Spent Nuclear Fuel," A00000000-01717-5705-00017, Rev. 01, Civilian Radioactive Waste Management System, Management and Operating Contractor. Las Vegas, Nevada, September 30, 1997.

Duguid, J. O., J. A. McNeish, and V. Vallikat, 1996. *Total System Performance Assessment of a Geologic Repository Containing Plutonium Waste Forms*, A00000000-01717-5705-00011, Rev. 00, Civilian Radioactive Waste Management System, Management & Operating Contractor. Las Vegas, Nevada.

Duguid, J. O., 1998. Letter to Abraham Van Luik, U. S. Department of Energy, Las Vegas, Nevada from Duke Engineering & Services, Austin, April 15, 1998.

EPA (U. S. Environmental Protection Agency), 1985. *Environmental Standards for the Management and Disposal of Spent Nuclear Fuel, High-level and Transuranic Radioactive Wastes*, (40 CFR 191), Federal Register, Vol. 50, No. 182, September 19, 1985, Washington, D.C., pp. 38066-38089.

EPA (U. S. Environmental Protection Agency), 1988. *Limiting Values of Radionuclide Intake and Air Concentration and Dose Conversion Factors for Inhalation, Submersion, and Ingestion*, EPA-520/1-88-020, Washington, D.C.

EPRI (Electric Power Research Institute), 1992. *Source Term in the EPRI Performance Assessment*, R. Shaw, presented to Nuclear Waste Technical Review Board, Las Vegas, Nevada, October 15, 1992.

INEEL Task Team on Spent Nuclear Fuel, 1997. *Technical Strategy for Management of INEEL Spent Nuclear Fuel*, Prepared for the U. S. Department of Energy, Office of Spent Fuel Management, Washington D.C., March, 1997.

Lappa, D. A., 1995. Letter Report to D. Harrison, U.S. Department of Energy, from Lawrence Livermore National Laboratory, Livermore, California, May 9, 1995.

NAS (National Research Council, National Academy of Sciences), 1983. Board on Radioactive Waste Management-Waste Isolation System Panel, *A Study of the Isolation System for Geologic Disposal of Radioactive Wastes*, National Academy Press, Washington, DC.

NRC (U.S. Nuclear Regulatory Commission), 1981. *Estimates of Internal Dose Equivalent to 22 Target Organs for Radionuclides Occurring in Routine Releases from Fuel-cycle Facilities, Vol. III*, Dunning, D., Killough, G., Bernard, S., Pleasant, J., and Walsh, P. NUREG/CR-0150 Vol. 3 (ORNL/NUREG/TM-190/V3), U.S. Nuclear Regulatory Commission, Washington, DC.

ORNL (Oak Ridge National Laboratory), no date. *Oak Ridge Isotope Generation (ORIGEN2), Isotope Generation and Depletion Code ORNL-CCC-371*, Contact the Radiation Shielding Information Center, Oak Ridge, Tennessee, (423) 574-6176.

Reeve, K. D., D. M. Levins, B. W. Seatonberry, R. K. Ryan, K. P. Hart, and G. T. Stevens, 1989. *Fabrication and Leach Testing of Synroc Containing Actinides and Fission Products*, Material Research Society Symposium Proceedings, Vol. 127, pp. 223-230.

Rechard, R. P., editor, 1995. *Performance Assessment of the Disposal in Unsaturated Tuff of Spent Nuclear Fuel and High-Level Waste Owned by U.S. Department of Energy*, SAND94-2563, Sandia National Laboratories, Albuquerque, New Mexico.

Research Reactor Spent Nuclear Fuel Task Team, 1996. *Technical Strategy for the Treatment, Packaging, and Disposal of Aluminum-Based Spent Nuclear Fuel*, Prepared for the U. S. Department of Energy, Office of Spent Fuel Management, Washington D.C., June, 1996.

Ringwood, A., Kesson, S., Reeve, K., Levins, D., and Ramm, E., 1988. *Synroc, Radioactive Waste Forms for the Future*, W. Lutze and R. Ewing, Des, North Holland, Amsterdam.

Stroupe, E. P., 1997. Memorandum to Distribution with Attachments, Complex-Wide Spent Nuclear Fuel (SNF) Work Planning Meeting Notes, INEEL, Idaho Falls, Idaho, February 14, 1997.

Stroupe, E. P., 1998 Letter to Robert W. Andrews, Duke Engineering & Services, Las Vegas, NV from Lockheed Martin Idaho Technologies Company, Idaho Falls, Idaho, May 4, 1998.

CHAPTER 6

APPENDIX A

FIGURES

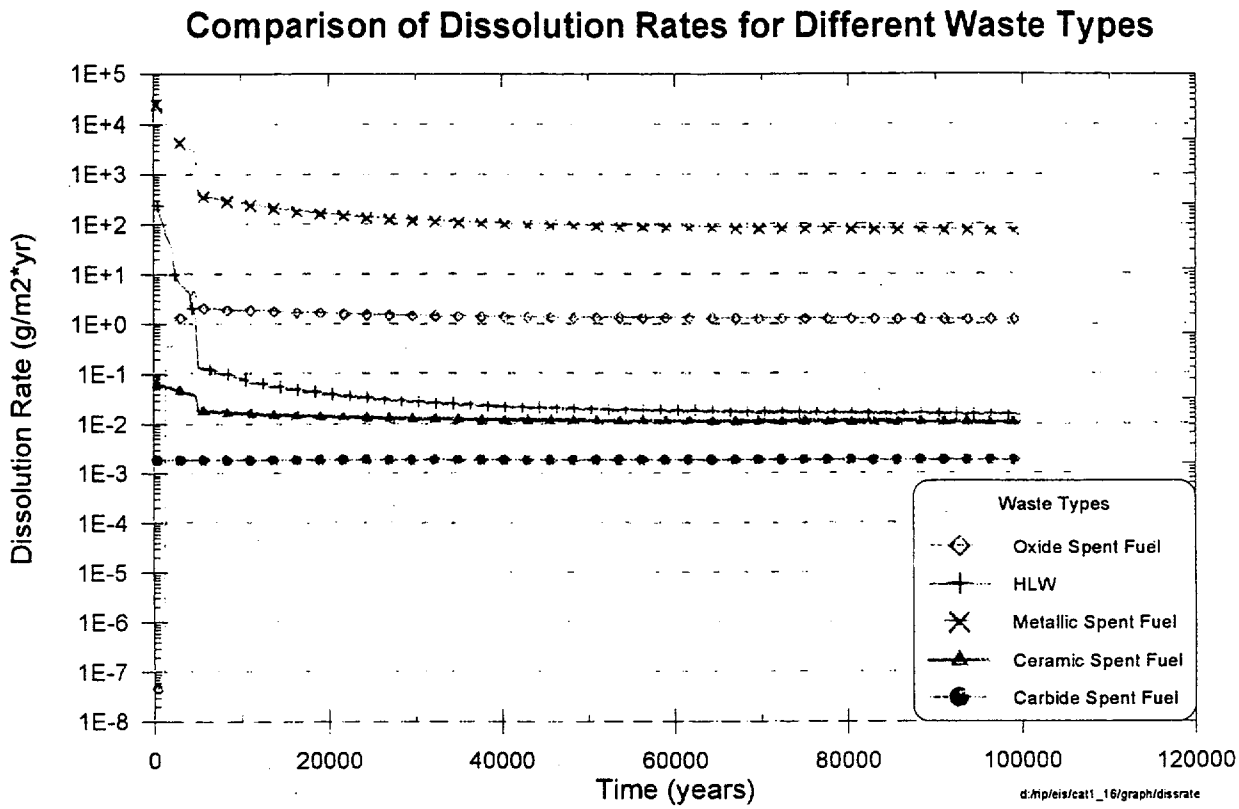

Figure 6A-1. Comparison of dissolution rates for high-level waste and oxide, metallic, carbide, and ceramic spent fuel.

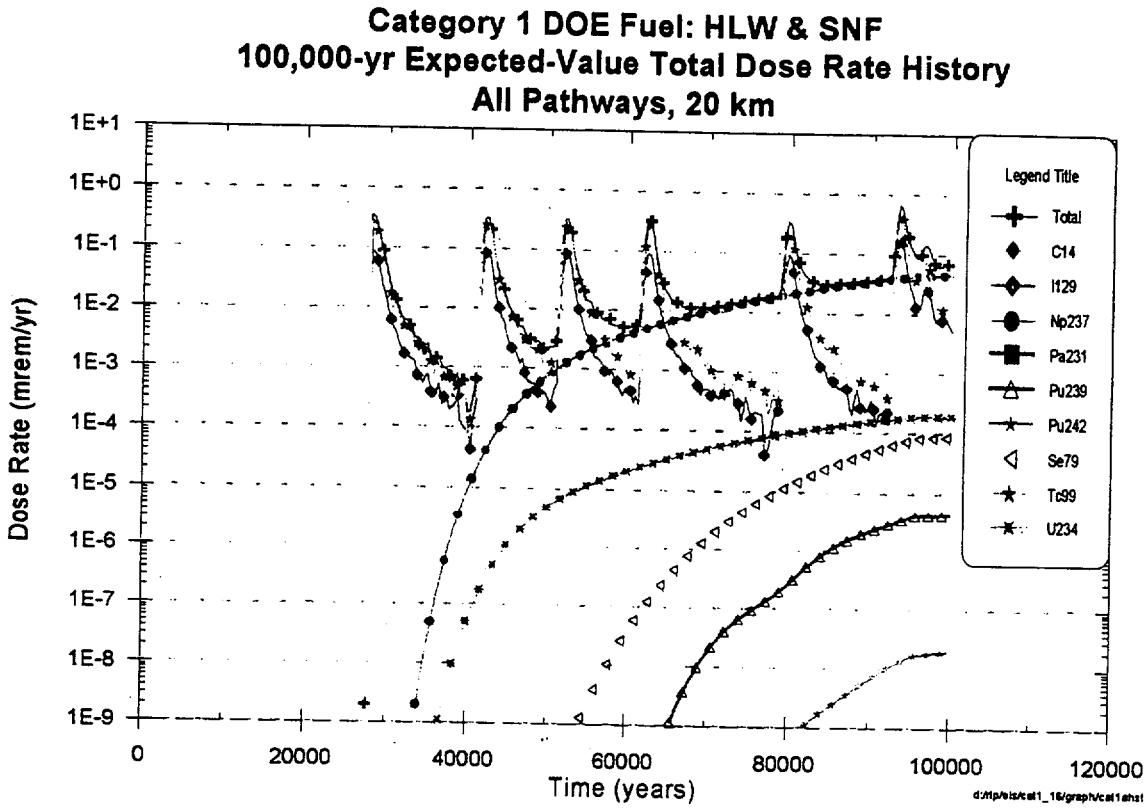

Figure 6A-2. Expected-Value Dose History at 20 Kilometers Over 100,000 Years from Category 1 Spent Fuel and HLW.

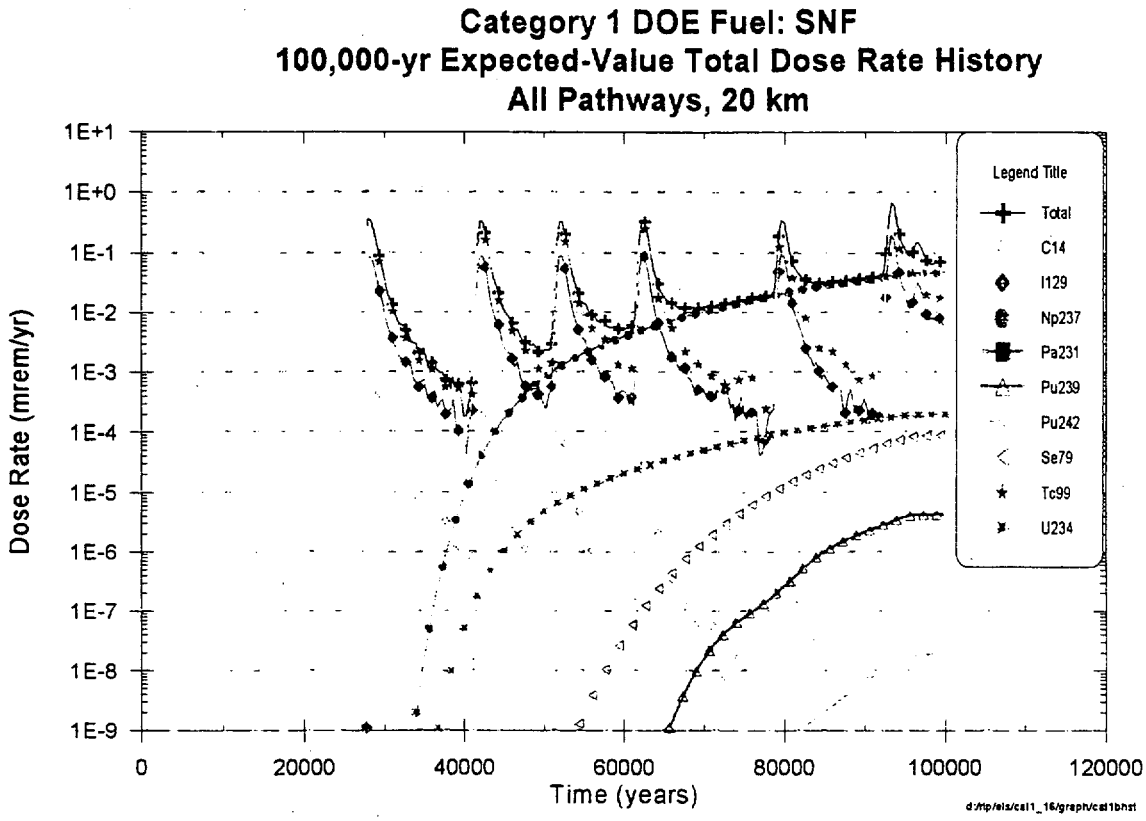

Figure 6A-3. Expected-Value Dose History at 20 Kilometers Over 100,000 years from Category 1 Spent Fuel.

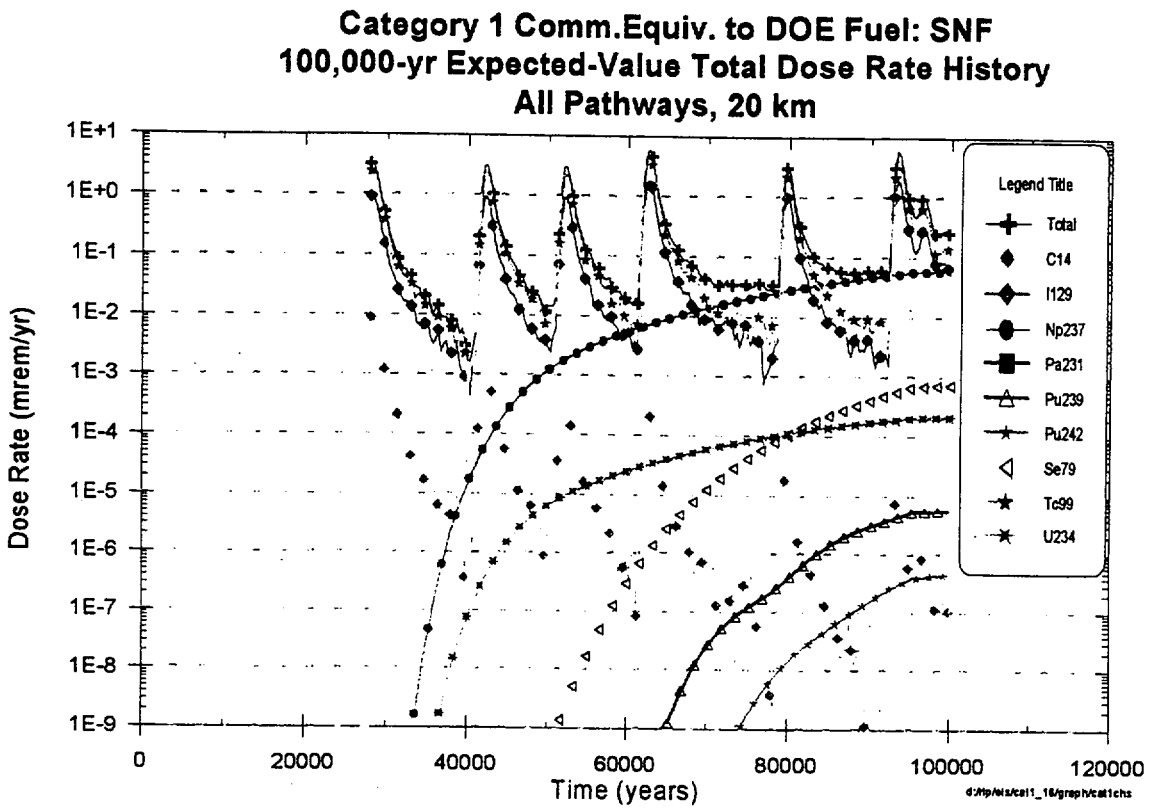

Figure 6A-4. Expected-Value Dose History at 20 Kilometers Over 100,000 Years from Commercial Spent Fuel Equivalent to Category 1 Spent Fuel.

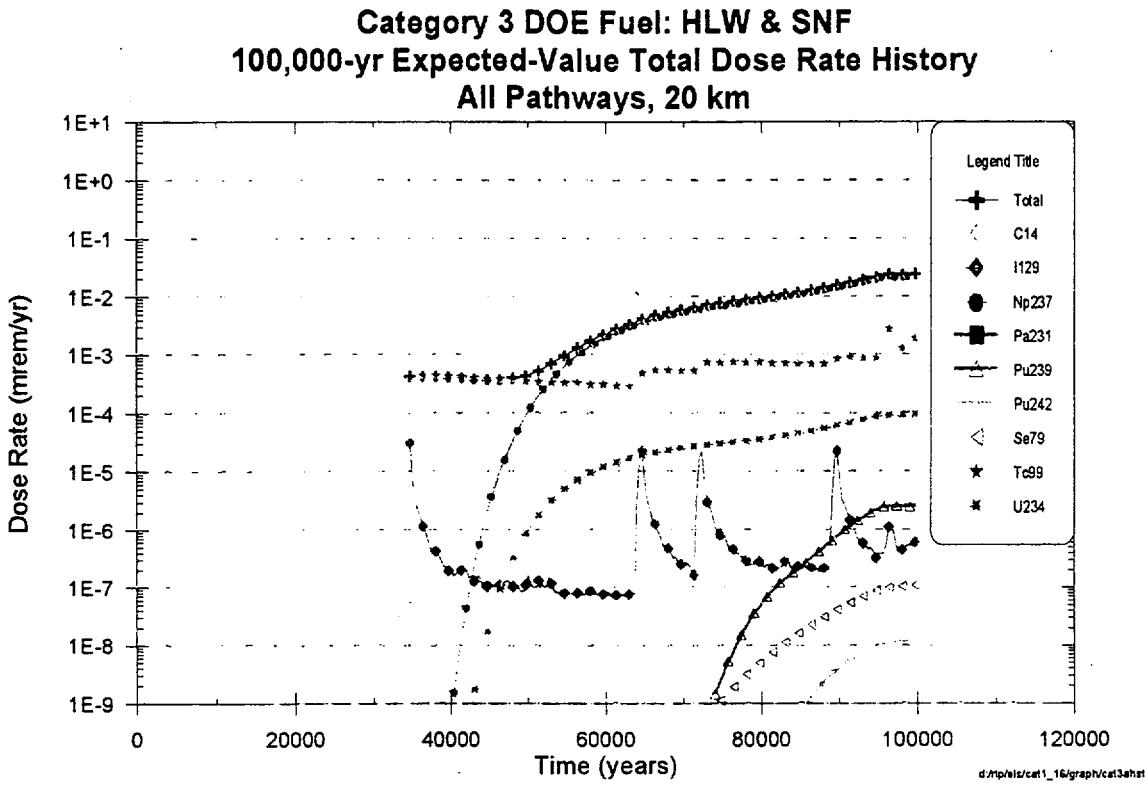

Figure 6A-5. Expected-Value Dose History at 20 Kilometers Over 100,000 Years from Category 3 Spent Fuel and HLW.

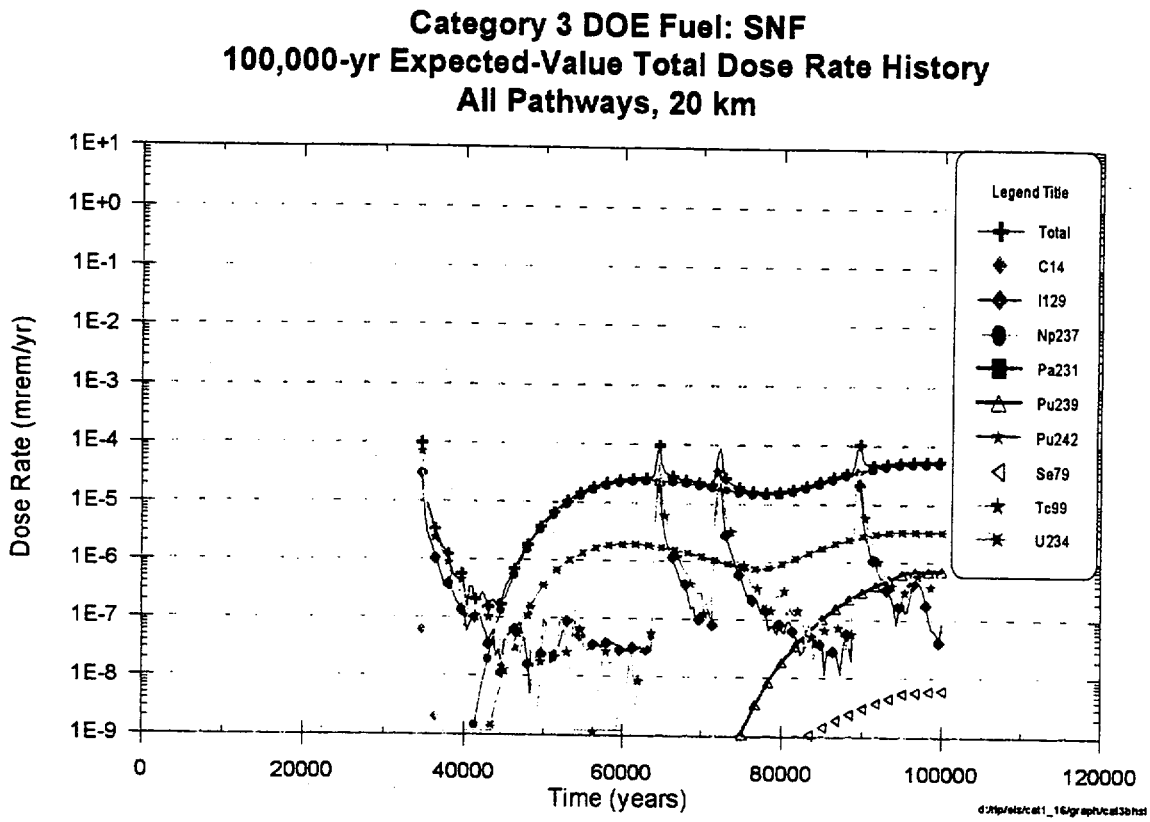

Figure 6A-6. Expected-Value Dose History at 20 Kilometers Over 100,000 Years from Category 3 Spent Fuel.

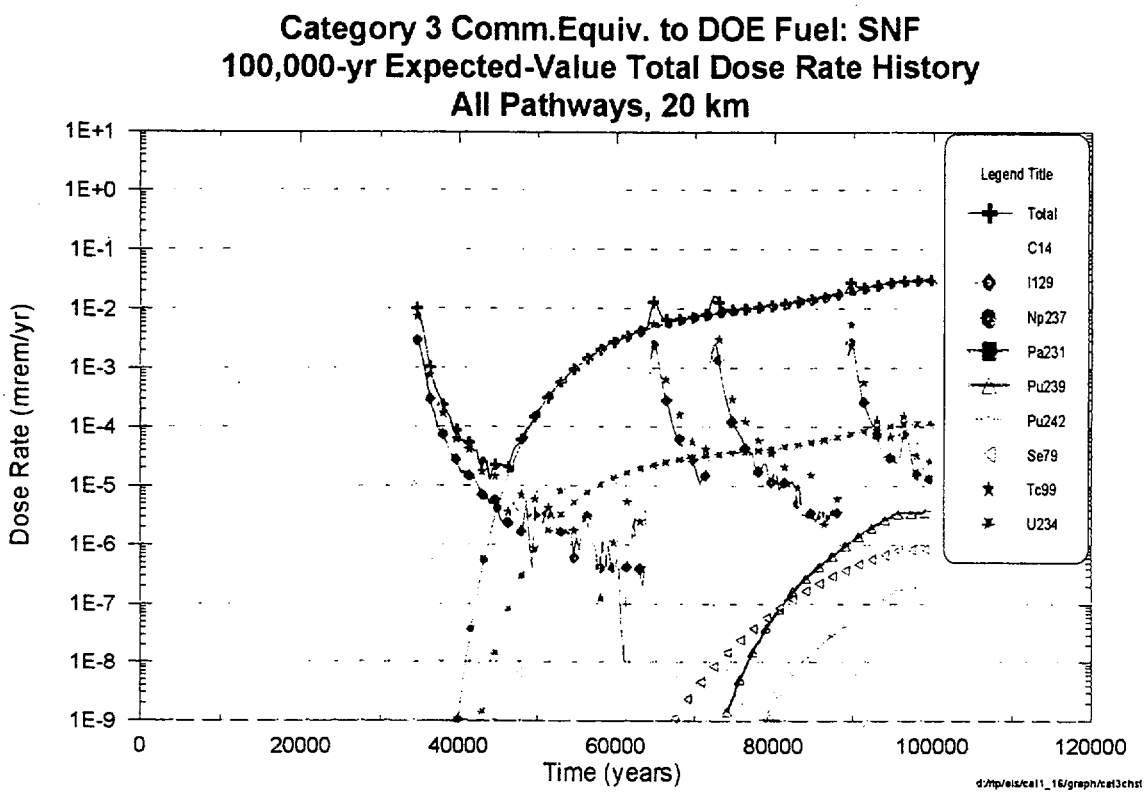

Figure 6A-7. Expected-Value Dose History at 20 Kilometers Over 100,000 Years from Commercial Spent Fuel Equivalent to Category 3 Spent Fuel.

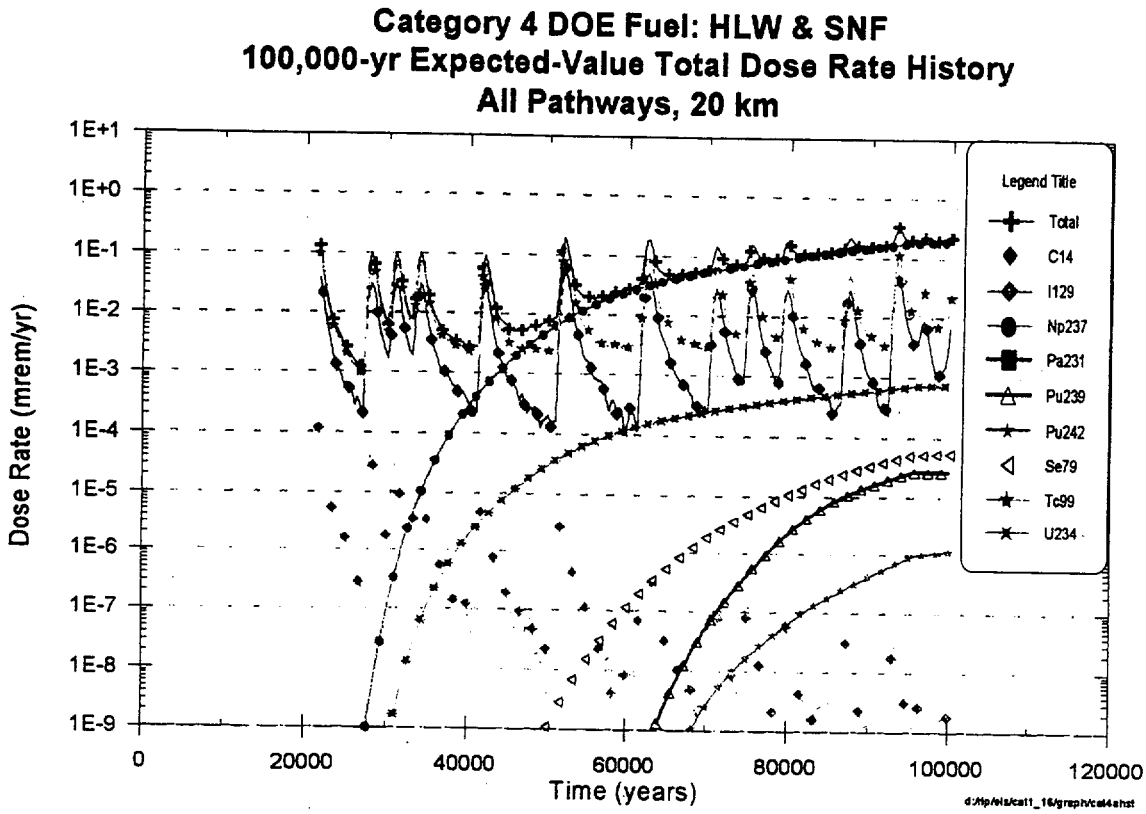

Figure 6A-8. Expected-Value Dose History at 20 Kilometers Over 100,000 Years from Category 4 Spent Fuel and HLW.

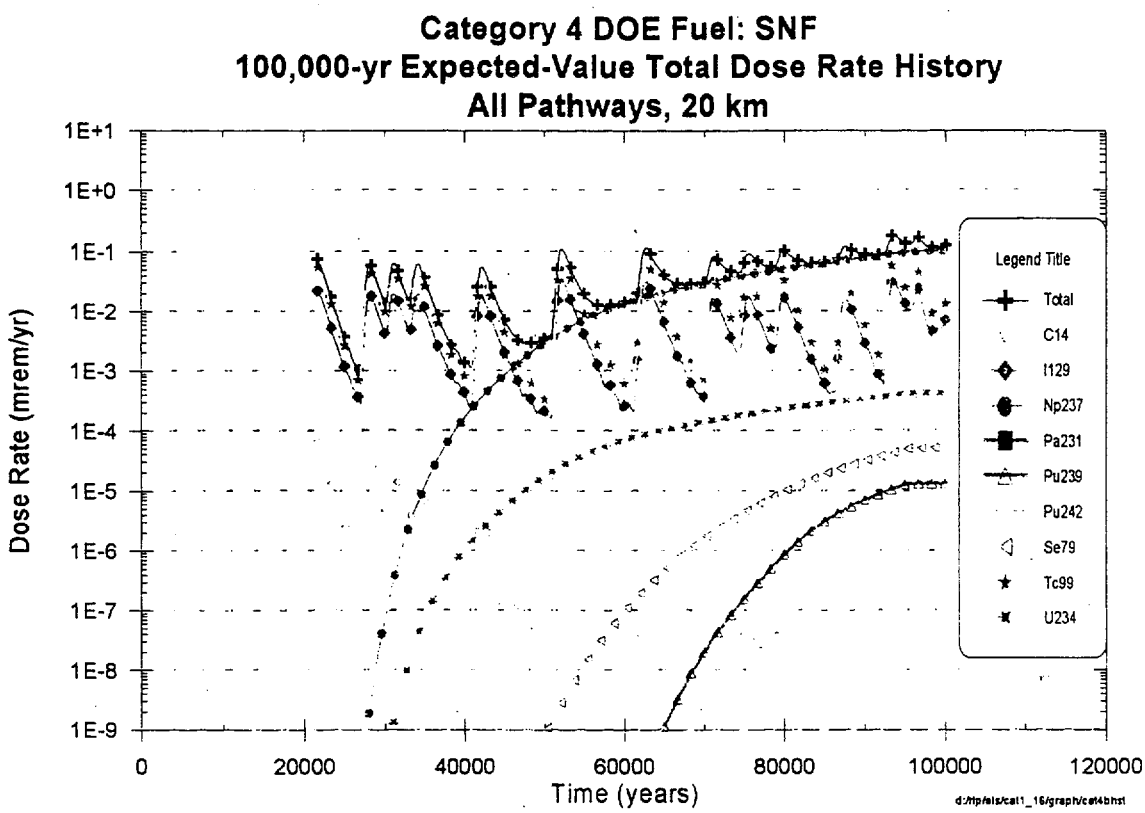

Figure 6A-9. Expected-Value Dose History at 20 Kilometers Over 100,000 Years from Category 4 Spent Fuel.

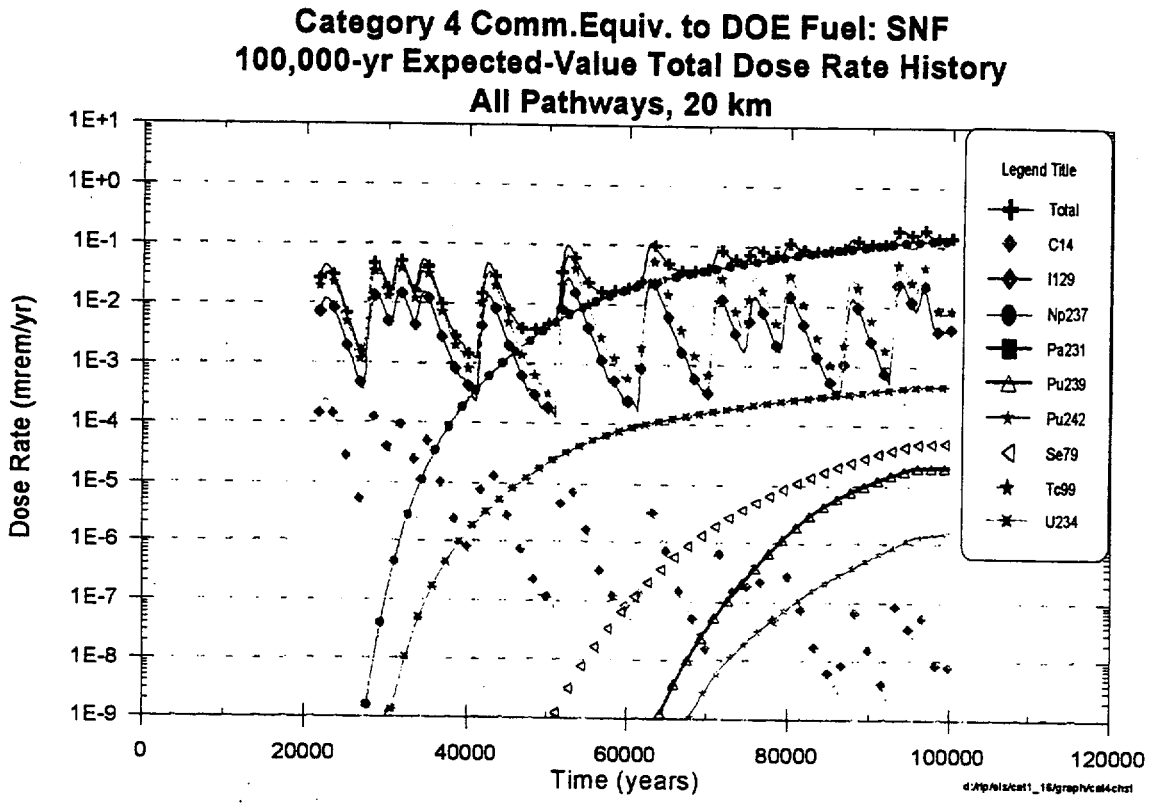

Figure 6A-10. Expected-Value Dose History at 20 Kilometers Over 100,000 Years from Commercial Spent Fuel Equivalent to Category 4 Spent Fuel.

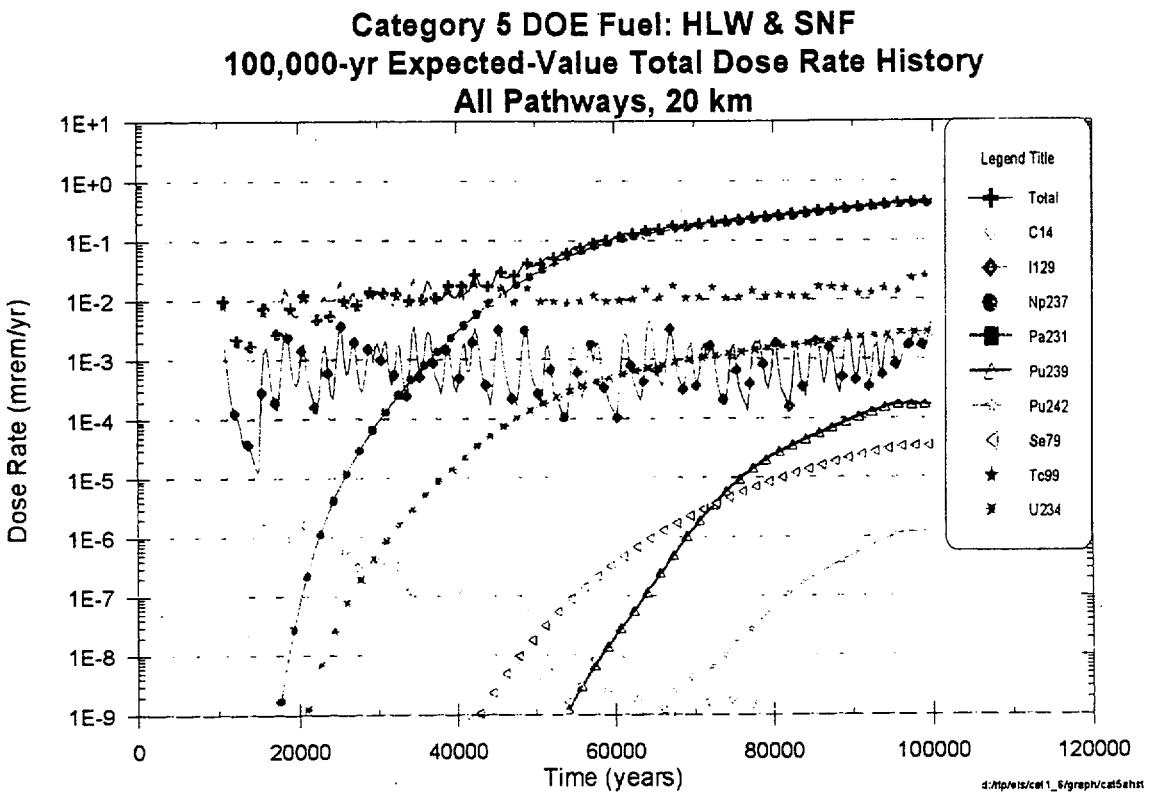

Figure 6A-11. Expected-Value Dose History at 20 Kilometers Over 100,000 Years from Category 5 Spent Fuel and HLW.

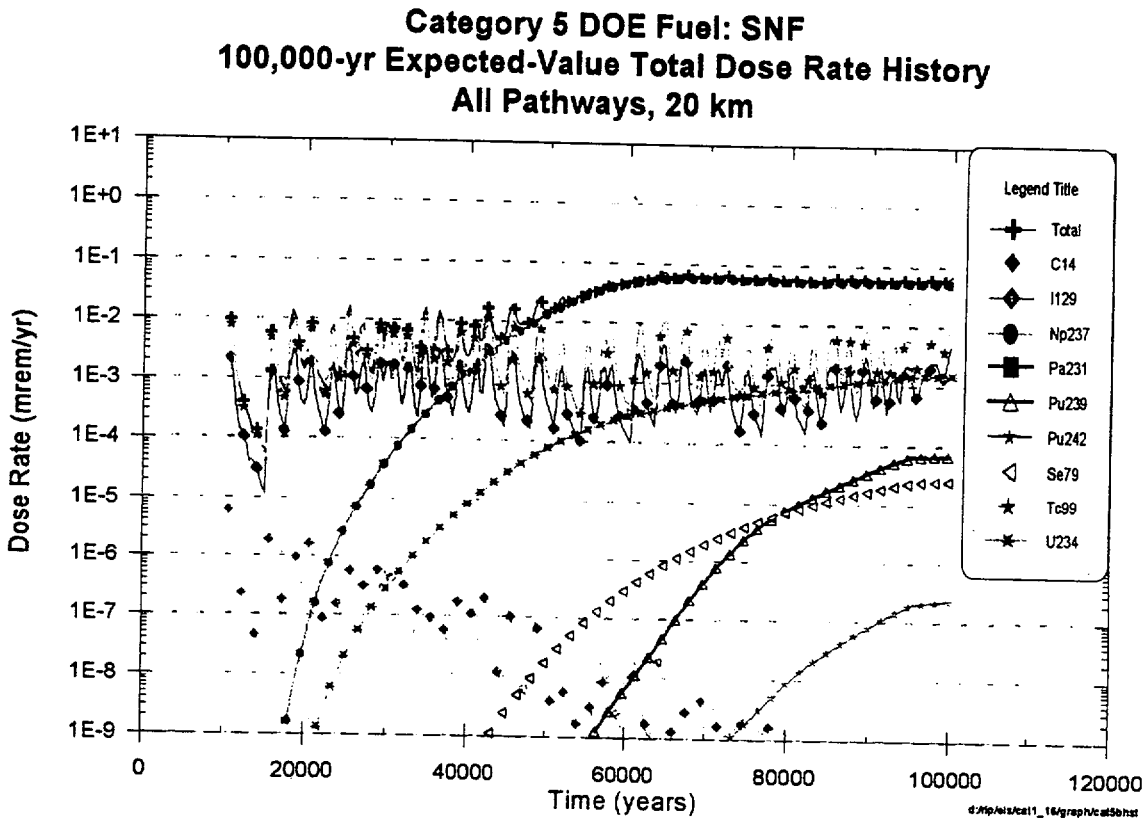

Figure 6A-12. Expected-Value Dose History at 20 Kilometers Over 100,000 Years from Category 5 Spent Fuel.

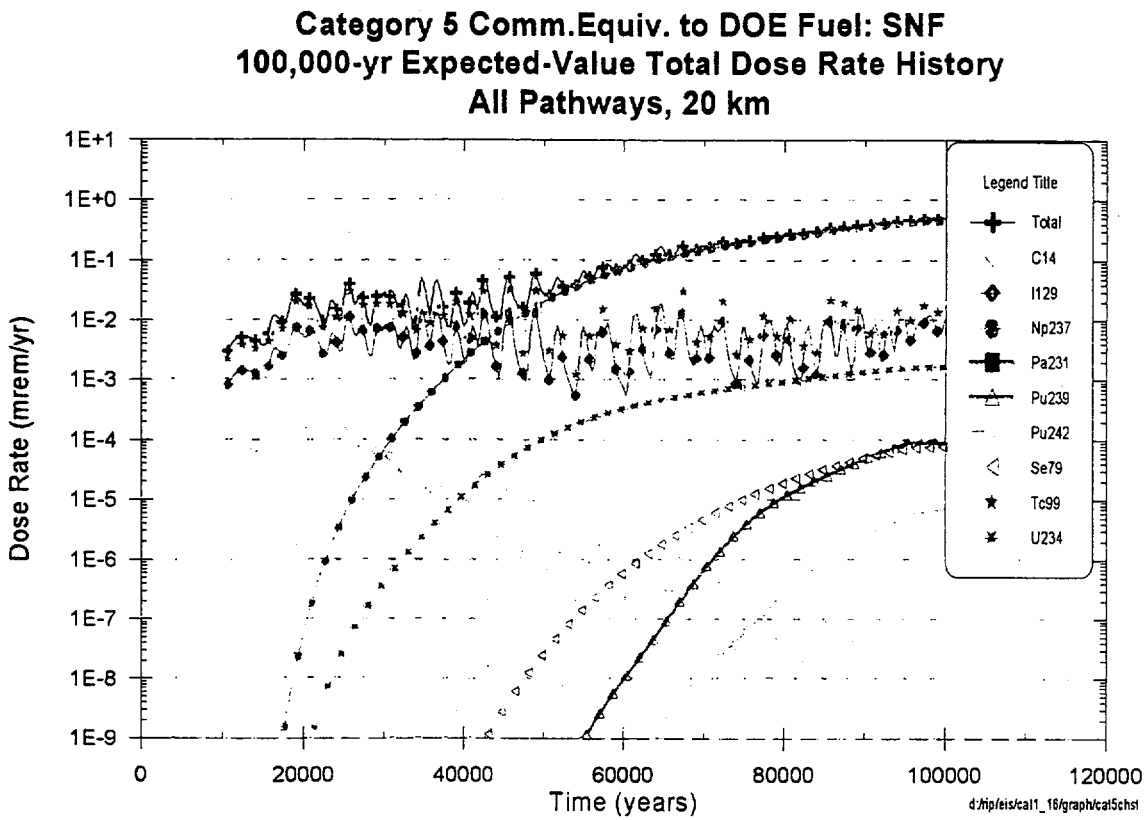

Figure 6A-13. Expected-Value Dose History at 20 Kilometers Over 100,000 Years from Commercial Spent Fuel Equivalent to Category 5 Spent Fuel.

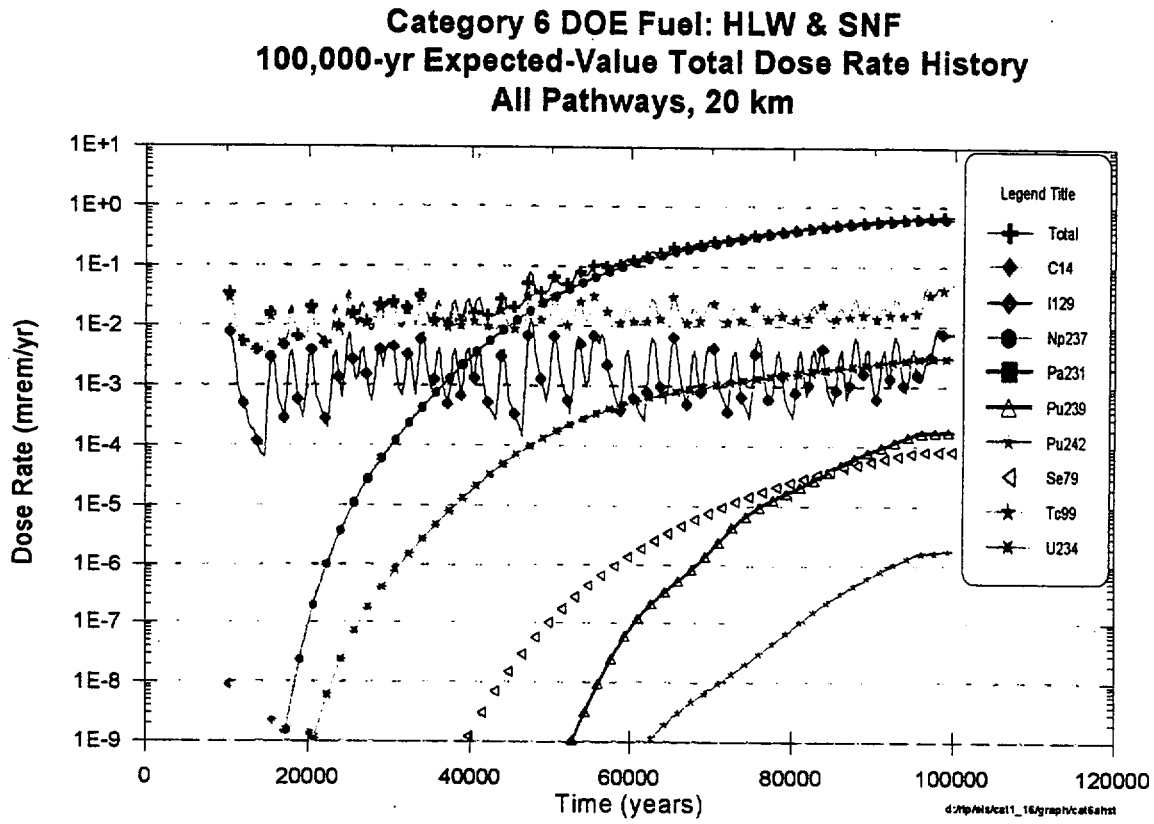

Figure 6A-14. Expected-Value Dose History at 20 Kilometers Over 100,000 Years from Category 6 Spent Fuel and HLW.

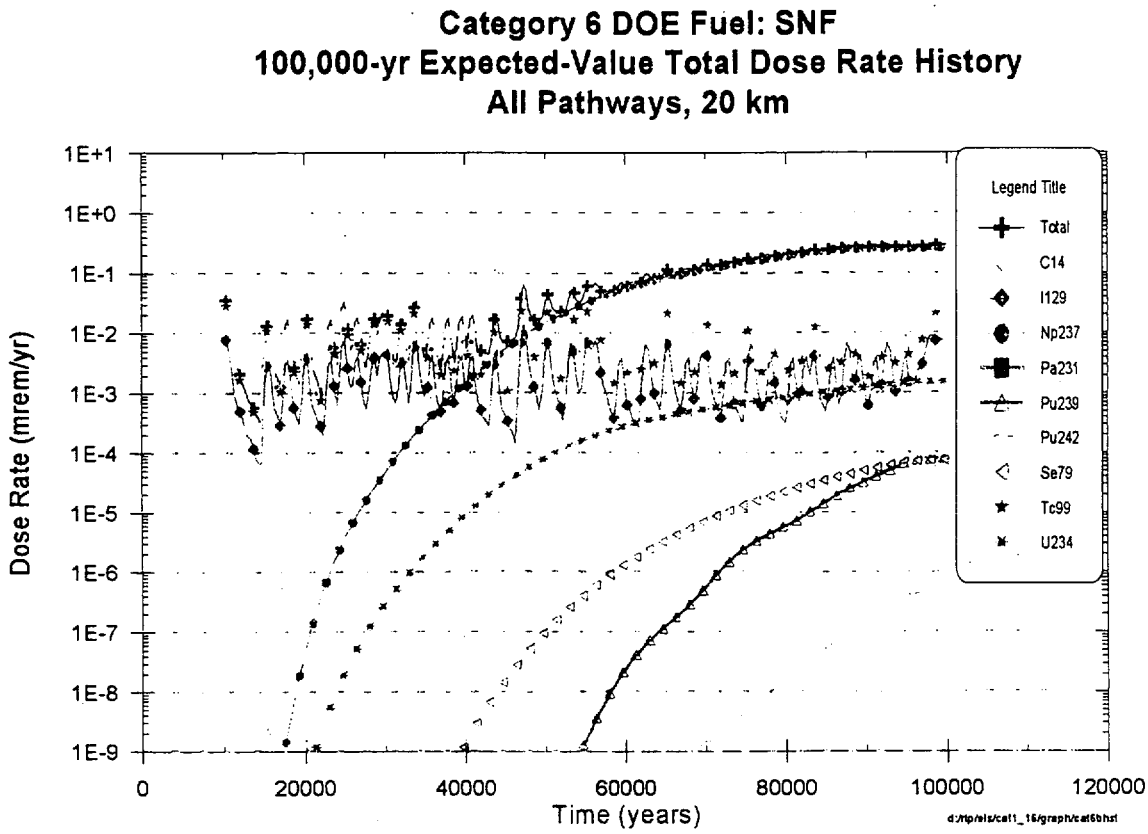

Figure 6A-15. Expected-Value Dose History at 20 Kilometers Over 100,000 Years from Category 6 Spent Fuel.

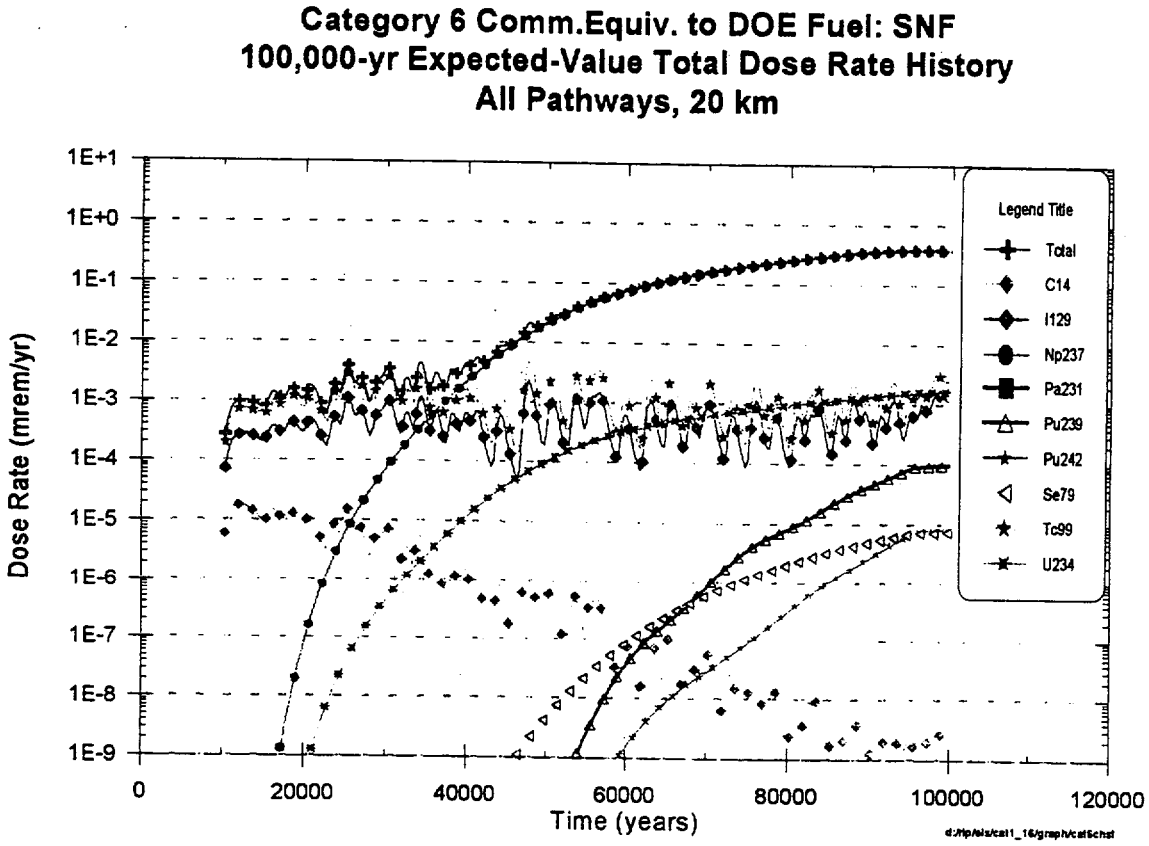

Figure 6A-16. Expected-Value Dose History at 20 Kilometers Over 100,000 Years from Commercial Spent Fuel Equivalent to Category 6 Spent Fuel.

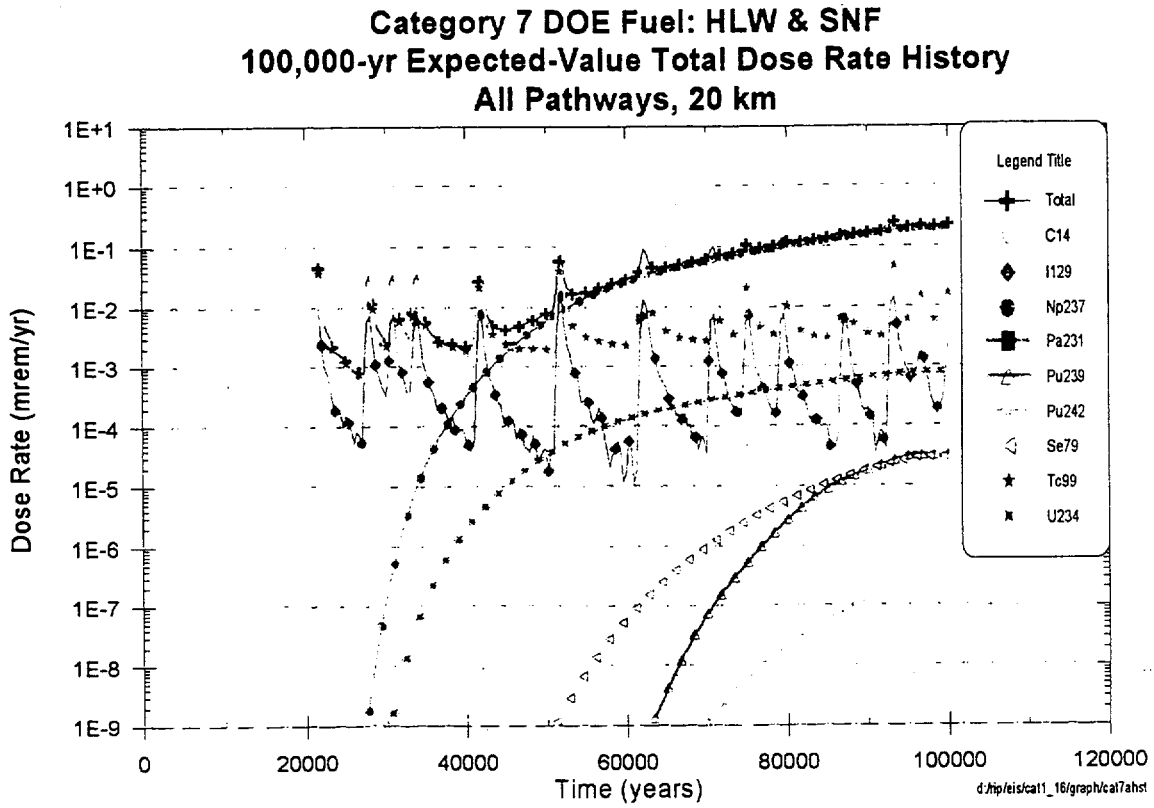

Figure 6A-17. Expected-Value Dose History at 20 Kilometers Over 100,000 Years from Category 7 Spent Fuel and HLW.

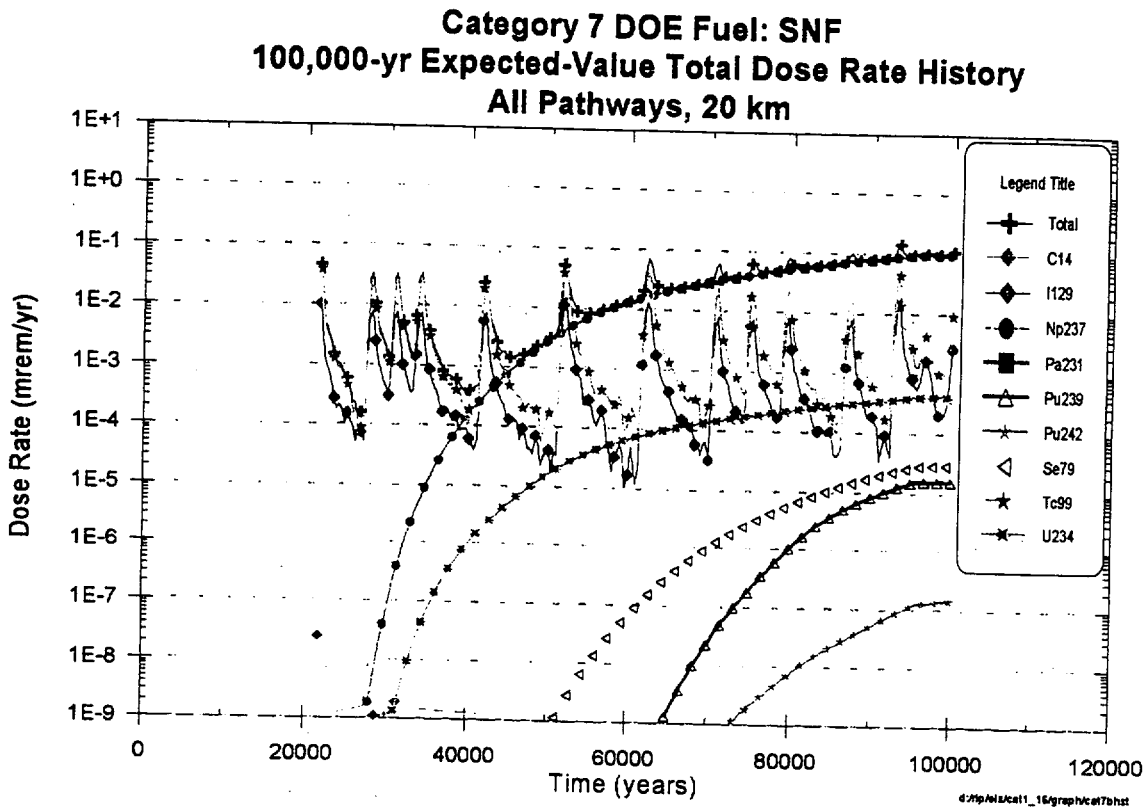

Figure 6A-18. Expected-Value Dose History at 20 Kilometers Over 100,000 Years from Category 7 Spent Fuel.

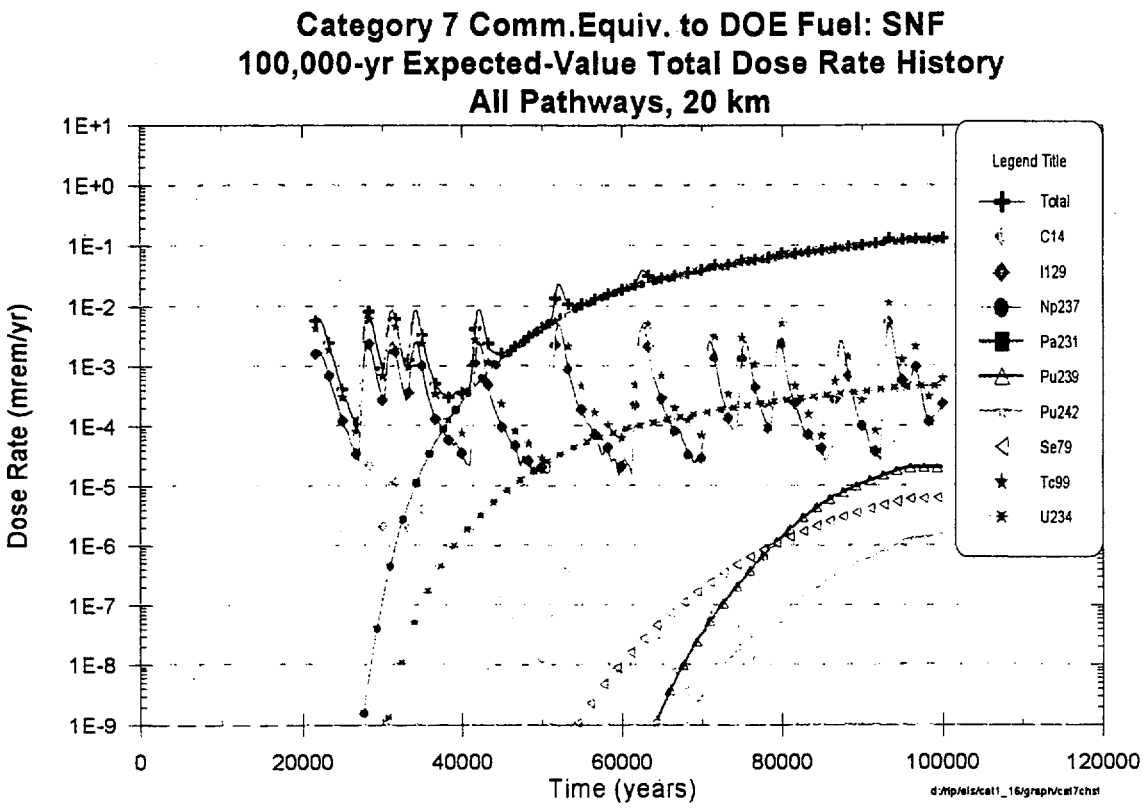

Figure 6A-19. Expected-Value Dose History at 20 Kilometers Over 100,000 Years from Commercial Spent Fuel Equivalent to Category 7 Spent Fuel.

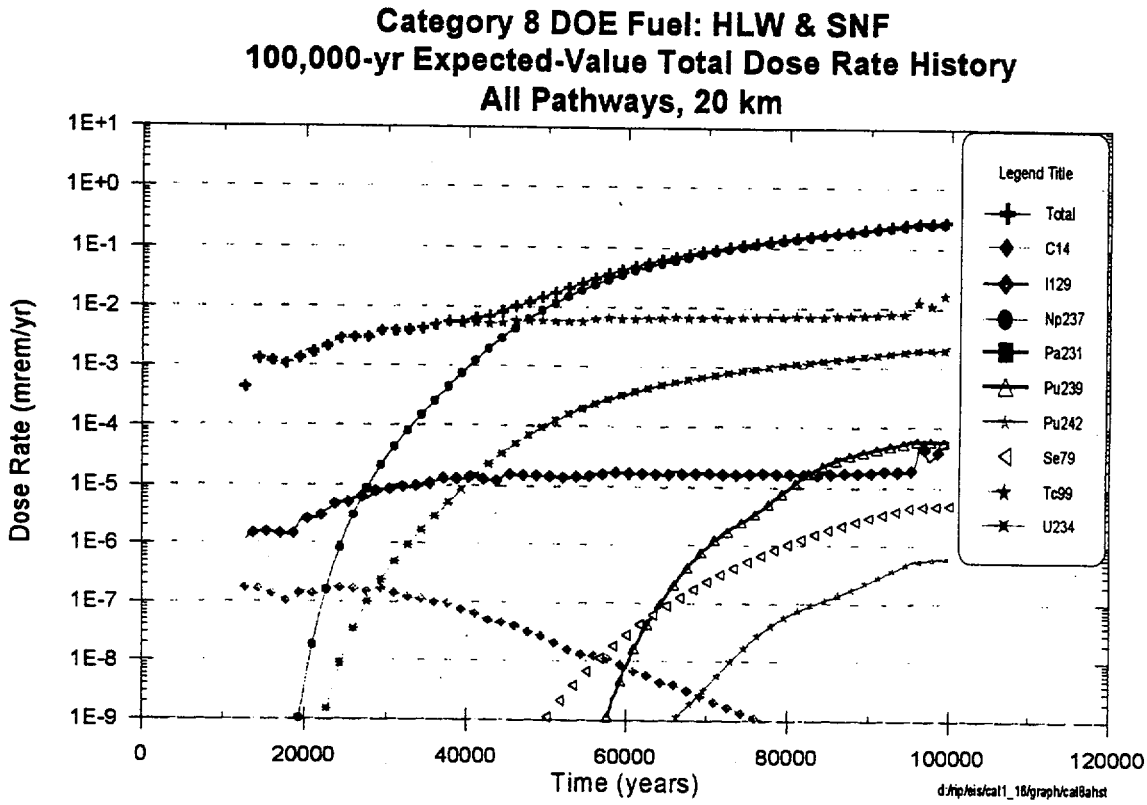

Figure 6A-20. Expected-Value Dose History at 20 Kilometers Over 100,000 Years from Category 8 Spent Fuel and HLW.

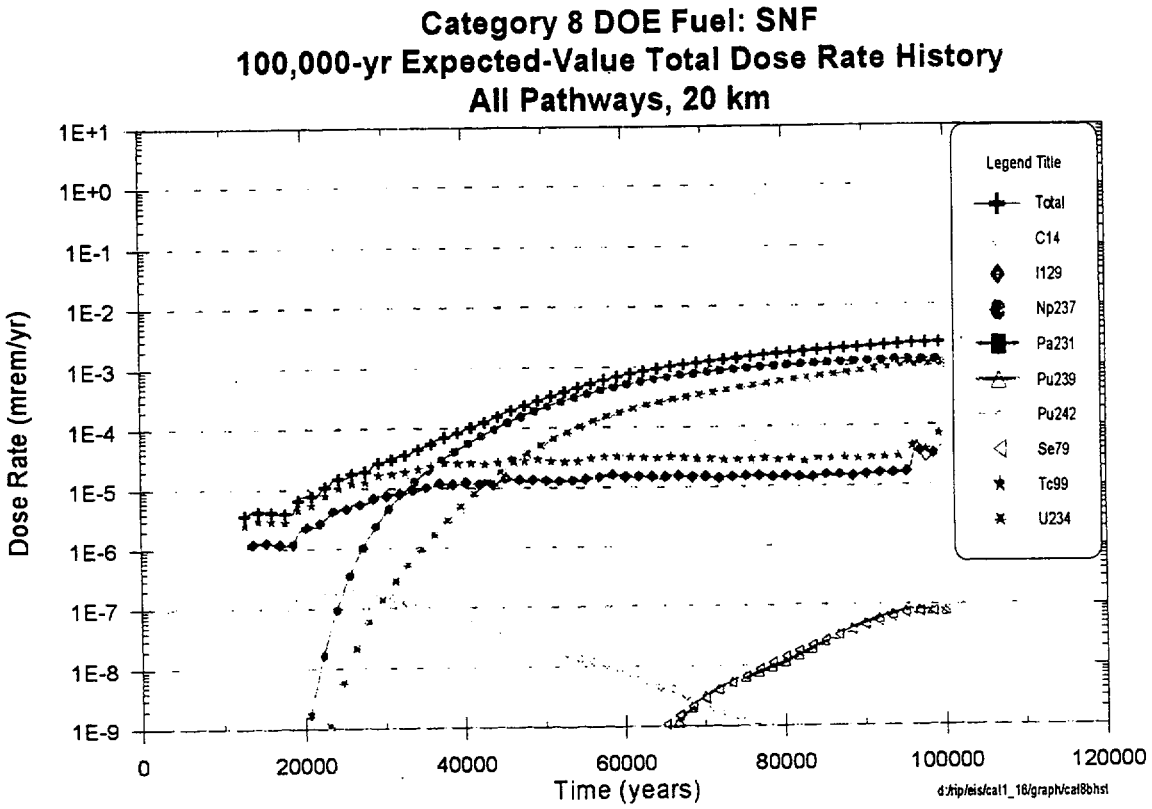

Figure 6A-21. Expected-Value Dose History at 20 Kilometers Over 100,000 Years from Category 8 Spent Fuel.

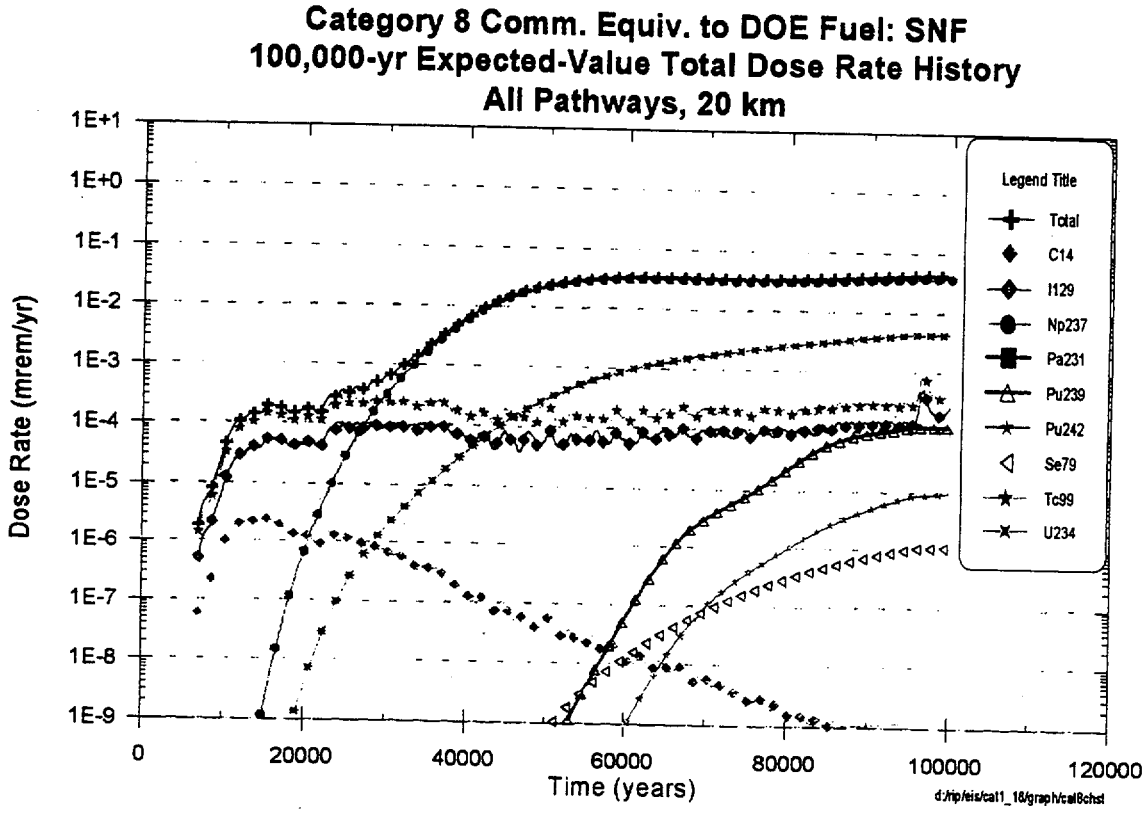

Figure 6A-22. Expected-Value Dose History at 20 Kilometers Over 100,000 Years from Commercial Spent Fuel Equivalent to Category 8 Spent Fuel.

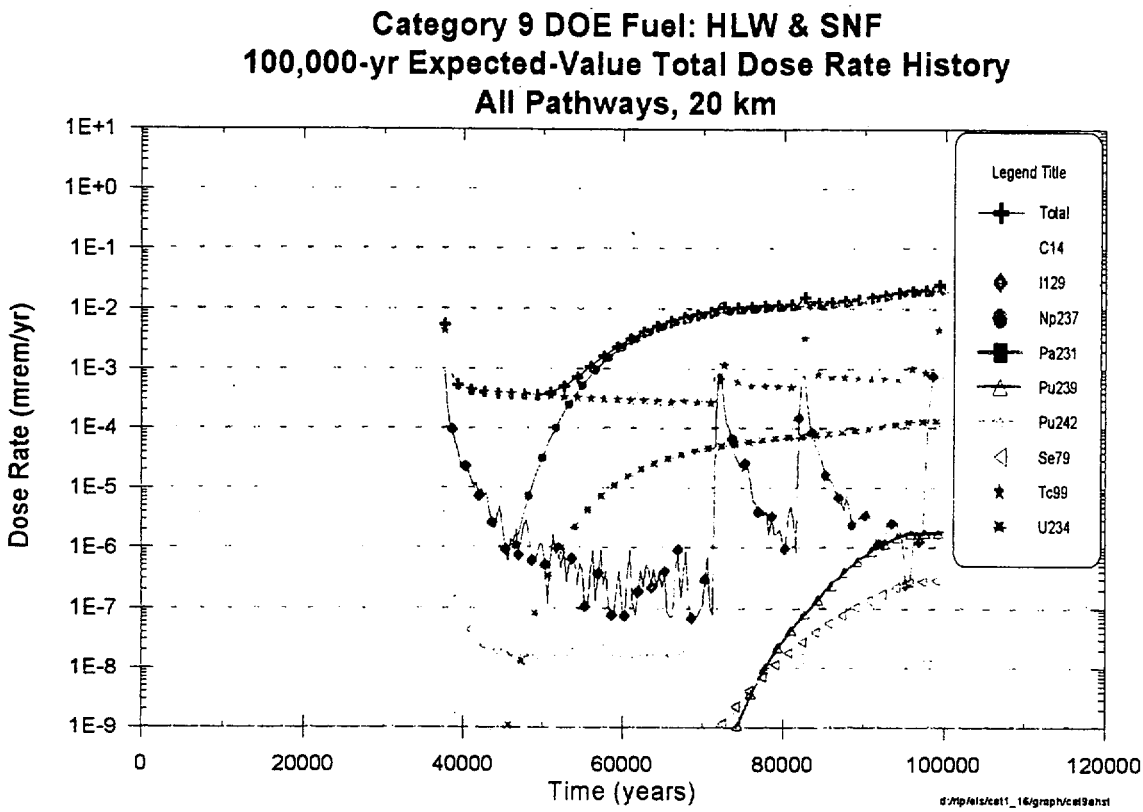

Figure 6A-23. Expected-Value Dose History at 20 Kilometers Over 100,000 Years from Category 9 Spent Fuel and HLW.

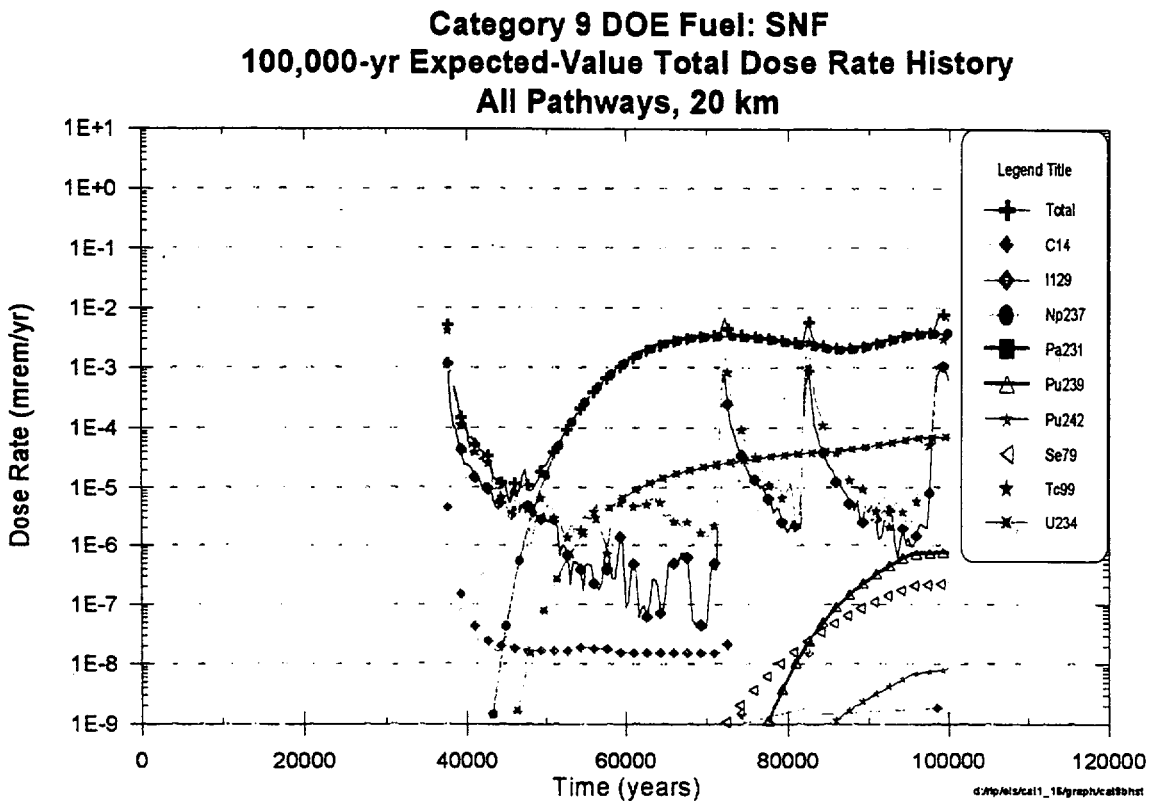

Figure 6A-24. Expected-Value Dose History at 20 Kilometers Over 100,000 Years from Category 9 Spent Fuel.

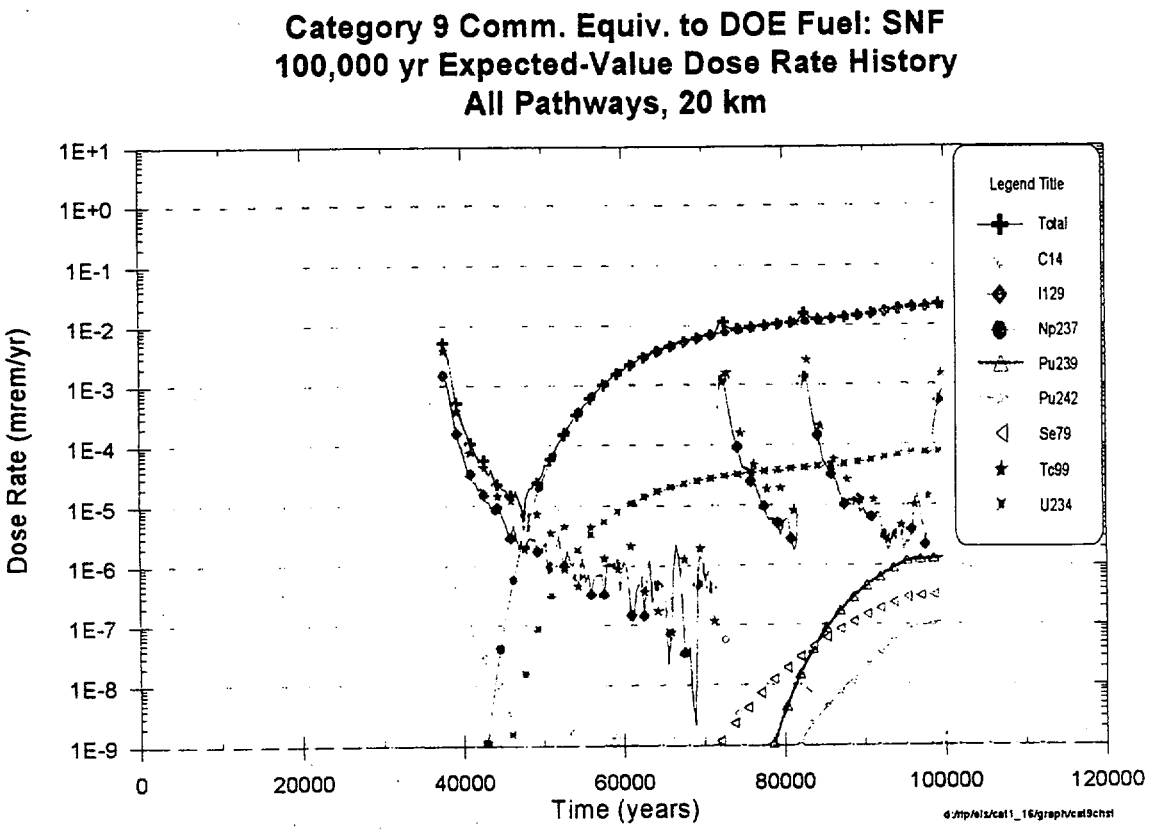

Figure 6A-25. Expected-Value Dose History at 20 Kilometers Over 100,000 Years from Commercial Spent Fuel Equivalent to Category 9 Spent Fuel.

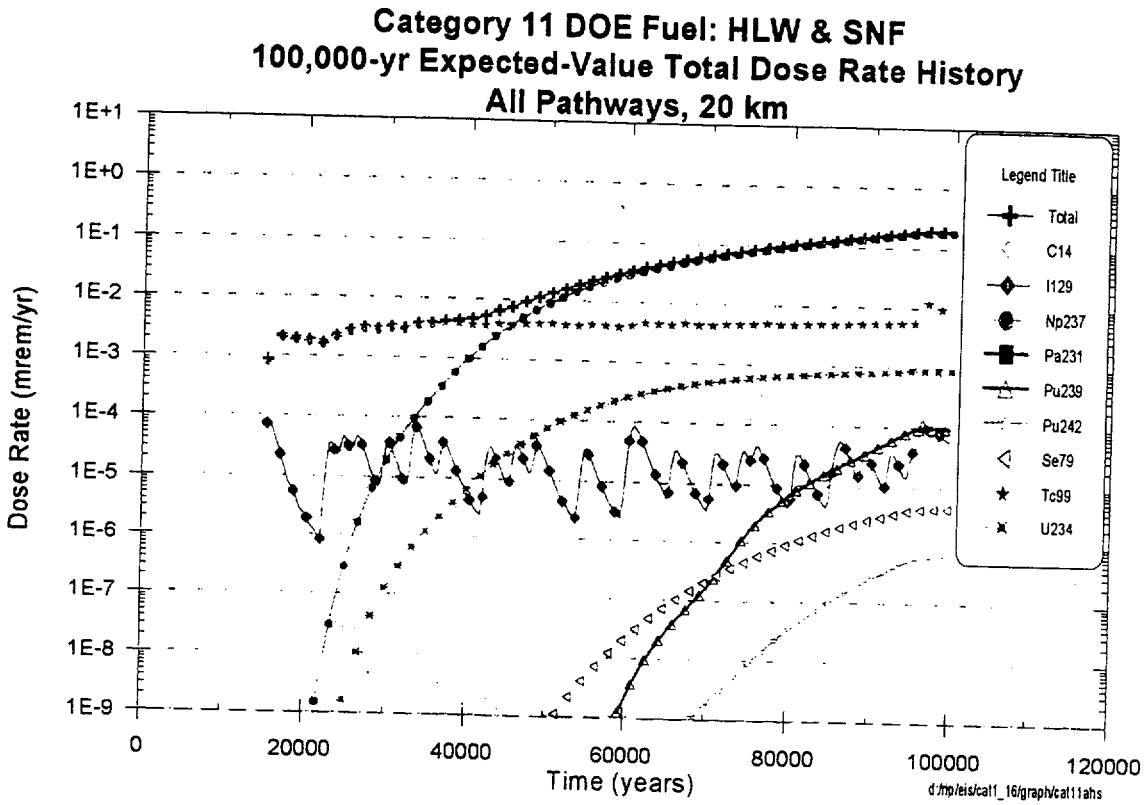

Figure 6A-26. Expected-Value Dose History at 20 Kilometers Over 100,000 Years from Category 11 Spent Fuel and HLW.

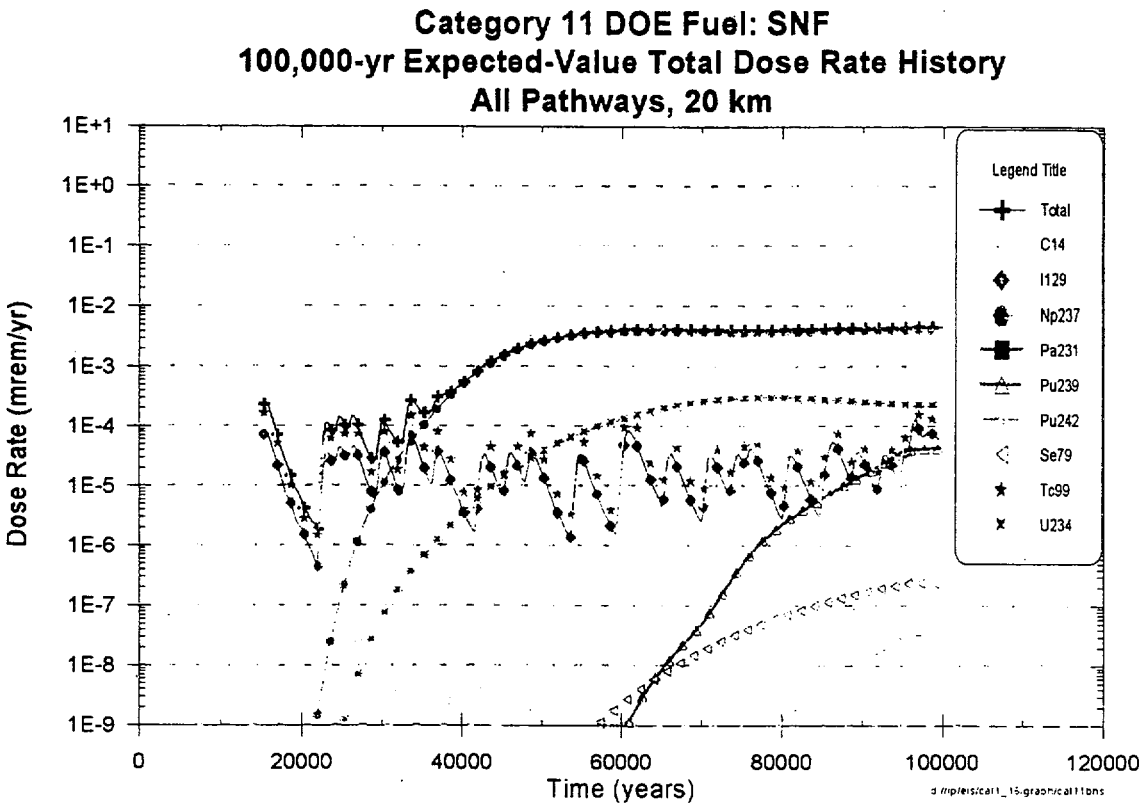

Figure 6A-27. Expected-Value Dose History at 20 Kilometers Over 100,000 Years from Category 11 Spent Fuel.

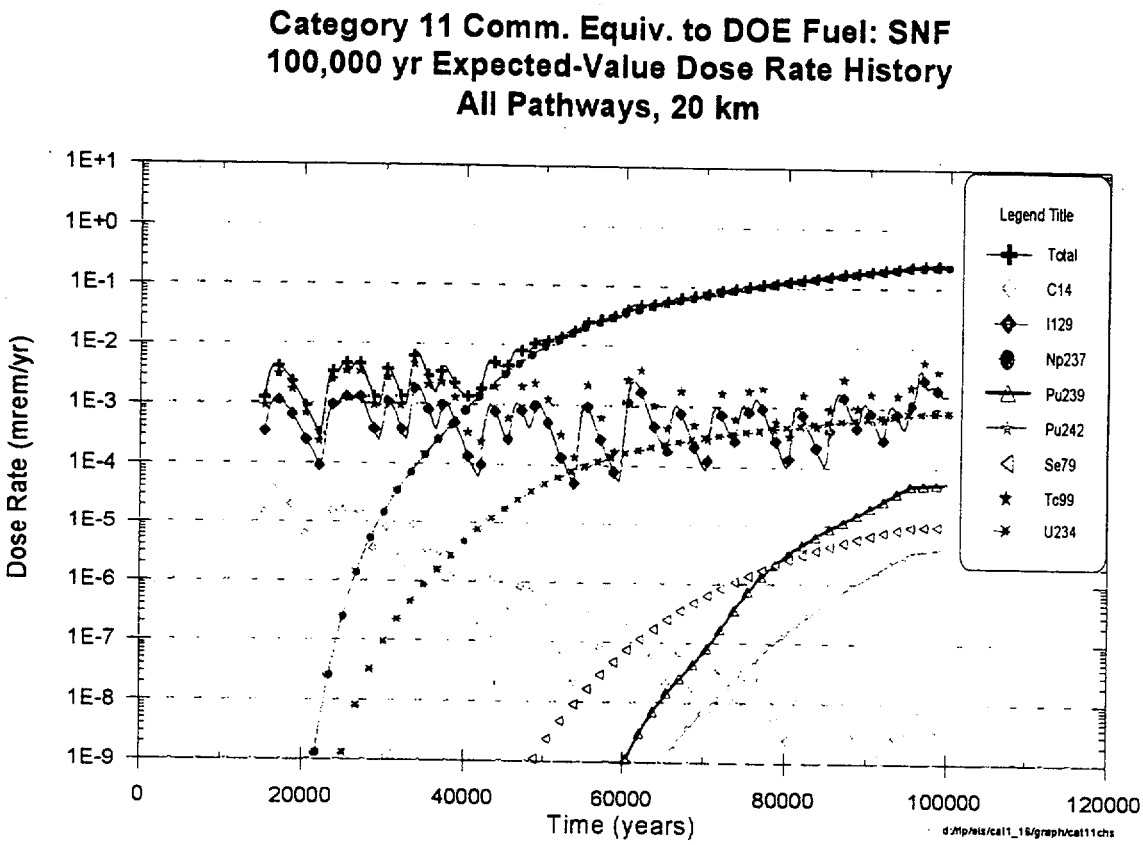

Figure 6A-28. Expected-Value Dose History at 20 Kilometers Over 100,000 Years from Commercial Spent Fuel Equivalent to Category 11 Spent Fuel.

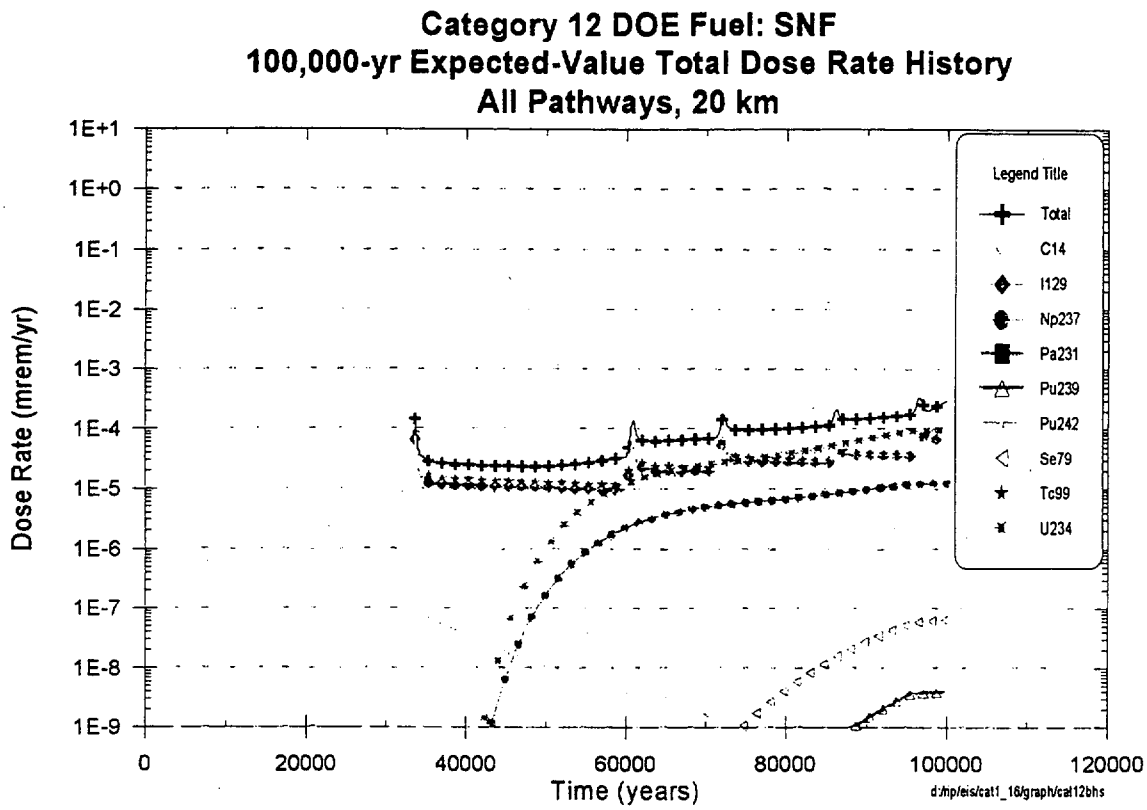

Figure 6A-29. Expected-Value Dose History at 20 Kilometers Over 100,000 Years from Category 12 Spent Fuel and HLW.

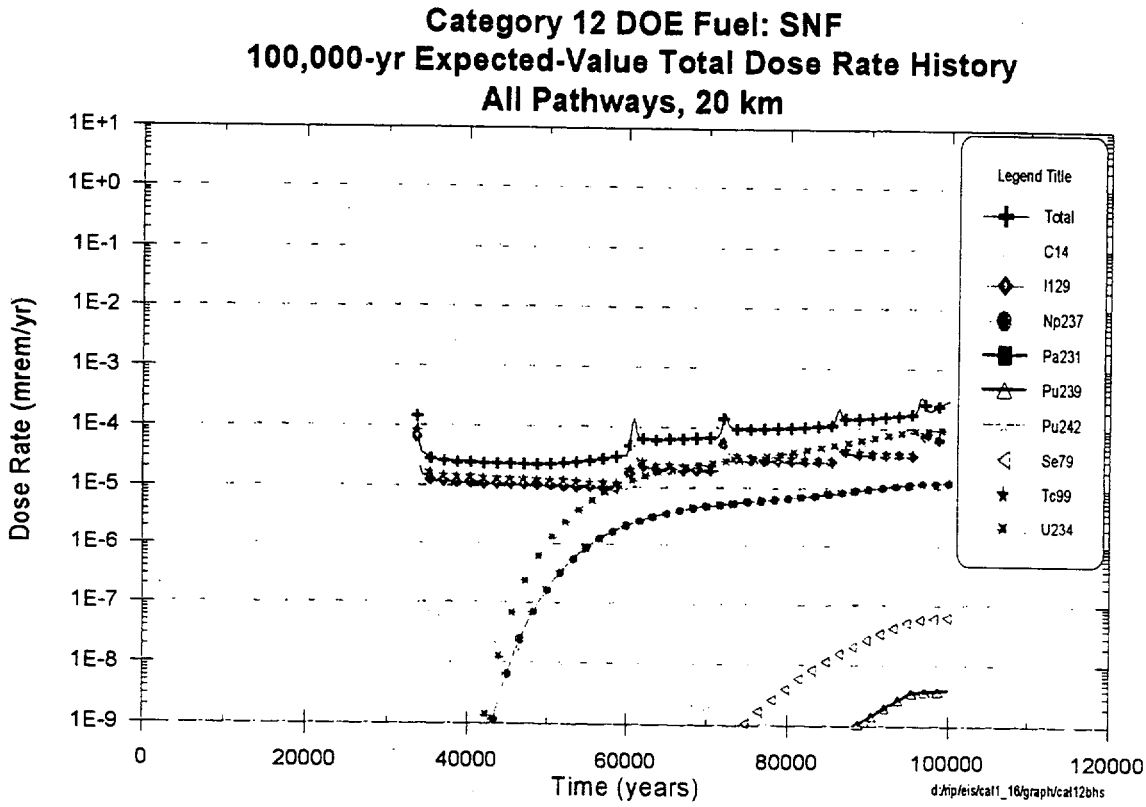

Figure 6A-30. Expected-Value Dose History at 20 Kilometers Over 100,000 Years from Category 12 Spent Fuel.

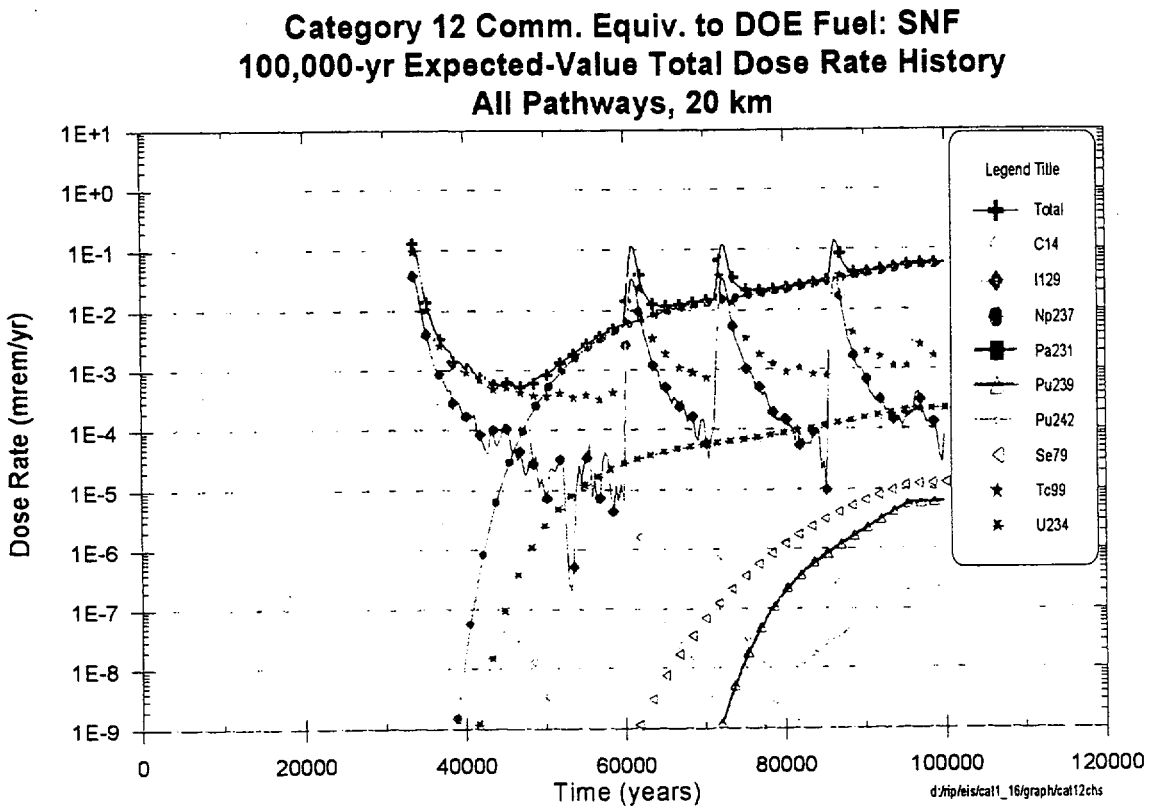

Figure 6A-31. Expected-Value Dose History at 20 Kilometers Over 100,000 Years from Commercial Spent Fuel Equivalent to Category 12 Spent Fuel.

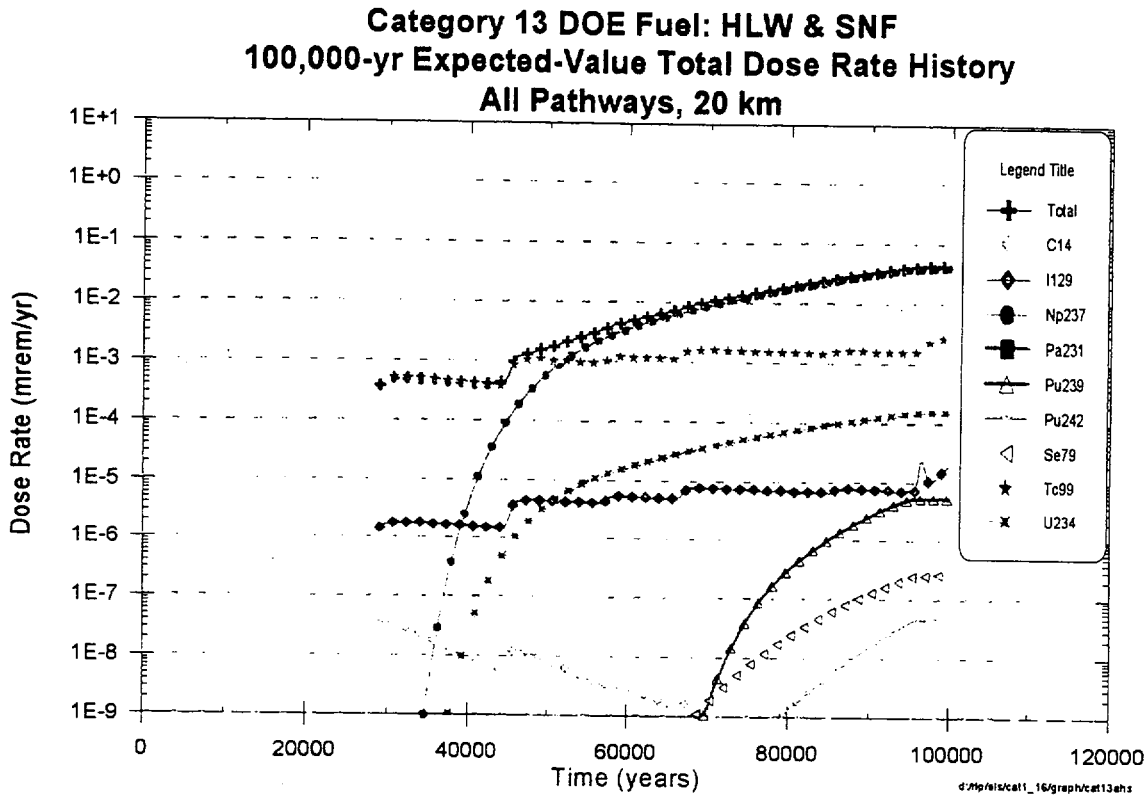

Figure 6A-32. Expected-Value Dose History at 20 Kilometers Over 100,000 Years from Category 13 Spent Fuel and HLW.

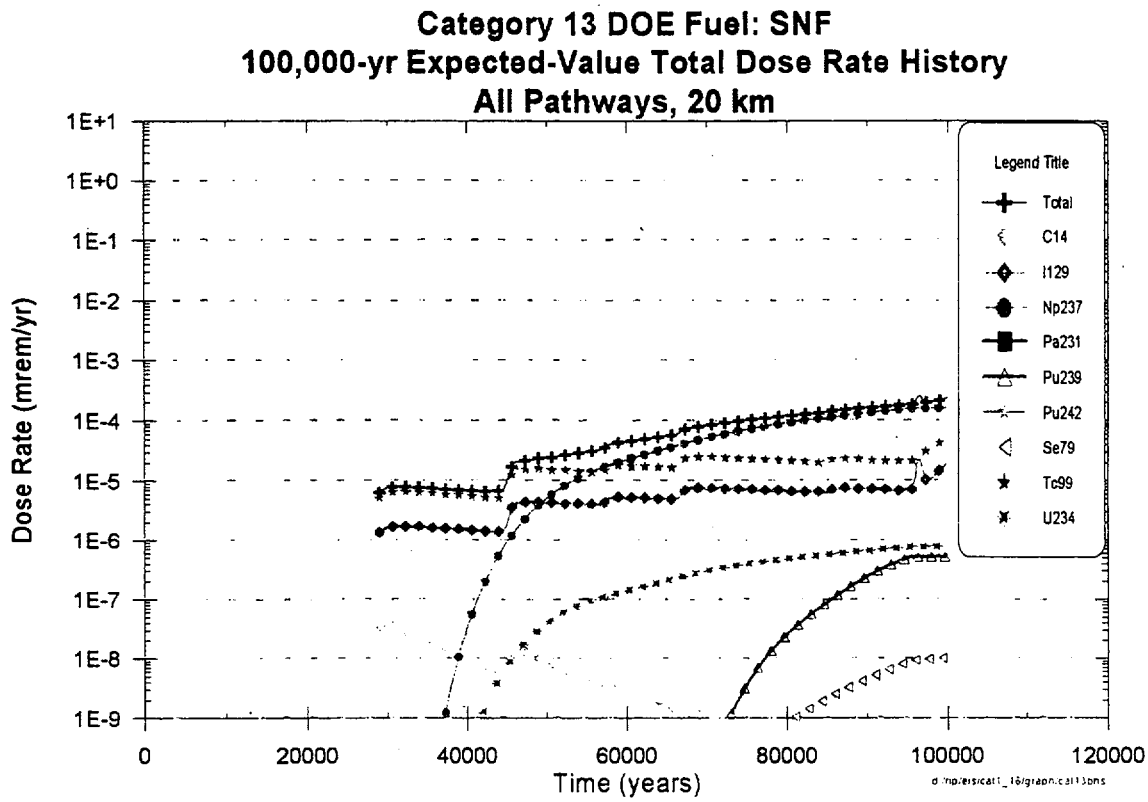

Figure 6A-33. Expected-Value Dose History at 20 Kilometers Over 100,000 Years from Category 13 Spent Fuel.

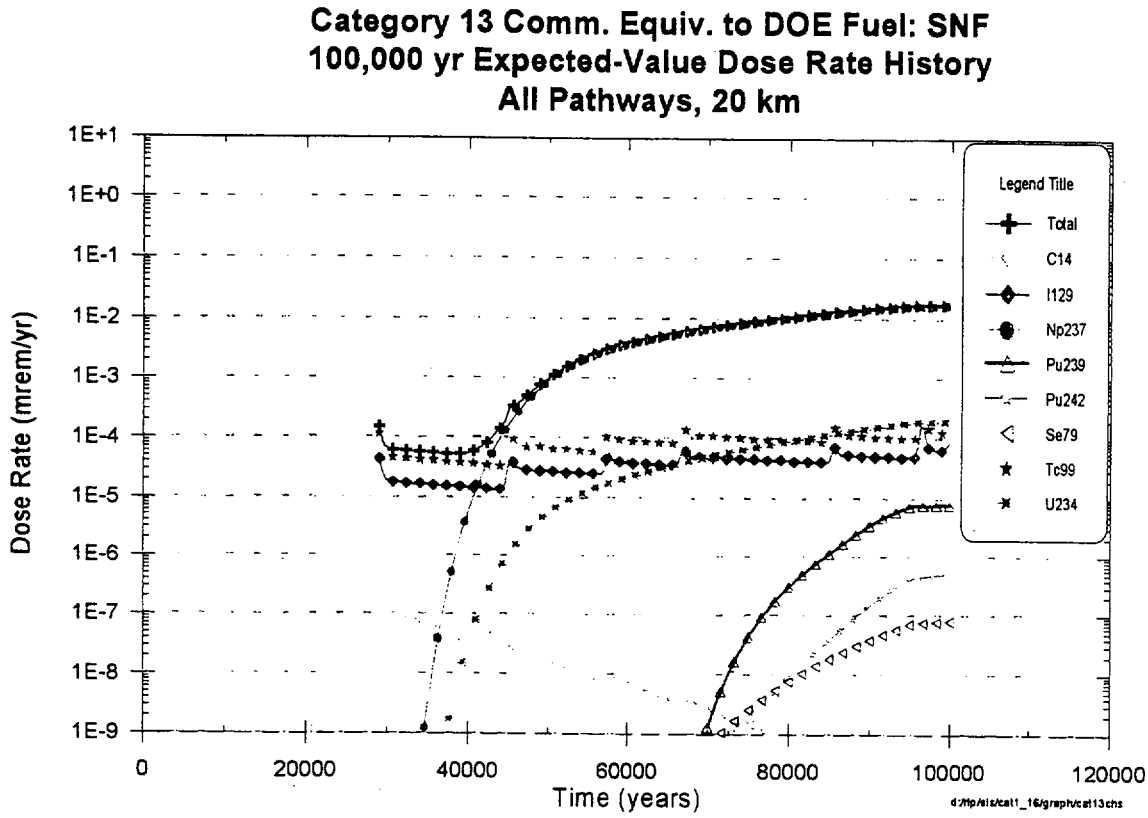

Figure 6A-34. Expected-Value Dose History at 20 Kilometers Over 100,000 Years from Commercial Spent Fuel Equivalent to Category 13 Spent Fuel.

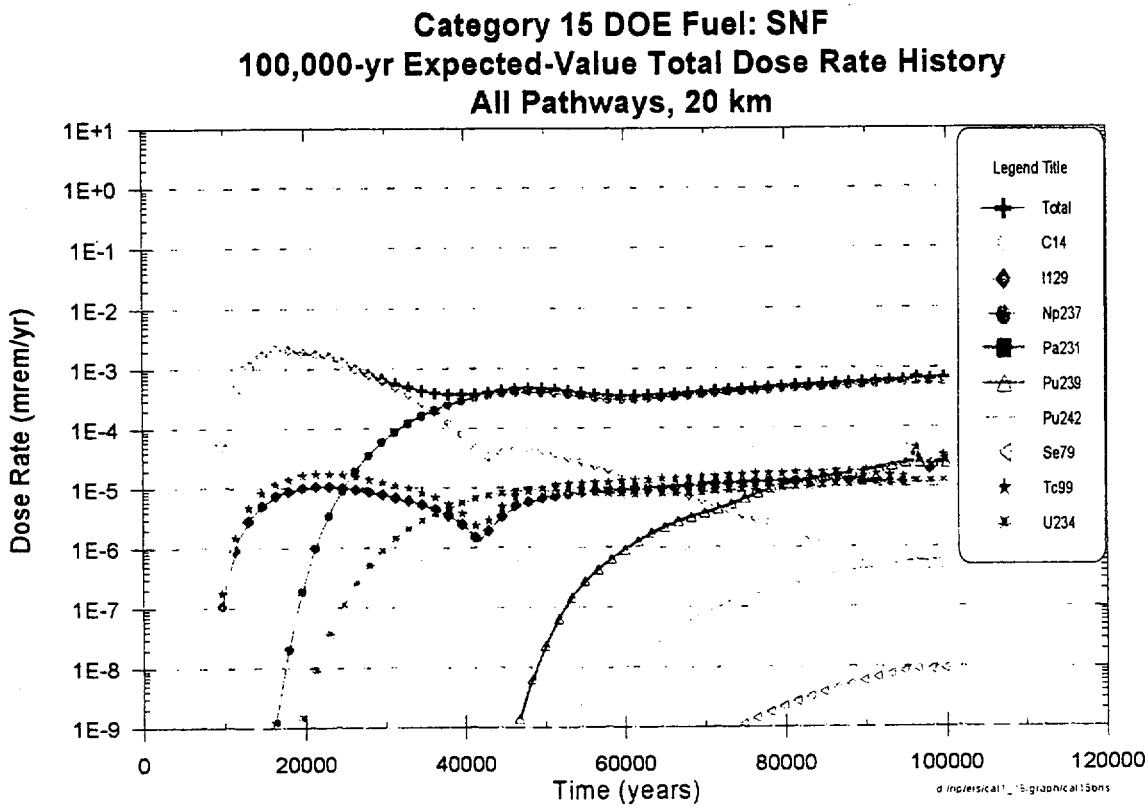

Figure 6A-35. Expected-Value Dose History at 20 Kilometers Over 100,000 Years from Category 15 Spent Fuel.

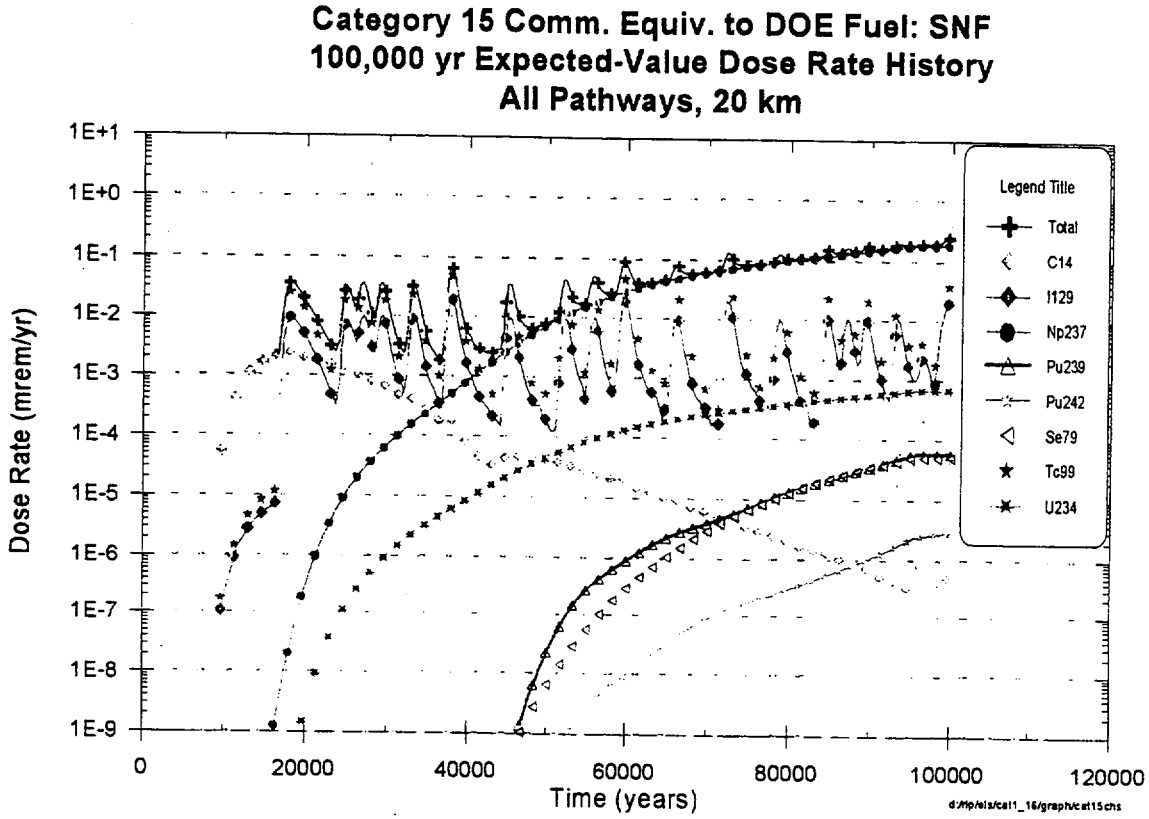

Figure 6A-36. Expected-Value Dose History at 20 Kilometers Over 100,000 Years from Commercial Spent Fuel Equivalent to Category 15 Spent Fuel.

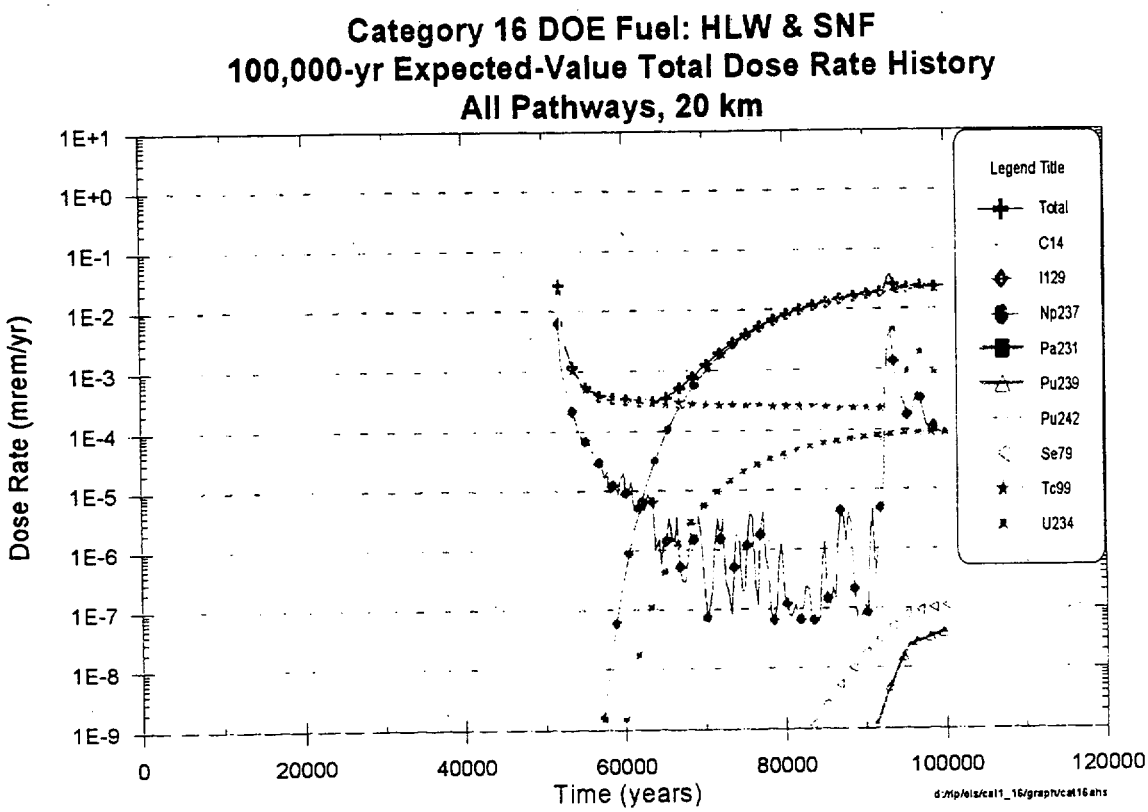

Figure 6A-37. Expected-Value Dose History at 20 Kilometers Over 100,000 Years from Category 16 Spent Fuel and HLW.

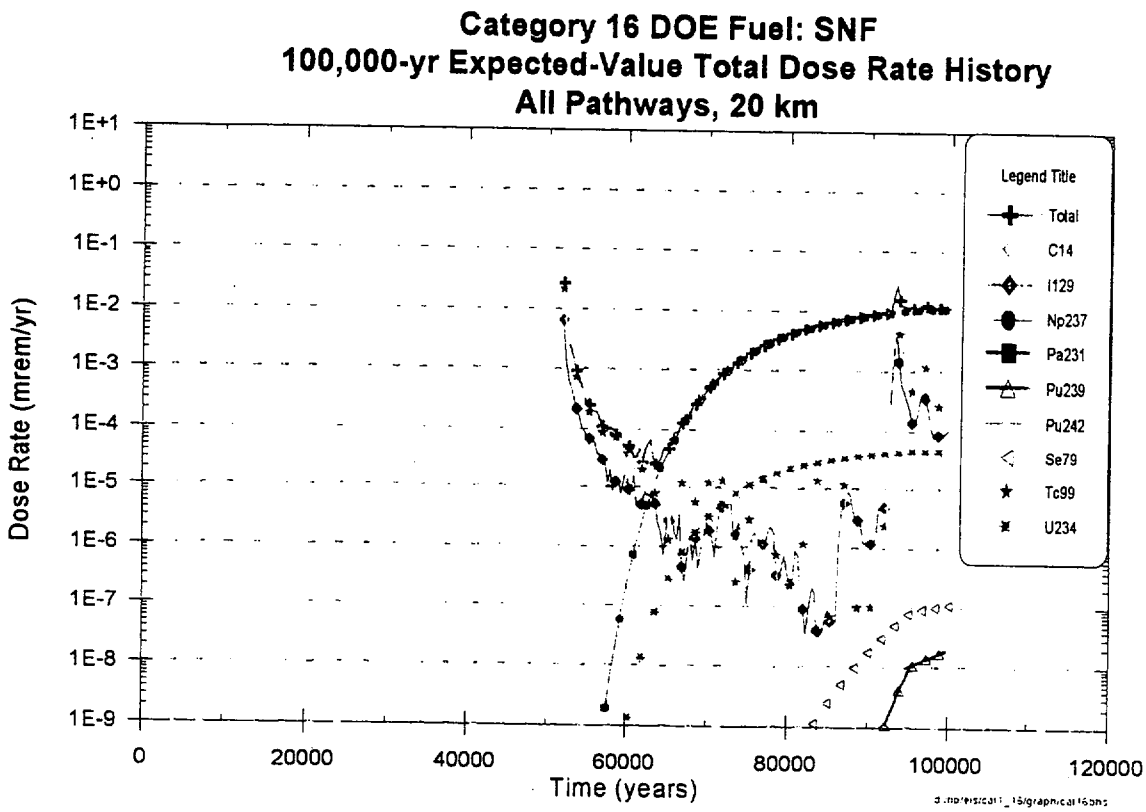

Figure 6A-38. Expected-Value Dose History at 20 Kilometers Over 100,000 Years from Category 16 Spent Fuel.

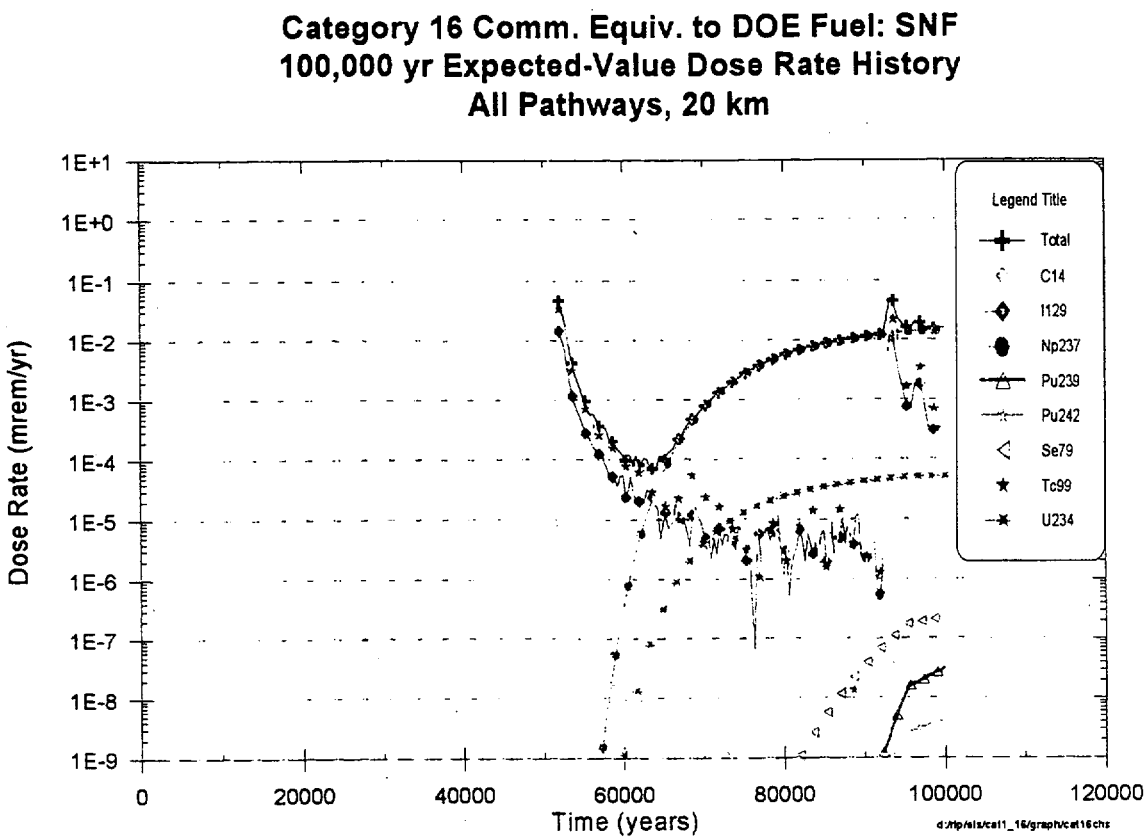

Figure 6A-39. Expected-Value Dose History at 20 Kilometers Over 100,000 Years from Commercial Spent Fuel Equivalent to Category 16 Spent Fuel.

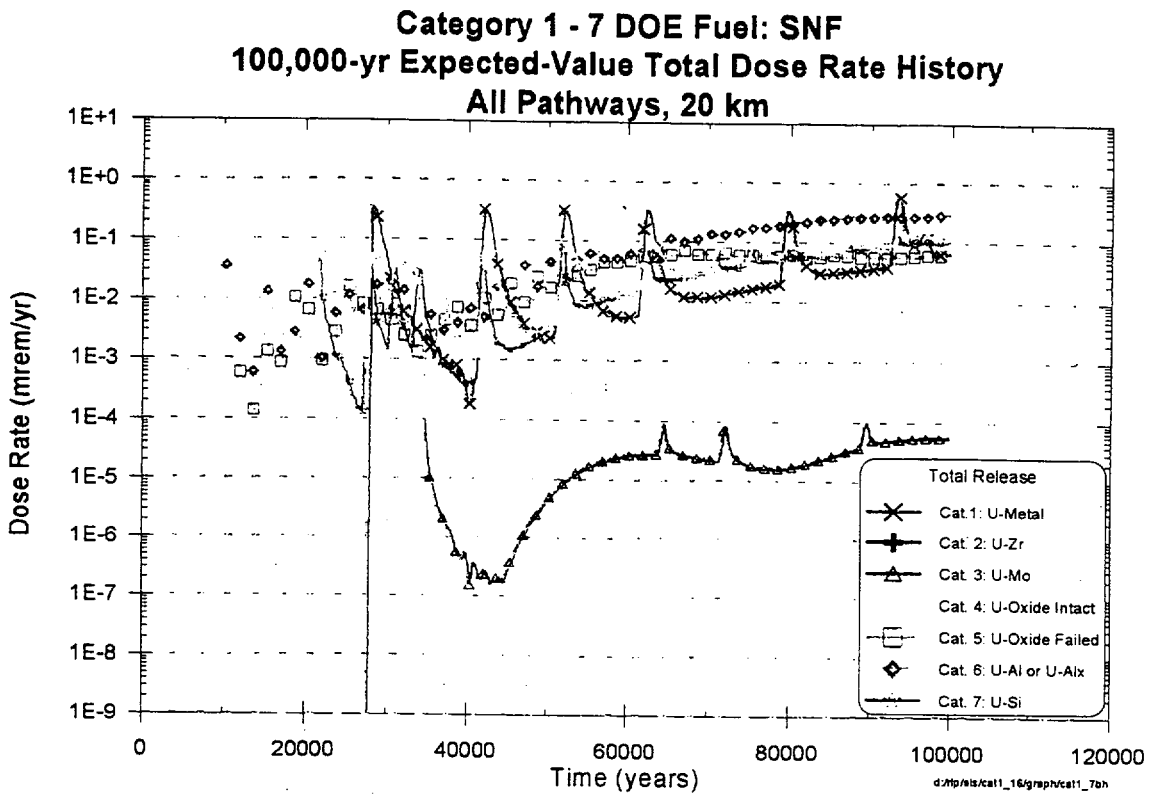

Figure 6A-40. Expected-Value Total Dose History at 20 Kilometers Over 100,000 Years from all of Categories 1 through 7 DOE SNF.

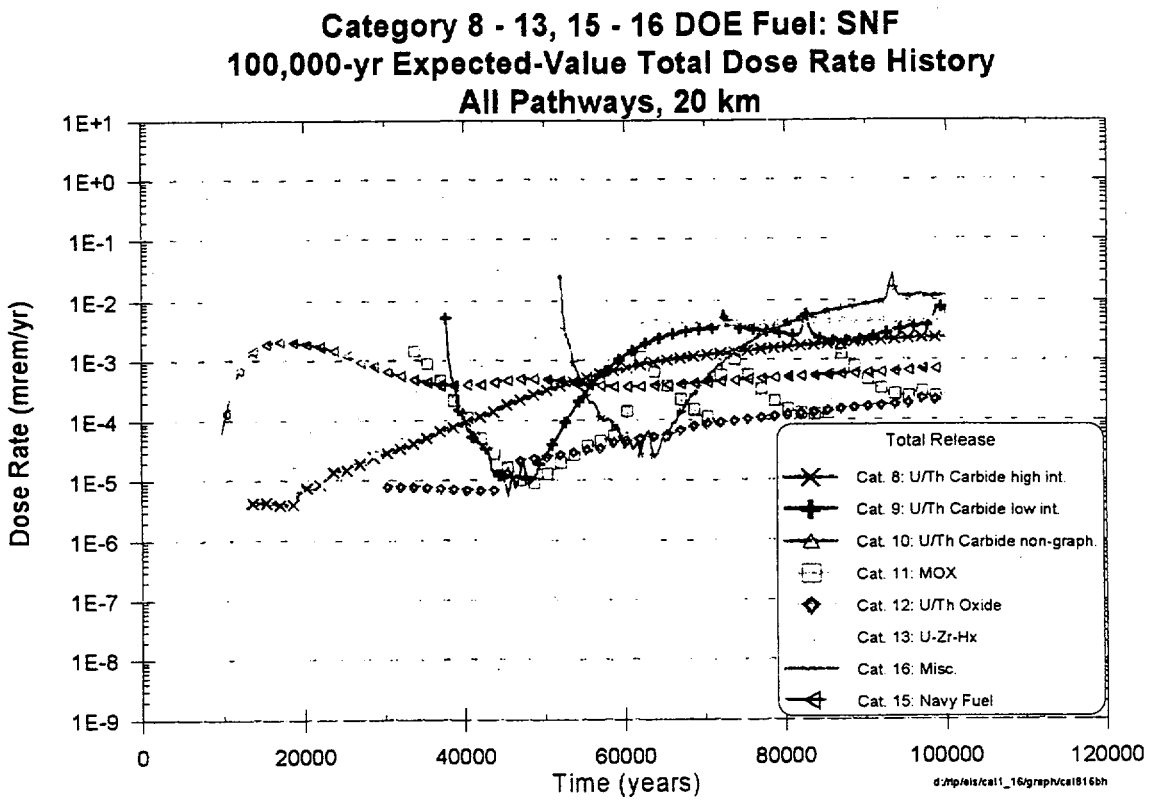

Figure 6A-41. Expected-Value Total Dose History at 20 Kilometers Over 100,000 Years from all of Categories 8 through 13, 15, and 16 DOE SNF.

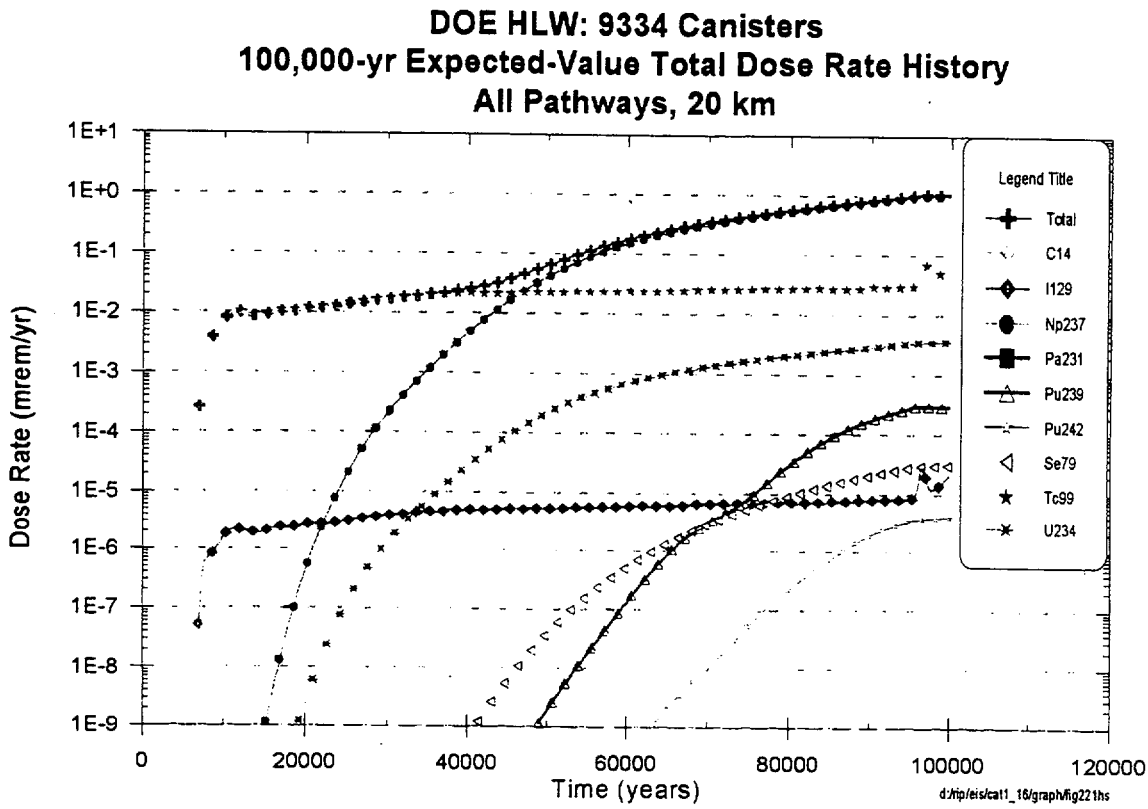

Figure 6A-42. Expected-Value Dose History at 20 Kilometers Over 100,000 Years from 9,334 Canisters of HLW.

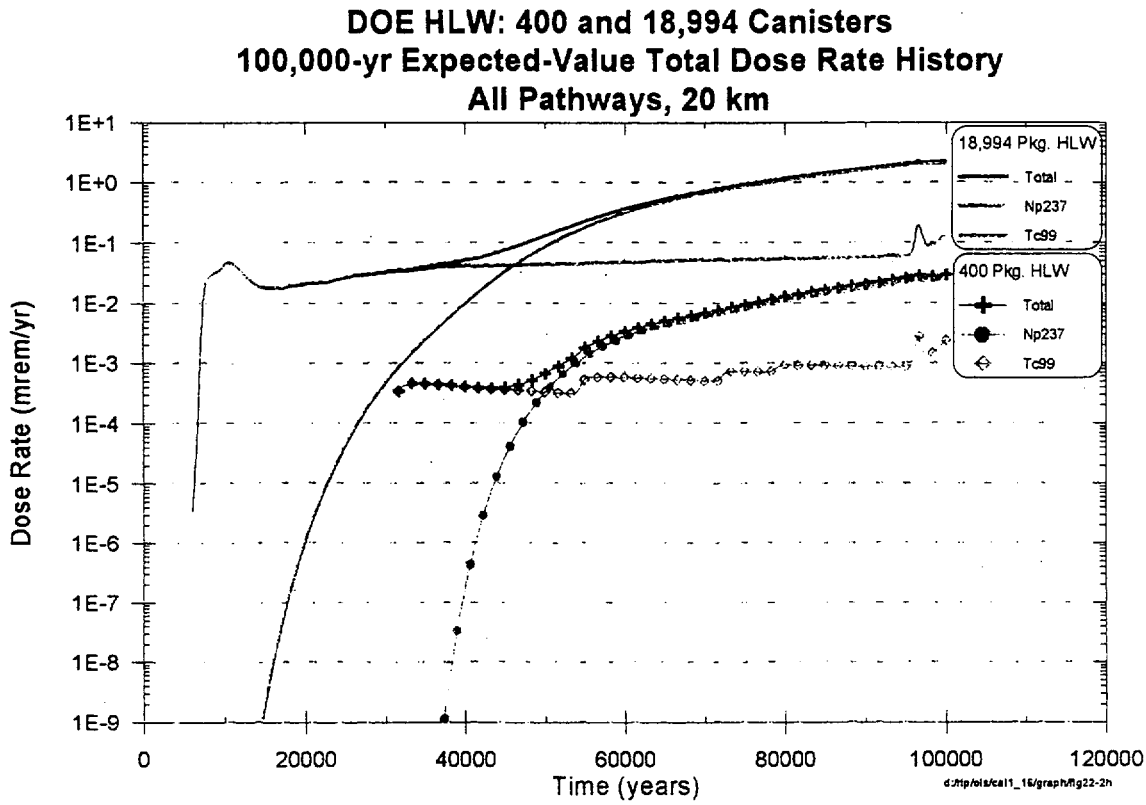

Figure 6A-43. Expected-Value Dose History at 20 Kilometers Over 100,000 Years from 400 and 18,994 Canisters of HLW.

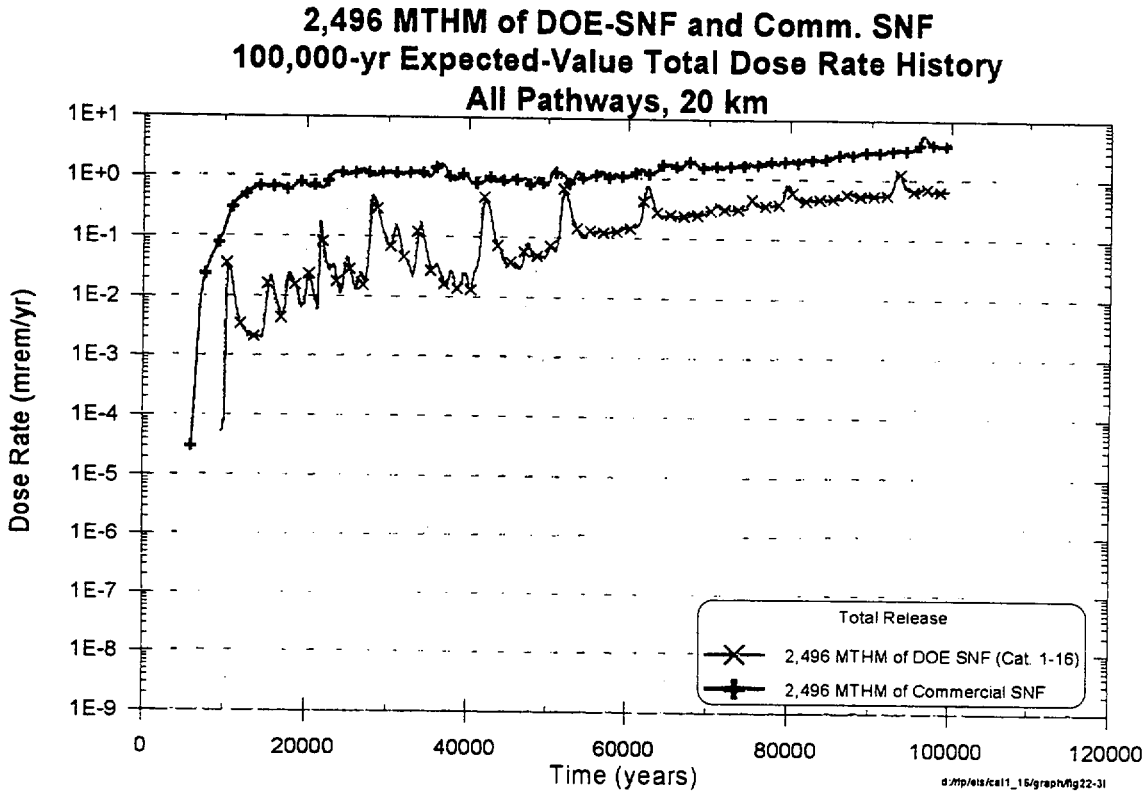

Figure 6A-44. Expected-Value Dose History at 20 Kilometers Over 100,000 Years from 2,496 MTHM of DOE SNF and from 2,496 MTHM of Commercial Spent Fuel.

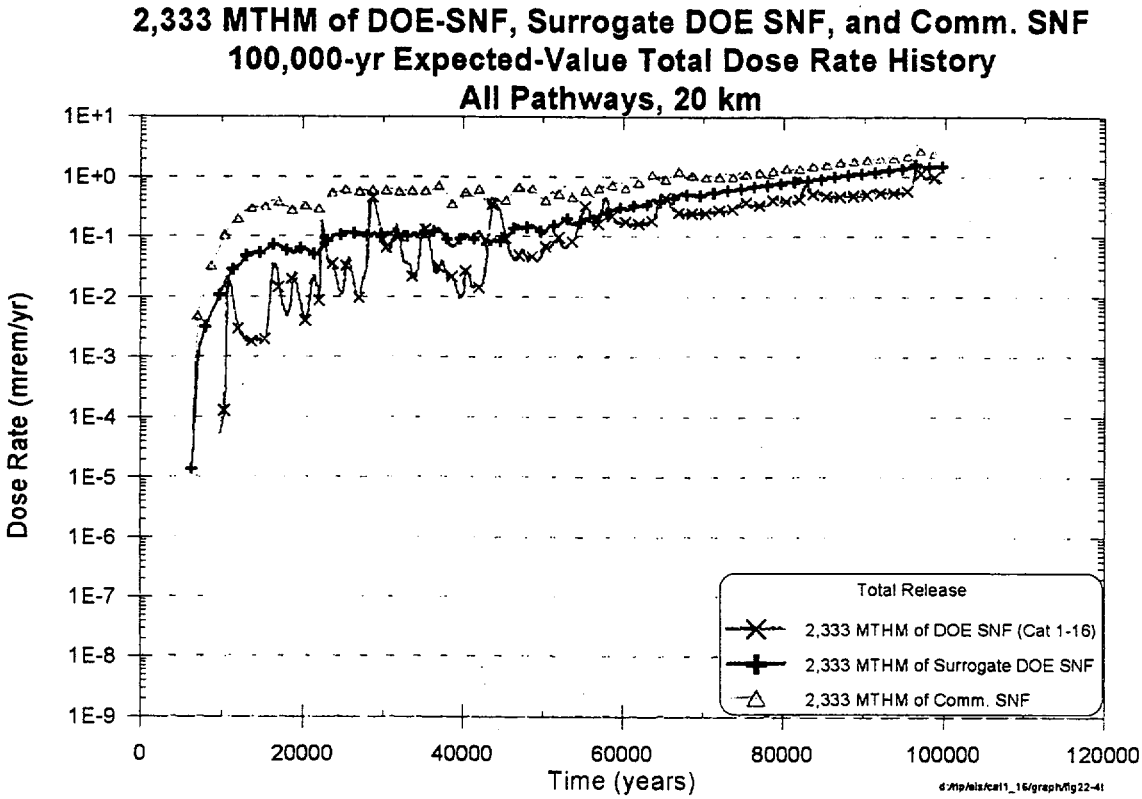

Figure 6A-45. Expected-Value Dose History at 20 Kilometers Over 100,000 Years from 2,333 MTHM of DOE SNF, from 2,333 MTHM of the Surrogate DOE SNF used in the Base case, and from 2,333 MTHM of Commercial Spent Fuel.

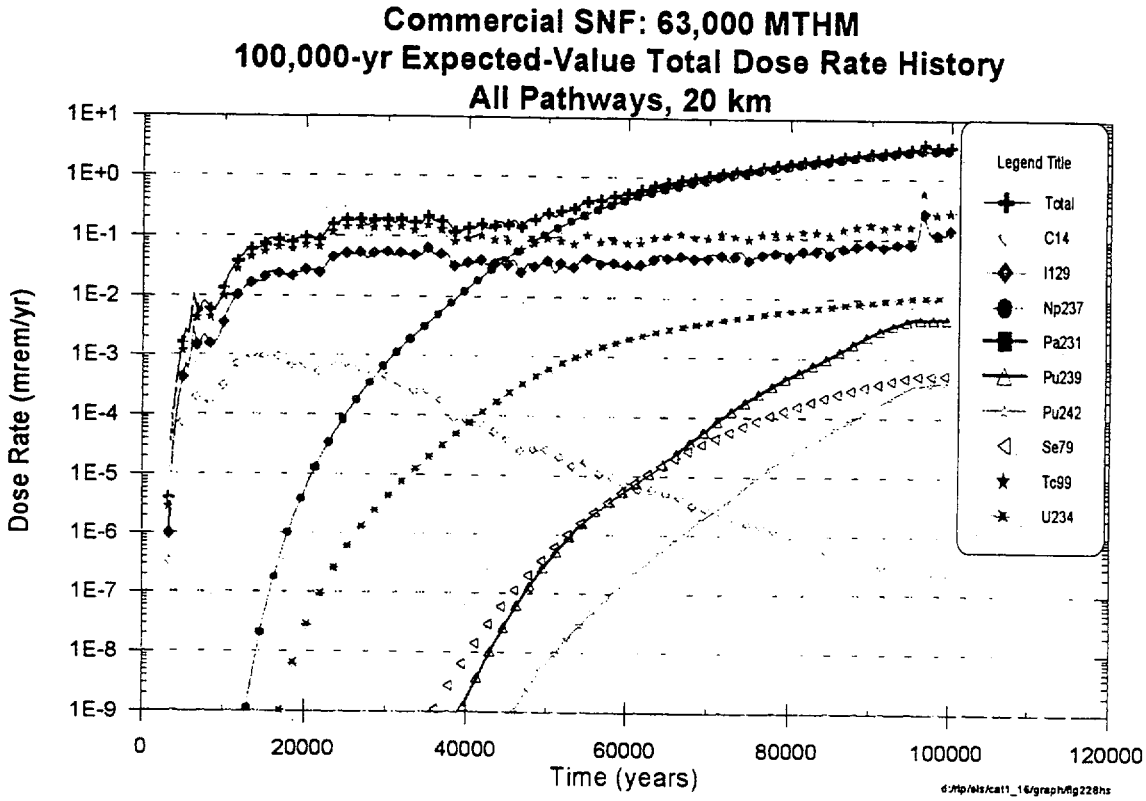

Figure 6A-46. Expected-Value Dose History at 20 Kilometers Over 100,000 Years from 63,000 MTHM of Commercial Spent Fuel.

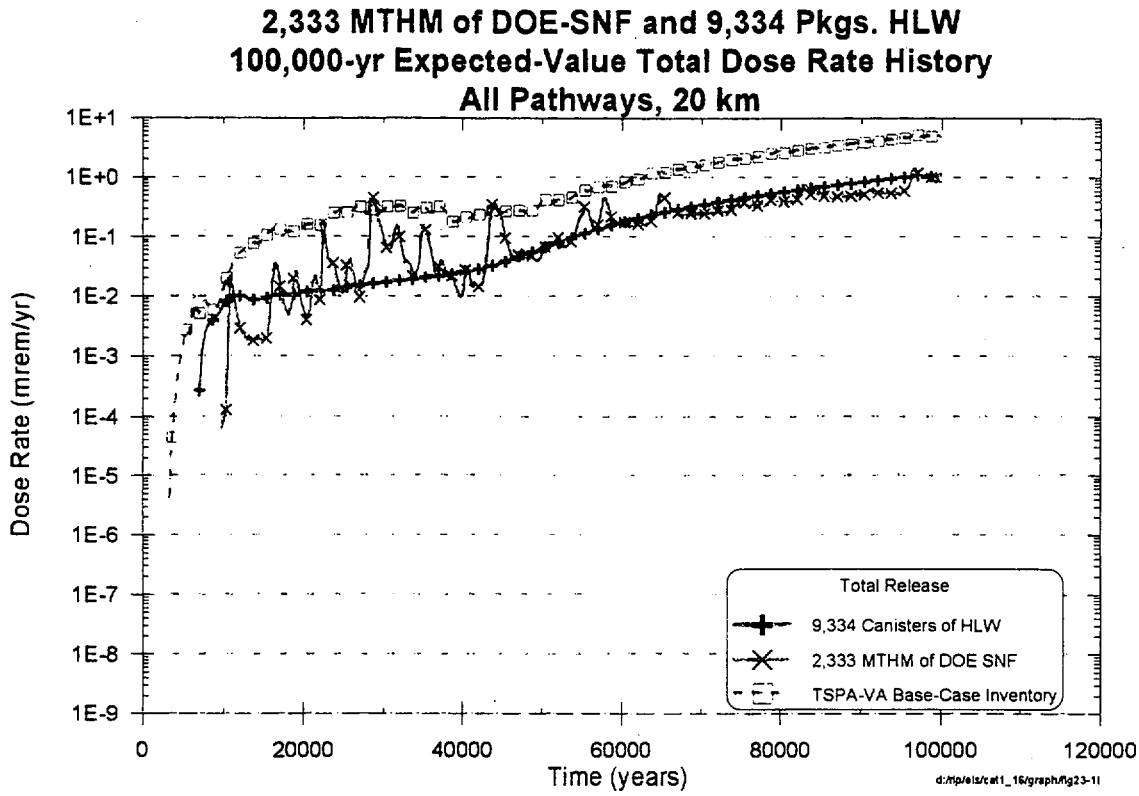

Figure 6A-47. Expected-Value Total Dose History at 20 Kilometers Over 100,000 Years from the Base Case Repository, 2,333 MTHM of DOE SNF, and 9,334 Canisters of HLW.

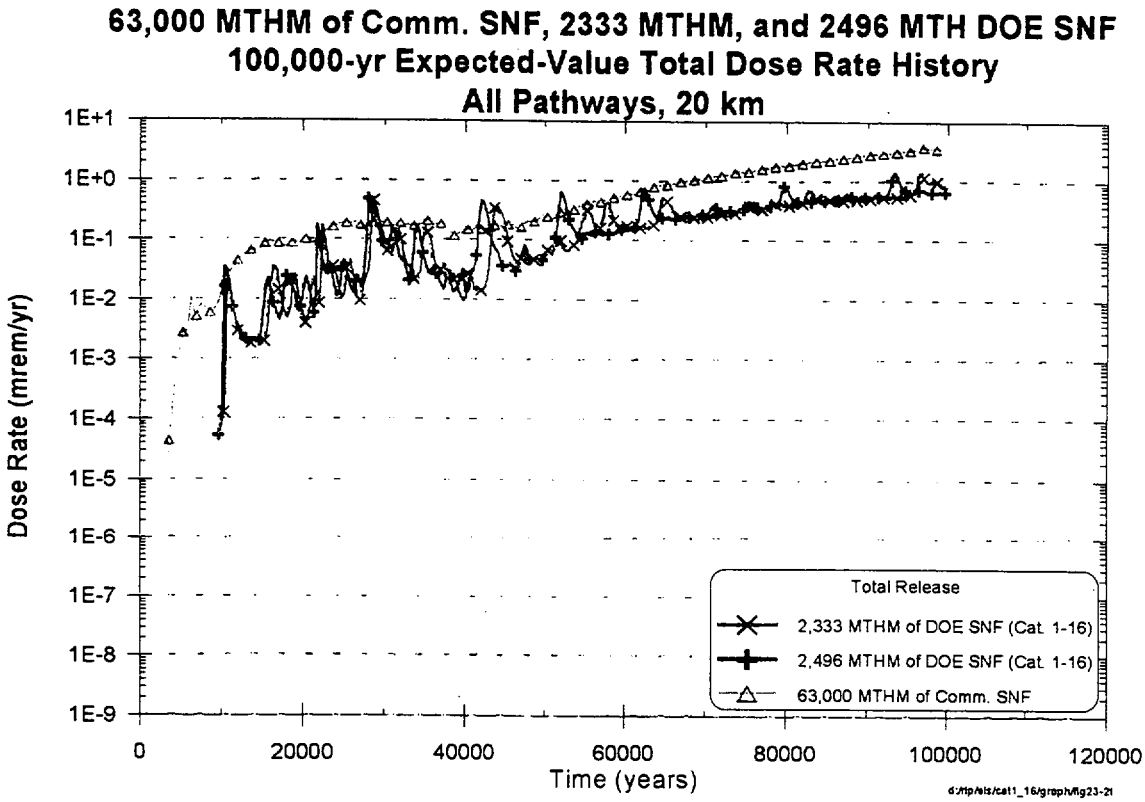

Figure 6A-48. Expected-Value Total Dose History at 20 Kilometers Over 100,000 Years from 63,000 MTHM of Commercial Spent Fuel, 2,333 MTHM of DOE SNF, 2,496 MTHM of DOE SNF.

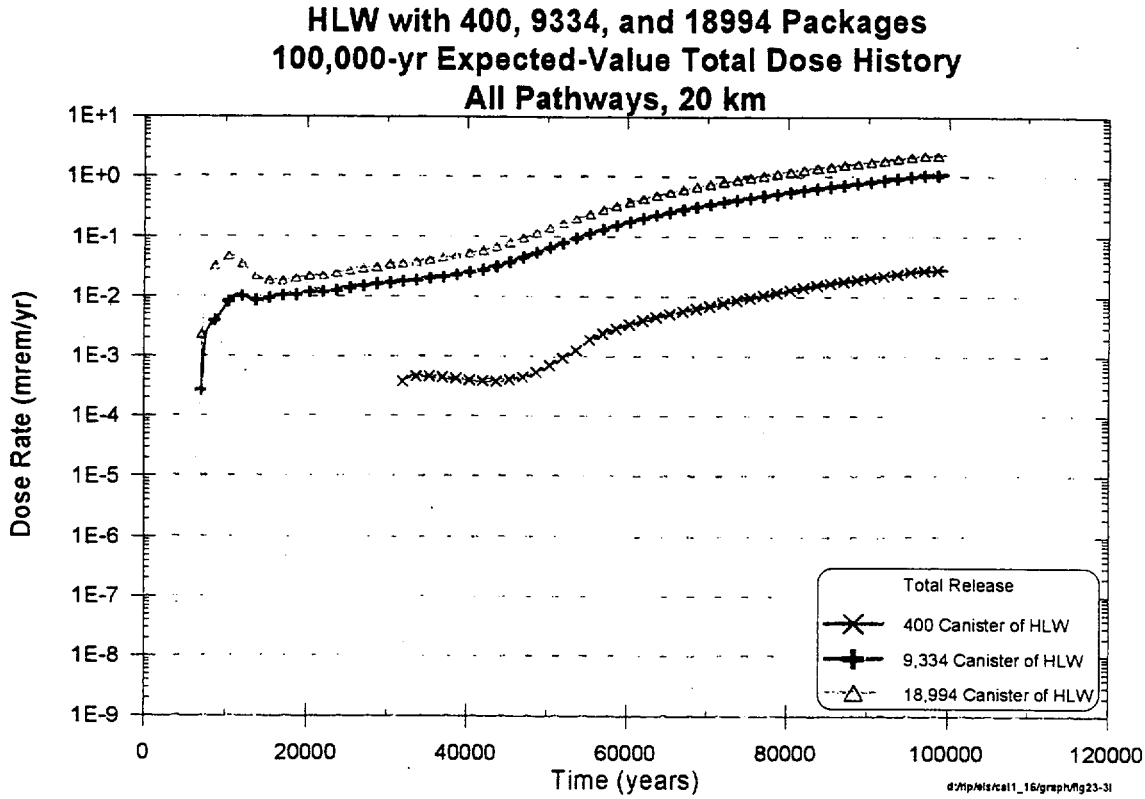

Figure 6A-49. Expected-Value Total Dose History at 20 Kilometers Over 100,000 Years from 400 Canisters of HLW, 9,334 Canisters of HLW, and 18,994 Canisters of HLW.

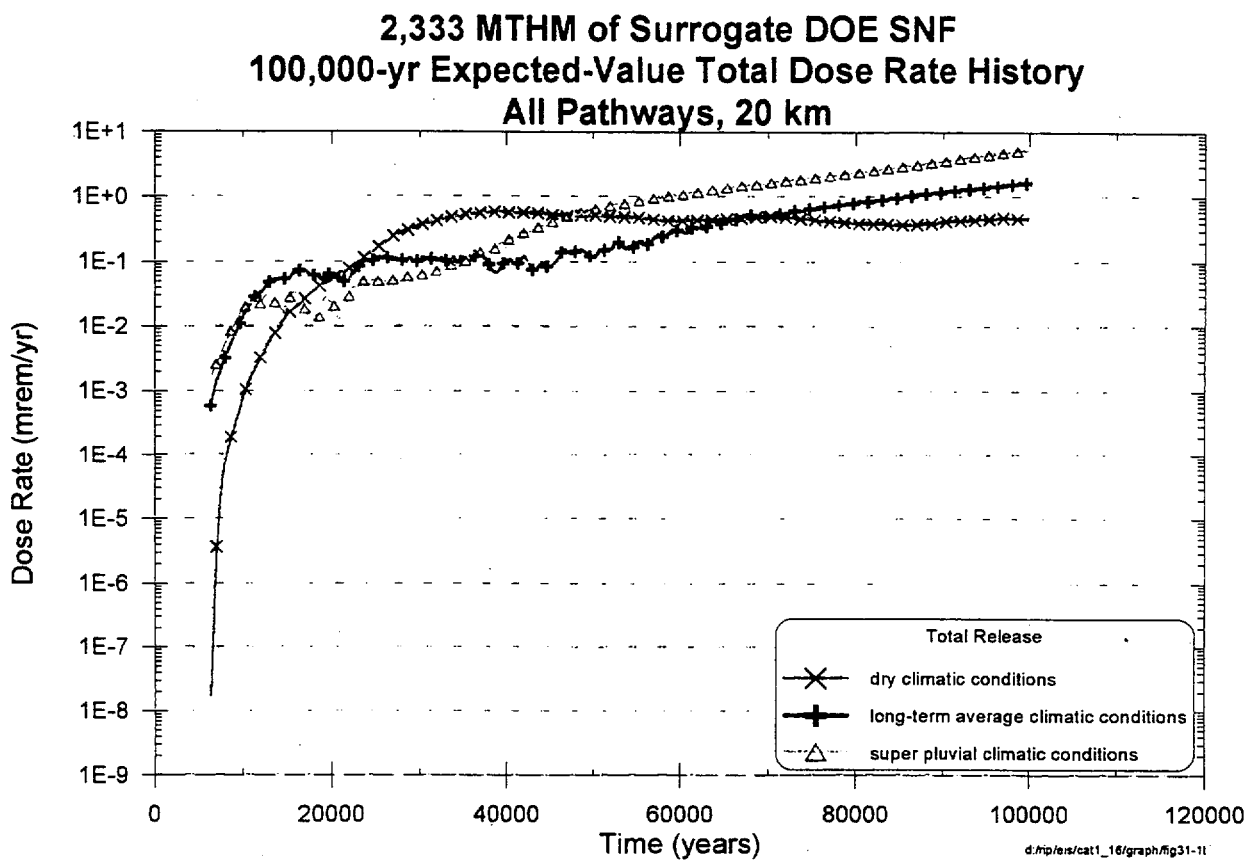

Figure 6A-50. Effects of Climatic Conditions on the Dose from the Surrogate DOE SNF used in the Base Case.

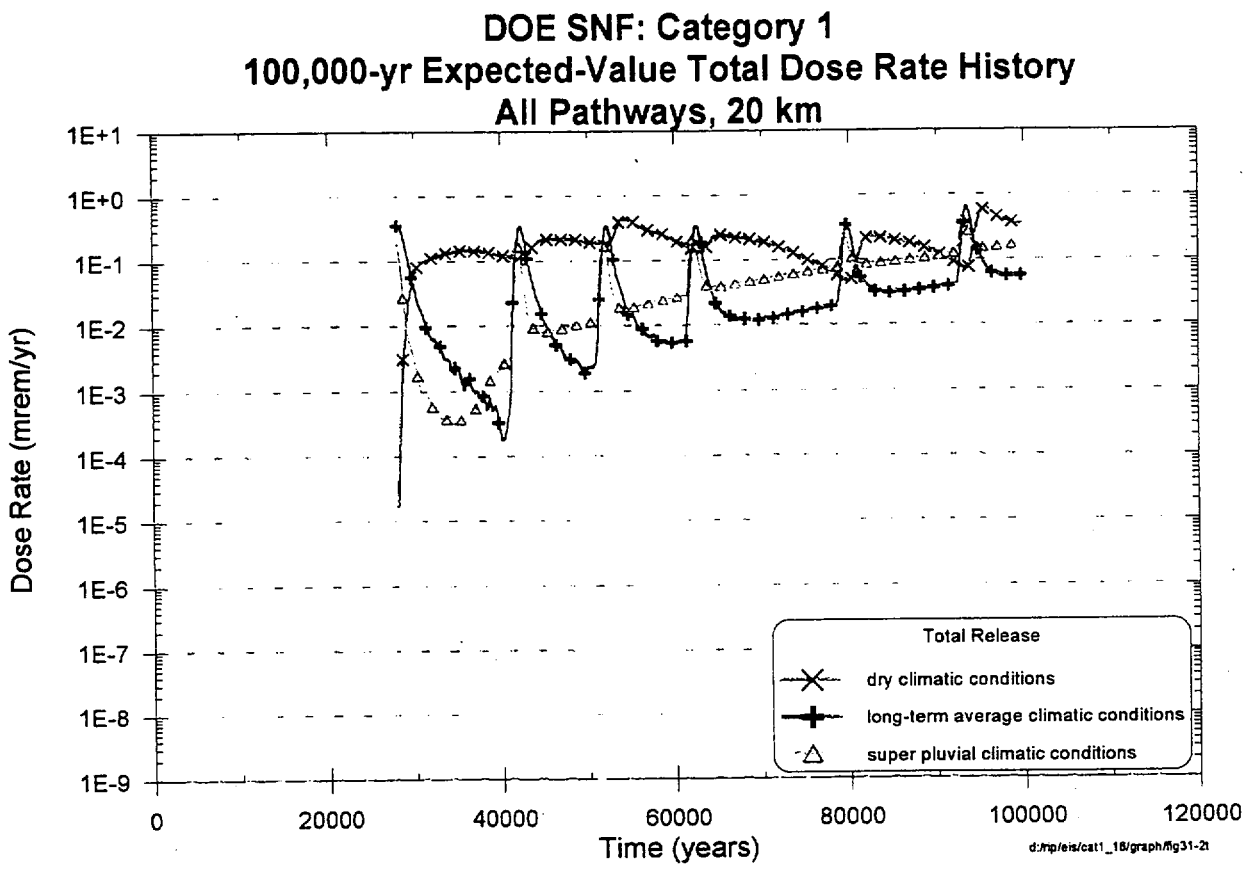

Figure 6A-51. Effects of Climatic Conditions on the Dose from Category 1 Spent Fuel.

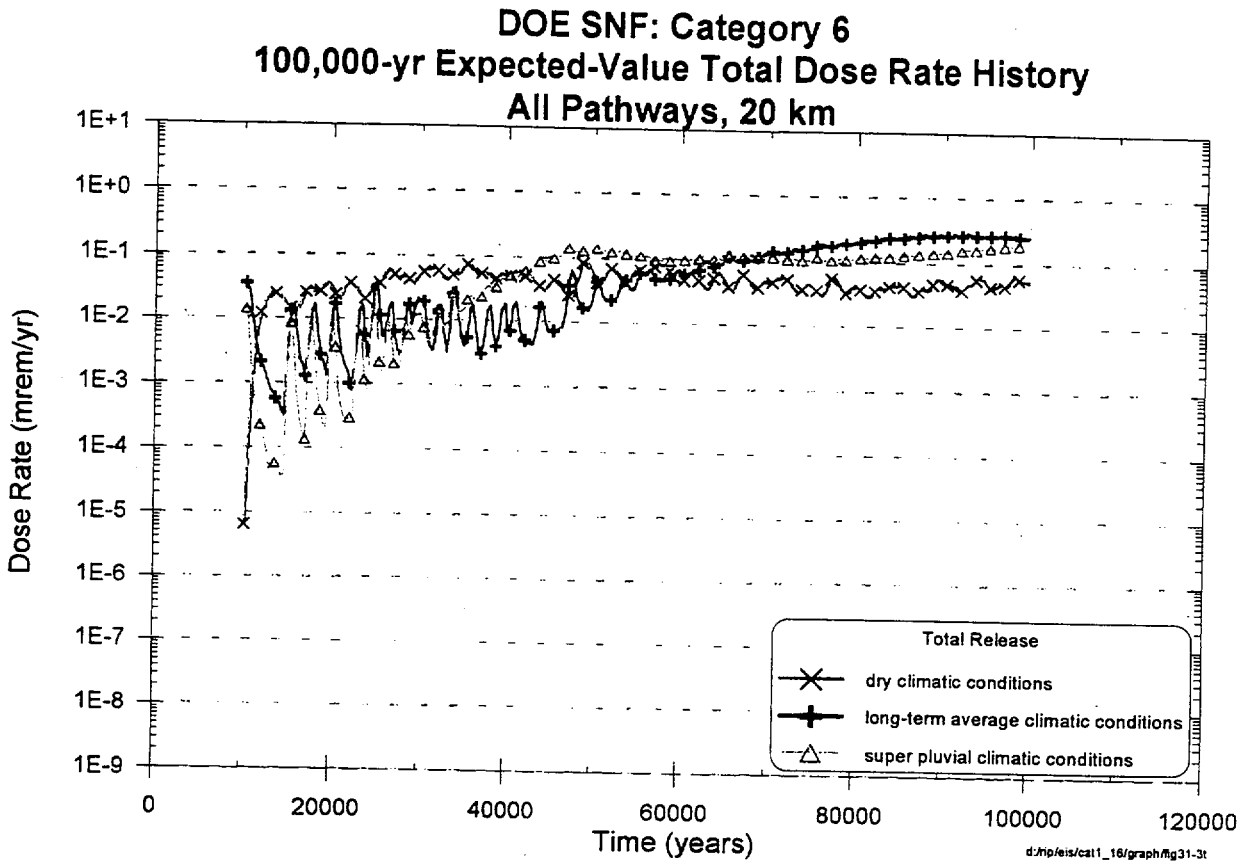

Figure 6A-52. Effects of Climatic Conditions on the Dose from Category 6 Spent Fuel.

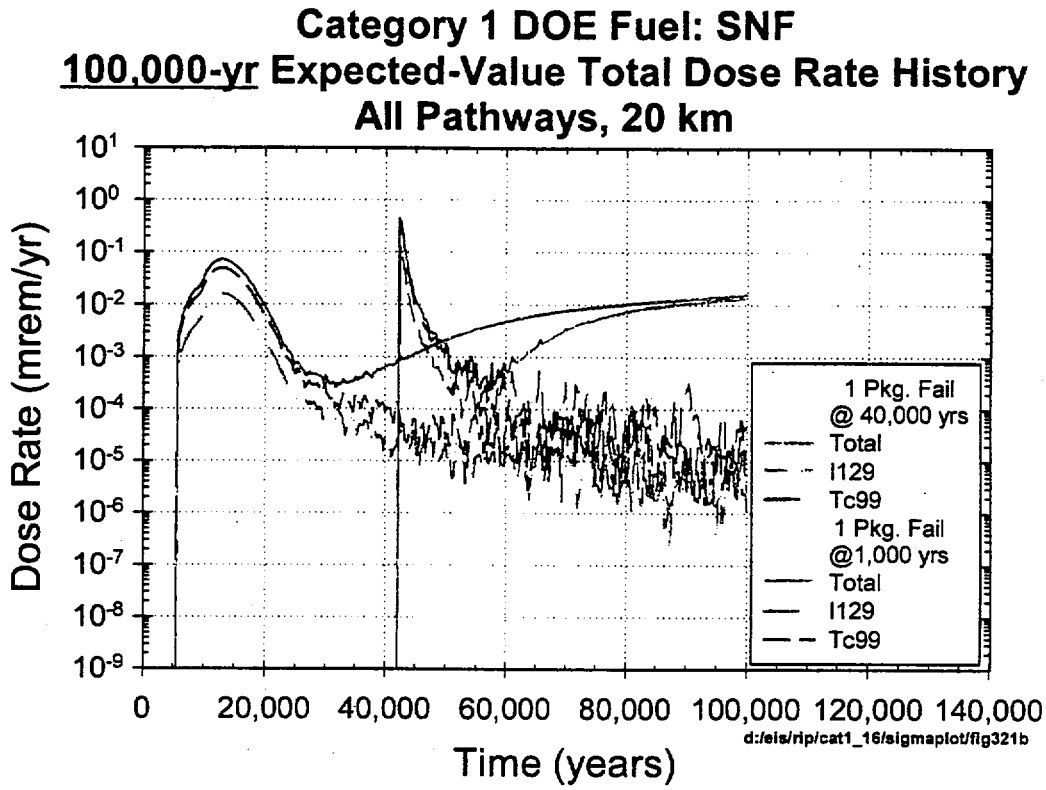

Figure 6A-53. Effects of Time of Waste Package Failure for Category 1 Spent Fuel.

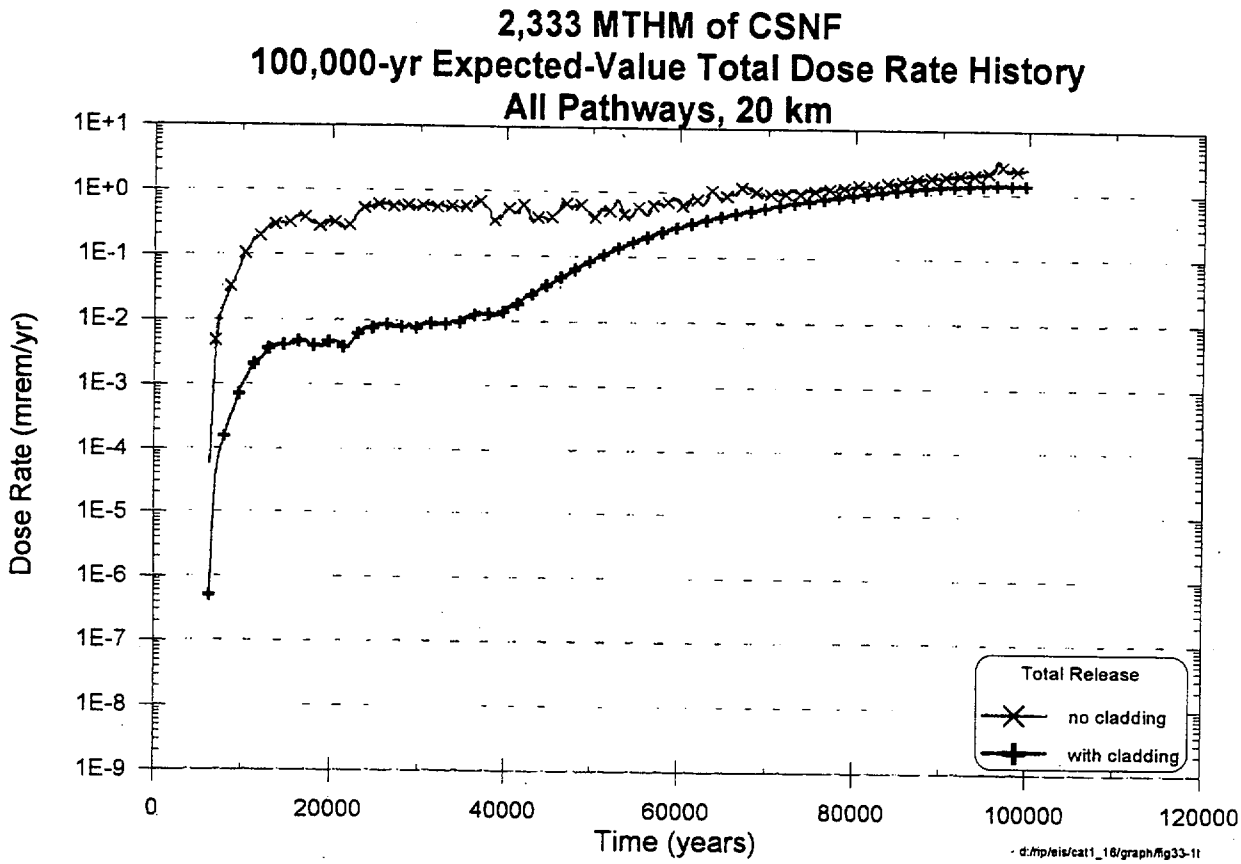

Figure 6A-54. Comparison of Cladding and No Cladding for 2,333 MTHM of Commercial Spent Fuel.

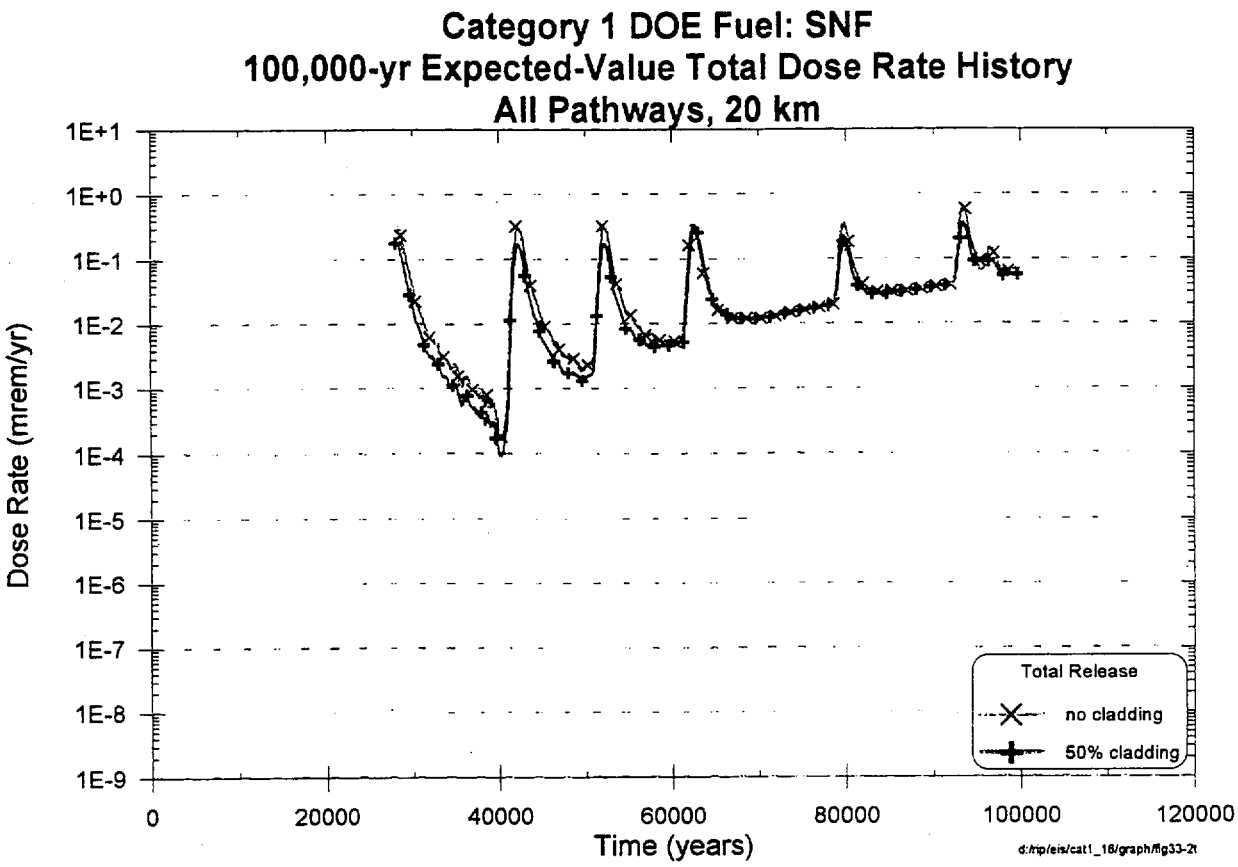

Figure 6A-55. Comparison of 50% Cladding and No Cladding for Category 1 Spent Fuel.

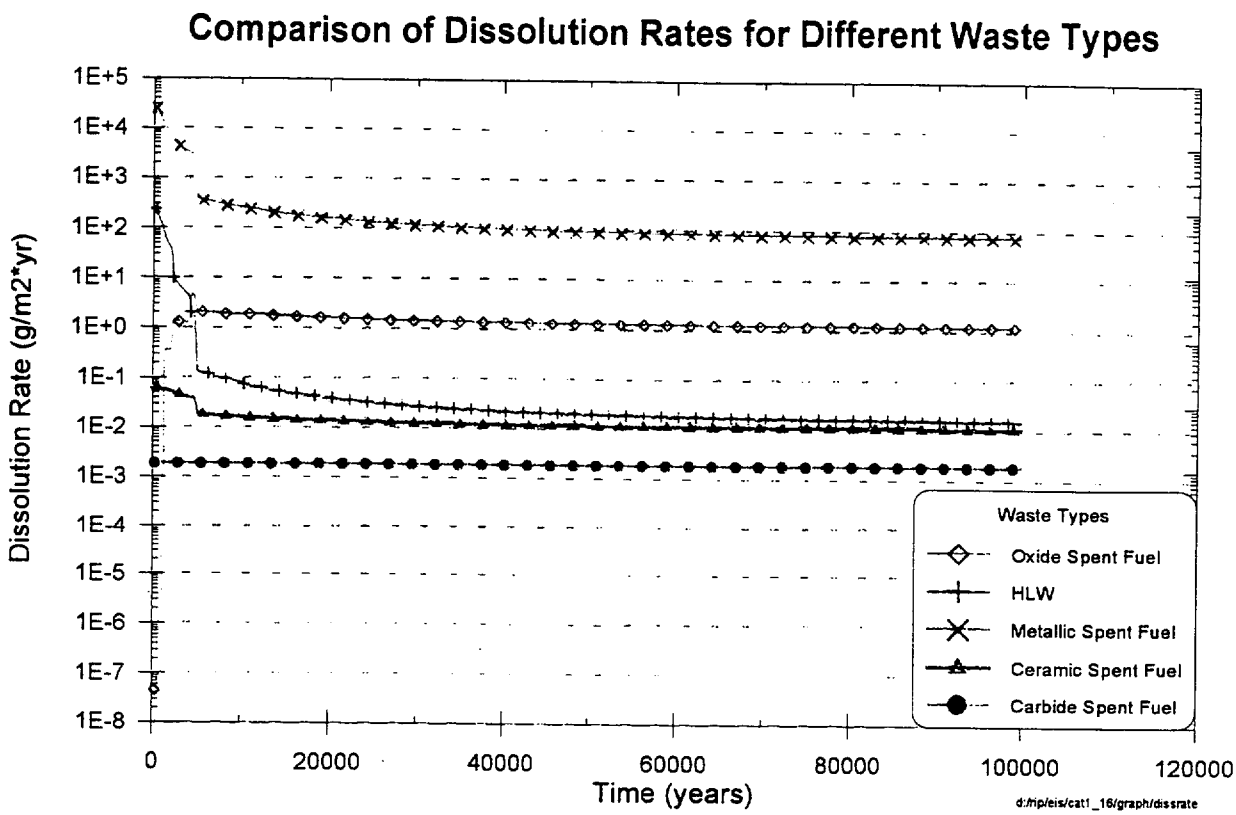

Figure 6A-56. Comparison of Dissolution Rates for HLW, Metallic Spent Fuel, Oxide Spent Fuel, Carbide Spent Fuel, and Ceramic Spent Fuel.

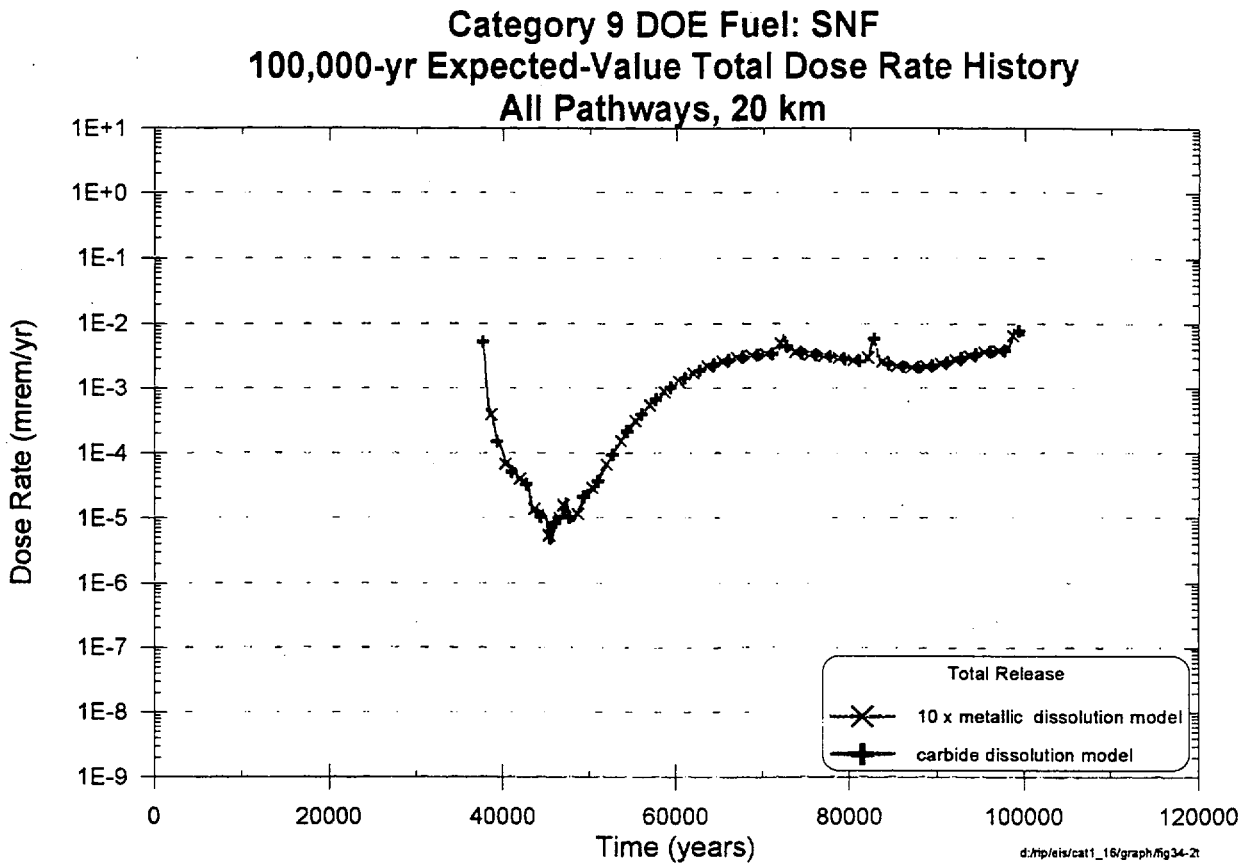

Figure 6A-57. Comparison of Using Ten-Times the Metallic Dissolution Model to Using the Carbide Dissolution Model For Category 9 Spent Fuel.

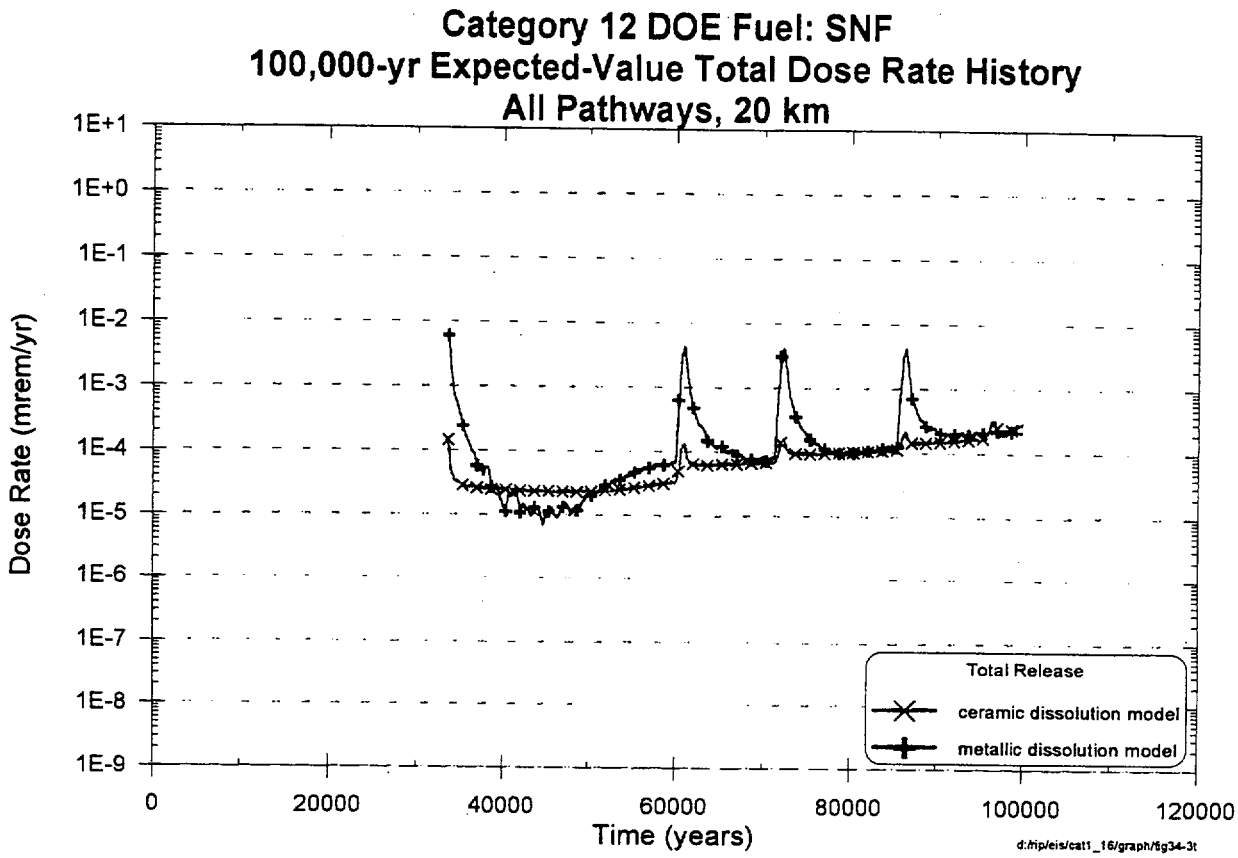

Figure 6A-58. Comparison of Using the Ceramic Dissolution Model for Category 12 Spent Fuel to Using the Congruent Dissolution of Thorium-Uranium Oxide.

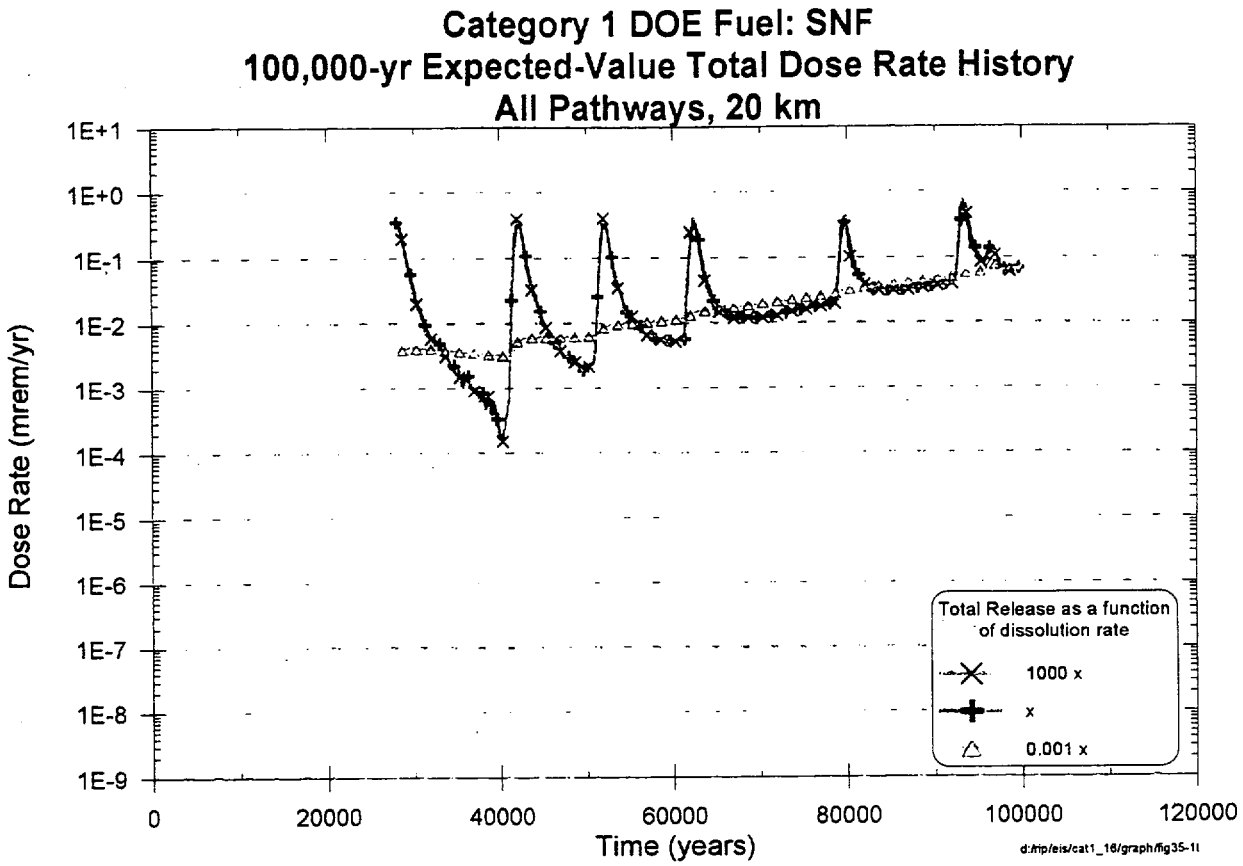

Figure 6A-59. Comparison of Dose from Category 1 Spent Fuel for Different Dissolution Rates for the Base Case Climate.

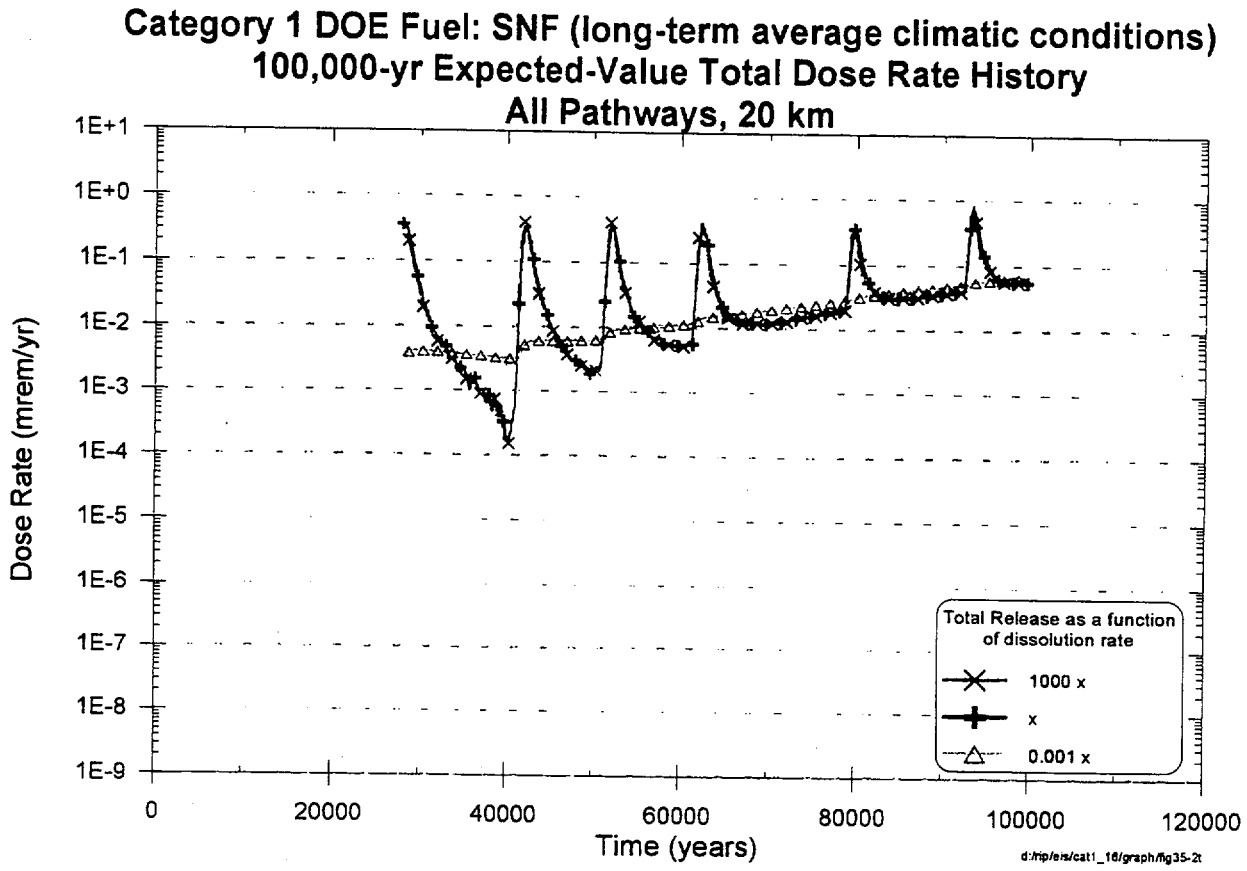

Figure 6A-60. Comparison of Dose from Category 1 Spent Fuel for Different Dissolution Rates for Long Term Average Climate for 100,000 Years Base.

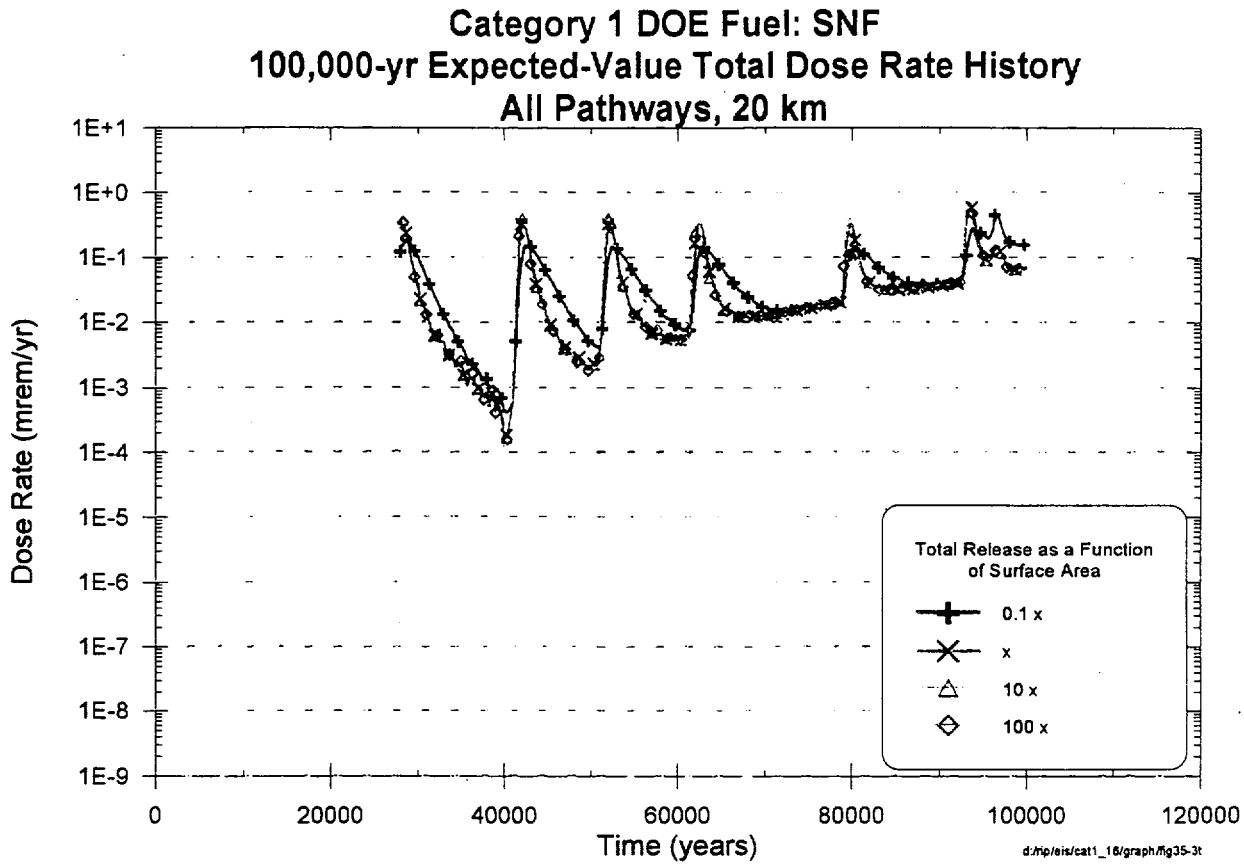

Figure 6A-61. Comparison of Dose from Category 1 Spent Fuel for Different Surface Areas for the Base Case Climate.

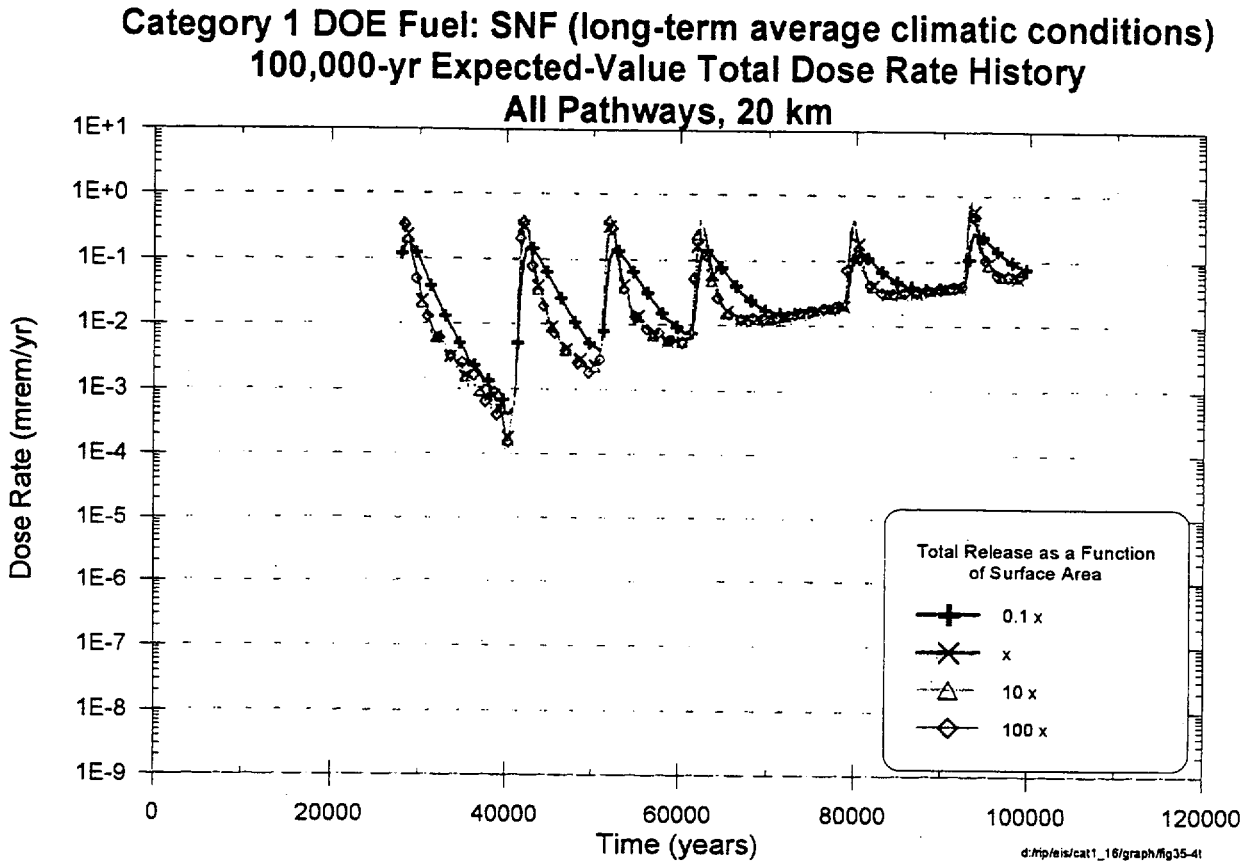

Figure 6A-62. Comparison of Dose from Category 1 Spent Fuel for Different Surface Areas for Long Term Average Climate for 100,000 Years Base.

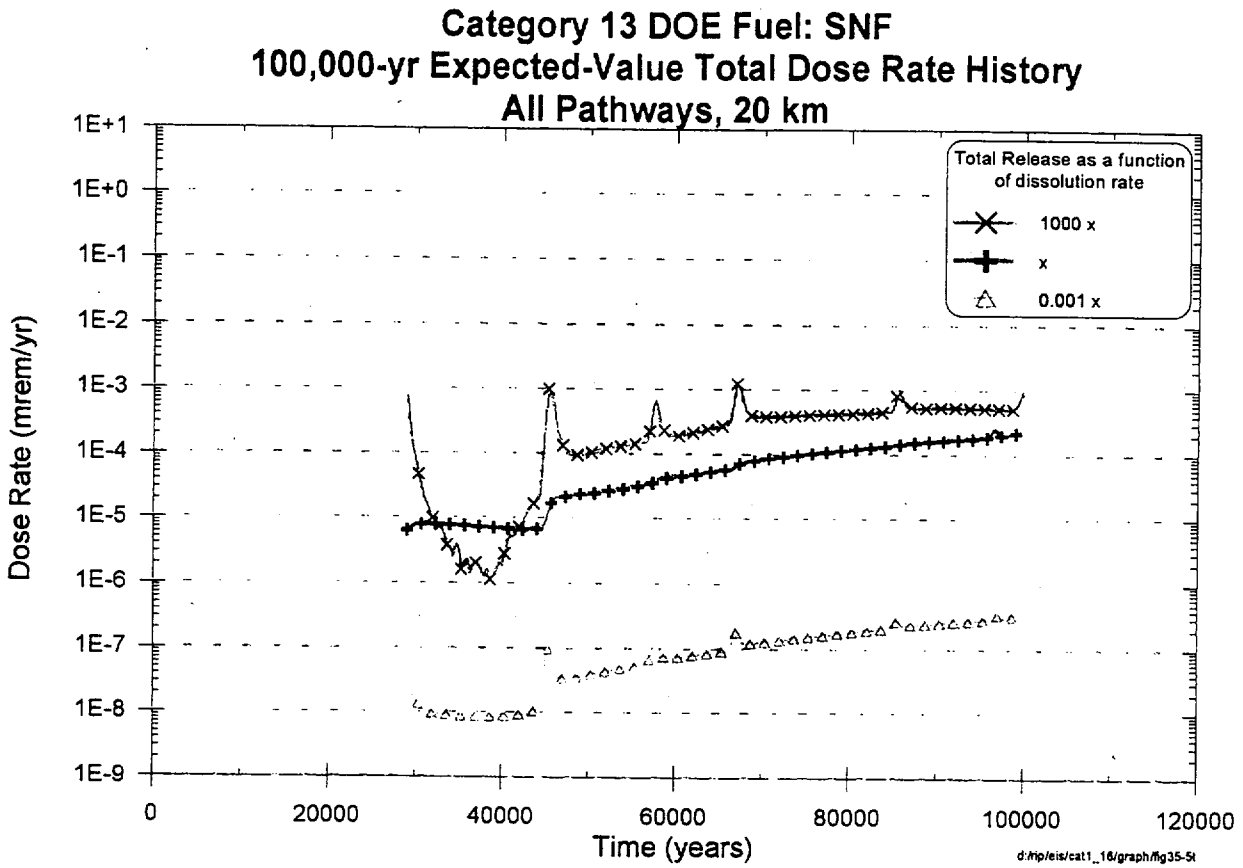

Figure 6A-63. Comparison of Dose from Category 13 Spent Fuel for Different Dissolution Rates for the Base Case Climate.

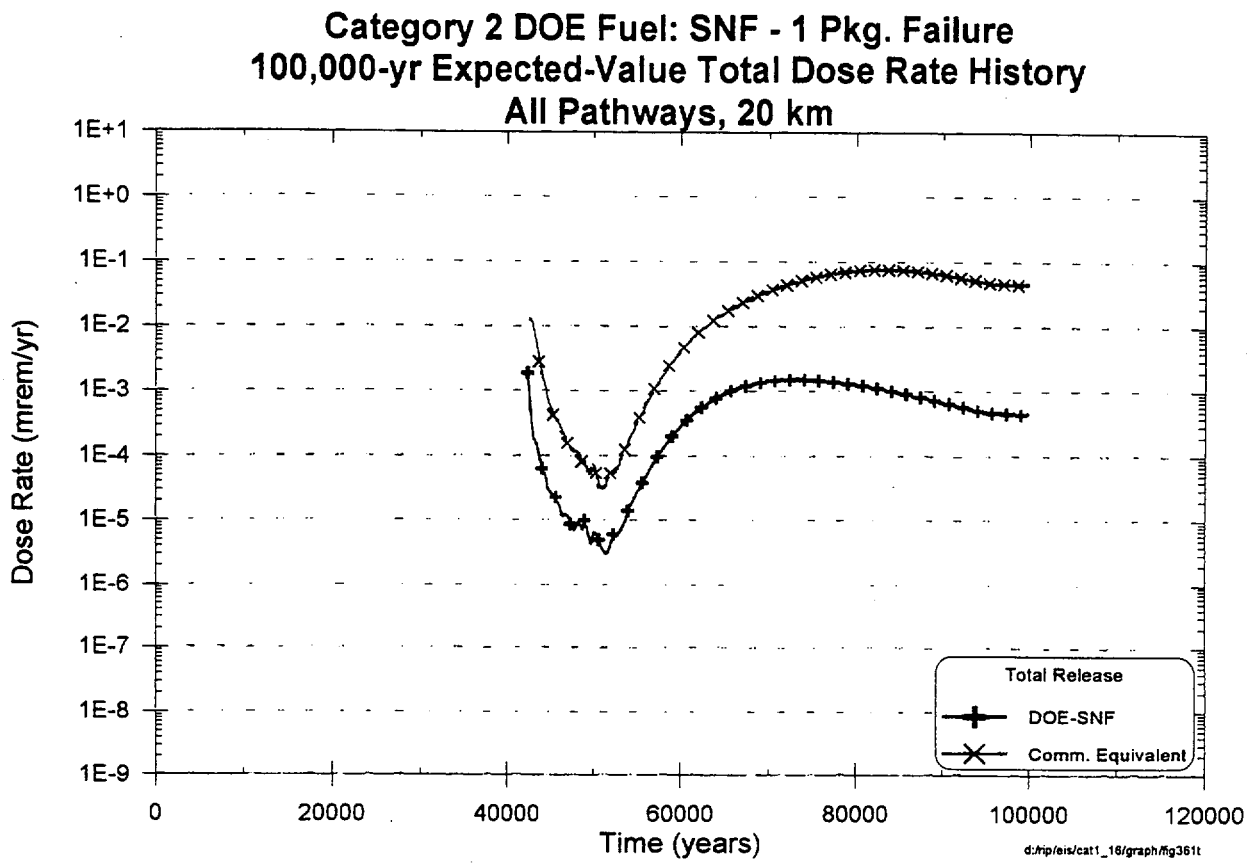

Figure 6A-64. Comparison of Dose from One Failed Package of Category 2 Spent Fuel to One Failed Package of Commercial Spent Fuel.

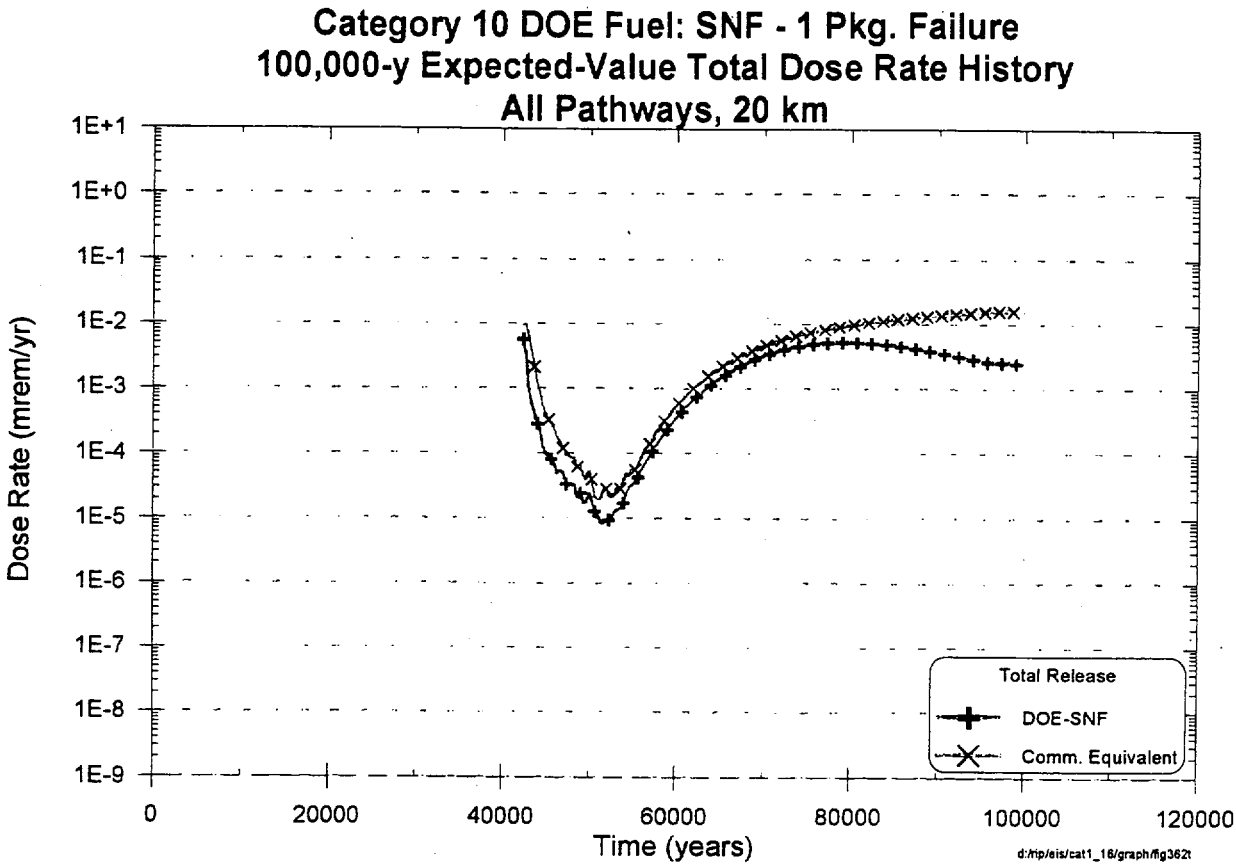

Figure 6A-65. Comparison of Dose from One Failed Package of Category 10 Spent Fuel to One Failed Package of Commercial Spent Fuel.

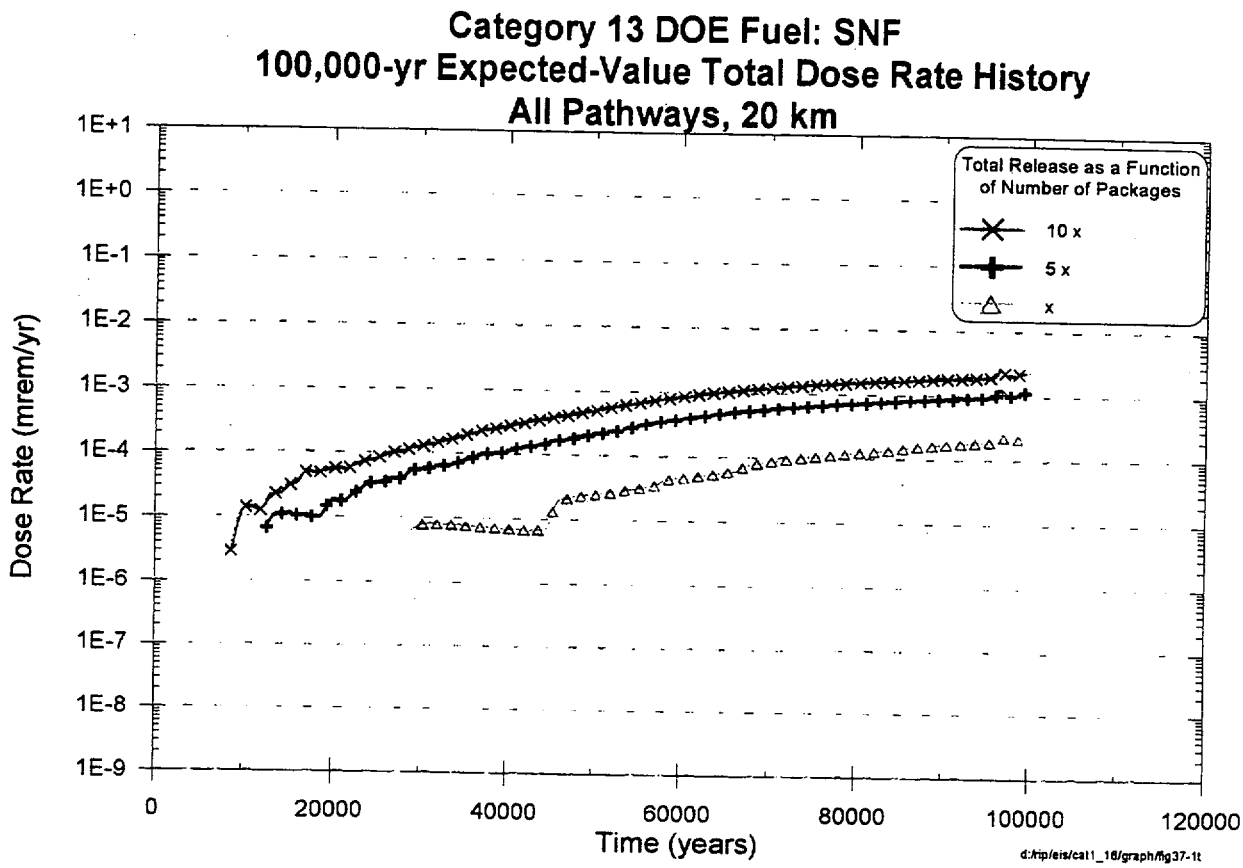

Figure 6A-66. Dose from Category 13 Spent Fuel for Different Numbers of Waste Packages.

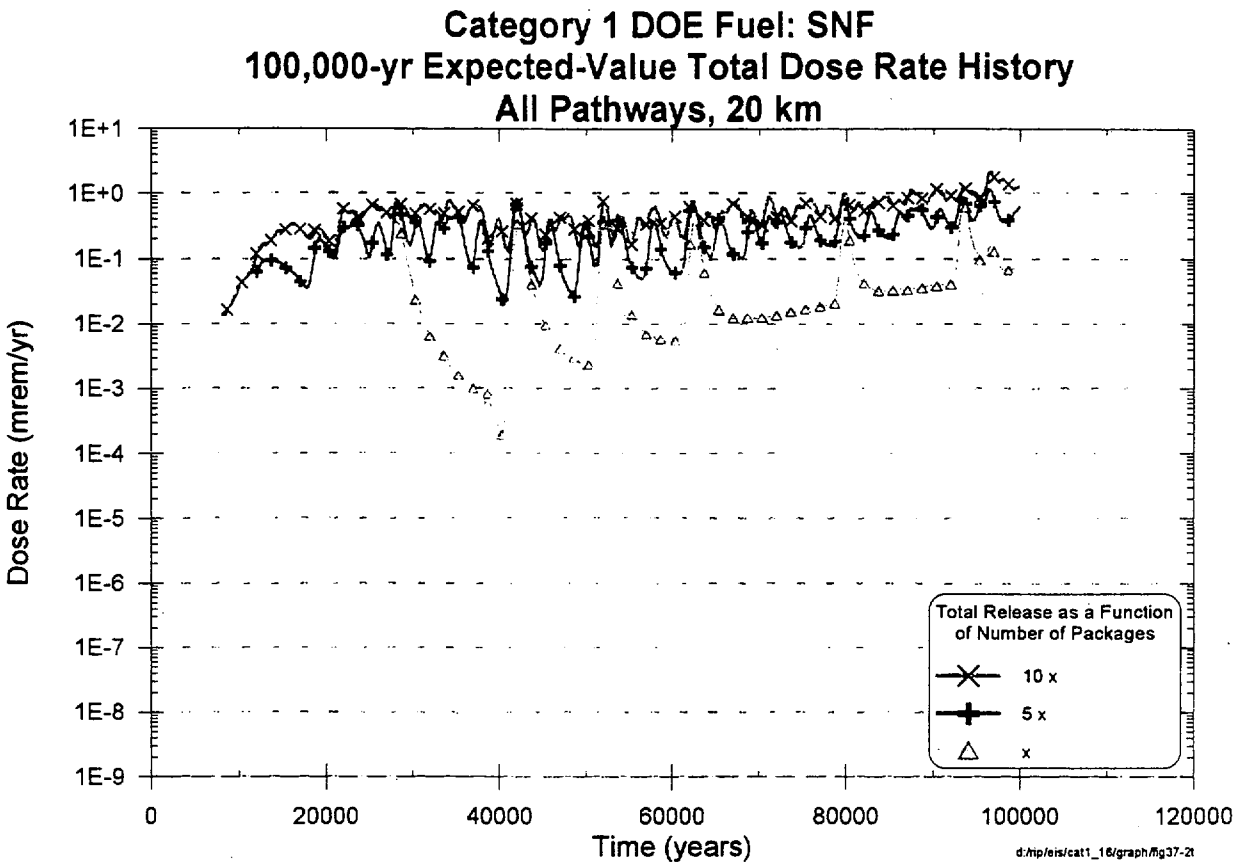

Figure 6A-67. Dose from Category 1 Spent Fuel for Different Numbers of Waste Packages.

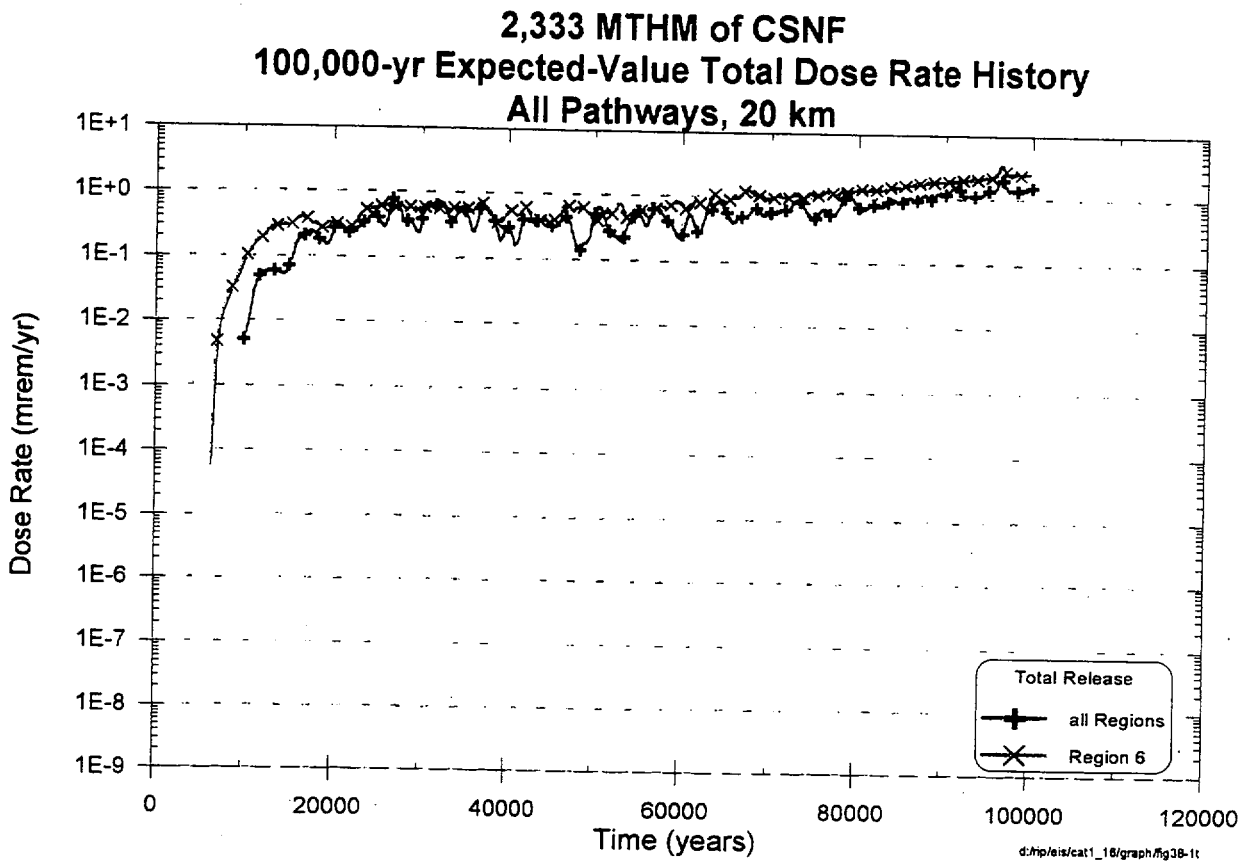

Figure 6A-68. Comparison of Disposal of 2,333 MTHM of Commercial Spent Fuel in One Region to Disposal in Six Regions.

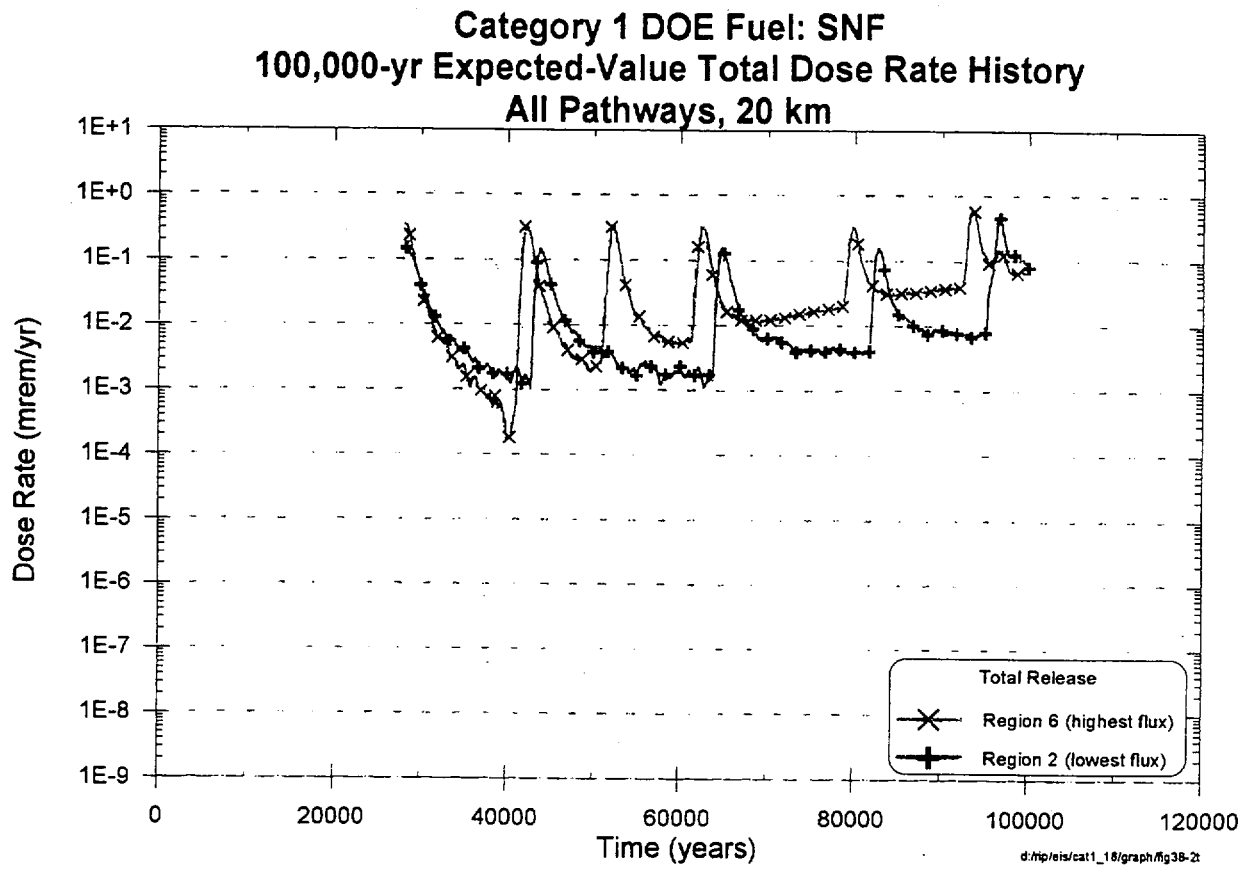

Figure 6A-69. Comparison of Disposal of Category 1 Spent Fuel in Region Six to Disposal of it in Region Two.

CHAPTER 6

APPENDIX A

TABLES

Table 6A-1. DOE spent fuel categories for total system performance assessment (TSPA) (modified from Stroupe 1997).

FUEL TYPES	SUMMARY CATEGORY
1. U metal, Disrupted Zr clad, Low Enriched Uranium (L-EU), N Reactor 2. U metal, Al clad, LEU, Single Pass Reactor	1. U metal
3. U-Zr, High Enriched Uranium (HEU), Chicago Pile 5 & Heavy Water component Test Reactor	2. Ud-Zr alloy
4. U-Mo, Zr clad, HEU, Enrico Fermi Reactor (FERMI)	3. U-Mo alloy
5. U oxide, Intact Zr clad, HEU, Shippingport Pressurized Water Reactor 6. U oxide, Intact Zr clad, Medium Enriched Uranium (MRU), Saxton 7. U oxide, Intact Zr clad, LEU, commercial 8. U oxide, Intact SST clad, HEU, Mobil Low Power Reactor 9. U oxide, Intact SST clad, MEU, Power Burst Facility 10. U oxide, Intact SST clad, LEU, Fast Flux Test Facility (FFTF)-Test Fuel Assembly (TFA)	4. U oxide
11. U oxide, Failed or declad, HEU, Stationary Medium Power Plant 12. U oxide, Failed or declad, MEU, Oak Ridge National Laboratory Fuel Scrap 13. U oxide, Failed or declad, LEU, Three Mile Island 14. U oxide, Al clad, HEU, High Flux Isotope Reactor 15. U oxide, Al clad, MEU, Foreign Research Reactor (FRR) & Materials Test Reactor (MTR)	5. U oxide (disrupted clad)

16. U-Al or U-Al alloy, Al clad, HEU, Advanced Test Reactor 17. U-Al or U-Al alloy, Al clad, MEU, FRR & MTR	6. U-Al alloy
18. U-Si, Al clad, HEU & MEU, FRR & MTR	7. U- Silicide
19. U-Th carbide, (high integrity graphite) HEU, Ft. St. Vrain	8. U-Th carbide (high integrity)
20. U-Th carbide, (low integrity graphite) HEU, Peach Bottom	9. U-Th carbide (low integrity)
21. U or U-Pu carbide, (low integrity non-graphite) MEU Fissile Gram Equivalent (FGE), Sodium Reactor Experiment & FFTF carb.	10. U-Th carbide (non-graphite)
22. Mixed oxide (MOX), Zr clad, HEU FGE, General Electric Test 23. MOX, SST clad, HEU FGE, FFTF –Driver Fuel Assembly 24. MOX, Misc. clad, MEU & LEU FGE), FFTF-Test Assembly-Advanced Oxide	11. Mixed Oxide
25. U-Th oxide, Zr clad, HEU FGE, Light Water Breeder Reactor 26. U-Th oxide, SST clad, HEU FGE, Dresden	12. U-Th oxide
27. U-Zr hydride, SST & Incoloy clad, HEU, Training Research Reactor General Atomic (TRIGA) Fuel Life Improvement Program 28. U-Zr Hydride, SST & Incoloy clad, MEU, TRIGA Std. 29. U-Zr hydride, Al clad, MEU, TRIGA Al 30. U-Zr hydride, Declad, HEU, Systems for Nuclear Auxiliary Power	13. U-Zr hydride

31. Na-Bonded, SSST & Misc. clad, HEU, MEU, &LEU, FERMI Blanket	14. Na-bonded (will be treated)
32. Navy, Classified HEU	15. Navy
33. Canyon Stabilization, HEU &LEU, Savannah River Site Target	Canyon (processed)
34. Misc. Spent Fuels, HEU, MEU & LEU, Unknown	16. Miscellaneous

Table 6A-2. Categories of DOE SNF and Typical Members of Each Category.

Category	Typical Spent Fuel
1. Uranium metal	N Reactor
2. Uranium-Zirconium alloy	Heavy Water Component Test Reactor
3. Uranium-Molybdenum alloy	FERMI (Enrico Fermi Reactor)
4. Uranium oxide	Commercial Pressurized Water Reactor (PWR)
5. Uranium oxide (disrupted clad)	Three Mile Island (TMI) core debris
6. Uranium-Aluminum alloy	Advanced Test Reactor (ATR)
7. Uranium silicide	Foreign Research Reactor-Materials Test Reactor (FRR-MTR)
8. Uranium-Thorium carbide (high integrity)	Fort St. Vrain
9. Uranium-Thorium carbide (low integrity)	Peach Bottom
10. Uranium-Thorium carbide (non-graphite)	Fast Flux Test Facility (FFTF) carbide
11. Mixed oxide	Fast Flux Test Facility (FFTF) oxide
12. Uranium-Thorium oxide	Shippingport Light Water Breeder Reactor (LWBR)
13. Uranium-Zirconium hydride	Training Research Isotope-General Atomic (TRIGA)
14 Sodium-bonded	Will be treated prior to disposal
15. Navy	Not specified
16. Miscellaneous	Not specified

Table 6A-3. Metric Tons Heavy Metal for Each Category of DOE SNF for the Total (2,496 MTHM) and Modified Inventories (2,333 MTHM).

bb	Spent Fuel Type	Total Inventory (MTHM)	Modified[12] Inventory (MTHM)
1	Uranium metal	2122.26	1979.88
2	Uranium-Zirconium alloy	0.04	0.04
3	Uranium-Molybdenum alloy	3.77	3.51
4	Uranium oxide	98.68	92.06
5	Uranium oxide (disrupted clad)	87.02	81.18
6	Uranium-Aluminum alloy	8.74	8.15
7	Uranium silicide	11.55	10.78
8	Uranium-Thorium carbide (high integrity)	24.67	23.01
9	Uranium-Thorium carbide (low integrity)	1.66	1.55
10	Uranium-Thorium carbide (non-graphite)	0.15	0.14
11	Mixed oxide	12.32	11.49
12	Uranium-Thorium oxide	49.63	46.30
13	Uranium-Zirconium hydride	2.03	1.89
15	Navy	63.00	63.00
16	Miscellaneous	10.73	10.01
Total		2496.25	2332.99

[1]Data provided by the National Spent Nuclear Fuel program (Stroupe, 1998).

[12]Total Inventory reduced by approximately 7%, except for Category 15, to obtain the modified inventory of approximately 2,333 MTHM.

Table 6A-4. ORIGEN2 Analyses Conducted to Obtain Radionuclide Inventories for DOE SNF.

Category	ORIGEN2 Analyses Used to Represent Fuels in the Category
1. Uranium metal	Commercial Pressurized Water Reactor (PWR) Fuel N Reactor Fuel Oak Ridge Research Reactor (ORR) Fuel Single Pass Reactor Fuel
2. Uranium-Zirconium alloy	Advanced Test Reactor (ATR) Fuel[1]
3. Uranium-Molybdenum alloy	Enrico Fermi Reactor (FERMI) Fuel
4. Uranium oxide	Commercial PWR Commercial Boiling Water Reactor (BWR) Fuel Pathfinder Fuel Power Burst Facility (PBF) Fuel Pulstar Buffalo Fuel Shippingport PWR Fuel Transient Reactor Test (TREAT) Fuel Fast Flux Test Facility (FFTF) Oxide Fuel ATR Fuel
5. Uranium oxide (disrupted clad)	Commercial PWR Pulstar Buffalo Fuel Three Mile Island (TMI) PBF Fuel ATR Fuel Missouri University Research Reactor (MURR) Fuel Rhode Island Nuclear Science Center (RINSC) Fuel ORR Fuel
6. Uranium-Aluminum alloy	MURR Fuel RINSC Fuel ORR Fuel
7. Uranium silicide	MURR Fuel RINSC Fuel ORR Fuel
8. Uranium-Thorium carbide (high integrity)	Fort St. Vrain (FSV) Fuel Peach Bottom Fuel General Atomics-High Temperature Gas Cooled Reactor (GA-HTGR) Fuel
9. Uranium-Thorium carbide (low integrity)	Peach Bottom Fuel
10. Uranium-Thorium carbide (non-graphite)	Fast Flux Test Facility (FFTF) Carbide Fuel FSV Fuel ATR Fuel
11. Mixed oxide	FFTF Oxide Fuel
12. Uranium-Thorium oxide	Shippingport Light Water Breeder Reactor (LWBR) Fuel
13. Uranium-Zirconium hydride	Train Research Isotope-General Atomic (TRIGA) Fuel
14. Sodium bonded	Not analyzed
15. Navy	Classified
16. Miscellaneous	N Reactor Fuel FFTF Oxide Fuel MURR Fuel RINSC Fuel ORR Fuel Commercial PWR Fuel ATR Fuel FERMI Fuel

Table 6A-5. Radionuclide Inventory for DOE SNF.[1]

Isotope	Category 1 (ci/mthm)	Category 2 (ci/mthm)	Category 3 (ci/mthm)	Category 4 (ci/mthm)	Category 5 (ci/mthm)	Category 6 (Ci/mthm)	Category 7 (Ci/mthm)
^{227}Ac	4.74E-06	9.51E-07	1.29E-04	3.93E-04	1.30E-04	2.95E-05	4.38E-06
^{241}Am	2.43E+02	7.69E+01	8.46E-04	3.59E+03	6.98E+01	2.84E+02	7.07E+02
^{242M}Am	1.41E-02	2.33E-01	0.00E+00	6.05E+00	1.35E-01	1.95E-01	2.55E-01
^{243}Am	5.96E-02	7.59E-01	1.36E-11	1.93E+01	2.14E-01	2.10E-01	6.96E-01
^{14}C	3.12E-01	1.63E-03	4.08E-02	2.37E-01	1.03E-02	8.53E-05	3.40E-04
^{36}Cl	0.00E+00	0.00E+00	1.04E-04	8.02E-04	1.63E-04	0.00E+00	0.00E+00
^{244}Cm	1.81E+00	3.13E+01	1.27E-12	8.13E+02	8.89E+00	1.80E+00	5.77E+00
^{245}Cm	7.67E-04	1.60E-03	3.46E-18	3.31E-01	3.61E-03	1.53E-04	3.86E-04
^{246}Cm	1.14E-04	1.10E-04	1.14E-21	5.62E-02	6.12E-04	7.36E-06	2.85E-05
^{135}Cs	3.77E-02	1.54E+00	8.40E-02	4.09E-01	2.08E-01	2.42E+00	3.65E-01
^{129}I	3.46E-03	3.26E-01	2.15E-03	4.11E-02	7.18E-03	1.57E-01	7.38E-02
^{93M}Nb	1.72E-01	1.73E+00	8.57E-02	1.56E+00	1.06E-01	1.33E+00	6.10E-01
^{94}Nb	1.21E-06	3.27E-04	1.56E-02	1.70E-02	4.01E-04	2.66E-04	1.44E-04
^{59}Ni	1.75E-02	0.00E+00	1.28E-01	2.18E-01	2.23E-03	0.00E+00	0.00E+00
^{63}Ni	1.66E+00	0.00E+00	2.66E+00	6.86E+02	2.43E-01	1.95E-20	0.00E+00
^{237}Np	3.65E-02	4.00E+00	6.19E-03	4.14E-01	2.92E-02	1.00E+00	3.47E-01
^{231}Pa	1.23E-05	4.57E-05	3.64E-04	6.90E-04	2.44E-04	3.57E-04	5.50E-05
^{210}Pb	6.89E-11	1.72E-10	2.67E-09	2.08E-07	5.01E-08	1.78E-09	2.25E-10
^{107}Pd	7.09E-03	2.28E-01	2.38E-03	1.11E-01	7.90E-03	7.94E-02	6.84E-02
^{238}Pu	5.34E+01	8.62E+03	3.09E-01	2.66E+03	5.51E+01	1.48E+03	5.45E+02
^{239}Pu	1.10E+02	2.14E+02	3.66E+01	3.57E+02	1.20E+02	2.05E+02	4.33E+02
^{240}Pu	6.49E+01	1.22E+02	1.14E-01	5.54E+02	4.22E+01	1.06E+02	3.09E+02
^{241}Pu	8.19E+02	4.20E+04	1.12E-02	3.24E+04	2.80E+03	5.38E+03	1.36E+04
^{242}Pu	3.43E-02	1.83E-01	7.10E-10	2.12E+00	2.90E-02	8.45E-02	3.02E-01
^{226}Ra	9.87E-07	4.38E-10	1.20E-08	6.03E-07	1.90E-07	3.26E-08	4.40E-09
^{228}Ra	8.02E-11	2.48E-11	7.49E-08	3.12E-04	1.06E-04	6.27E-11	2.21E-11
^{79}Se	5.52E-02	5.88E+00	3.10E-02	4.41E-01	1.53E-01	4.25E+00	2.01E+00
^{131}Sm	6.97E+01	5.30E+03	1.29E+02	1.22E+03	2.35E+02	3.56E+03	6.68E+02
^{126}Sn	7.43E-02	5.26E+00	7.04E-02	5.57E-01	1.11E-01	1.42E+00	7.91E-01
^{99}Tc	1.65E+00	1.98E+02	8.40E-01	1.52E+01	3.97E+00	8.83E+01	4.20E+01
^{229}Th	8.36E-09	2.12E-08	4.38E-08	9.26E-04	3.04E-04	1.88E-07	2.35E-08
^{230}Th	9.32E-07	1.71E-06	2.13E-06	8.57E-05	2.79E-05	1.54E-05	2.31E-06
^{232}Th	1.09E-10	4.05E-10	7.89E-08	3.28E-04	1.12E-04	1.61E-09	5.78E-10
^{233}U	5.28E-06	1.82E-04	1.83E-05	3.59E-01	1.16E-01	2.27E-04	3.41E-05
^{234}U	4.19E-01	1.71E-01	9.20E-03	3.85E-01	1.01E-01	1.87E-01	3.41E-02
^{235}U	1.79E-02	1.63E+00	5.85E-01	3.93E-02	1.15E-01	1.54E+00	2.48E-01
^{236}U	7.00E-02	6.71E+00	3.21E+01	3.19E-01	1.11E-01	3.14E+00	1.15E+00
^{238}U	3.32E-01	3.00E-02	2.66E-01	3.00E-01	3.23E-01	7.63E-02	3.03E-01
^{93}Zr	2.16E-01	3.02E+01	1.24E-01	2.12E+00	4.80E-01	8.69E+00	4.06E+00

Isotope	Category 8 (Ci/MTHM)	Category 9 (Ci/MTHM)	Category 10 (Ci/MTHM)	Category 11 (Ci/MTHM)	Category 12 (Ci/MTHM)	Category 13 (Ci/MTHM)	Category 15 (Ci/MTHM)	Category 16 (Ci/MTHM)
^{227}Ac	0.00E+00	1.02E-01	2.91E-07	4.47E-08	6.14E-01	2.78E-06	N/A[42]	2.93E-06
^{241}Am	7.57E+01	9.58E+01	7.68E+03	1.28E+04	1.19E+00	1.00E+01	N/A	4.97E+02
^{242M}Am	2.05E-02	4.91E-02	1.34E+01	2.23E+01	1.25E-02	1.11E-01	N/A	6.62E-01
^{243}Am	5.41E-01	4.76E-02	2.20E-01	5.36E+00	2.38E-03	1.23E-02	N/A	2.08E+00
^{14}C	4.39E+00	1.35E+00	4.73E-04	2.95E-02	9.56E-01	4.19E+00	N/A	7.32E-03
^{36}Cl	5.51E-02	3.83E-02	0.00E+00	3.12E-04	2.13E-02	1.26E-01	N/A	1.81E-05
^{244}Cm	1.70E+01	1.25E+00	9.06E+00	2.25E+02	2.29E-01	3.35E-01	N/A	8.19E+01
^{245}Cm	2.84E-03	1.44E-04	4.62E-04	9.22E-02	4.74E-05	6.84E-06	N/A	3.06E-02
^{246}Cm	1.41E-03	4.69E-06	3.18E-05	1.57E-02	3.13E-06	1.92E-07	N/A	5.16E-03
^{135}Cs	3.52E-01	9.52E-01	4.44E-01	9.53E-02	2.87E-01	1.59E+00	N/A	5.86E-01
^{129}I	4.21E-02	2.64E-02	9.42E-02	1.07E-02	1.58E-02	3.57E-02	N/A	9.90E-02
^{93M}Nb	1.88E-01	1.67E+00	5.02E-01	3.76E-01	4.40E-01	3.49E-01	N/A	7.07E-01
^{94}Nb	2.70E-03	1.77E-02	9.46E-05	5.67E-04	2.22E-02	2.29E-01	N/A	1.50E-04
^{59}Ni	3.51E-01	5.27E-02	0.00E+00	6.09E-02	7.32E-02	2.45E+01	N/A	3.53E-03
^{63}Ni	8.43E+00	5.43E+00	1.62E+02	2.58E+02	8.92E+00	3.03E+03	N/A	4.36E-01
^{237}Np	3.31E-01	2.66E-01	1.22E+00	1.92E-01	1.01E-03	9.51E-02	N/A	1.03E+00
^{231}Pa	3.79E-01	1.74E-01	1.33E-05	3.70E-06	1.55E+00	4.44E-05	N/A	4.47E-05
^{210}Pb	9.32E-05	9.39E-06	4.98E-11	9.22E-09	1.12E-04	6.74E-11	N/A	3.22E-09
^{107}Pd	1.77E-02	1.72E-02	6.59E-02	3.04E-02	3.43E-03	2.95E-02	N/A	7.82E-02
^{238}Pu	1.65E+03	6.63E+02	3.62E+03	2.36E+03	3.94E+00	1.05E+02	N/A	2.26E+03
^{239}Pu	4.58E+00	1.48E+01	6.17E+03	9.52E+03	2.55E-01	2.24E+02	N/A	2.23E+02
^{240}Pu	7.71E+00	1.16E+01	5.32E+03	8.28E+03	1.46E-01	8.72E+01	N/A	1.56E+02
^{241}Pu	0.00E+00	1.08E+03	5.62E+04	7.70E+04	3.47E+01	6.50E+03	N/A	1.51E+04
^{242}Pu	0.00E+00	1.53E-02	5.32E-02	5.90E-01	3.27E-04	1.21E-02	N/A	3.01E-01
^{226}Ra	9.90E-05	3.37E-05	7.38E-08	1.58E-07	6.44E-05	1.12E-10	N/A	1.77E-08
^{228}Ra	1.33E-01	8.60E-02	2.25E-11	6.00E-10	1.01E-01	1.72E-07	N/A	6.42E-11
^{79}Se	5.99E-01	4.86E-01	1.70E+00	1.08E-01	3.52E-01	6.36E-01	N/A	1.99E+00
^{131}Sm	9.18E+02	9.19E+02	5.98E+03	7.20E+03	1.30E+02	1.18E+03	N/A	1.61E+03
^{126}Sn	2.82E-01	4.49E-01	1.52E+00	1.42E-01	3.95E-01	5.89E-01	N/A	1.43E+00
^{99}Tc	1.51E+01	1.46E+01	5.73E+01	3.78E+00	3.27E+00	2.14E+01	N/A	5.82E+01
^{229}Th	5.65E-01	2.47E-01	8.00E-09	5.03E-08	2.60E-01	5.66E-08	N/A	3.72E-08
^{230}Th	3.87E-02	4.76E-03	1.67E-05	3.46E-05	9.84E-03	1.90E-07	N/A	4.98E-06
^{232}Th	1.03E-01	9.06E-02	1.43E-10	1.62E-09	1.20E-01	5.09E-07	N/A	4.20E-10
^{233}U	1.40E+02	9.45E+01	5.61E-05	2.76E-05	1.69E+02	2.77E-04	N/A	6.81E-05
^{234}U	1.14E+01	1.57E+01	1.61E-01	2.37E-01	8.39E+00	1.04E-02	N/A	7.70E-02
^{235}U	4.40E-02	2.44E-01	4.73E-01	6.39E-03	5.65E-04	4.87E-01	N/A	5.02E-01
^{236}U	4.33E-01	6.16E-01	1.97E+00	1.23E-01	1.16E-03	6.54E-01	N/A	1.91E+00
^{238}U	1.09E-03	2.55E-03	8.67E-03	8.08E-02	1.84E-05	2.85E-01	N/A	1.01E-01
^{93}Zr	2.19E+01	2.31E+00	8.74E+00	5.05E-01	8.21E-01	3.84E+00	N/A	8.05E+00

[1]Data provided by the National Spent Nuclear Fuel program (Stroupe 1998).

[42]No inventory is given for Navy SNF; analyses are conducted using a release term at the boundary of the waste package.

Table 6A-6. Radionuclide Inventory for Commercial Spent Nuclear Fuel (CSNF), Surrogate DOE SNF, and High-Level Waste (HLW) and Used in the TSPA-VA Base Case

Isotope	Commercial Spent Fuel (Ci/MTHM)	Surrogate DOE SNF (Ci/MTHM)	High-Level Waste (Ci/MTHM)
^{227}Ac	1.86E-05	2.57E-05	9.43E-04
^{241}Am	3.87E+03	4.42E+02	3.47E+02
^{242M}Am	2.26E+01	3.89E-01	3.31E-02
^{243}Am	2.63E+01	9.04E-01	8.20E-02
^{14}C	1.44E+00	3.38E-01	0.00E+00
^{36}Cl	1.15E-02	6.19E-04	0.00E+00
^{244}Cm	1.24E+03	3.74E+01	2.09E+01
^{245}Cm	3.65E-01	1.52E-02	8.83E-05
^{246}Cm	7.60E-02	2.58E-03	1.00E-05
^{135}Cs	5.36E-01	7.21E-02	3.09E-01
^{129}I	3.57E-02	6.19E-03	1.49E-05
^{93M}Nb	1.89E+00	2.33E-01	1.55E+00
^{94}Nb	8.47E-01	7.62E-04	5.31E-05
^{59}Ni	2.44E+00	2.90E-02	1.49E-01
^{63}Ni	3.20E+02	3.17E+01	1.31E+01
^{237}Np	4.54E-01	5.96E-02	1.90E-01
^{231}Pa	3.42E-05	4.02E-03	1.53E-03
^{210}Pb	6.94E-07	9.88E-07	4.56E-08
^{107}Pd	1.31E-01	1.20E-02	4.42E-02
^{238}Pu	3.22E+03	1.97E+02	6.50E+02
^{239}Pu	3.68E+02	1.69E+02	8.66E+00
^{240}Pu	5.47E+02	1.27E+02	5.51E+00
^{241}Pu	3.52E+04	2.63E+03	2.25E+02
^{242}Pu	2.10E+00	1.24E-01	7.12E-03
^{226}Ra	2.57E-06	1.96E-06	1.59E-07
^{228}Ra	3.21E-10	1.41E-03	1.64E-04
^{79}Se	4.58E-01	9.66E-02	1.02E-01
^{131}Sm	3.67E+02	1.83E+02	7.63E+02
^{126}Sn	8.85E-01	1.04E-01	6.76E-01
^{99}Tc	1.45E+01	2.78E+00	1.05E+01
^{229}Th	3.77E-07	5.97E-03	2.36E-05
^{230}Th	3.69E-04	4.12E-04	2.14E-05
^{232}Th	4.50E-10	1.10E-03	1.65E-04
^{233}U	7.31E-05	1.49E+00	9.33E-04
^{234}U	1.39E+00	5.19E-01	8.69E-02
^{235}U	1.71E-02	2.83E-02	3.16E-04
^{236}U	2.81E-01	9.75E-02	1.14E-03
^{238}U	3.15E-01	3.25E-01	9.91E-03
^{93}Zr	2.47E+00	5.66E-01	1.87E+00

Table 6A-7. Release Source Term at the Boundary of a Failed Waste Package for Category 15 (Navy) Spent Fuel.[1]

	^{241}Am (Ci/Yr)	^{243}Am (Ci/Yr)	^{14}C (Ci/Yr)	^{36}Cl (Ci/Yr)	^{245}Cm (Ci/Yr)	^{135}Cs (Ci/Yr)	^{129}I (Ci/Yr)
7000	0.0E+00	0.0E+00	0.0E+00	0.0E+00	0.0E+00	0.0E+00	0.0E+00
7500	0.0E+00	0.0E+00	0.0E+00	0.0E+00	0.0E+00	0.0E+00	0.0E+00
8000	6.3E-12	2.6E-10	9.3E-06	4.6E-08	6.3E-12	9.1E-12	9.4E-11
8500	1.0E-11	4.3E-10	1.7E-05	7.8E-08	1.0E-11	1.6E-11	1.9E-10
9000	7.5E-12	3.7E-10	2.7E-05	6.1E-08	8.0E-12	1.2E-11	3.1E-10
9500	6.6E-11	2.6E-09	5.3E-05	5.7E-07	6.7E-11	1.1E-10	6.3E-10
10000	1.2E-10	4.7E-09	7.7E-05	1.1E-06	1.2E-10	2.2E-10	9.4E-10
11000	3.0E-10	1.1E-08	1.3E-04	3.0E-06	3.0E-10	5.9E-10	1.7E-09
12000	4.4E-10	1.7E-08	1.7E-04	4.8E-06	4.5E-10	9.6E-10	2.5E-09
13000	5.6E-10	2.1E-08	2.0E-04	6.6E-06	5.7E-10	1.3E-09	3.2E-09
14000	6.5E-10	2.4E-08	2.2E-04	8.4E-06	6.6E-10	1.7E-09	4.0E-09
5000	7.4E-10	2.7E-08	2.3E-04	1.0E-05	7.5E-10	2.0E-09	4.8E-09
16000	8.4E-10	3.0E-08	2.2E-04	1.3E-05	8.4E-10	2.5E-09	5.1E-09
18000	1.0E-09	3.6E-08	2.0E-04	1.8E-05	1.0E-09	3.6E-09	5.8E-09
20000	1.2E-09	3.9E-08	1.8E-04	2.4E-05	1.2E-09	4.8E-09	6.4E-09
25000	9.7E-10	3.1E-08	9.0E-05	3.1E-05	9.7E-10	6.1E-09	5.0E-09
30000	7.4E-10	2.2E-08	4.3E-05	3.3E-05	7.4E-10	7.2E-09	3.6E-09
35000	3.2E-10	8.9E-09	1.4E-05	2.1E-05	3.2E-10	4.6E-09	2.1E-09
40000	9.9E-11	2.7E-09	2.6E-06	9.9E-06	9.9E-11	2.1E-09	4.8E-10
45000	1.3E-10	3.3E-09	5.2E-06	2.0E-05	1.3E-10	4.3E-09	3.1E-09
50000	1.0E-10	2.3E-09	3.7E-06	2.3E-05	1.0E-10	5.0E-09	4.3E-09
55000	7.4E-11	1.6E-09	2.2E-06	2.5E-05	7.4E-11	5.3E-09	4.9E-09
60000	5.3E-11	1.1E-09	1.4E-06	2.7E-05	5.4E-11	5.8E-09	5.4E-09
65000	3.9E-11	7.4E-10	8.1E-07	2.7E-05	3.9E-11	6.4E-09	5.9E-09
70000	2.9E-11	5.1E-10	4.8E-07	2.9E-05	2.6E-11	6.8E-09	6.6E-09
75000	2.0E-11	3.5E-10	2.8E-07	3.2E-05	2.0E-11	7.5E-09	7.0E-09
80000	1.4E-11	2.3E-10	1.6E-07	3.4E-05	1.4E-11	7.7E-09	7.3E-09
85000	1.1E-11	1.6E-10	9.6E-08	3.7E-05	1.1E-11	8.4E-09	7.7E-09
90000	6.4E-12	8.3E-11	4.5E-08	3.2E-05	6.2E-12	7.3E-09	6.8E-09
95000	4.2E-12	5.1E-11	2.3E-08	3.1E-05	3.9E-12	6.9E-09	6.1E-09
100000	2.0E-12	2.3E-11	9.4E-09	2.3E-05	1.9E-12	5.2E-09	4.6E-09

Table 6A-7. (continued)[1]

Year	^{93M}Nb (Ci/Yr)	^{94}Nb (Ci/Yr)	^{59}Ni (Ci/Yr)	^{237}Np (Ci/Yr)	^{210}Pb (Ci/Yr)	^{107}Pd (Ci/Yr)	^{239}Pu (Ci/Yr)
7000	0.0E+00	0.0E+00	0.0E+00	0.0E+00	0.0E+00	0.0E+00	0.0E+00
7500	0.0E+00	0.0E+00	0.0E+00	0.0E+00	0.0E+00	0.0E+00	0.0E+00
8000	3.2E-07	3.6E-07	6.5E-06	3.3E-11	9.8E-13	2.4E-12	1.5E-08
8500	5.4E-07	7.0E-07	1.3E-05	5.7E-11	1.8E-12	4.1E-12	2.6E-08
9000	4.3E-07	1.1E-06	2.2E-05	4.5E-11	1.6E-12	3.2E-12	2.1E-08
9500	4.0E-06	2.3E-06	4.3E-05	4.2E-10	1.5E-11	3.0E-11	1.8E-07
10000	7.6E-06	3.3E-06	6.4E-05	7.9E-10	3.1E-11	5.7E-11	3.3E-07
11000	2.1E-05	5.9E-06	1.2E-04	2.2E-09	9.6E-11	1.5E-10	8.8E-07
12000	3.3E-05	8.2E-06	1.7E-04	3.5E-09	1.7E-10	2.5E-10	1.4E-06
13000	4.6E-05	1.0E-05	2.1E-04	4.8E-09	2.6E-10	3.5E-10	1.8E-06
14000	5.9E-05	1.2E-05	2.6E-04	6.2E-09	3.6E-10	4.4E-10	2.3E-06
15000	7.2E-05	1.4E-05	3.1E-04	7.5E-09	4.6E-10	5.4E-10	2.7E-06
16000	8.8E-05	1.5E-05	3.3E-04	9.2E-09	7.1E-10	6.5E-10	3.2E-06
18000	1.3E-04	1.6E-05	3.6E-04	1.3E-08	1.1E-09	9.5E-10	4.4E-06
20000	1.7E-04	1.6E-05	3.9E-04	1.7E-08	1.7E-09	1.3E-09	5.4E-06
25000	2.1E-04	1.1E-05	2.9E-04	2.2E-08	2.6E-09	1.6E-09	6.1E-06
30000	2.5E-04	6.6E-06	2.0E-04	2.6E-08	3.6E-09	1.9E-09	6.1E-06
35000	1.6E-04	3.1E-06	1.1E-04	1.7E-08	2.5E-09	1.2E-09	3.4E-06
40000	7.4E-05	6.3E-07	2.3E-05	7.8E-09	1.3E-09	5.6E-10	1.4E-06
45000	1.5E-04	3.3E-06	1.5E-04	1.5E-08	2.8E-09	1.1E-09	2.3E-06
50000	1.7E-04	3.9E-06	2.0E-04	1.8E-08	3.7E-09	1.3E-09	2.3E-06
55000	1.8E-04	3.7E-06	2.2E-04	1.9E-08	4.1E-09	1.4E-09	2.3E-06
60000	2.0E-04	3.4E-06	2.3E-04	2.1E-08	4.7E-09	1.5E-09	2.1E-06
65000	2.2E-04	3.2E-06	2.4E-04	2.3E-08	5.4E-09	1.7E-09	2.0E-06
70000	2.3E-04	2.9E-06	2.6E-04	2.4E-08	6.3E-09	1.8E-09	1.8E-06
75000	2.6E-04	2.6E-06	2.6E-04	2.7E-08	6.9E-09	2.0E-09	1.8E-06
80000	2.7E-04	2.3E-06	2.6E-04	2.8E-08	7.7E-09	2.1E-09	1.6E-06
85000	3.0E-04	2.1E-06	2.6E-04	3.1E-08	8.7E-09	2.3E-09	1.6E-06
90000	2.6E-04	1.5E-06	2.2E-04	2.7E-08	7.9E-09	2.0E-09	1.1E-06
95000	2.4E-04	1.1E-06	1.9E-04	2.6E-08	7.8E-09	1.9E-09	9.5E-07
100000	1.8E-04	7.3E-07	1.4E-04	1.9E-08	5.9E-09	1.4E-09	6.3E-07

Table 6A-7. (continued)[1]

Year	^{240}Pu (Ci/Yr)	^{241}Pu (Ci/Yr)	^{242}Pu (Ci/Yr)	^{226}Ra (Ci/Yr)	^{79}Se (Ci/Yr)	^{126}Sn (Ci/Yr)	^{99}Tc (Ci/Yr)
7000	0.0E+00	0.0E+00	0.0E+00	0.0E+00	0.0E+00	0.0E+00	0.0E+00
7500	0.0E+00	0.0E+00	0.0E+00	0.0E+00	0.0E+00	0.0E+00	0.0E+00
8000	2.3E-09	6.0E-12	4.5E-11	9.8E-13	1.2E-11	1.9E-11	2.3E-08
8500	3.8E-09	9.6E-12	8.0E-11	1.8E-12	2.1E-11	3.5E-11	4.6E-08
9000	3.2E-09	7.1E-12	7.5E-11	1.6E-12	2.2E-11	4.5E-11	7.6E-08
9500	2.3E-08	6.6E-11	5.3E-10	1.5E-11	1.3E-10	1.8E-10	1.5E-07
10000	4.1E-08	1.2E-10	9.8E-10	3.1E-11	2.4E-10	3.1E-10	2.3E-07
11000	9.9E-08	3.0E-10	2.6E-09	9.6E-11	6.3E-10	7.7E-10	4.2E-07
12000	1.4E-07	4.4E-10	4.2E-09	1.7E-10	9.6E-10	1.2E-09	6.0E-07
13000	1.8E-07	5.6E-10	5.8E-09	2.6E-10	1.3E-09	1.6E-09	7.8E-07
14000	2.1E-07	6.5E-10	7.4E-09	3.6E-10	1.7E-09	2.0E-09	9.7E-07
15000	2.3E-07	7.4E-10	9.0E-09	4.6E-10	2.0E-09	2.4E-09	1.1E-06
16000	2.5E-07	8.4E-10	1.1E-08	7.1E-10	2.4E-09	2.9E-09	1.2E-06
18000	2.9E-07	1.0E-09	1.6E-08	1.1E-09	3.4E-09	4.1E-09	1.4E-06
20000	3.0E-07	1.2E-09	2.1E-08	1.7E-09	4.2E-09	5.0E-09	1.5E-06
25000	2.3E-07	9.9E-10	2.6E-08	2.6E-09	5.1E-09	5.9E-09	1.2E-06
30000	1.5E-07	7.4E-10	3.0E-08	3.6E-09	5.6E-09	6.6E-09	8.4E-07
35000	5.9E-08	3.2E-10	2.0E-08	2.5E-09	3.4E-09	4.1E-09	4.7E-07
40000	1.7E-08	9.9E-11	9.1E-09	1.3E-09	1.5E-09	1.8E-09	1.1E-07
45000	2.0E-08	1.3E-10	1.8E-08	2.8E-09	2.9E-09	3.5E-09	6.7E-07
50000	1.3E-08	1.0E-10	2.0E-08	3.7E-09	3.2E-09	4.2E-09	9.3E-07
55000	8.5E-09	7.4E-11	2.1E-08	4.1E-09	3.2E-09	4.3E-09	1.0E-06
60000	5.4E-09	5.3E-11	2.3E-08	4.7E-09	3.4E-09	4.4E-09	1.1E-06
65000	3.5E-09	3.9E-11	2.5E-08	5.4E-09	3.5E-09	4.8E-09	1.2E-06
70000	2.2E-09	2.9E-11	2.7E-08	6.3E-09	3.5E-09	4.9E-09	1.3E-06
75000	1.4E-09	2.0E-11	2.9E-08	6.9E-09	3.6E-09	5.4E-09	1.4E-06
80000	9.0E-10	1.4E-11	3.1E-08	7.7E-09	3.8E-09	5.3E-09	1.4E-06
85000	5.8E-10	1.1E-11	3.3E-08	8.7E-09	3.8E-09	5.5E-09	1.5E-06
90000	3.0E-10	6.2E-12	2.9E-08	7.9E-09	3.3E-09	4.8E-09	1.3E-06
95000	1.7E-10	3.9E-12	2.7E-08	7.8E-09	2.9E-09	4.2E-09	1.1E-06
100000	7.4E-11	1.9E-12	2.0E-08	5.9E-09	2.1E-09	3.2E-09	8.5E-07

Table 6A-7. (continued)[1]

Year	^{229}Th (Ci/Yr)	^{230}Th (Ci/Yr)	^{233}U (Ci/Yr)	^{234}U (Ci/Yr)	^{236}U (Ci/Yr)	^{93}Zr (Ci/Yr)
7000	0.0E+00	0.0E+00	0.0E+00	0.0E+00	0.0E+00	0.0E+00
7500	0.0E+00	0.0E+00	0.0E+00	0.0E+00	0.0E+00	0.0E+00
8000	3.5E-11	1.4E-12	6.7E-11	1.9E-11	9.5E-13	3.2E-07
8500	6.6E-11	2.5E-12	1.1E-10	3.2E-11	1.6E-12	5.5E-07
9000	5.2E-11	2.0E-12	8.9E-11	2.5E-11	1.3E-12	4.4E-07
9500	4.8E-10	2.0E-11	8.3E-10	2.4E-10	1.3E-11	4.0E-06
10000	1.0E-09	4.0E-11	1.6E-09	4.5E-10	2.5E-11	7.6E-06
11000	2.7E-09	1.2E-10	4.3E-09	1.2E-09	7.1E-11	2.1E-05
12000	4.8E-09	2.1E-10	7.0E-09	1.9E-09	1.2E-10	3.4E-05
13000	7.1E-09	3.1E-10	9.6E-09	2.7E-09	1.7E-10	4.6E-05
14000	9.1E-09	4.2E-10	1.2E-08	3.4E-09	2.2E-10	5.9E-05
15000	1.1E-08	5.4E-10	1.5E-08	4.2E-09	2.8E-10	7.2E-05
16000	1.4E-08	7.1E-10	1.8E-08	5.1E-09	3.5E-10	8.8E-05
18000	2.2E-08	1.1E-09	2.7E-08	7.3E-09	5.2E-10	1.3E-04
20000	2.9E-08	1.7E-09	3.5E-08	9.6E-09	7.0E-10	1.7E-04
25000	4.0E-08	2.6E-09	4.2E-08	1.2E-08	9.4E-10	2.1E-04
30000	5.0E-08	3.6E-09	5.0E-08	1.4E-08	1.1E-09	2.5E-04
35000	3.2E-08	2.5E-09	3.2E-08	8.9E-09	7.5E-10	1.6E-04
40000	1.5E-08	1.3E-09	1.5E-08	4.0E-09	3.5E-10	7.4E-05
45000	2.9E-08	2.8E-09	2.9E-08	8.0E-09	6.9E-10	1.5E-04
50000	3.5E-08	3.7E-09	3.5E-08	9.2E-09	8.3E-10	1.7E-04
55000	3.7E-08	4.1E-09	3.5E-08	9.7E-09	8.8E-10	1.8E-04
60000	3.8E-08	4.7E-09	3.8E-08	1.0E-08	9.6E-10	2.0E-04
65000	4.2E-08	5.4E-09	4.2E-08	1.1E-08	1.1E-09	2.2E-04
70000	4.5E-08	6.3E-09	4.5E-08	1.2E-08	1.1E-09	2.3E-04
75000	4.9E-08	6.9E-09	4.9E-08	1.3E-08	1.2E-09	2.6E-04
80000	5.2E-08	7.7E-09	5.2E-08	1.3E-08	1.3E-09	2.7E-04
85000	5.7E-08	8.7E-09	5.4E-08	1.5E-08	1.4E-09	3.0E-04
90000	5.0E-08	7.9E-09	4.7E-08	1.3E-08	1.3E-09	2.6E-04
95000	4.7E-08	7.8E-09	4.4E-08	1.2E-08	1.2E-09	2.4E-04
100000	3.6E-08	5.9E-09	3.3E-08	8.8E-09	9.0E-10	1.8E-04

[1]Isotopes having releases of 10^{-10} Ci/yr or lower are omitted from the table.

Table 6A-8. Number and Type of Waste Packages for the Total Inventory of DOE SNF (2,496 MTHM) by Category.*

Category	Package Type (5 × 1)[1] Short[2]	Package Type (5 × 1) Long[3]	Package Type (3 × 1)[4] Short	Package Type (3 × 1) Long	Package Type (0 × 4)[5] Long	Package Type (21)[6] Long
1	2	4			101	
2	2	6				
3	70					
4	66	127			5	16
5	298	388				
6	673	33				
7	165	50				
8		503				
9		60				
10	3	2				
11	38	329				
12	15	9		47		
13	92	8				
15						
16	24	20				
Total	1448	1539		47	106	16

*Data provided by the National Spent Nuclear Fuel program (Stroupe, 1998).

[1]A 5 × 1 package contains five 610 mm (24 inch) canisters of HLW and one 432 mm (17 inch) canister of spent fuel.

[2]A short package contains canisters that are 3.05 m (10 feet) in length.

[3]A long package contains canisters that are 4.57 m (15 feet) in length.

[4]A 3 × 1 package contains three 610 mm (24 inch) canisters of HLW and one 610 mm (24 inch) canister of spent fuel.

[5]A 0 × 4 package contains four 610 mm (24 inch) canisters of spent fuel.

[6]A 21 package is a standard PWR package for 21 spent fuel assemblies.

Table 6A-9. Number of Waste Packages and HLW Canisters for Disposal of the Total Inventory of DOE Spent Fuel (2,496 MTHM).

Category	Number of Packages	Number of Short[1] HLW Canisters	Number of Long[2] HLW Canisters
1	107	10	20
2	8	10	30
3	70	350	
4	214	330	635
5	686	1490	1940
6	706	3365	165
7	215	825	250
8	503		2515
9	60		300
10	5	15	10
11	367	190	1645
12	71	75	186
13	100	460	40
15			
16	44	120	100
Total	3156	7240	7836

[1]A short package contains canisters that are 3.05 m (10 feet) in length.

[2]A long package contains canisters that are 4.57 m (15 feet) in length.

Table 6A-10. Number and Type of Waste Packages for the Modified Inventory of DOE SNF (2,333 MTHM) by Category.*

Category	Package Type (5 × 1)[1] Short[2]	Package Type (5 × 1) Long[3]	Package Type (3 × 1)[4] Short	Package Type (3 × 1) Long	Package Type (0 × 4)[5] Long	Package Type (21)[6] Long
1	2	4			95	
2	2	6				
3	66					
4	62	120			5	15
5	279	363				
6	628	31				
7	154	47				
8		470				
9		56				
10	3	2				
11	36	308				
12	14	9		44		
13	86	8				
15						
16	23	19				
Total	1355	1443		44	100	15

*Data provided by the National Spent Nuclear Fuel program (Stroupe, 1998).

[1]A 5 × 1 package contains five 610 mm (24 inch) canisters of HLW and one 432 mm (17 inch) canister of spent fuel.

[2]A short package contains canisters that are 3.05 m (10 feet) in length.

[3]A long package contains canisters that are 4.57 m (15 feet) in length.

[4]A 3 × 1 package contains three 610 mm (24 inch) canisters of HLW and one 610 mm (24 inch) canister of spent fuel.

[5]A 0 × 4 package contains four 610 mm (24 inch) canisters of spent fuel.

[6]A 21 package is a standard PWR package for 21 spent fuel assemblies.

Table 6A-11. Number of Waste Packages and HLW Canisters for Disposal of the Modified Inventory of DOE Spent Fuel (2,333 MTHM).

Category	Number of Packages	Number of Short[1] HLW Canisters	Number of Long[2] HLW Canisters
1	101	10	20
2	8	10	30
3	66	330	
4	202	310	600
5	642	1395	1815
6	659	3140	155
7	201	770	235
8	470		2350
9	56		280
10	5	15	10
11	344	180	1540
12	67	70	177
13	94	430	40
15			
16	42	115	95
Total	2957	6775	7347

[1]A short package contains canisters that are 3.05 m (10 feet) in length.

[2]A long package contains canisters that are 4.57 m (15 feet) in length.

Table 6A-12. Physical Characteristics of DOE SNF.[1]

Category	Air Alteration Rate (fraction/yr)	Matrix Dissolution Rate ($g/m^2/yr$)	Matrix Surface Area (m^2/g)	Failed Cladding (%)	Free Radionuclide Inventory (fraction)	Gap Radionuclide Inventory (fraction)
1	0	metal model	7.0E-05	100	0.001	0
2	0	metal model	6.5E-03	10	0.00001	0
3	0	metal model x 10	4.0E-04	10	0.00001	0
4	0	oxide model	9.5E-04	100	0	.01-.02
5	0	oxide model	9.5E-02	100	0	0.0001
6	0	metal model x 0.1	7.4E-03	100	0.0001	0
7	0	metal model x 0.1	1.4E-02	100	0.0001	0
8	0	Si carbide model	2.2E-02	1	0.00001	0
9	0	metal model x 10	2.2E-02	60	0.1	0.001
10	0	metal model x 100	2.6E-03	10	0	.01-.02
11	0	oxide model	9.5E-04	10	0	.01-.02
12	0	ceramic model	5.0E-04	10	0	.01-.02
13	0	oxide model x 0.1	1.0E-04	10	0.00001	0.00001
15	N/A[2]	N/A	N/A	N/A	N/A	N/A
16	0	metal model	7.0E-05	100	0.001	0

[1]Data provided by the National Spent Nuclear Fuel program (Stroupe 1998).

[2]Navy SNF is analyzed using a release source term at the boundary of the waste package.

CHAPTER 6

APPENDIX B

ANALYSIS OF PLUTONIUM DISPOSITION WASTES

INTENTIONALLY LEFT BLANK

CONTENTS

B-1. SOURCE TERM FOR plutonium waste forms B6-1

B-1.1 WASTE FORMS B6-1

B-1.2 RADIONUCLIDE INVENTORIES B6-1

B-1.3 WASTE PACKAGE TYPES AND LOADING B6-1

B-1.4 PHYSICAL CHARACTERISTICS OF WASTE FORMS B6-2

B-1.5 WASTE FORM DISSOLUTION MODELS B6-2
- B-1.5.1 Ceramic B6-2
- B-1.5.2 Oxide (Commercial) Spent Fuel B6-3
- B-1.5.3 High-Level Waste Glass B6-3

B-2. DOSE TO HUMANS B6-3

B-2.1 DOSE ATTRIBUTED TO EACH WASTE FORM B6-3
- B-2.1.1 Mixed Oxide (MOX) Spent Fuel B6-4
- B-2.1.2 Can-In-Canister Ceramic B6-4

B-2.2 DOSE ATTRIBUTED TO COMBINED WASTE FORMS B6-4
- B-2.2.1 Combinations of Plutonium Waste Forms B6-4
- B-2.2.2 TSPA-VA Base Case B6-5

B-2.3 COMPARISON OF RESULTS B6-5

B-3. EVALUATION OF SENSITIVITY AND UNCERTAINTY B6-6

B-3.1 WASTE FORM DISSOLUTION RATE AND SURFACE AREA B6-6

B-3.2 WASTE FORM DISSOLUTION MODEL B6-6

B-3.3 NUMBER OF WASTE PACKAGES B6-7

B-4. CONCLUSIONS B6-8

B-4.1 REFERENCES B6-10

FIGURES

Figure 6B-1. Schematic Diagram of Can-in-Canister Waste Form B6-11

Figure 6B-2. Waste Package Used for Disposal of High-Level Waste and Can-in-Canister Ceramic. B6-12

Figure 6B-3. Expected-Value Dose History at 20 Kilometers Over 100,000 Years from 75 Packages of Mixed Oxide Spent Fuel (33 metric ton case). B6-13

Figure 6B-4 Expected-Value Dose History at 20 Kilometers over 100,000 Years from 75 Packages of Commercial Spent Fuel. B6-14

Figure 6B-5. Expected-Value Dose History at 20 Kilometers over 100,000 Years from 159 Packages of Can-in-Canister Ceramic (17 metric ton case). B6-15

Figure 6B-6. Expected-Value Dose History at 20 Kilometers over 100,000 Years from 159 Packages of HLW. B6-16

Figure 6B-7. Expected-Value Dose History at 20 Kilometers over 100,000 Years from 75 Packages of Mixed Oxide Spent Fuel and 159 packages of Can-in-Canister Ceramic (33 metric tons of MOX and 17 metric tons of ceramic). B6-17

Figure 6B-8. Expected-Value Dose History at 20 Kilometers Over 100,000 Years from 436 Packages of Can-in-Canister Ceramic (50 metric ton case). B6-18

Figure 6B-9. Expected-Value Dose History at 20 Kilometers Over 100,000 Years from 436 Packages of HLW. B6-19

Figure 6B-10. Expected-Value Dose History at 20 Kilometers Over 100,000 Years from TSPA-VA Base Case. B6-20

Figure 6B-11 Expected-Value Dose History at 20 Kilometers over 100,000 Years from 75 Packages of MOX Spent Fuel Compared to 75 Packages of Commercial Spent Fuel. B6-21

Figure 6B-12. Expected-Value Dose History at 20 Kilometers over 100,000 Years from 159 Packages of Can-in-Canister Ceramic Compared to 159 Packages of HLW. B6-22

Figure 6B-13. Expected-Value Dose History at 20 Kilometers Over 100,000 Years from 436 Packages of Can-in-Canister Ceramic Compared to 436 Packages of HLW B6-23

Figure 6B-14. Effects of Uncertain Dissolution Rate on Dose from Mixed Oxide Spent Fuel. B6-24

Figure 6B-15. Effects of Uncertain Surface Area on Dose from Mixed Oxide Spent Fuel. B6-25

Figure 6B-16. Effects of Uncertain Dissolution Rate on Dose from Plutonium Ceramic. B6-26

Figure 6B-17. Effects of Uncertain Surface Area on Dose from Plutonium Ceramic. B6-27

Figure 6B-18. Effects of Uncertain Dissolution Model on Dose from Plutonium Ceramic; Ceramic Using the Ceramic Dissolution Model Compared to Ceramic Using the HLW Glass Model for 50 metric tons of Plutonium in 436 Packages. B6-28

Figure 6B-19. Effects of Uncertain Dissolution Model on Dose from Plutonium Ceramic; Ceramic Using the Ceramic Dissolution Model Compared to Ceramic Using the HLW Glass Model for 50 metric tons of Plutonium in 872 Packages. B6-29

Figure 6B-20. Sensitivity of Dose from Mixed Oxide Spent Fuel to Number of Waste Packages; 75 Packages Compared to 150 Packages for the 33 Metric Ton Case. B6-30

TABLES

Table 6B-1. Radionuclide Inventory for Mixed Oxide (MOX) Spent Fuel..... B6-31

Table 6B-2. Radionuclide Inventories for Commercial Spent Fuel and High-Level Waste (HLW). B6-32

Table 6B-3. Radionuclide Inventory for Surplus Plutonium Used in Can-In-Canister Ceramic. B6-33

Table 6B-4. Physical Characteristics of Commercial Spent Fuel, HLW, and Plutonium Ceramic. B6-33

APPENDIX B
ANALYSIS OF PLUTONIUM DISPOSITION WASTES

B-1. SOURCE TERM FOR PLUTONIUM WASTE FORMS

The source term is a description of the rate and duration of radionuclide release from the engineered barrier system. It is a function of: the total radionuclide inventory; the number of waste packages; the package failure rate, the waste form alteration/dissolution (leaching) rate; waste form surface area; solubility of radionuclides; and the mode of radionuclide migration through the failed barrier system (i.e., by advection or diffusion). Temperature, amount water, water movement, and water chemistry affect the source term. This chapter describes the primary components of the source term used for each waste form. It includes the radionuclide inventory, the waste packaging, the physical characteristics of the waste, and the dissolution/alteration model.

B-1.1 WASTE FORMS

For disposal of plutonium two waste forms are being considered, mixed oxide (MOX) nuclear fuel and can-in-canister ceramic. About 5% plutonium, by weight, is incorporated into the (MOX) fuel and it is assumed to be burned in a current pressurized water reactor (PWR). The resulting spent fuel is assumed to be a mixture of two- and three-cycle burn, with the two-cycle being burned for 35 GWd/ton and the three-cycle being burned for 52.5 GWd/ton (Murphy, 1997). The mixture is assumed to be 46.3% two-cycle and 53.7% three-cycle (Murphy 1998). These percentages were used to determine the average radionuclide inventory for the MOX spent fuel analyzed based on ORIGIN analyses inventory for two-cycle (Murphy, 1998) and three-cycle (Primm 1997; Murphy 1998) MOX spent fuel that is 30 years old.

The can-in-canister ceramic is a waste form where plutonium ceramic disks are contained in 28 cans that are then encapsulated in high-level waste (HLW) in a HLW canister (Gould, 1998). The 28 cans displace about 12% of the volume of a standard HLW canister (Figure 6B-1).

B-1.2 RADIONUCLIDE INVENTORIES

The radionuclide inventory for the MOX spent fuel is presented in Table 6B-1. Both the two- and three-cycle inventories are presented along with the average inventory. As stated earlier the average inventory is assumed to be 46.3% two-cycle and 53.7 percent three-cycle MOX (Murphy 1998). For comparison Table 6B-2 shows the radionuclide inventories for commercial spent fuel and HLW that are used in the base case. Table 6B-3 shows the Radionuclide inventory for the surplus plutonium used in the ceramic of the can-in-canister ceramic for both the 17-ton case and the 50-ton case (Gould, 1998).

B-1.3 WASTE PACKAGE TYPES AND LOADING

The MOX spent fuel is packaged in 21 assembly Pressurized Water Reactor spent fuel packages. For disposal of 33 metric tons of plutonium as MOX spent fuel there are 1,567 spent fuel assemblies that can be disposed in 75 PWR packages.

The can-in-canister ceramic is encapsulated in four canisters that are contained in a HLW package (Figure 6B-2). For the 17 ton case disposal requires 159 packages, and for the 50 ton case disposal requires 436 packages (Gould 1998). The former case is called the 17-ton case for historical reasons even though the total quantity of material in it is closer to 18.2 metric tons. The 18.2 tons of plutonium is impure and is only suitable for disposal as an encapsulated waste form. This nomenclature has been extended to the MOX spent fuel that is referred to as the 33-ton case.

B-1.4 PHYSICAL CHARACTERISTICS OF WASTE FORMS

The MOX spent fuel is assumed to have the same physical properties as commercial spent fuel. The HLW is assumed to have the same physical characteristics as the HLW in the TSPA-VA base case with the exception that there is about 12% (by volume) less per canister because of the displacement of the cans of ceramic. Table 6B-4 shows the physical characteristics of Commercial spent fuel, HLW and plutonium ceramic. The MOX spent fuel is assumed to have the same physical characteristics as commercial spent fuel.

B-1.5 WASTE FORM DISSOLUTION MODELS

B-1.5.1 Ceramic

The dissolution model for ceramic was taken from Lappa (1995). The composition of the ceramic was assumed by Lappa to be similar to that of Synroc-C, a titanate ceramic. Reeve et al. (1989) proposed that the cumulative release from Synroc to be:

$$Q = Q_0 + \theta + SFt/A \qquad (6B\text{-}1)$$

where

Q = release rate per unit surface area (g/m^2),

Q_0 = instantaneous release from grain boundaries and metastable phases (g/m^2),

θ = kinetic function that accounts for ionic diffusion, selective matrix attack, etc (g/m^2),

S = solubility of the matrix (g/m^2),

F = ground-water flow rate (m^3/ day),

A = surface area (m^2), and

T = time (days).

Lappa states that it is likely that the long-term release from the Synroc is controlled by the third term of the equation. Existing data indicate that S is less than or equal to 0.007 g/m^3 based on a long-term leaching rate of less than or equal to 10^{-4} g/m^2/day when SA/C is 10 m^{-1} at 70 degrees

Centigrade in deionized water (Lappa, 1995). The leaching rate also increases with increasing temperature (Ringwood et. al., 1988). This temperature effect is described by:

$$R = \alpha\ 10^{-\beta(1000/T)} \tag{6B-2}$$

where

R	=	leaching rate ^{2}-(g/m^2 day)
T	=	temperature in degrees K, and
α and β =		are constants.

Based on the Synroc data of Ringwood et. al. (1988), $\beta \approx 1.0$ and $\alpha \approx 0.082$ g/m^2/day when SA/C is 10 m^{-1} at 70 degrees Centigrade. These are the same conditions that were assumed in TSPA 1995 for HLW glass. The release rate can be calculated by multiplying R by the surface area (S) and the elapsed time (t). The radionuclides are released from the waste form based on its alteration rate, and are then transported at a rate dependant on whether they are alteration controlled or solubility-limited radionuclides.

The alteration/dissolution rate presented above is for a monolithic form, and if the monolith is cracked the release rate could be significantly different. The release rate should be measured in the ongoing research and development program to provide a more valid release in the repository environment.

B-1.5.2 Oxide (Commercial) Spent Fuel

See Section 6.3.1.3.2.

B-1.5.3 High-Level Waste Glass

See Section 6.3.3.3.

B-2. DOSE TO HUMANS

The plutonium waste forms were analyzed by placing them, one at a time, in the environment of the TSPA-VA base case and calculating the expected-value dose history attributed to that waste form for an individual using water from a well 20 kilometers down gradient from the repository. The dose to the individual is from all sources: ingestion of food and water, inhalation, and exposure to contaminated areas and water.

B-2.1 DOSE ATTRIBUTED TO EACH WASTE FORM

Two waste forms are analyzed. They are MOX spent fuel and can-in-canister ceramic. Two cases of disposal of 50 metric tons of surplus plutonium were analyzed; the first for disposal of

33 tons as MOX spent fuel and 17 tons as can-in-canister ceramic, and the second for disposal of 50 tons as can-in-canister ceramic. The 17-ton case for can-in-canister actually uses 18.2 metric tons of plutonium.

B-2.1.1 Mixed Oxide (MOX) Spent Fuel

The expected-value dose history attributed to the MOX spent fuel that is disposed in 75 PWR packages is shown in Figure 6B-3. The 75 packages contain the MOX spent fuel that results from disposal of 33 tons of surplus plutonium. The four spikes in dose observed on this figure, for alteration-controlled radionuclides (Tc-99, I-129, and C-14), represent individual waste package failures. Of the 75 packages analyzed, only four are expected to fail over 100,000 years. When a package fails, the alteration-controlled radionuclides are "rapidly" flushed from the package. Here, "rapidly" is over a period of a few thousand years. The dose curves for other radionuclides are smoother because of three factors: the effects of the Zircaloy cladding, there solubility limit, and sorption along the transport pathway. For comparison, the expected value dose history for 75 packages of commercial spent fuel is shown in Figure 6B-4. Comparison of Figures 6B-3 and 6B-4 shows that the dose from the MOX spent fuel is about the same as that from an equivalent amount of commercial spent fuel.

B-2.1.2 Can-In-Canister Ceramic

The expected-value dose history from disposal of 159 packages of can-in-canister is shown in Figure 6B-5. The figure was developed by adding the results of analyses of 159 packages of only the ceramic to the analysis of 159 packages of only the HLW used to encapsulate the ceramic. This approach was used in order to apply the ceramic dissolution model to the ceramic and the glass dissolution model to the HLW, because two different dissolution models cannot be applied within the same waste package. The result is conservative because the approach assumes that leaching of both waste forms, the ceramic and the glass, begins at the time the package is breached. A less conservative approach would be to delay the leaching of the ceramic for a time equal to that necessary to dissolve enough glass to expose the cans of ceramic. Figure 6B-6 shows the expected-value dose history for 159 packages of HLW. Comparison of the two figures, Figure 6B-5 and 6B-6, shows that the total dose for the two are essentially the same, but there is an increase in the dose from Pu-239 and Pu-242 for the can-in-canister ceramic, as would be expected. However, this increase is not enough to affect the total dose.

B-2.2 DOSE ATTRIBUTED TO COMBINED WASTE FORMS

B-2.2.1 Combinations of Plutonium Waste Forms

Figure 6B-7 shows the expected-value dose history for disposal of 50 metric tons of surplus plutonium as a combination of MOX and can-in-canister ceramic (33 tons in MOX and 17 tons in ceramic). The total dose form these combined waste forms may be compared to disposal of 50 tons of surplus plutonium as can-in-canister ceramic, Figure 6b-8(b). Comparison of Figures 6B-7 and 6B-8(b) indicates that the total dose from disposal of 50 metric tons of plutonium as a combination of MOX and can-in-canister ceramic is somewhat lower than disposal of all of it as can-in-canister ceramic. The expected value dose history for disposal of 436 packages of HLW is

shown in Figure 6B-9, and is nearly identical to that of an equal number of packages of can-in-canister ceramic.

B-2.2.2 TSPA-VA Base Case

The base case for the TSPA-VA is for a repository that contains 63,000 MTHM of commercial spent fuel, 2,333 MTHM of DOE spent fuel, and 4,667 MTHM of HLW. The plutonium waste forms are not explicitly included in the base case. However, if a portion of the base case HLW is considered to be can-in-canister ceramic and a portion of the commercial spent fuel is consider to be MOX, then the plutonium waste forms would be implicitly in the base case. This implied inclusion in the base case is possible because the dose from the MOX and the can-in-canister ceramic is not significantly different than that from commercial spent fuel and HLW, respectively. The expected-value dose history for the TSPA-VA base case is shown in Figure 6B-10.

B-2.3 COMPARISON OF RESULTS

Figure 6B-4 shows the comparison of expected-value total dose history for 75 packages of MOX spent fuel as compared to 75 packages of commercial spent fuel. The two dose curves are nearly equivalent with the curve for the MOX being somewhat higher than that for the commercial spent fuel. The difference between the two curves is due to the inventory analyzed in each case. The MOX spent fuel was packaged with 21 assemblies per package (about 9.7 MTHM per package) and this was compared to average commercial spent fuel packages used in the base case that contain about 8.1 MTHM per package. This indicates that disposal of 33 tons of plutonium as MOX would have an insignificant affect on the dose from the entire repository, especially when it is assumed to replace an equivalent amount of commercial spent fuel. If the MOX were assumed to be in addition to the commercial spent fuel the affect would still be insignificant. To see this, compare Figure 6B-11 with Figure 6B-10. This comparison shows that the dose from the MOX is about two orders of magnitude below that from the entire repository (i.e., about 700 MTHM of MOX as compared to 63,000 MTHM of commercial spent fuel).

Figure 6B-12 shows the expected-value total dose history for 159 packages of can-in-canister ceramic compared to the same number of packages of HLW. These curves are nearly identical because the ceramic waste form does not contribute significantly to the total dose. The curves differ by only about 12% due to the decrease of 12% in HLW in the packages of can-in-canister ceramic. Figure 6B-13 shows the expected–value dose history for disposal of 436 packages of can-in-canister ceramic as compared to an equivalent number of packages of HLW.

B-3. EVALUATION OF SENSITIVITY AND UNCERTAINTY

B-3.1 WASTE FORM DISSOLUTION RATE AND SURFACE AREA

The dissolution model for commercial spent fuel was used for the MOX spent fuel because both are oxide fuels. The dissolution rate of MOX spent fuel is somewhat uncertain because of the differences in composition of the fuel. To determine the potential effects of this uncertainty, the dissolution rate was increased and decreased by three orders of magnitude and the results are shown in Figure 6B-14. The increase in dissolution rate, of three orders of magnitude, had no effect, and the decrease reduced the peak dose by about an order of magnitude.

The dissolution of the MOX spent fuel is also affected by surface area that is also somewhat uncertain because of differences between commercial spent fuel and MOX spent fuel. Figure 6B-15 shows the results for a two order of magnitude increase and decrease in surface area of the MOX spent fuel. The increase has no significant effect and the decrease tends to reduce the dose from Tc-99 and I-129 but has little influence on the dose from Np-237 (i.e., it smoothes out the spikes caused by release of Tc-99 and I-129). For individual radionuclides see Figure 6B-3. The reason that there is no effect of the increased dissolution rate is that the Tc-99 and I-129 are released nearly instantaneously in either case as compared to the length of a model time step, and release of Np-237 release is controlled by its solubility. The decrease in dissolution rate begins to effect even the highly soluble elements (Tc-99 and I-129) because it limits the amount available for transport. Even at the lower dissolution rate there is still more Np-237 dissolved than can be transported at its solubility limit so its release is not affected.

The sensitivity of dose from the plutonium ceramic to uncertainty in dissolution rate is shown in Figure 6B-16. There is a significant effect for both a three order of magnitude increase or decrease in dissolution rate. However, the peak dose for the increase is the same as that for no increase. The three order of magnitude decrease in dissolution rate has a corresponding decrease in dose of about a factor of eight.

The sensitivity of dose to uncertainty in surface area is shown in Figure 6B-17. As in the case of dissolution rate, the increase in surface area does not change the peak dose. Also, the decrease in surface area, by three orders of magnitude, does not change the peak dose. However, the dose from the plutonium ceramic is sensitive to changes in both dissolution rate and surface area prior to the peak dose that occurs at 100,000 years (Figures 6B-16 and 6B-17, respectively).

B-3.2 WASTE FORM DISSOLUTION MODEL

The choice of the oxide spent fuel dissolution model for the MOX spent fuel is relatively certain because of the similarity of the radionuclides contained in the fuel and the fact that the manufacture of the fuel would be similar to the manufacture of commercial fuel for a PWR. Because of this similarity, the sensitivity of dose to choice of dissolution model for MOX was not analyzed.

The sensitivity of the dose from the plutonium ceramic is analyzed to investigate the effect of uncertainty in the choice of dissolution model. In the extreme, it is felt that the ceramic

dissolution could be no faster than that of the HLW glass. Figure 6B-18 shows a comparison between the glass and ceramic models for the plutonium ceramic contained in 436 packages. The two curves are almost identical and the peak dose for the glass and ceramic dissolution model is the same.

B-3.3 NUMBER OF WASTE PACKAGES

The number of waste packages needed for disposal of MOX spent fuel and can-in-canister ceramic is uncertain because the analyses of criticality are being conducted in parallel with the analyses of performance. For the analyses of performance discussed in this report, the two waste forms are assumed to be packaged in the minimum number of packages. The waste forms are assumed to be packaged with 21 assemblies of MOX spent fuel in a PWR package and four canisters of can-in-canister ceramic in a HLW package. Figure 3.3-1 shows dose attributed to disposing the can-in-canister ceramic in twice as many packages (872 packages), and the assumption of glass and ceramic models for the plutonium ceramic. A comparison of Figure B-19 to 6B-18 shows the difference in disposing of 50 tons of plutonium ceramic in 872 and 436 packages, respectively. This comparison is done to examine the potential effect of having to dispose of the can-in-canister ceramic with only two canisters per waste package because of criticality considerations. As can be seen, the increase in the number of waste packages by a factor of two has a corresponding increase in peak dose.

Figure 6B-20 shows the effect of disposing of the MOX spent fuel in twice as many packages (150 as compared to 75). The dose peaks for Tc-99 and I-129 are lower for the larger number of packages because of the decreased inventory of these radionuclides in each package (by a factor of two). The dose from Np-237 increases because for the larger number of packages because there are more waste package failures (i.e., there are more failed packages releasing Np-237 at its solubility limit).

B-4. CONCLUSIONS

The analyses of performance of plutonium waste forms were conducted by placing the waste forms, one at a time, in the environment of the base case repository for the viability assessment of the Yucca Mountain repository site. The base case repository contains 70,000 MTHM of waste that is comprised of 63,000 MTHM of commercial spent fuel, 2,333 MTHM of DOE spent fuel, and 4,667 MTHM of HLW (DOE 1998). The area mass loading of the repository is 85 metric tons per acre based on commercial spent fuel. The plutonium waste forms were assumed to be disposed in Region 6 of the base case repository. It Region 6 has the highest flux of the six regions in the footprint of the repository is divided into for the purpose of calculations, and the results are expected to be conservative. The MOX spent fuel was assumed to have Zircaloy cladding and was compared to an equivalent amount of commercial spent fuel that identical cladding.

The expected value base case model assumes current dry climate for the first 5,000 years that switches to the long-term average for the remainder of the 100,000 year period that is simulated for the analyses of plutonium waste forms. The expected value percolation flux (net infiltration) is 7.7 mm/yr for the current dry climate and 42 mm/yr for the long-term average climate. For the central-central region (Region 6), 9.3% of the waste packages are expected to be exposed to drips for the current dry climate and 33% are expected to be exposed to drips for the long-term average climate.

Two cases were examined for disposal of 50 metric tons of surplus plutonium; a combination of 33 tons in MOX spent fuel and 17 tons in can-in-canister ceramic, and 50 tons of plutonium in can-in-canister ceramic. The MOX spent fuel is packaged in 75 PWR waste packages, the 17 tons of can-in-canister plutonium is in 159 four canister HLW packages, and the 50 tons of can-in-canister plutonium is packaged in 436 HLW packages.

The waste packages have a 10-cm corrosion allowance outer barrier and a 2-cm corrosion resistant inner barrier. The outer barrier is composed of carbon steel and the inner barrier is composed of Alloy C-22. Because the Alloy C-22 is expected to fail by general corrosion, the lifetime of the waste package has been increased when compared to prior analyses (Duguid et. al. 1997).

The analyses for two plutonium waste forms were conducted: MOX spent fuel and can-in-canister ceramic. The MOX spent fuel is similar in composition and manufacture, is burned in a commercial PWR reactor, and the spent fuel is disposed in a 21 assembly PWR waste package. The can-in-canister ceramic is a plutonium waste form that contains small cans of plutonium ceramic that are encapsulated in HLW in a HLW canister. Four canisters are disposed in a HLW package. Both the PWR and HLW waste packages have the same inner and outer barrier materials and thickness (described above).

The expected-value dose history of an individual located 20 kilometers down gradient from the repository was analyzed for each of the plutonium waste forms. The results for the MOX spent fuel were compared to an equivalent amount of commercial spent fuel, and the results for the can-in-canister ceramic were compared to the same number of canisters of HLW.

Based on comparisons of analyses, MOX spent fuel and can-in-canister ceramic and the comparison of these waste forms to commercial spent fuel and HLW, respectively, the following conclusions are drawn:

- The disposal of 50 metric tons of surplus plutonium in the repository has an insignificant effect on the dose from the entire repository

- The dose from MOX spent fuel is about the same as that from an equivalent amount of commercial spent fuel. Any difference is insignificant compared to the dose from the entire repository, and substitution of the MOX for an equivalent amount of commercial spent fuel (about 700 MTHM) would not have a significant effect on dose from the repository.

- The dose from can-in-canister ceramic, either 159 packages or 436 packages, is nearly identical to that from an equivalent number of HLW packages. This means that disposal of plutonium in the form of can-in-canister ceramic would have no effect on the dose from the repository if an equal number of packages of can-in-canister ceramic were substituted for HLW.

- Assuming a three order of magnitude higher dissolution rate for MOX spent fuel has no significance on the dose. This is attributed to there being more radionuclides dissolved than can be transported from the failed waste package. A three order of magnitude decrease in dissolution rate for MOX spent fuel reduces the peak dose by about one order of magnitude. The reduced dissolution rate is the limiting factor in transport from the failed waste package.

- Assuming a two order of magnitude increase in MOX spent fuel, surface area has no effect on dose. The dissolution rate of the fuel is proportional to surface area (i.e., there are more radionuclides dissolved than can be transported from the failed waste package). A two order of magnitude decrease in surface area reduces the dose spikes that are caused by Tc-99 and I-129, but has little affect on the dose from Np-237. The dissolution rate decreases the availability of alteration controlled radionuclides, but is not low enough to affect the solubility limited radionuclide (i.e., there is more Np-237 dissolved than can be transported from the failed waste package).

- There is little sensitivity of peak dose from plutonium ceramic to a three order of magnitude increase in dissolution rate. A corresponding decrease in dissolution rate decreases the peak dose by about a factor of eight.

- There is little sensitivity of the peak dose from plutonium ceramic to either a two order of magnitude increase or a corresponding decrease in surface area.

- Doubling the number of waste packages by a factor of two has a corresponding increase in peak dose from the plutonium ceramic.

- The peak dose from the plutonium ceramic in can-in-canister ceramic is more than three orders of magnitude below that of the HLW used to encapsulate it.

- Increasing the number of waste packages of the MOX spent fuel by a factor of two lowers the dose spikes caused by Tc-99 and I-129 by a factor of two (i.e., there is half as much of these radionuclides per waste package). The same increase in waste packages increases the dose from Np-237 (i.e., there are more failed packages releasing Np-237 at its solubility limit).

B-4.1 REFERENCES

Gould, T., 1998. Letter Report to Sarvajit S. Sareen, TRW Safety Systems, Inc., Vienna VA, from Lawrence Livermore National Laboratory, Livermore, CA, January 23, 1998.

Lappa, D. A., 1995. Letter Report to D. Harrison, U.S. Department of Energy, from Lawrence Livermore National Laboratory, Livermore, CA, May 9, 1995.

Murphy, B. D., 1997. *Characteristics of Spent Fuel from Plutonium Disposition Reactors, Vol. 3: A Westinghouse Pressurized-Water Reactor Design*, Oak Ridge National Laboratory, ORNL/TM-13170/V3, July, 1997.

Murphy, B. D., 1998. Letter to James Duguid, Duke Engineering & Services, Vienna, VA from Oak Ridge National Laboratory, Oak Ridge, TN, April 20, 1998.

Primm, R. T., 1997. Letter to James Duguid, Duke Engineering & Services, Vienna, VA from Oak Ridge National Laboratory, Oak Ridge, TN, December 10, 1997.

Ringwood, A., Kesson, S., Reeve, K., Levins, D., and Ramm, E., 1988. *Synroc, Radioactive Waste Forms for the Future*, W. Lutze and R. Ewing, Des, North Holland, Amsterdam.

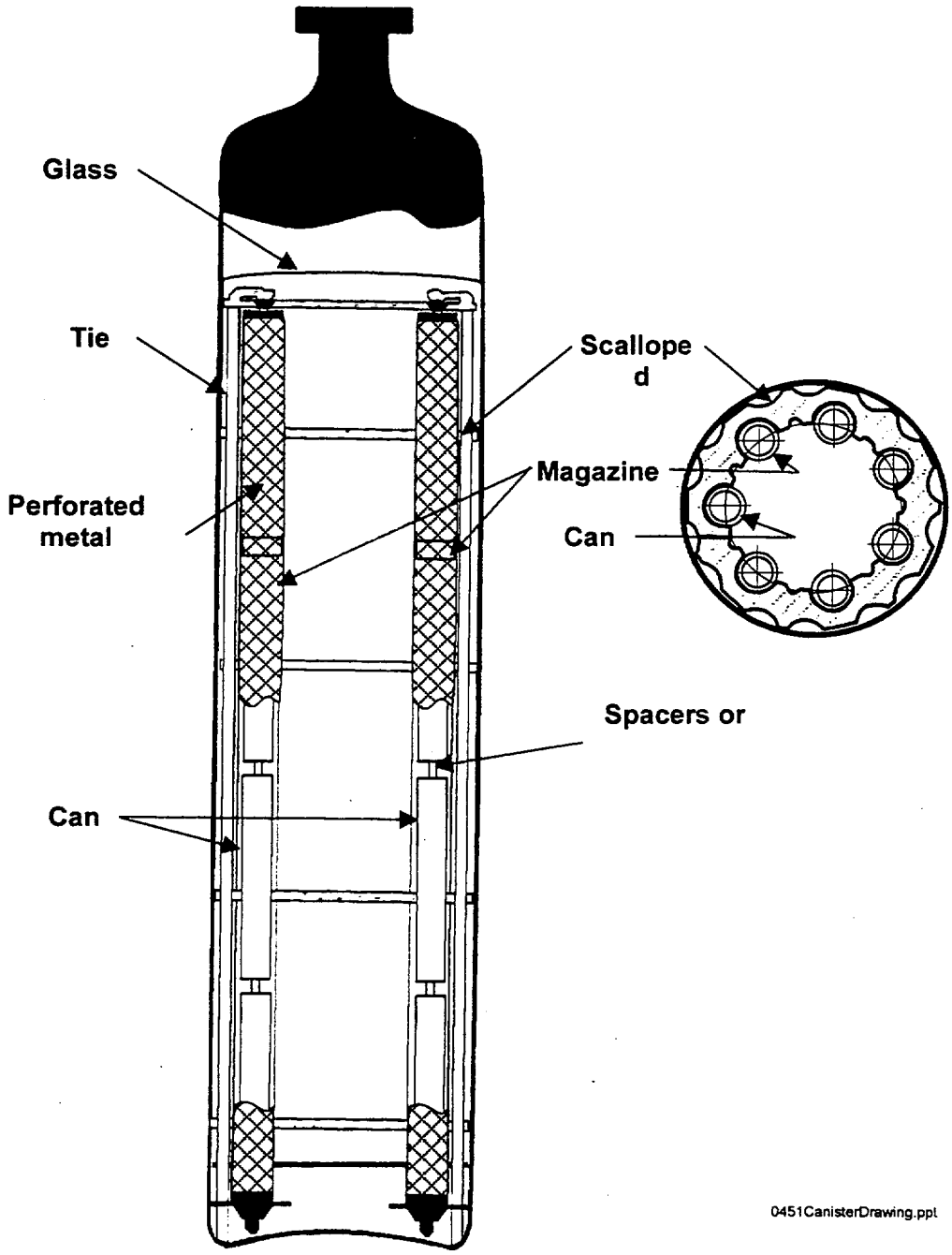

Figure 6B-1. Schematic Diagram of Can-in-Canister Waste Form

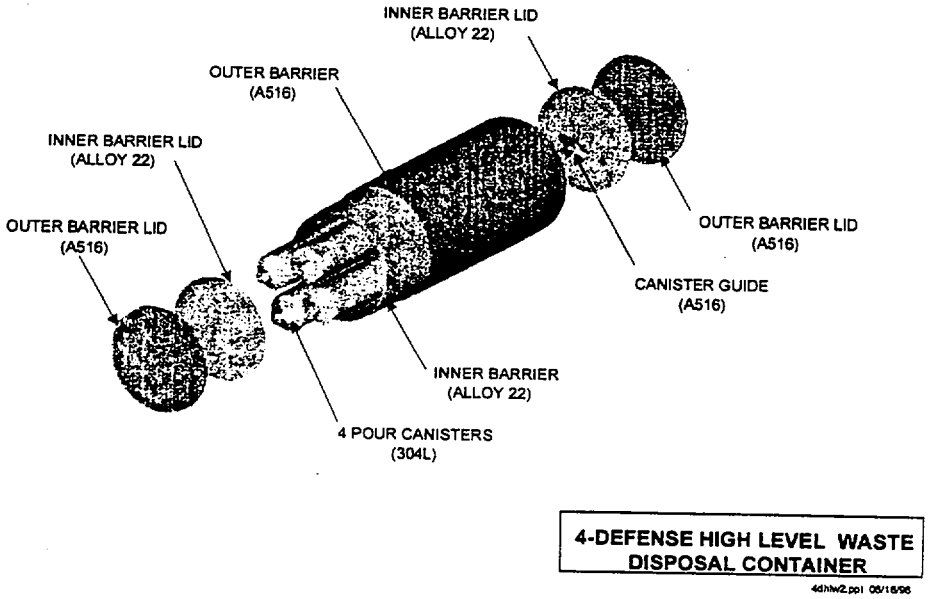

Figure 6B-2. Waste Package Used for Disposal of High-Level Waste and Can-in-Canister Ceramic.

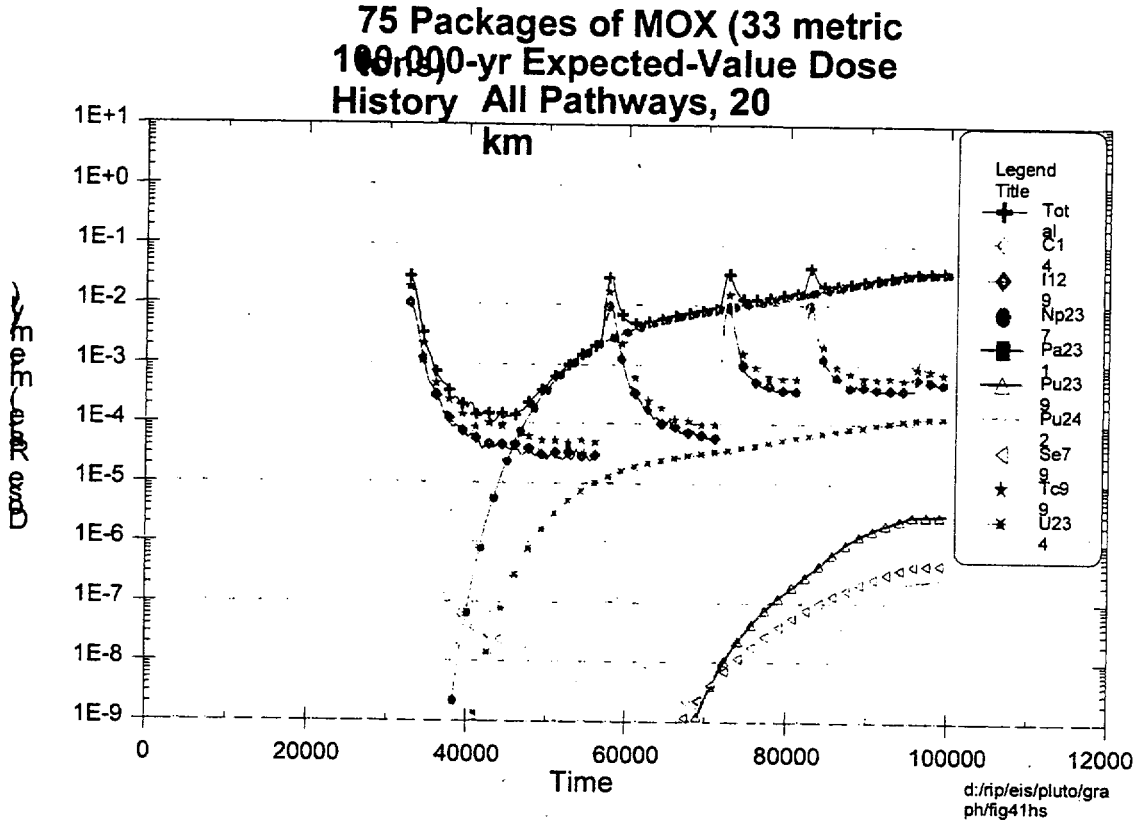

Figure 6B-3. Expected-Value Dose History at 20 Kilometers Over 100,000 Years from 75 Packages of Mixed Oxide Spent Fuel (33 metric ton case).

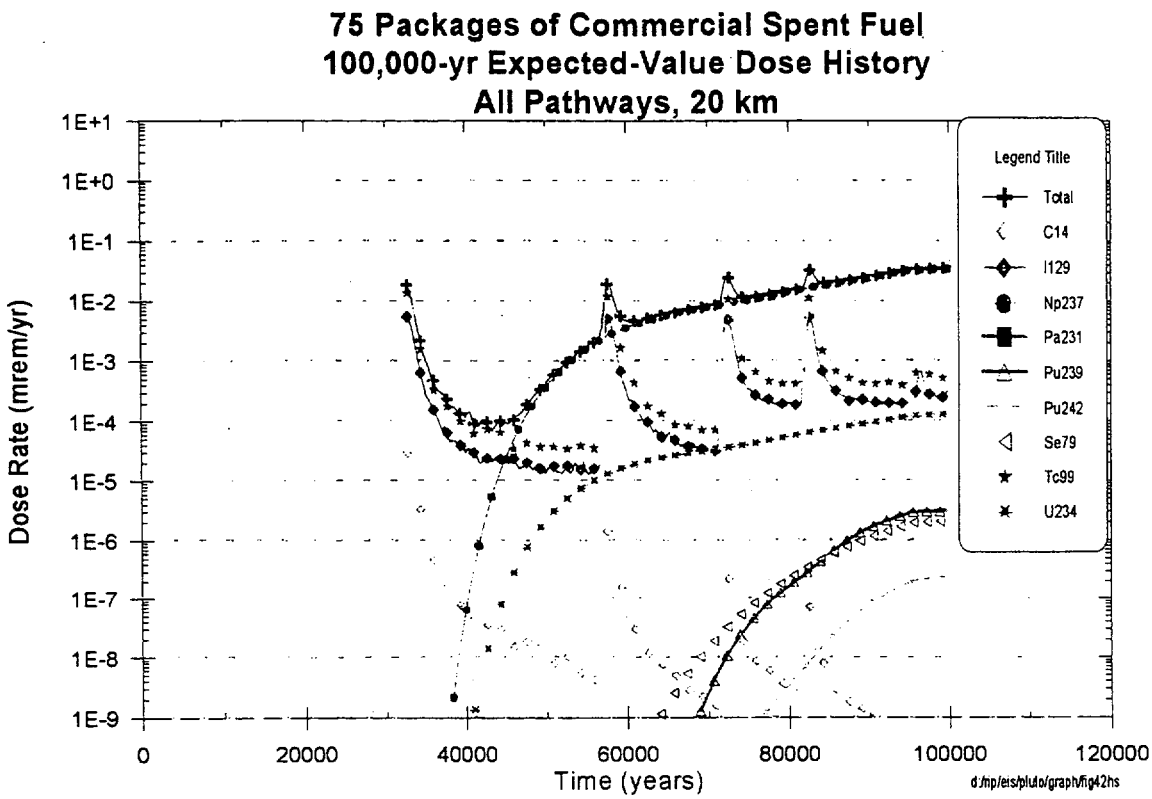

Figure 6B-4 Expected-Value Dose History at 20 Kilometers over 100,000 Years from 75 Packages of Commercial Spent Fuel.

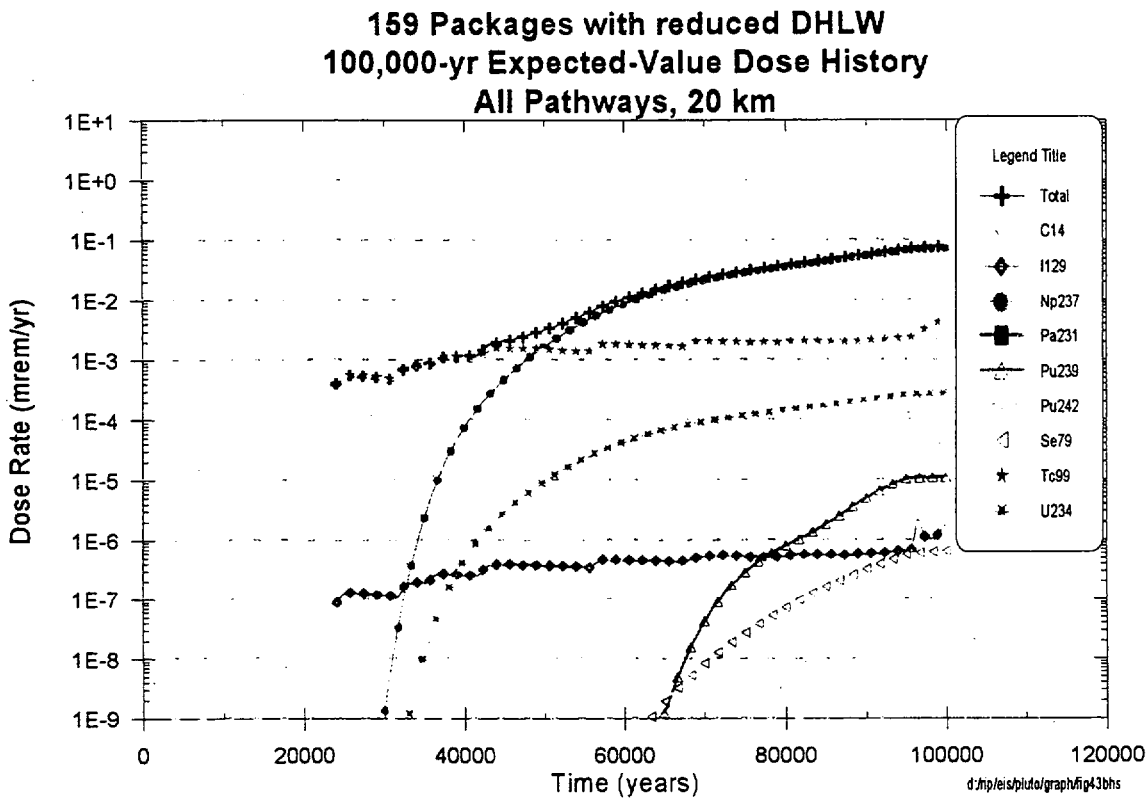

Figure 6B-5. Expected-Value Dose History at 20 Kilometers over 100,000 Years from 159 Packages of Can-in-Canister Ceramic (17 metric ton case).

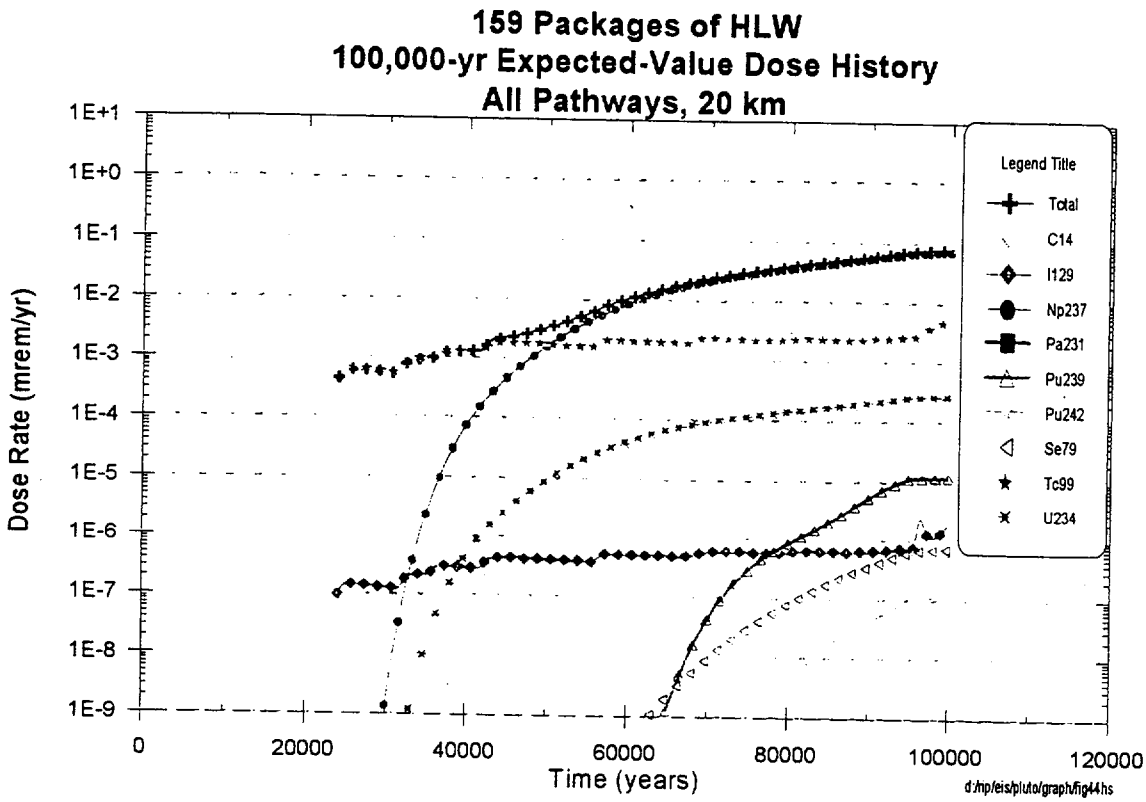

Figure 6B-6. Expected-Value Dose History at 20 Kilometers over 100,000 Years from 159 Packages of HLW.

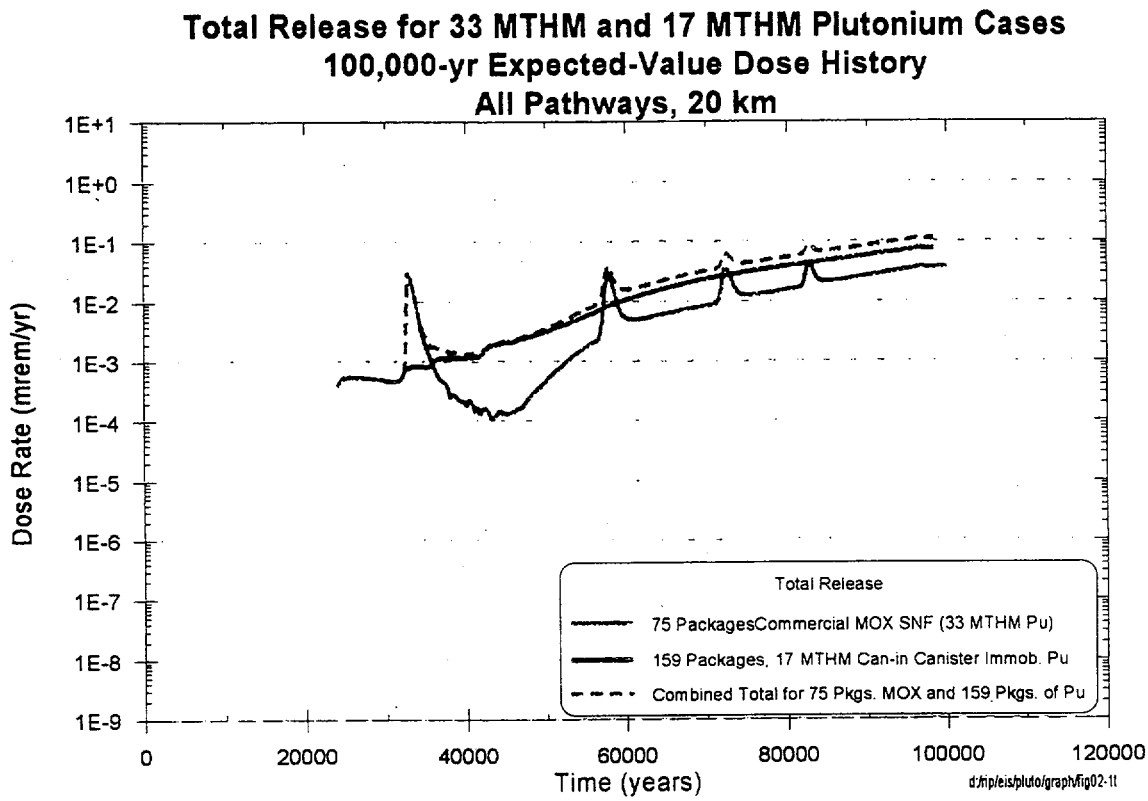

Figure 6B-7. Expected-Value Dose History at 20 Kilometers over 100,000 Years from 75 Packages of Mixed Oxide Spent Fuel and 159 packages of Can-in-Canister Ceramic (33 metric tons of MOX and 17 metric tons of ceramic).

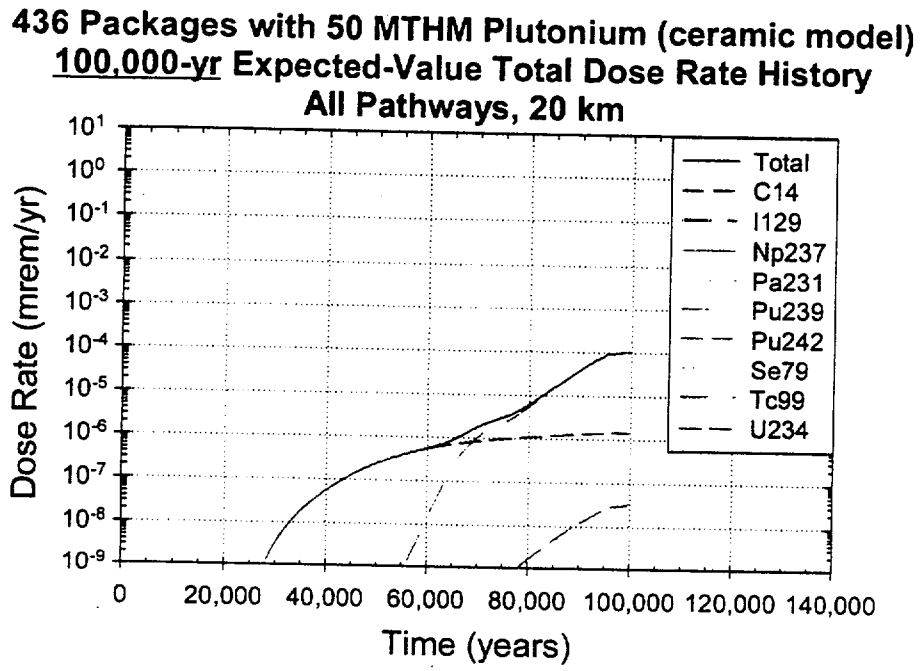

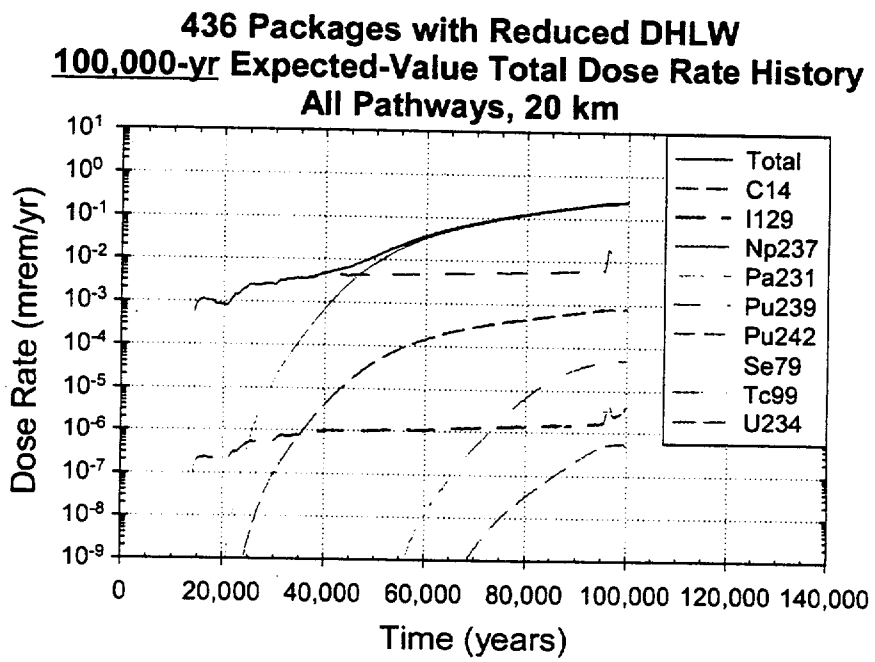

Figure 6B-8. Expected-Value Dose History at 20 Kilometers Over 100,000 Years from 436 Packages of Can-in-Canister Ceramic (50 metric ton case).

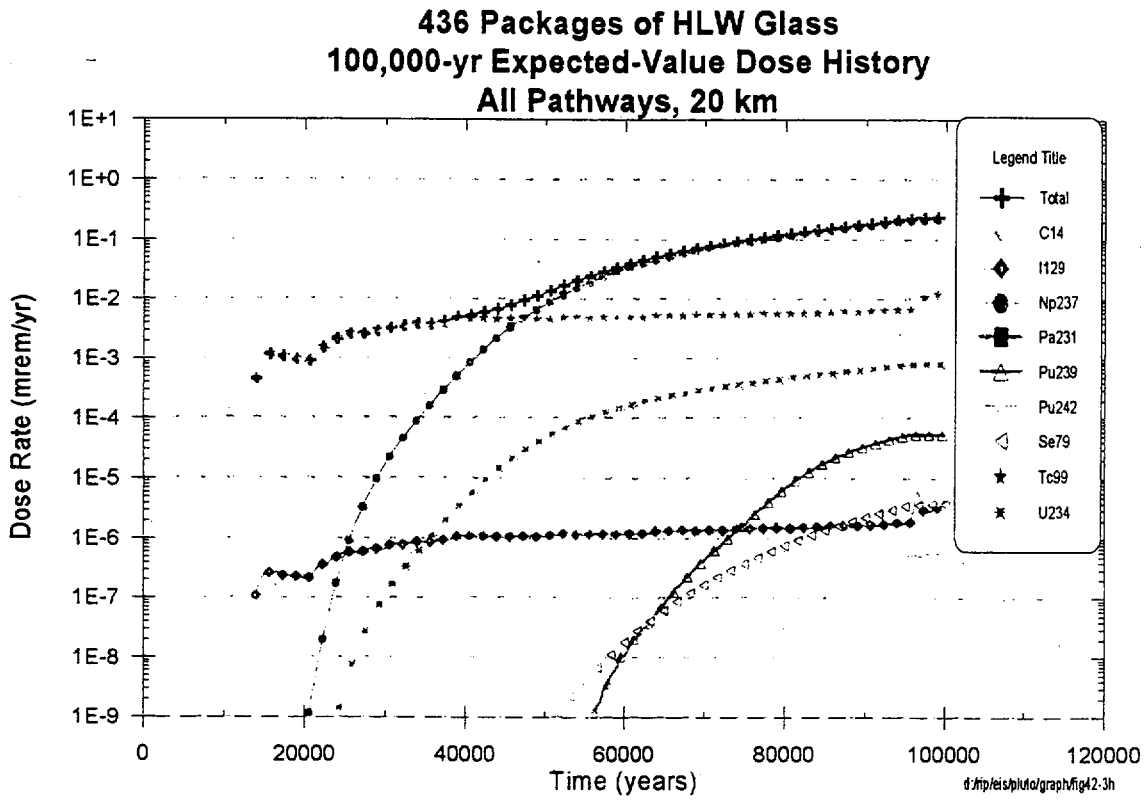

Figure 6B-9. Expected-Value Dose History at 20 Kilometers Over 100,000 Years from 436 Packages of HLW.

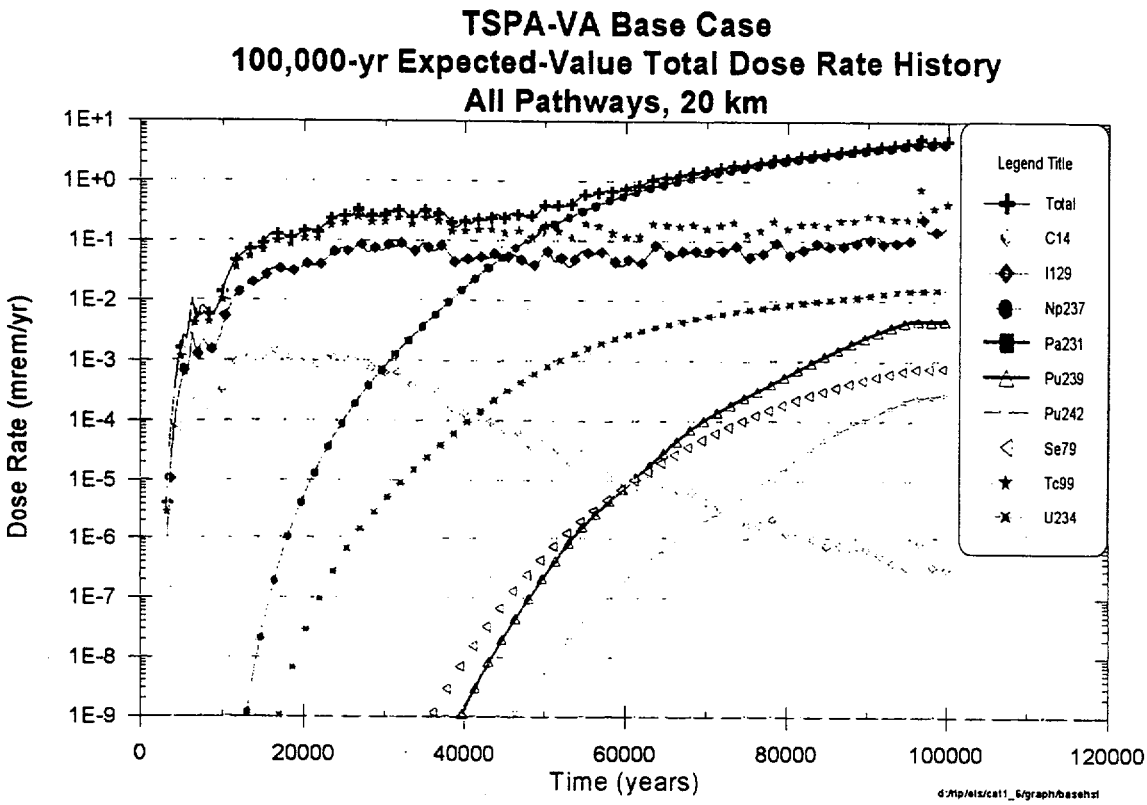

Figure 6B-10. Expected-Value Dose History at 20 Kilometers Over 100,000 Years from TSPA-VA Base Case.

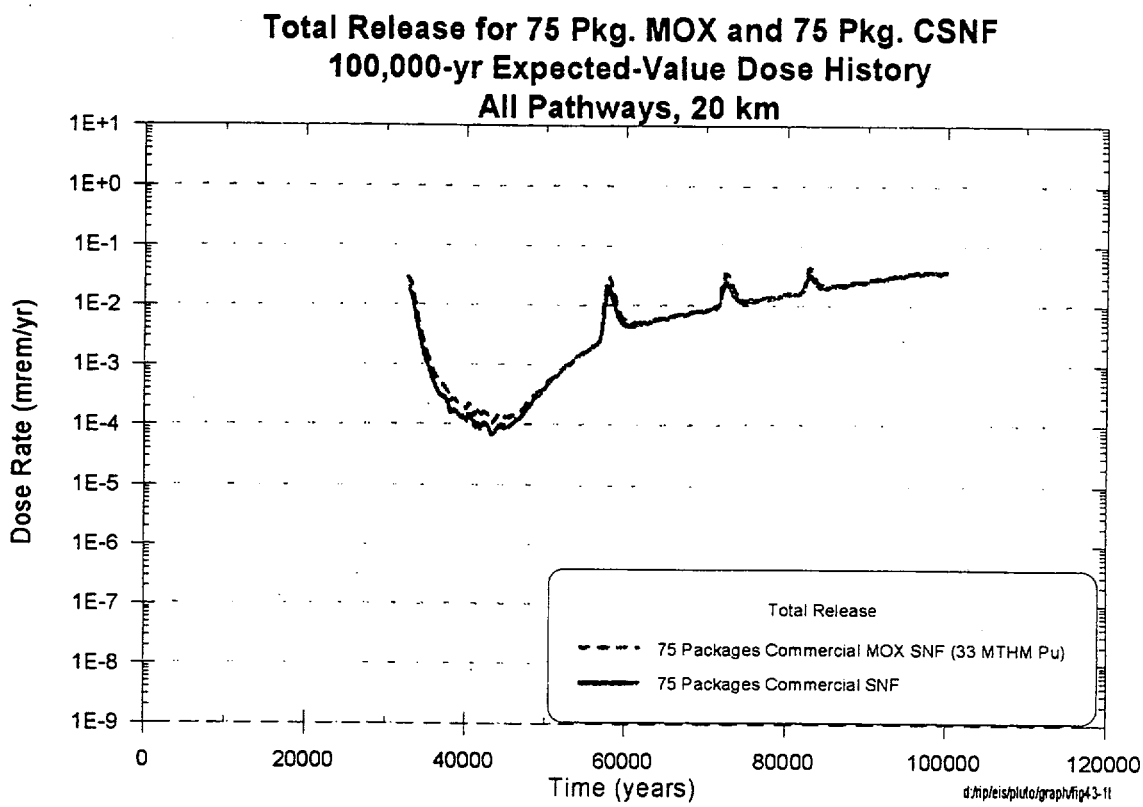

Figure 6B-11 Expected-Value Dose History at 20 Kilometers over 100,000 Years from 75 Packages of MOX Spent Fuel Compared to 75 Packages of Commercial Spent Fuel.

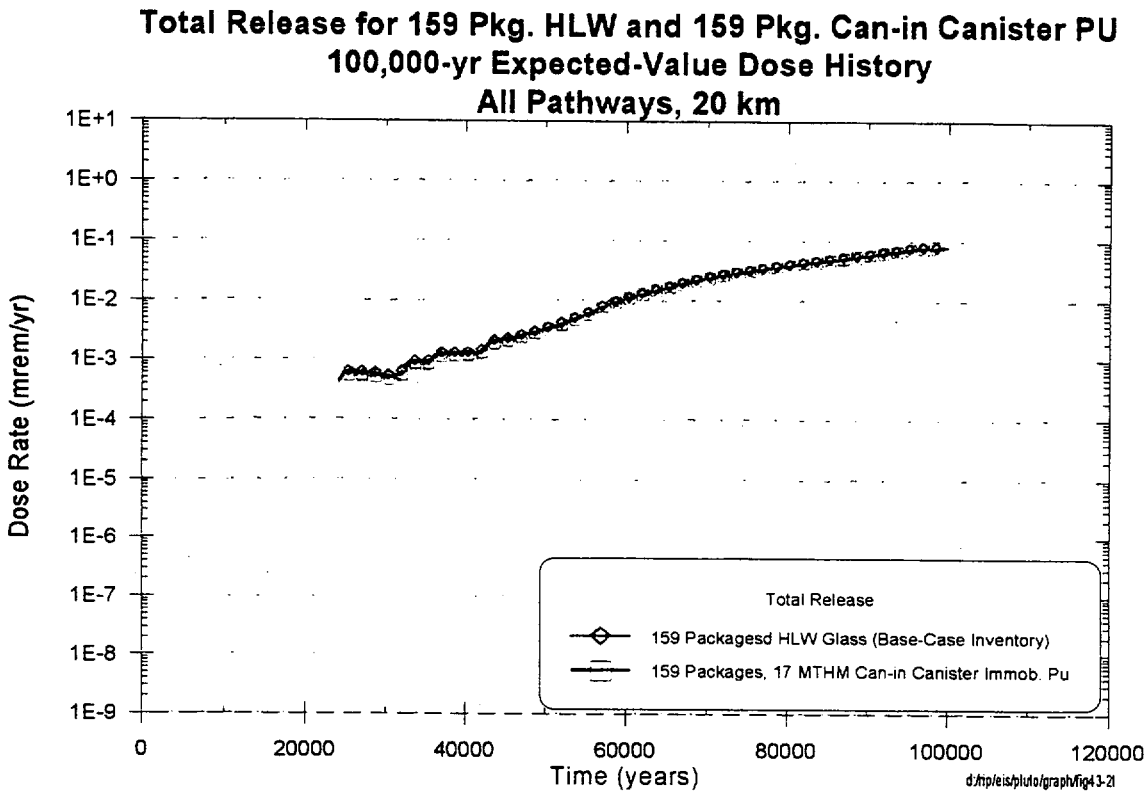

Figure 6B-12. Expected-Value Dose History at 20 Kilometers over 100,000 Years from 159 Packages of Can-in-Canister Ceramic Compared to 159 Packages of HLW.

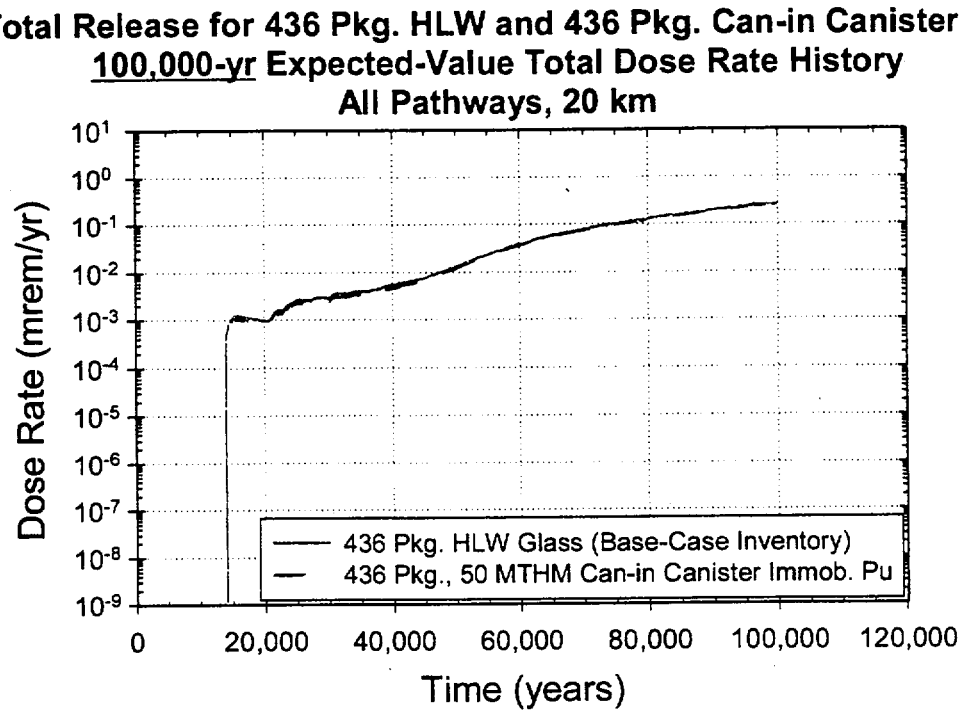

Figure 6B-13. Expected-Value Dose History at 20 Kilometers Over 100,000 Years from 436 Packages of Can-in-Canister Ceramic Compared to 436 Packages of HLW

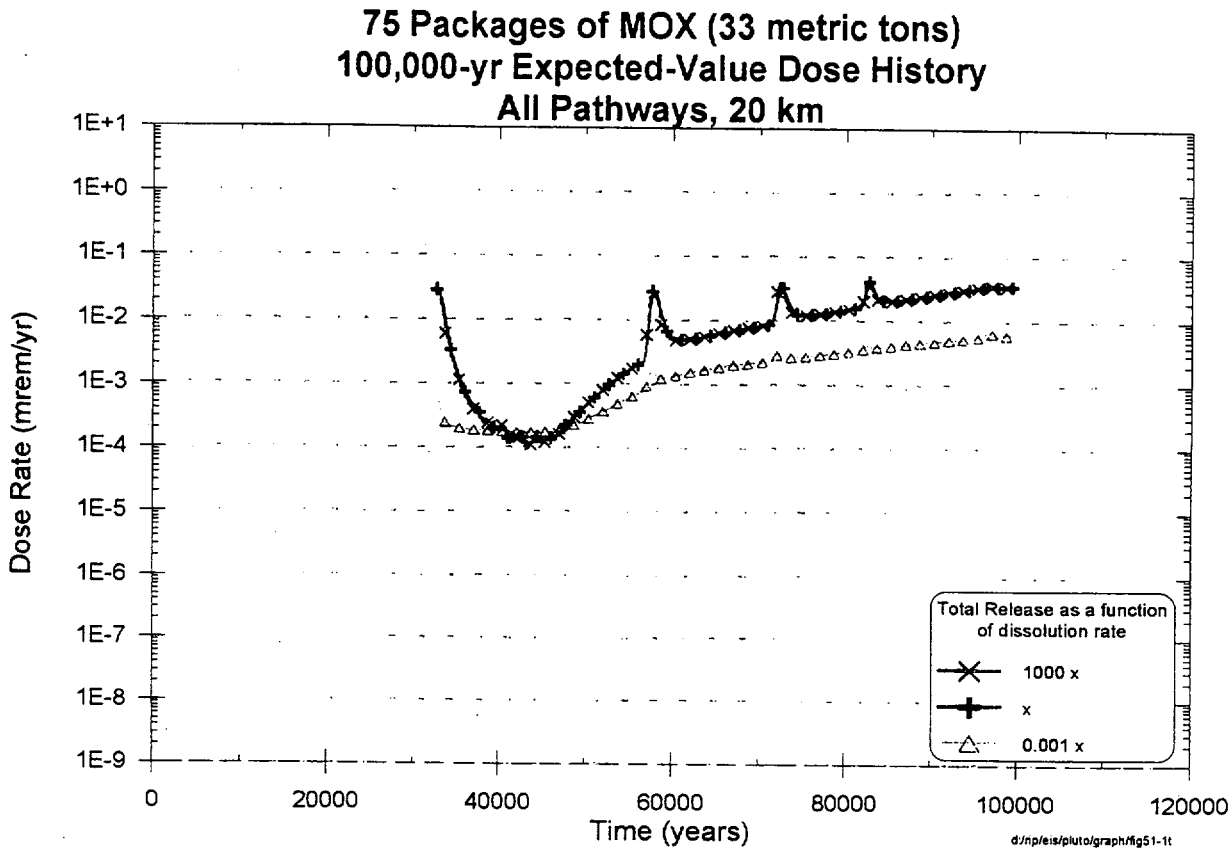

Figure 6B-14. Effects of Uncertain Dissolution Rate on Dose from Mixed Oxide Spent Fuel.

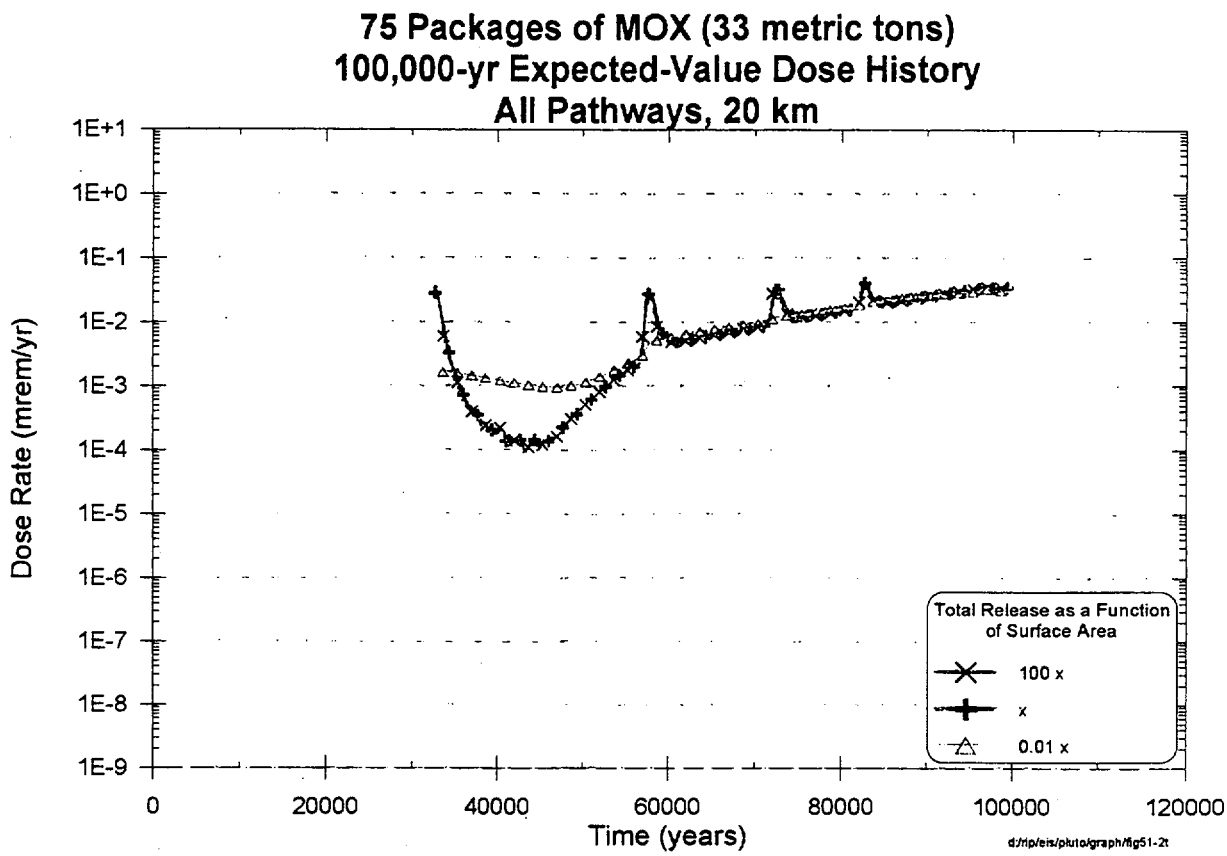

Figure 6B-15. Effects of Uncertain Surface Area on Dose from Mixed Oxide Spent Fuel.

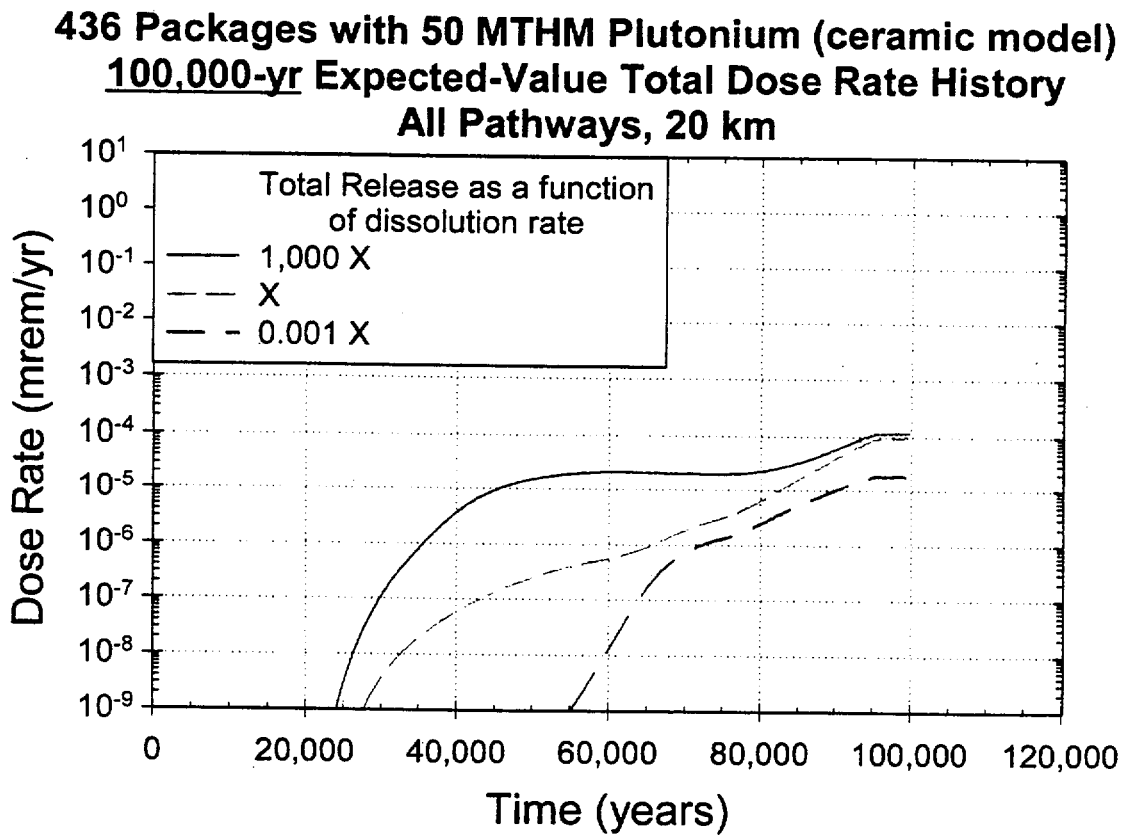

Figure 6B-16. Effects of Uncertain Dissolution Rate on Dose from Plutonium Ceramic.

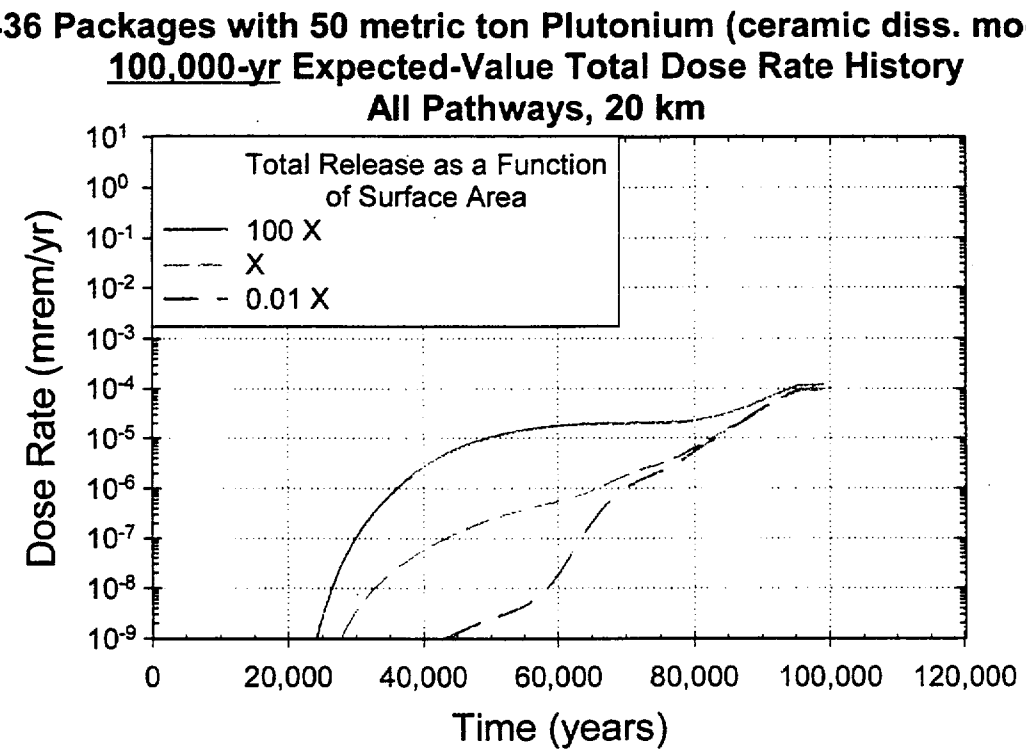

Figure 6B-17. Effects of Uncertain Surface Area on Dose from Plutonium Ceramic.

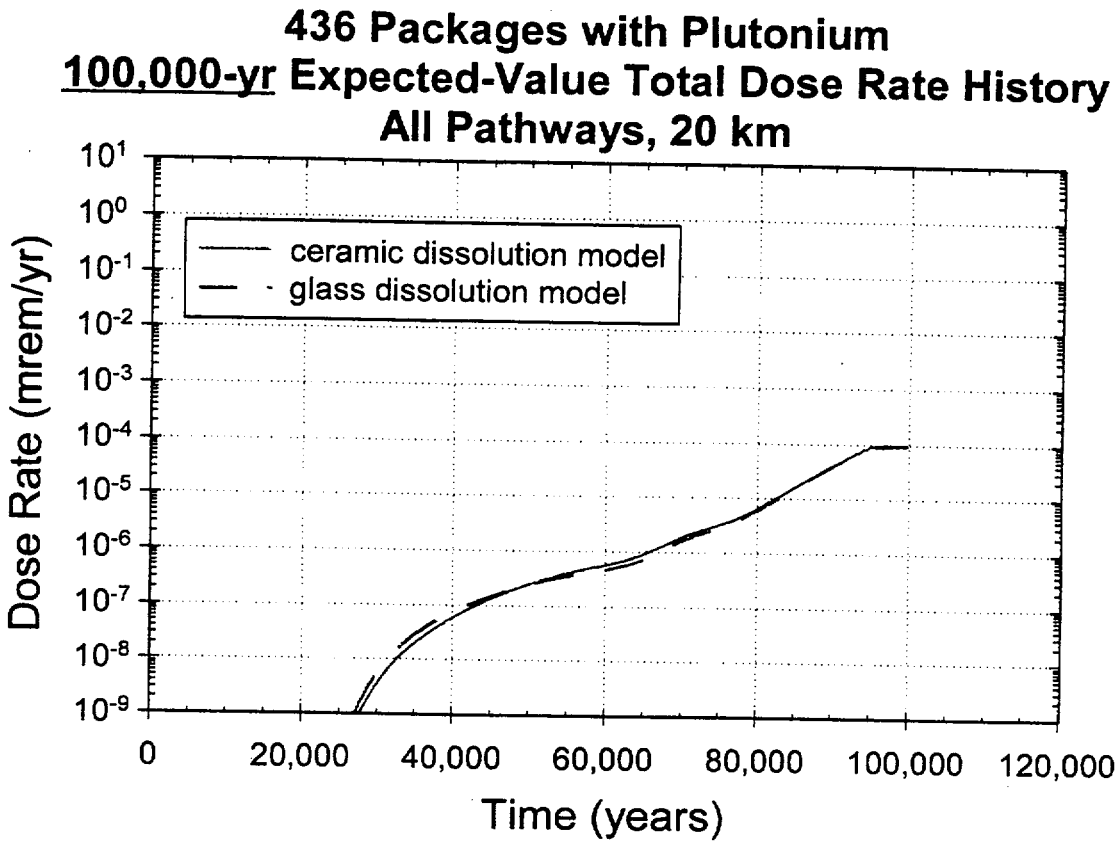

Figure 6B-18. Effects of Uncertain Dissolution Model on Dose from Plutonium Ceramic; Ceramic Using the Ceramic Dissolution Model Compared to Ceramic Using the HLW Glass Model for 50 metric tons of Plutonium in 436 Packages.

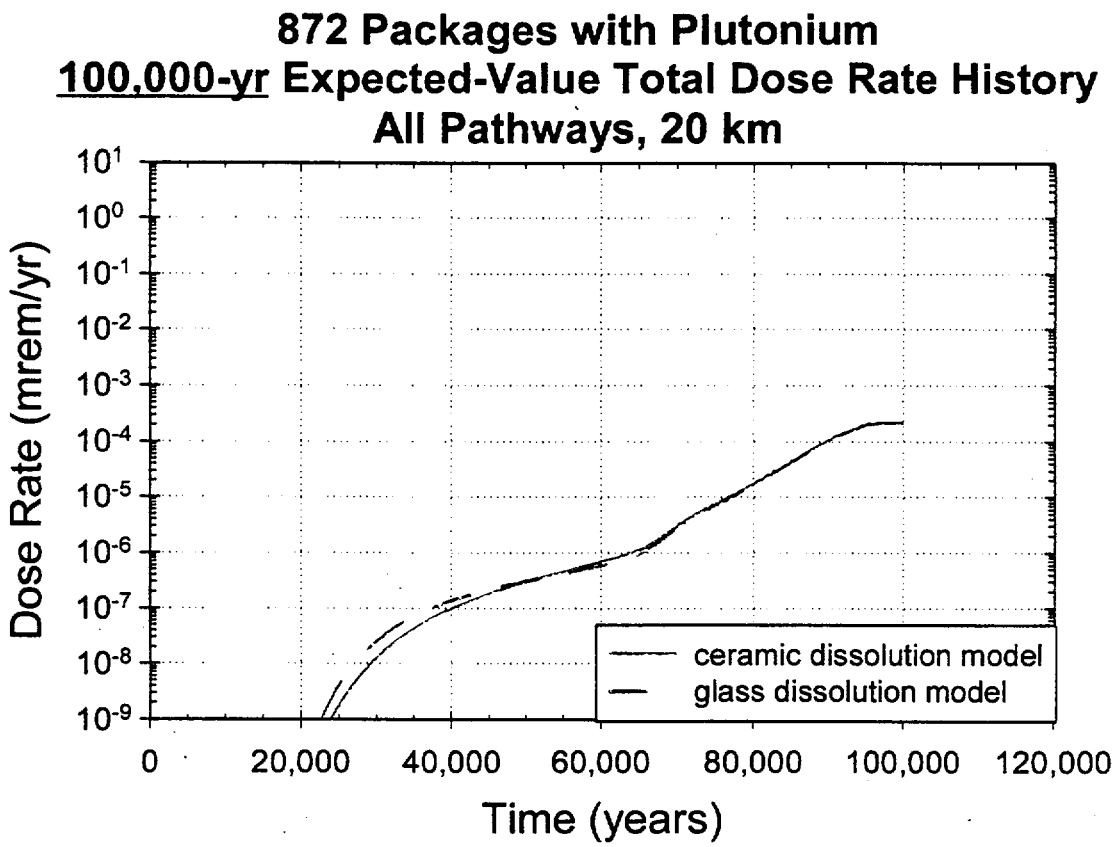

Figure 6B-19. Effects of Uncertain Dissolution Model on Dose from Plutonium Ceramic; Ceramic Using the Ceramic Dissolution Model Compared to Ceramic Using the HLW Glass Model for 50 metric tons of Plutonium in 872 Packages.

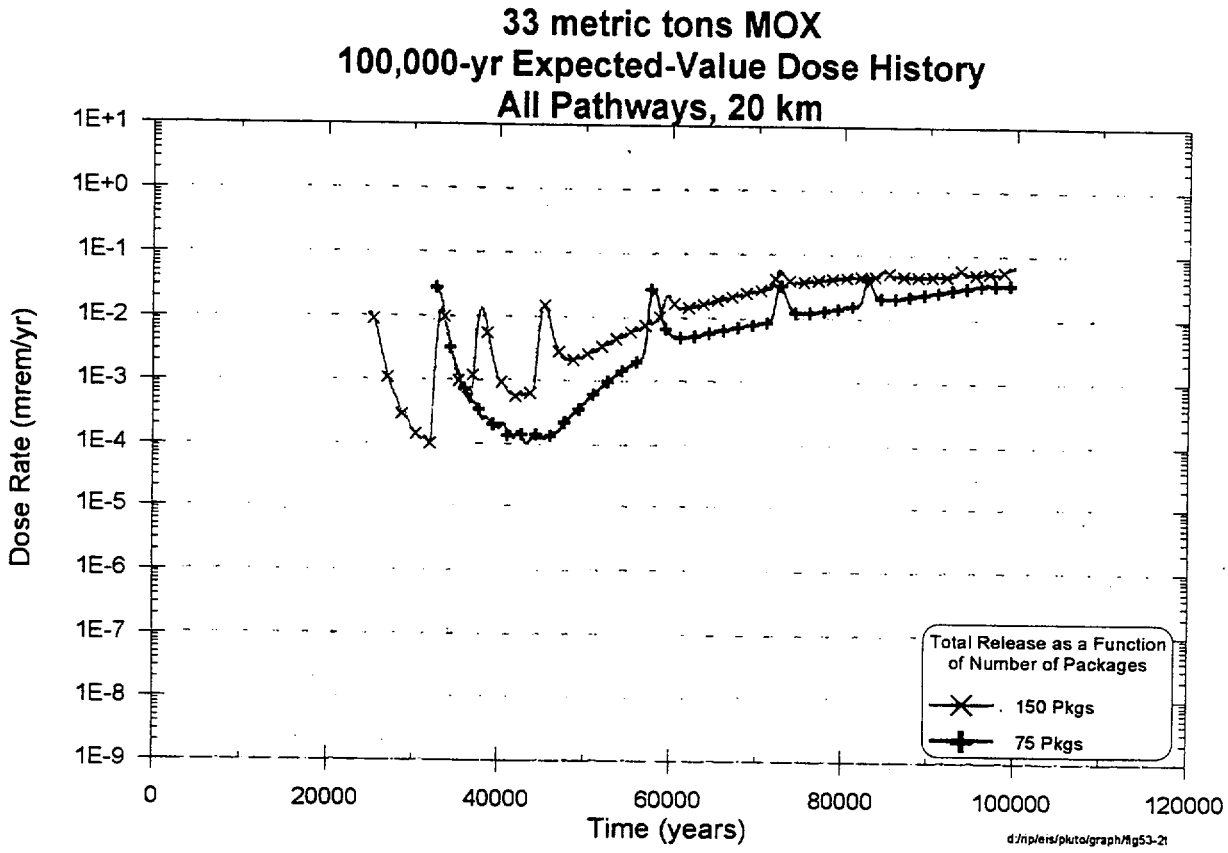

Figure 6B-20. Sensitivity of Dose from Mixed Oxide Spent Fuel to Number of Waste Packages; 75 Packages Compared to 150 Packages for the 33 Metric Ton Case.

Table 6B-1. Radionuclide Inventory for Mixed Oxide (MOX) Spent Fuel.

Isotope	Two-Cycle MOX (Ci/assembly)	Three-Cycle MOX (Ci/assembly)	Average[1] MOX (Ci/assembly)
^{227}Ac	8.32E-07	1.10E-06	9.76E-07
^{241}Am	6.33E+03	6.82E+03	6.59E+03
^{242M}Am	2.56E+01	3.70E+01	3.17E+01
^{243}Am	2.39E+01	5.75E+01	4.19E+01
^{14}C	3.36E-01	5.54E-01	4.53E-01
^{36}Cl	1.26E-08	3.89E-08	2.67E-08
^{244}Cm	9.35E+02	3.42E+03	2.27E+03
^{245}Cm	3.63E-01	1.71E+00	1.09E+00
^{246}Cm	3.10E-02	2.64E-01	1.56E-01
^{135}Cs	3.94E-01	5.48E-01	4.77E-01
^{129}I	2.10E-02	3.00E-02	2.58E-02
^{93M}Nb	3.09E-01	4.57E-01	3.88E-01
^{94}Nb	8.03E-05	1.09E-04	9.57E-05
^{59}Ni	1.13E+00	1.74E+00	1.46E+00
^{63}Ni	1.22E+02	1.99E+02	1.63E+02
^{237}Np	8.34E-02	1.04E-01	9.45E-02
^{231}Pa	1.60E-06	1.90E-06	1.76E-06
^{210}Pb	2.88E-08	4.27E-08	3.63E-08
^{107}Pd	1.22E-01	1.84E-01	1.55E-01
^{238}Pu	8.75E+02	2.14E+03	1.55E+03
^{239}Pu	5.58E+02	3.91E+02	4.68E+02
^{240}Pu	8.73E+02	8.69E+02	8.71E+02
^{241}Pu	5.70E+04	6.04E+04	5.88E+04
^{242}Pu	1.94E+00	3.77E+00	2.92E+00
^{226}Ra	1.22E-07	1.92E-07	1.60E-07
^{228}Ra	---	---	---
^{79}Se	3.16E-02	4.54E-02	3.90E-02
^{131}Sm	3.72E+02	3.87E+02	3.80E+02
^{126}Sn	5.04E-01	7.17E-01	6.18E-01
^{99}Tc	6.43E+00	9.03E+00	7.83E+00
^{229Th}	1.31E-08	2.14E-08	1.76E-08
^{230Th}	2.20E-05	3.82E-05	3.07E-05
^{232}Th	---	---	---
^{233}U	8.92E-06	1.15E-05	1.03E-05
^{234}U	1.18E-01	2.34E-01	1.80E-01
^{235}U	9.95E-04	6.43E-04	8.06E-04
^{236}U	6.84E-03	8.30E-03	7.62E-03
^{238}U	1.44E-01	1.42E-01	1.43E-01
^{93}Zr	4.18E-01	6.10E-01	5.21E-01

[1]Average based on 46.3% two-cycle and 53.7% three-cycle MOX.

Table 6B-2. Radionuclide Inventories for Commercial Spent Fuel and High-Level Waste (HLW).

Isotope	Commercial Spent Fuel (Ci/MTHM)	High-Level Waste (Ci/MTHM)
^{227}Ac	1.86E-05	9.43E-04
^{241}Am	3.87E+03	3.47E+02
^{242M}Am	2.26E+01	3.31E-02
^{243}Am	2.63E+01	8.20E-02
^{14}C	1.44E+00	0.00E+00
^{36}Cl	1.15E-02	0.00E+00
^{244}Cm	1.24E+03	2.09E+01
^{245}Cm	3.65E-01	8.83E-05
^{246}Cm	7.60E-02	1.00E-05
^{135}Cs	5.36E-01	3.09E-01
^{129}I	3.57E-02	1.49E-05
^{93M}Nb	1.89E+00	1.55E+00
^{94}Nb	8.47E-01	5.31E-05
^{59}Ni	2.44E+00	1.49E-01
^{63}Ni	3.20E+02	1.31E+01
^{237}Np	4.54E-01	1.90E-01
^{231}Pa	3.42E-05	1.53E-03
^{210}Pb	6.94E-07	4.56E-08
^{107}Pd	1.31E-01	4.42E-02
^{238}Pu	3.22E+03	6.50E+02
^{239}Pu	3.68E+02	8.66E+00
^{240}Pu	5.47E+02	5.51E+00
^{241}Pu	3.52E+04	2.25E+02
^{242}Pu	2.10E+00	7.12E-03
^{226}Ra	2.57E-06	1.59E-07
^{228}Ra	3.21E-10	1.64E-04
^{79}Se	4.58E-01	1.02E-01
^{131}Sm	3.67E+02	7.63E+02
^{126}Sn	8.85E-01	6.76E-01
^{99}Tc	1.45E+01	1.05E+01
^{229}Th	3.77E-07	2.36E-05
^{230}Th	3.69E-04	2.14E-05
^{232}Th	4.50E-10	1.65E-04
^{233}U	7.31E-05	9.33E-04
^{234}U	1.39E+00	8.69E-02
^{235}U	1.71E-02	3.16E-04
^{236}U	2.81E-01	1.14E-03
^{238}U	3.15E-01	9.91E-03
^{93}Zr	2.47E+00	1.87E+00

Table 6B-3. Radionuclide Inventory for Surplus Plutonium Used in Can-In-Canister Ceramic.

Isotope	17-Ton Case (Ci/canister)[1]	50-Ton Case (Ci/canister)[1]
^{238}Pu	122.0	60.0
^{239}Pu	1613.0	1653.0
^{240}Pu	550.0	430.0
^{241}Pu	4732.0	2849.0
^{242}Pu	9.8 E –2	4.6 E -2
^{241}Am	718.0	432.0
^{234}U	< 1.5 E –5	< 1.5 E -5
^{235}U	2.34 E –3	1.1 E –3
^{238}U	1.89 E –5	1.91 E -2
^{232}Th	< 1.5 E –5	< 1.5 E -5

[1]Includes only the radionuclides in the ceramic in the year 2010. Does not include radionuclides in the HLW.

Table 6B-4. Physical Characteristics of Commercial Spent Fuel, HLW, and Plutonium Ceramic.

Waste Type	Air Alteration Rate (fraction/yr)	Matrix Dissolution Rate ($g/m^2/yr$)	Matrix Surface Area (m^2/g)	Failed Cladding (%)	Gap Radionuclide Inventory (fraction)
Commercial Spent Fuel	0	Oxide model	3.96E-03	1.25	0.02
High-Level Waste	0	Glass model	5.705E-05	N/A	N/A
Plutonium Ceramic	0	Ceramic model	1.51E-4	N/A	N/A

CHAPTER 6

APPENDIX C

RADIONUCLIDE SELECTION AND CHAIN DECAY

INTENTIONALLY LEFT BLANK

CONTENTS

C-1. Selection of Radionuclides for TSPA-VA C6-1

C-2. Modeling of Chain-Decay Processes in the Unsaturated-Zone Transport Model..... C6-4

FIGURES

Figure C6-1. Normalized dose rate at water table using the concentrations of the out flowing unsaturated zone groundwater for the thirty-nine radionuclide case. C6-7

Figure C6-2. Expected-value dose rate time history over a period of 1,000,000 years for the radionuclides in the Np-237 chain. Only Np-237, U-233 and Th-229 show up in the plot. C6-8

Figure C6-3. Comparison of Np-237 dose rate from the 39 radionuclide case, where decay chains and ingrowth are included with the 9 radionuclide case, where the decay and ingrowth from the parents are accounted at time zero. C6-9

Figure C6-4. Cumulative activity released from different boundaries of the repository system. C6-10

Figure C6-5. Comparison of mass flow rate curves from RIP and FEHM including chain-decay. The mass flow rates of species 1, 2, and 6 are too low to be seen in the plot. C6-11

Figure C6-6. Normalized cumulative breakthrough curves from FEHM including chain-decay. The values of species 1, 2, and 6 are too low to be seen in the plots. C6-12

TABLES

Table 6C-1. Radionuclides Used in TSPA Simulations, along with their half-lives—Arranged by chains. The nine radionuclides used for the TSPA-VA base case are highlighted in bold..... C6-13

Table 6C-2. Radionuclide inventory for the 39 radionuclides with decay chains.. ..... C6-15

Table 6C- 3. Radionuclide inventory for the nine radionuclides used in TSPA-VA..... C6-17

INTENTIONALLY LEFT BLANK

APPENDIX C
RADIONUCLIDE SELECTION AND CHAIN DECAY

C-1. SELECTION OF RADIONUCLIDES FOR TSPA-VA

Nine radionuclides are selected for all the performance assessment analyses in TSPA-VA. These nine radionuclides are a subset of the thirty-nine radionuclides considered in TSPA-1995 (CRWMS M&O 1995). A listing of these radionuclides along with their decay chains and half-lives is given in Table 6C-1, with the ones selected in TSPA-VA highlighted in bold. The set of thirty-nine radionuclides were obtained by screening the different waste streams based on contribution of the radionuclide to : (1) potential release normalized to 40 CFR 191 Table 1 values over time periods from 1,000 to 1,000,000 years, and (2) potential average annual whole body dose over time periods from 1,000 to 1,000,000 years. More information on the screening methodology can be found in TSPA-1995.

For TSPA-VA, fewer radionuclides are selected, because of computational limitations in modeling all the thirty-nine radionuclides with decay chains and ingrowth, in the models used for the radionuclide transport in the unsaturated zone (UZ) and the engineered barrier system (EBS). The three dimensional, dual-permeability, FEHM particle tracker (Robinson et al. 1997; Zyvoloski et al. 1996) is used for simulating radionuclide transport in the unsaturated zone. Simulations run for long time frames (1,000,000 years) require using large number of particles (1,000,000) for each radionuclide to capture the transport processes accurately. This would impose a huge computational restraint when all the thirty-nine radionuclides are considered along with decay chains and ingrowth. Spatial heterogeneity in infiltration and thermal behavior is modeled by dividing the repository into six regions. This combined with the three waste types and the three different dripping conditions to which waste packages are exposed in the three climate states, would result in a large network of mixing cells[1], requiring huge computational times, when decay chains are included for modeling EBS transport in RIP (Golder 1998). Especially these computational constraints are magnified while running probabilistic analyses, which are an integral part of performance assessment calculations.

The nine radionuclides listed in bold in Table 6C-1, were chosen based on six criteria (not necessarily in order of significance): high solubility, low sorption affinity, size of inventory (plus ingrowth generated by parent radionuclide), high biosphere dose conversion factor, half-life long enough to survive transport, and existence as colloidal particles. The experience obtained from previous Yucca Mountain TSPA's (Wilson et al. 1994; CRWMS M&O 1995; NRC 1995; Kessler and McGuire 1996) also helped in excluding many radionuclides out of the thirty-nine, which were found to be inconsequential in their dose effects. Also some verification simulations were performed using all the thirty-nine radionuclides with their decay chains in order prevent the exclusion of important radionuclides from the performance assessment calculations. The results of these simulations will be presented in the following sections. Since the selected nine radionuclides, do not include decay chains and ingrowth, the inventory of these radionuclides

[1] A series of mixing cells are used within RIP for modeling EBS transport. Mixing cells are equivalent to equilibrium batch reactors, with all the mass assumed to be instantaneously and completely mixed throughout the cell.

need to be adjusted. This is a concern only for the actinides (Pa-231, Pu-239, Pu-242, Np-237 and U-234) listed in the table. For the actinides (Pu-239, Pu-242, Np-237 and U-234) that have longer half-lives than that of their parents, the adjustment to their inventory is done by assuming artificial decay of all their parents at time zero and thus increasing their inventory. This is a conservative assumption as all the parents in a given chain are assumed to decay instantaneously rather than progressively over time. For Pa-231, this procedure is not appropriate because, the half-life is much shorter than that of the parent U-235, which has a half-life of almost a billion years. So to allow for the neglect of decay, it was assumed that Pa-231 was, at all time, in secular equilibrium with the U-235 parent (that is for every curie of U-235 in the waste form there was a curie of Pa-231). This was done by specifying the inventory of Pa-231 in grams (not activity) that would be in secular equilibrium with U-235. To avoid an unnatural "rapid" decay of the Pa-231, the half-life of U-235 was used to characterize the decay of Pa-231. This will result in an over-estimate of Pa-231 inventory at early times till it reaches secular equilibrium, but after that correct inventory of Pa-231 will be present. The radionuclide inventory in curies for all the thirty-nine radionuclides is given in Table 6C-2. The inventory for the nine radionuclides with the adjustments for ingrowth as discussed above is presented in Table 6C-3.

The results of the simulations conducted to verify the effects of using a smaller subset of radionuclides in performance assessment calculations are presented in various forms to discuss the inaccuracy caused due to this assumption. In Figure 6C-1, the normalized dose using the concentration at the water table from the outflowing unsaturated zone groundwater is presented. These calculations are done by using all the thirty-nine radionuclides with decay chains in the FEHM particle tracker till the base of the UZ. The methodology in the FEHM particle tracker for modeling decay chains with ingrowth is discussed in Section C6-2 of this appendix. The average concentrations from the outflowing unsaturated zone groundwater, flowing into the saturated zone at the water table was calculated using the total liquid flux and the total activity released at the base of the UZ. These concentrations are converted to dose using the biosphere dose conversion factors for all the thirty-nine radionuclides. Further the normalized dose, instead of the actual dose is presented, as these values do not reach the accessible environment, but instead helps in identifying the important radionuclides at the water table. For 10,000 years, these normalized dose are computed by dividing all calculated dose by the peak Tc-99 dose within 10,000 years. For 100,000 and 1,000,000 years, the peak Np-237 dose is used as the normalizing factor. In the 10,000 year case, the top four radionuclides are plotted and as seen in the figure, Tc-99 is clearly the dominant radionuclide. The only radionuclide which does not belong to the list of nine that appears in this time frame is Cl-36, but the contribution from this is very minimal compared to other radionuclides. For 100,000 years, none of the additional thirty radionuclides were found to be important and are not plotted. For 1,000,000 years, two additional radionuclides are shown that become somewhat important after 200,000 years, that is, after the point at which Np-237 is no longer solubility limited. These radionuclides are U-233 and Th-229, which are in the Np-237 chain. U-233 is the daughter of Np-237 and Th-229 is the daughter of U-233. After 200,000 years, U-233 and Th-229 have dose rates that are slightly less than Pu-242. Omitting these radionuclides makes the total dose at the water table about 15 to 20 percent lower than it should be.

Because U-233 and Th-229 are found to be important at the water table, the Np-237 chain containing these two radionuclides is modeled all the way through the saturated zone to calculate the impact of omitting these two radionuclides on the total dose at the accessible environment.

The transport through the unsaturated zone is modeled using the FEHM particle tracker with the entire decay chain and ingrowth. The saturated zone transport is modeled with six one dimensional flow tubes using FEHMN ((Zyvoloski et al. 1995)), a computer code for simulating heat and mass transfer for finite elements. The mass flux at the water table is used as the input for each of the streamtubes and the output concentrations at the end of the SZ is converted to dose using biosphere dose conversion factors. This methodology is different from that used for the nine radionuclides case, where the convolution integral is used to combine the unit breakthrough curves obtained using one-dimensional flow tubes. This is done due to the limitation in the convolution approach for including decay chains and ingrowth. The results of the expected-value simulation are presented in Figure 6C-2. Similar to Figure 6C-1, both U-233 and Th-229 show up on the plot in addition to Np-237, but the relative importance of these radionuclides compared to Np-237 has decreased. U-233 is about a factor of 50 lower than Np-237 in peak dose rate, and the difference is higher during early times till 300,000 years and then decreases to about a factor of 20 at 1,000,000 years. Th-229 is about four orders of magnitude lower than Np-237, making its contribution very minimal to the total dose rate. Since Np-237 is the radionuclide contributing the most to the peak dose in 100,000 years and 1,000,000 years, the dose from this is compared from the thirty-nine radionuclides case, where the entire decay chain with ingrowth is included against the nine radionuclides case, where the ingrowth from the parents of Np-237 is accounted by decaying them at time zero. The dose rate time histories for both these cases is shown in Figure C6-3. This figure shows, the approach taken for accounting the radionuclide inventory for Np-237 due to ingrowth from the parent radionuclides is reasonable for performance assessment calculations.

The cumulative activity released at the various boundaries of the repository system is presented in Figure C6-4 for both the thirty-nine and nine radionuclide case. Along with this, the total inventory as a function of time is also plotted, showing the decrease of inventory over a period of 1,000,000 years just due to radioactive decay. The release from the EBS is nearly equal for both cases till 20,000 years, but after that they diverge and by one million years, the release from thirty-nine radionuclide case is about 20 times greater than that from nine radionuclides. But this difference disappears after the transport of radionuclides through the unsaturated zone, due to sorption of radionuclides to the rock matrix and also the radionuclides with short half-lives undergoing decay to insignificant levels by the time they exit at the base of the UZ. This indicates the nine radionuclides are adequate for conducting performance assessment analyses and provide reasonable estimates of activity released over time.

C-2. MODELING OF CHAIN-DECAY PROCESSES IN THE UNSATURATED-ZONE TRANSPORT MODEL

In this section, the details of the process-based chain decay model developed for simulating radionuclide transport in the unsaturated zone with radioactive decay and ingrowth is discussed. First the mathematical details for modeling this process is discussed and then the results conducted for verifying the alogrithm is presented.

Process Model of Chain-Decay - The equation to include decay-ingrowth calculation for species i with a decay rate λ decays into species j is:

$$N_j = \sum_{m=1}^{N_i} \{1 - \exp[-\lambda(t - t_m)] \tag{6C-1}$$

where N_j is the number of particles of species j decayed from species i, N_i is the number of particles of species i, and t_m is the time at which the m th particle is injected into the system. In this case, the decay products, N_j, may be radionuclides. Using this equation, if 500,000 particles of species I are injected into the system, then at each time step, the number of mathematical operations for decay calculations alone are around 2.5 million. To simulate a time period of 1 million years, the typical calculation requires about 200 timesteps. Therefore, the total number of operations will reach 0.5 billion. This suggests that for large-scale simulations, the use of Equation (C-1) is inefficient.

To reduce the computational burden in simulations, the decay-ingrowth Equation (C-1) is approximated with an integral. Multiplying both sides of Equation (C-1) by dt_m and approximating the summation by an integral from t_1 to t_{Ni} , the average injection time interval between particles, the equation becomes:

$$N_j = \left\{(\tau_2 - \tau_1) + \frac{1}{\lambda}[\exp(-\lambda\tau_2) - \exp(-\lambda\tau_1)]\right\} / dt_m \tag{6C-2}$$

where $\tau_1 = t - t_{Ni}$ and $\tau_2 = t - t_1$. Using Equation (C-2), the amount of operations within one time step is reduced from millions of operations to just 10, which greatly increases the speed of simulations.

The accuracy of the integral approach depends on the number of particles and their release history. In general, the use of more particles increases the accuracy. When the same number of particles is used in simulations, the one with the constant release rate has less error. If the release rate changes with time, the release period is divided into several segments, such that, within each segment the release rate can be treated as constant. Then, the decay-ingrowth calculations are carried out corresponding to each segment. The accuracy of the approximation (Equation [C-2]) is also dependent on the magnitude of the injection time between particles (dt) times the decay

constant, λ. If this product is small compared with one, then the approximation is accurate, that is if:

$$e^{-\lambda dt} \approx 1 - \lambda\, dt \qquad \text{(6C-3)}$$

The integral approach was tested against the discrete formula given in Equation (C-1). For most of the simulations, at least 100,000 particles were released for each species over the repository area (represented by 100 nodes) at a constant rate. The duration of releasing period varied from 1,000 to 10,000 years. The results from the integral approach was generally in close agreement with those obtained using Equation (C-1). The relative error was less than 1%. But, the computational burden was greatly reduced from millions of operations to just 10 operations within each time step.

Another issue that relates to decay simulations is the spatial distribution of the decayed radionuclides. This problem is treated by using the rule of first in and first out. This rule states that the decay will proceed from the oldest to the youngest particle such that the total number of particles that have decayed equals the number computed in Equation (C-2). This implemented by assigning an injection time to each particle. This "rule" is not strictly correct, however, because radionuclide decay is a statistical process based on age, it cannot be deterministically predicted. To improve this approximation, the radionuclides are assigned to groups based on injection times. The time intervals for each group is based on the time-step selections used for the TSPA-VA calculations. Then the radionuclide decay calculation (Equation [C-2]), along with the first in, first out rule, is applied to each injection-time-interval group. In the case where several particles are injected at the same time, a uniform random number generator is used to randomly select the decayed particle(s). The new particle(s) generated due to decay-ingrowth takes over the location of the old particle(s) but with its (their) own transport properties.

Comparison of Chain-Decay Algorithm used in FEHM Particle Tracker with RIP - The multiple species ingrowth particle tracking model was tested against the RIP(Golder, 1998) using a 1 meter long, 1-dimensional saturated field with artificial (with user-defined half lives) radionuclides. A constant flow field was established so that the travel time for conservative tracers was 3,900 years. Also a dispersivity of 0.025 m was used in both the calculations. A total of 7 species with the same transport properties were simulated. A multiple decay chain starting from species 1 and then sequentially decaying into species 6 (1->2->3->4->5->6) was assumed in the simulations. The half-lives of species 1 to species 5 were: 10, 100, 1,000, 10,000, and 100,000 years, respectively. 500,000 particles of species 1 (representing 100 gram radionuclides) were injected into the system at a constant rate from 0 to 5,000 years. Species 2 to species 6 had initial concentrations of zero. Species 7, was assumed to be similar to species 1 but without decay and was used for comparison.

The mass flow rate curves at the outflow boundary from FEHM and RIP simulations are plotted in Figure C6-5. Due to numerical dispersion, the RIP curves have longer tails than the FEHM curves. The mass flow rates of species 1 and 2 at the outflow boundary are extremely low because of their short half lives, 10 and 100 years, respectively, and the relative long travel time (3,900 years). In fact, species 1 was not observed at the outflow boundary during the simulations. On the other hand, the long half life of species 5 (100,000 years) and the relative

short travel time (3,900 years) resulted in very little decay of species 5. Thus, the mass flow rate of species 6 is also very low. It is clear that the FEHM curves match the RIP curves very well. The normalized cumulative curves from the FEHM simulation are plotted in Figure C6-6. At any given time, the summation of the cumulative breakthrough values for species 1 through species 6 equals the cumulative breakthrough value for species 7, which is a check on conservation of mass in the system.

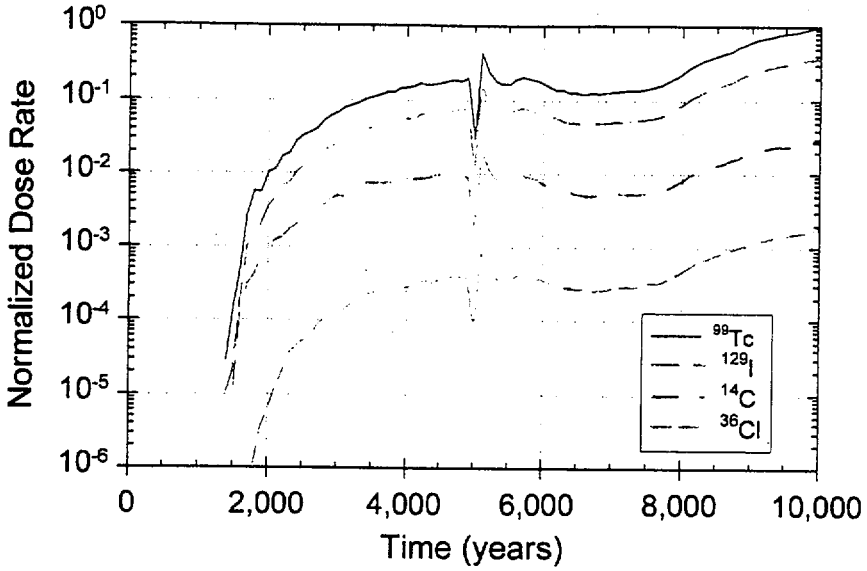

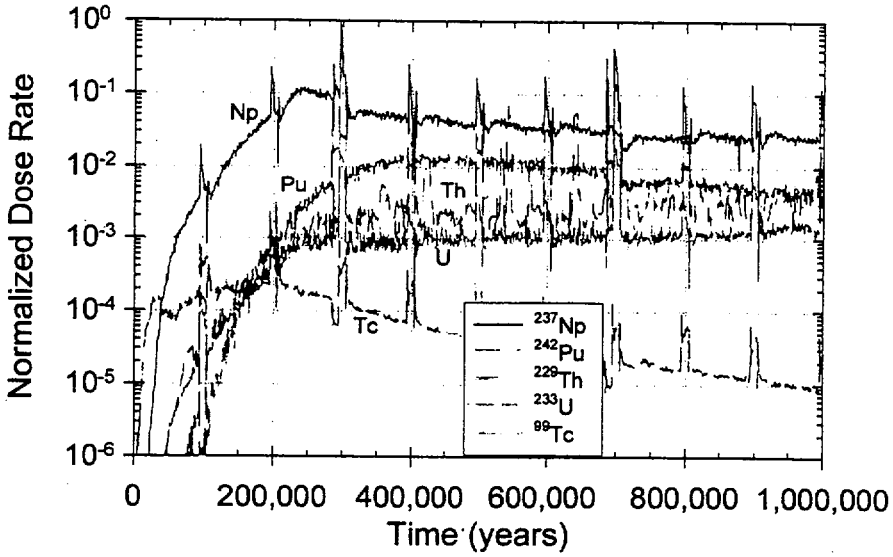

Figure C6-1. Normalized dose rate at water table using the concentrations of the out flowing unsaturated zone groundwater for the thirty-nine radionuclide case.

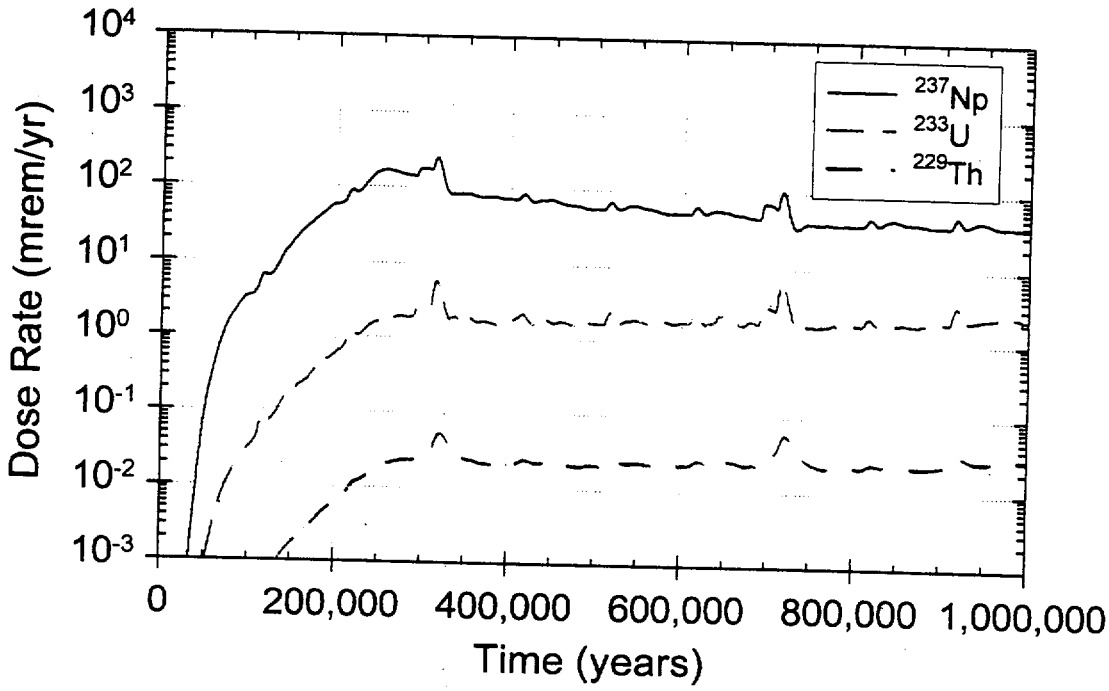

Figure C6-2. Expected-value dose rate time history over a period of 1,000,000 years for the radionuclides in the Np-237 chain. Only Np-237, U-233 and Th-229 show up in the plot.

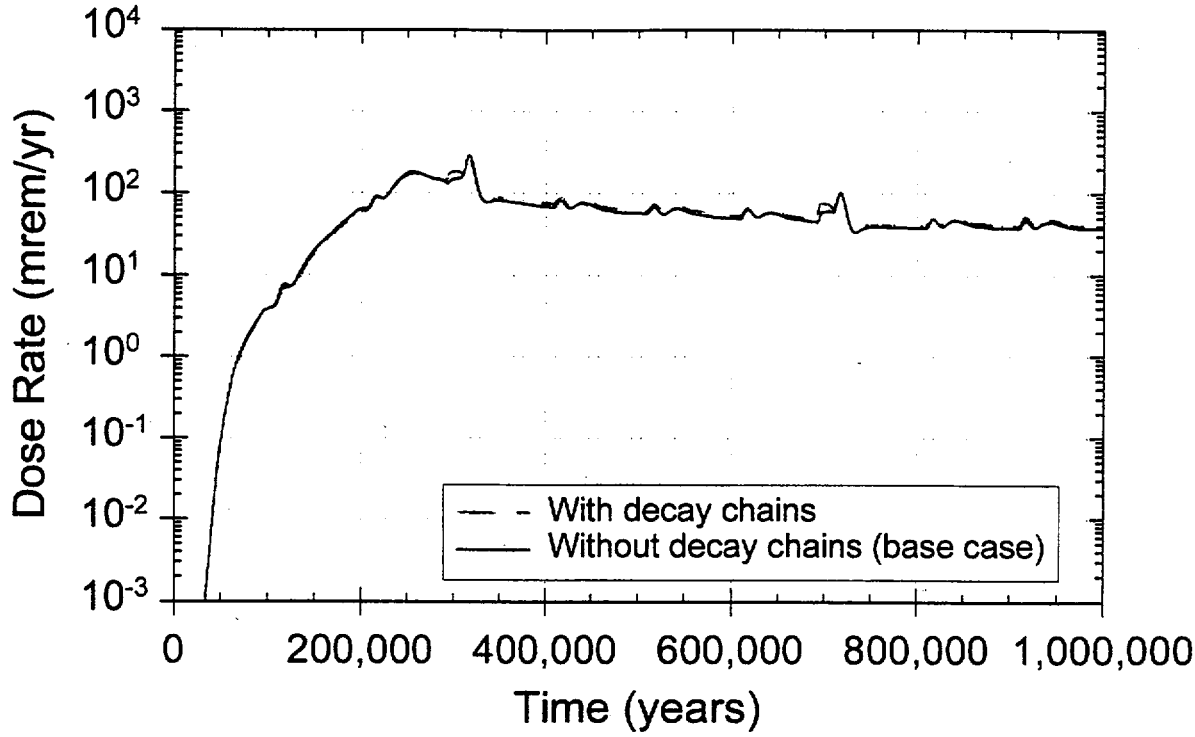

Figure C6-3. Comparison of Np-237 dose rate from the 39 radionuclide case, where decay chains and ingrowth are included with the 9 radionuclide case, where the decay and ingrowth from the parents are accounted at time zero.

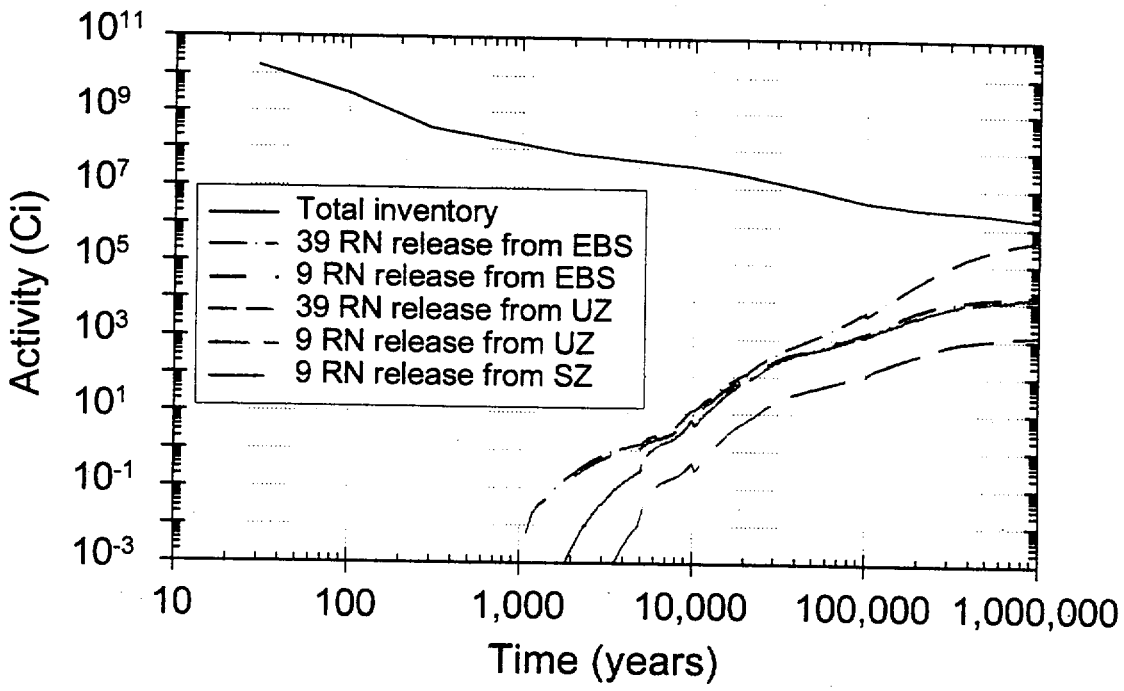

Figure C6-4. Cumulative activity released from different boundaries of the repository system.

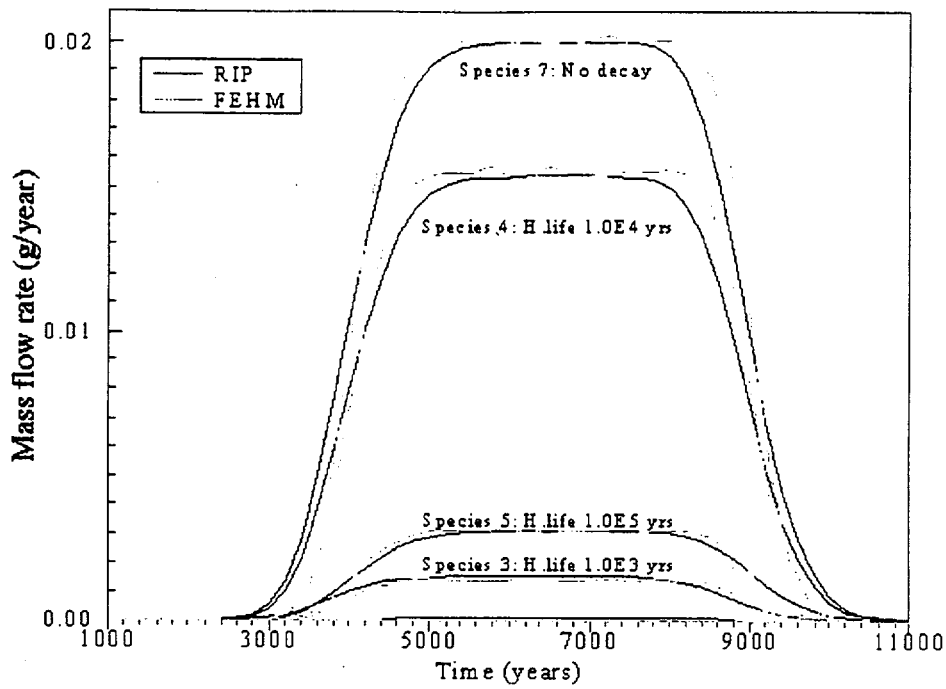

Figure C6-5. Comparison of mass flow rate curves from RIP and FEHM including chain-decay. The mass flow rates of species 1, 2, and 6 are too low to be seen in the plot.

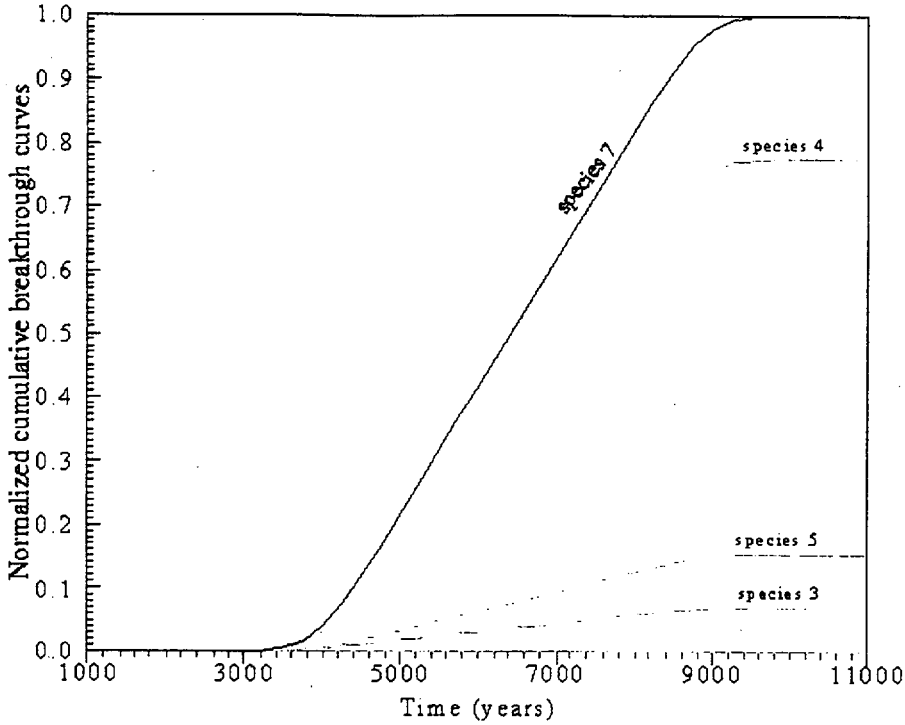

Figure C6-6. Normalized cumulative breakthrough curves from FEHM including chain-decay. The values of species 1, 2, and 6 are too low to be seen in the plots.

Table 6C-1. Radionuclides Used in TSPA Simulations, along with their half-lives—Arranged by chains. The nine radionuclides used for the TSPA-VA base case are highlighted in bold.

No.	Chain	Radionuclide	Half life (years)
1	Am-243	Am-243	7.38E+03
2		**Pu-239**	2.41E+04
3		U-235	7.04E+08
4		**Pa-231**	3.28E+04
5		Ac-227	2.16E+01
6	Cm-245	Cm-245	8.50E+03
7		Pu-241	1.44E+01
8		Am-241	4.32E+02
9		**Np-237**	2.14E+06
10		U-233	1.59E+05
11		Th-229	7.34E+03
12	Cm-246	Cm-246	4.73E+03
13		**Pu-242**	3.87E+05
14		U-238	4.47E+09
15		Am-242m	1.52E+02
16		Pu-238	8.77E+01
17		**U-234**	2.45E+05
18		Th-230	7.70E+04
19		Ra-226	1.60E+03
20		Pb-210	2.23E+01
21	Cm-244	Cm-244	1.81E+01
22		Pu-240	6.54E+03
23		U-236	2.34E+07
24		Th-232	1.41E+10
25		Ra-228	6.7E+00
26	No Chain	**C-14**	5.73E+03
27		Cl-36	3.01E+05
28		Cs-135	2.30E+06
29		**I-129**	1.57E+07
30		Nb-93m	1.36E+01
31		Nb-94	2.03E+04

Table 6C-1.

No.	Chain	Radionuclide	Half life (years)
32		Ni-59	8.0E+04
33		Ni-63	9.20E+01
34		Pd-107	6.50E+06
35		**Se-79**	6.50E+04
36		Sm-151	9.00E+01
37		Sn-126	1.00E+05
38		**Tc-99**	2.13E+05
39		Zr-93	1.53E+06

Table 6C-2. Radionuclide inventory for the 39 radionuclides with decay chains.

No	Radionuclide	Total Curies (Ci)		
		CSNF[1]	HLW[2]	DSNF[3]
1	Ac-227	1.17E+00	4.40E+00	5.99E-02
2	Am-241	2.44E+08	1.62E+06	1.03E+06
3	Am-242m	1.42E+06	1.54E+02	9.07E+02
4	Am-243	1.66E+06	3.83E+02	2.11E+03
5	C-14	9.06E+04	0.00E+00	7.89E+02
6	Cl-36	7.22E+02	0.00E+00	1.44E+00
7	Cm-244	7.84E+07	9.74E+04	8.73E+04
8	Cm-245	2.30E+04	4.12E-01	3.55E+01
9	Cm-246	4.79E+03	4.67E-02	6.02E+00
10	Cs-135	3.37E+04	1.44E+03	1.68E+02
11	I-129	2.25E+03	6.94E-02	1.44E+01
12	Nb-93m	1.19E+05	7.25E+03	5.43E+02
13	Nb-94	5.34E+04	2.48E-01	1.78E+00
14	Ni-59	1.54E+05	6.97E+02	6.77E+01
15	Ni-63	2.02E+07	6.09E+04	7.40E+04
16	Np-237	2.86E+04	8.89E+02	1.39E+02
17	Pa-231	2.16E+00	7.12E+00	9.39E+00
18	Pb-210	4.37E-02	2.13E-04	2.30E-03
19	Pd-107	8.27E+03	2.06E+02	2.80E+01
20	Pu-238	2.03E+08	3.03E+06	4.60E+05
21	Pu-239	2.32E+07	4.04E+04	3.95E+05
22	Pu-240	3.45E+07	2.57E+04	2.97E+05
23	Pu-241	2.22E+09	1.05E+06	6.12E+06
24	Pu-242	1.32E+05	3.32E+01	2.90E+02
25	Ra-226	1.62E-01	7.44E-04	4.58E-03
26	Ra-228	2.02E-05	7.67E-01	3.29E+00
27	Se-79	2.89E+04	4.75E+02	2.25E+02
28	Sm-151	2.31E+07	3.56E+06	4.28E+05
29	Sn-126	5.58E+04	3.16E+03	2.41E+02
30	Tc-99	9.16E+05	4.90E+04	6.48E+03
31	Th-229	2.38E-02	1.10E-01	1.39E+01
32	Th-230	2.32E+01	9.99E-02	9.60E-01
33	Th-232	2.84E-05	7.70E-01	2.56E+00
34	U-233	4.61E+00	4.36E+00	3.47E+03

Table 6C-2. (Continued)

No	Radionuclide	Total Curies (Ci)		
		CSNF[1]	HLW[2]	DSNF[3]
35	U-234	8.73E+04	4.06E+02	1.21E+03
36	U-235	1.08E+03	1.48E+00	6.60E+01
37	U-236	1.77E+04	5.32E+00	2.27E+02
38	U-238	1.99E+04	4.62E+01	7.57E+02
39	Zr-93	1.56E+05	8.74E+03	1.32E+03

[1]CSNF = Commercial spent nuclear fuel

[2] HLW = High level waste

[3] DSNF = DOE spent nuclear fuel

Table 6C- 3. Radionuclide inventory for the nine radionuclides used in TSPA-VA.

No	Radionuclide	Total Curies (Ci)		
		CSNF	HLW	DSNF
1	C-14	9.08E+04	0	7.89E+02
2	I-129	2.25E+03	6.93E-02	1.44E+01
3	Np-237	8.85E+04	1.22E+03	3.90E+02
4	Pa-231	3.95E+04	6.06E+01	1.68E+03
5	Pu-239	2.37E+07	4.04E+04	3.95E+05
6	Pu-242	1.32E+05	3.33E+01	2.90E+02
7	Se-79	2.89E+04	4.76E+02	2.25E+02
8	Tc-99	9.16E+05	4.91E+04	6.49E+03
9	U-234	1.64E+05	1.49E+03	1.38E+03

CHAPTER 6

APPENDIX D

Data Status and Tracking Tables

CHAPTER 6

APPENDIX D

Data Status and Tracking Tables

Table D6-1 Data Tracking for Chapter 6 Figures

Fig.	Code and Version	Input Filename	Output Filename	Data Tracking Number	Q Stat.
6-5	Lotus 123, R5	REFs	CD_SUM.WK4	vinod's clad deg fig	NQ
6-6	None	Ref., Garde 91	Fig. Reproduced	ES lit.	NQ
6-7	None	Ref. Mardon 97	Fig. Reproduced	ES lit.	NQ
6-8	None	Ref. Schrire 94	Fig. Reproduced	ES lit.	NQ
6-9	None	Ref. Manzel 97	Fig. Reproduced	ES lit.	NQ
6-10	Lotus 123, R5	REF, Manzel 97	CD_TMPR.WK4	MO9808RDITHERM.000	NQ
6-11	WAPDEG	Chap. 5 Calc.	Fig. From Chap.5	MO9807MWDWAPDEG.000	NQ
6-12	WAPDEG	B00000000-01717-0210-00033	B00000000-01717-0210-00033	MO9807MWDWAPDEG.000	NQ
6-13	WAPDEG	B00000000-01717-0210-00033	B00000000-01717-0210-00033	MO9807MWDWAPDEG.000	NQ
6-14	Lotus 123, R5		MATSUEO.WK4	ES lit.	NQ
6-15	None	Ref., Kreynes 96	Fig. Reproduced	ES lit.	NQ
6-16	None	Ref., Shi Puls 96	Fig. Reproduced	ES lit.	NQ
6-17	None	Ref., Pescatore 89	No calculations, data from Ref. Plotted.	ES lit.	NQ
6-18	MathCad +, V6	BBA000000-01717-0200-00054, Rev. 01	BBA000000-01717-0200-00054, Rev. 01	MO9808CLADDING.000	NQ
6-22			Fig. Reproduced	ES lit.	NQ
6-23	None	Ref. Einziger and Strain 86	Fig. Reproduced	ES lit.	NQ
6-24		Data from WFCR Rev. 1.2		LL980803451022.014	NQ
6-25		Data from WFCR Rev. 1.2		LL980803451022.014	NQ
6-26		Data from WFCR Rev. 1.2		LL980803451022.014	NQ
6-27		Data from WFCR Rev. 1.2		LL980803451022.014	NQ
6-28				MO9808SPADNFPU.000	NQ
6-30	NA	From WFCR Rev. 1.2, Table 3.5.2.2	NA	LL-???	NQ
6-31	NA	From WFCR Rev. 1.2, Table 3.5.1.1	NA	LL-???	NQ
6-32	None	Ref., Ross and Mendel 97	Fig. Reproduced	LL lit.	NQ
6-36	DRIPTESTANALYSIS V2.0 (MS Excel97)	dtanalysis5!atm103data	dtanalysis5!atm103results	LL980803451022.014	NQ
6-37	DRIPTESTANALYSIS V2.0 (MS	dtanalysis5!atm106data	dtanalysis5!atm106results	LL980803451022.014	NQ

Table D6-1 Data Tracking for Chapter 6 Figures

Fig.	Code and Version	Input Filename	Output Filename	Data Tracking Number	Q Stat.
6-5	Lotus 123, R5	REFs	CD_SUM.WK4	vinod's clad deg fig	NQ
6-6	None	Ref., Garde 91	Fig. Reproduced	ES lit.	NQ
6-7	None	Ref. Mardon 97	Fig. Reproduced	ES lit.	NQ
6-8	None	Ref. Schrire 94	Fig. Reproduced	ES lit.	NQ
6-9	None	Ref. Manzel 97	Fig. Reproduced	ES lit.	NQ
6-10	Lotus 123, R5	REF, Manzel 97	CD_TMPR.WK4	MO9808RDITHERM.000	NQ
6-11	WAPDEG	Chap. 5 Calc.	Fig. From Chap.5	MO9807MWDWAPDEG.000	NQ
6-12	WAPDEG	B00000000-01717-0210-00033	B00000000-01717-0210-00033	MO9807MWDWAPDEG.000	NQ
6-13	WAPDEG	B00000000-01717-0210-00033	B00000000-01717-0210-00033	MO9807MWDWAPDEG.000	NQ
6-14	Lotus 123, R5		MATSUEO.WK4	ES lit.	NQ
6-15	None	Ref., Kreynes 96	Fig. Reproduced	ES lit.	NQ
6-16	None	Ref., Shi Puls 96	Fig. Reproduced	ES lit.	NQ
6-17	None	Ref., Pescatore 89	No calculations, data from Ref. Plotted.	ES lit.	NQ
6-18	MathCad +, V6	BBA000000-01717-0200-00054, Rev. 01	BBA000000-01717-0200-00054, Rev. 01	MO9808CLADDING.000	NQ
6-22			Fig. Reproduced	ES lit.	NQ
6-23	None	Ref. Einziger and Strain 86	Fig. Reproduced	ES lit.	NQ
6-24		Data from WFCR Rev. 1.2		LL980803451022.014	NQ
6-25		Data from WFCR Rev. 1.2		LL980803451022.014	NQ
6-26		Data from WFCR Rev. 1.2		LL980803451022.014	NQ
6-27		Data from WFCR Rev. 1.2		LL980803451022.014	NQ
6-28				MO9808SPADNFPU.000	NQ
6-30	NA	From WFCR Rev. 1.2, Table 3.5.2.2	NA	LL-???	NQ
6-31	NA	From WFCR Rev. 1.2, Table 3.5.1.1	NA	LL-???	NQ
6-32	None	Ref., Ross and Mendel 97	Fig. Reproduced	LL lit.	NQ
6-36	DRIPTESTANALYSIS V2.0 (MS Excel97)	dtanalysis5!atm103data	dtanalysis5!atm103results	LL980803451022.014	NQ
6-37	DRIPTESTANALYSIS V2.0 (MS	dtanalysis5!atm106data	dtanalysis5!atm106results	LL980803451022.014	NQ

	Excel97)				
6-38	DRIPTESTANALYSIS V2.0 (MS Excel97)	dtanalysis5!atm103results; dtanalysis5!atm106results	dtanalysis5!tspacomparison	LL980803451022.014	NQ
6-40	AREST-CT V1.2	csfnf01.actin, sptfl02.time	csfnf01.out2h, csfnf01.out2b	MO9807SPAAREST.000	NQ
6-41	AREST-CT V1.2	csfnf01.actin,sptfl02.time	csfnf01.out2h, csfnf01.out2b	MO9807SPAAREST.000	NQ
6-43	AREST-CT V1.2	csfnf01.actin,sptfl02.time	csfnf01.out2h, csfnf01.out2b	MO9807SPAAREST.000	NQ
6-44	AREST-CT V1.2	corr201.actin,sptfl02.time	corr201.out2h,corr201.out2b	MO9807SPAAREST.000	NQ
6-45	AREST-CT V1.2	corr201.actin,sptfl02.time	corr201.out2h,corr201.out2b	MO9807SPAAREST.000	NQ
6-46	AREST-CT V1.2	corr201.actin,sptfl02.time	corr201.out2h,corr201.out2b	MO9807SPAAREST.000	NQ
6-47	AREST-CT V1.2	corr201.actin,sptfl02.time	corr201.out2h,corr201.out2b	MO9807SPAAREST.000	NQ
6-48	AREST-CT V1.2	corr201.actin,corr202.actin, corr203.actin,corr204.actin, corr301.actin,corr302.actin, corr303.actin,corr304.actin sptfl02.time	corr201.out2h,corr201.out2b, corr202.out2h,corr202.out2b, corr203.out2h,corr203.out2b, corr204.out2h,corr204.out2b, corr301.out2h,corr301.out2b, corr302.out2h,corr302.out2b, corr303.out2h,corr303.out2b, corr304.out2h,corr304.out2b	MO9807SPAAREST.000	NQ
6-51	*	see SNT05080598001.001	see SNT05080598001.001	SNT05080598001.001	NQ
6-52	*	see SNT05080598001.001	see SNT05080598001.001	SNT05080598001.001	NQ
6-53	*	see SNT05080598001.001	see SNT05080598001.001	SNT05080598001.001	NQ
6-54	*	see SNT05080598001.001	see SNT05080598001.001	SNT05080598001.001	NQ
6-55	*	see SNT05080598001.001	see SNT05080598001.001	SNT05080598001.001	NQ
6-56	*	Case31e6,case0ee6,case82e6,case84e6	See footnote ***	MO9807MWDRIP00.000	NQ
6-57	*	Case0ee5,case98e5	See footnote ***	MO9807MWDRIP00.000	NQ
6-58	*	Case0ee5,casee98e5	See footnote ***	MO9807MWDRIP00.000	NQ
6-59	*	Case0ee5,case98e5	See footnote ***	MO9807MWDRIP00.000	NQ
6-60	*	Case0ee5,case94e5	See footnote ***	MO9807MWDRIP00.000	NQ
6-61	*	Case0ee6,case94e6	See footnote ***	MO9807MWDRIP00.000	NQ
6-62	*	Case0ee6,case32ee6	See footnote ***	MO9807MWDRIP00.000	NQ
6-63	*	see SNT05080598001.001	see SNT05080598001.001	SNT05080598001.001	NQ
6-64	*	see SNT05080598001.001	see SNT05080598001.001	SNT05080598001.001	NQ
6-65	*	see SNT05080598001.001	see SNT05080598001.001	SNT05080598001.001	NQ
6-66	*	see SNT05080598001.001	see SNT05080598001.001	SNT05080598001.001	NQ
6-67	*	see SNT05080598001.001	see SNT05080598001.001	SNT05080598001.001	NQ
6-68	*	see SNT05080598001.001	see SNT05080598001.001	SNT05080598001.001	NQ

6-69	*	see SNT05080598001.001	see SNT05080598001.001	SNT05080598001.001	NQ
6-70	*	cat1b.rp - cat7b.rp	cat1b.btr - cat7b.btr cat1bhst.dat - cat7bhst.dat	MO9808SPADNFPU.001	NQ
6-71	*	cat8b.rp - cat16b.rp	cat8b.btr - cat16b.btr cat8bhst.dat - cat16bhs.dat	MO9808SPADNFPU.001	NQ
6-72	*	fig227.rp, fig227.btf cat1b.rp - cat16b.rp	fig227.btr, fig227.dat cat1b.btr - cat16b.btr cat1b.dat - cat16b.dat jcatbsm1.dat: Sum of 'b'-runs	MO9808SPADNFPU.001	NQ
6-73	*	fig225.rp, fig225.btf fig311.rp, fig311.btf cat1d.rp - cat16d.rp	fig225.btr, fig225.dat fig311.btr, fig311.dat cat1d.btr - cat16d.btr jcatdsm1.dat: Sum of 'd'-runs	MO9808SPADNFPU.001	NQ
6-74	*	fig221.rp, fig221.btf cat1d.rp - cat16d.rp	fig221.btr, fig221.dat cat1d.btr - cat16d.btr cat1d.dat - cat16d.dat jcatdsm1.dat: Sum of 'd'-runs	MO9808SPADNFPU.001	NQ
6-75	*	fig228.rp, fig228.btf cat1b.rp - cat16b.rp cat1d.rp - cat16d.rp	fig228.btr, fig228.dat cat1b.btr - cat16b.btr cat1b.dat - cat16b.dat jcatbsm1.dat: Sum of 'b'-runs cat1d.btr - cat16d.btr cat1d.dat - cat16d.dat jcatdsm1.dat: Sum of 'd'-runs	MO9808SPADNFPU.001	NQ
6-76	*	fig221.rp, fig221.btf fig222.rp, fig222.btf fig223.rp, fig223.btf	fig221.btr, fig221.dat fig222.btr, fig222.dat fig223.btr, fig223.dat	MO9808SPADNFPU.001	NQ
6-77	*	fig41.rp, fig41.btf fig43ac.rp, fig43ac.btf fig43b.rp, fig43b.btf	fig41.btr, fig41.dat fig43ab.dat (sum of total: fig43ac.dat fig43b.dat) fig021.dat (sum of total: fig41.dat, fig43ab.dat)	MO9808SPADNFPU.000	NQ
6-78	*	fig42-3.rp, fig42-3.btf fig422ac.rp, fig422ac.btf fig422b.rp, fig422b.btf	fig42-3.btr, fig42-3.dat fig422ab.dat (sum of total: fig422ac.dat, fig422b.dat)	MO9808SPADNFPU.000	NQ
6-79	*	fig41.rp, fig41.btf fig42.rp, fig42.btf	fig41.btr, fig41.dat fig42.btr, fig42.dat	MO9808SPADNFPU.000	NQ

* Total System Model includes RIP (v. 5.19.01), fehmn.dll, szconv.dll, gldis.dll, edc.dll, sfdis.dll
** Name listed is the generic file name ("filename") for the input of Total System Model. It represents the following files with different extensions:

filename.bak	filename.bpf	filename.bsr	filename.btf
filename.rp	filename.t01	filename.t02	filename.t03
filename.t04	filename.t05	filename.t06	filename.t07
filename.t08	filename.t09	filename.t10	filename.t11
filename.t12	filename.t13	filename.t14	filename.t15
filename.t16	filename.t17	filename.t18	filename.t19
filename.t20	filename.t21	filename.t22	filename.t23
filename.t24	filename.t25	filename.t26	filename.t27
filename.t28	filename.t29	filename.t30	filename.t31
filename.t32	filename.t33	filename.t34	filename.t35
filename.t36	filename.t37		

plus the following Total System Model files:

baserun1.dat	fehmn.files	fmQb.dpdp	fmQb.grid
fmQb.rock	fmQb.stor	fmQb.zone	fmQb.zone6
ptrk.expval(exp. val.)	ptrk.multrlz(mult. real.)	ff0100.ini	ff0300.ini
ff0500.ini	ff1100.ini	ff1300.ini	ff1500.ini
ff2100.ini	ff2300.ini	ff2500.ini	

SZ Files (Expected Value Run):

sz01_01.0001	sz01_02.0001	sz01_03.0001	sz01_04.0001
sz01_05.0001	sz01_06.0001	sz02_01.0001	sz02_02.0001
sz02_03.0001	sz02_04.0001	sz02_05.0001	sz02_06.0001
sz03_01.0001	sz03_02.0001	sz03_03.0001	sz03_04.0001
sz03_05.0001	sz03_06.0001	sz04_01.0001	sz04_02.0001
sz04_03.0001	sz04_04.0001	sz04_05.0001	sz04_06.0001
sz05_01.0001	sz05_02.0001	sz05_03.0001	sz05_04.0001
sz05_05.0001	sz05_06.0001	sz06_01.0001	sz06_02.0001
sz06_03.0001	sz06_04.0001	sz06_05.0001	sz06_06.0001
sz07_01.0001	sz07_02.0001	sz07_03.0001	sz07_04.0001
sz07_05.0001	sz07_06.0001	sz08_01.0001	sz08_02.0001
sz08_03.0001	sz08_04.0001	sz08_05.0001	sz08_06.0001
sz09_01.0001	sz09_02.0001	sz09_03.0001	sz09_04.0001
sz09_05.0001	sz09_06.0001	sz10_01.0001	sz10_02.0001
sz10_03.0001	sz10_04.0001	sz10_05.0001	sz10_06.0001
sz11_01.0001	sz11_02.0001	sz11_03.0001	sz11_04.0001
sz11_05.0001	sz11_06.0001		

*** The output filename for each Total System Model simulation is its generic filename with the extension of ".btr".

Table D6-2 Data Tracking for Figures in Appendix A of Chapter 6

Figure	Code and Version	Input Filename (DELL-400 Austin)	Output Filename	Data Tracking Number	Q Status
6A-2	RIP 5.19	cat1a.rp, cat1a.btf	cat1a.btr, cat1ahst.dat	MO9808SPADNFPU.002	NQ
6A-3	RIP 5.19	cat1b.rp, cat1b.btf	cat1b.btr, cat1bhst.dat	MO9808SPADNFPU.002	NQ
6A-4	RIP 5.19	cat1c.rp, cat1c.btf	cat1c.btr, cat1chst.dat	MO9808SPADNFPU.002	NQ
6A-5	RIP 5.19	cat3a.rp, cat3a.btf	cat3a.btr, cat3ahst.dat	MO9808SPADNFPU.002	NQ
6A-6	RIP 5.19	cat3b.rp, cat3b.btf	cat3b.btr, cat3bhst.dat	MO9808SPADNFPU.002	NQ
6A-7	RIP 5.19	cat3c.rp, cat3c.btf	cat3c.btr, cat3chst.dat	MO9808SPADNFPU.002	NQ
6A-8	RIP 5.19	cat4a.rp, cat4a.btf	cat4a.btr, cat4ahst.dat	MO9808SPADNFPU.002	NQ
6A-9	RIP 5.19	cat4b.rp, cat4b.btf	cat4b.btr, cat4bhst.dat	MO9808SPADNFPU.002	NQ
6A-10	RIP 5.19	cat4c.rp, cat4c.btf	cat4c.btr, cat4chst.dat	MO9808SPADNFPU.002	NQ
6A-11	RIP 5.19	cat5a.rp, cat5a.btf	cat5a.btr, cat5ahst.dat	MO9808SPADNFPU.002	NQ
6A-12	RIP 5.19	cat5b.rp, cat5b.btf	cat5b.btr, cat5bhst.dat	MO9808SPADNFPU.002	NQ
6A-13	RIP 5.19	cat5c.rp, cat5c.btf	cat5c.btr, cat5chst.dat	MO9808SPADNFPU.002	NQ
6A-14	RIP 5.19	cat6a.rp, cat6a.btf	cat6a.btr, cat6ahst.dat	MO9808SPADNFPU.002	NQ
6A-15	RIP 5.19	cat6b.rp, cat6b.btf	cat6b.btr, cat6bhst.dat	MO9808SPADNFPU.002	NQ
6A-16	RIP 5.19	cat6c.rp, cat6c.btf	cat6c.btr, cat6chst.dat	MO9808SPADNFPU.002	NQ
6A-17	RIP 5.19	cat7a.rp, cat7a.btf	cat7a.btr, cat7ahst.dat	MO9808SPADNFPU.002	NQ
6A-18	RIP 5.19	cat7b.rp, cat7b.btf	cat7b.btr, cat7bhst.dat	MO9808SPADNFPU.002	NQ

6A-19	RIP 5.19	cat7c.rp, cat7c.btf	cat7c.btr, cat7chst.dat	MO9808SPADNFPU.002	NQ
6A-20	RIP 5.19	cat8a.rp, cat8a.btf	cat8a.btr, cat8ahst.dat	MO9808SPADNFPU.002	NQ
6A-21	RIP 5.19	cat8b.rp, cat8b.btf	cat8b.btr, cat8bhst.dat	MO9808SPADNFPU.002	NQ
6A-22	RIP 5.19	cat8c.rp, cat8c.btf	cat8c.btr, cat8chst.dat	MO9808SPADNFPU.002	NQ
6A-23	RIP 5.19	cat9a.rp, cat9a.btf	cat9a.btr, cat9ahst.dat	MO9808SPADNFPU.002	NQ
6A-24	RIP 5.19	cat9b.rp, cat9b.btf	cat9b.btr, cat9bhst.dat	MO9808SPADNFPU.002	NQ
6A-25	RIP 5.19	cat9c.rp, cat9c.btf	cat9c.btr, cat9chst.dat	MO9808SPADNFPU.002	NQ
6A-26	RIP 5.19	cat11a.rp, cat11a.btf	cat11a.btr, cat11ahs.dat	MO9808SPADNFPU.002	NQ
6A-27	RIP 5.19	cat11b.rp, cat11b.btf	cat11b.btr, cat11bhs.dat	MO9808SPADNFPU.002	NQ
6A-28	RIP 5.19	cat11c.rp, cat11c.btf	cat11c.btr, cat11chs.dat	MO9808SPADNFPU.002	NQ
6A-29	RIP 5.19	cat12a.rp, cat12a.btf	cat12a.btr, cat12ahs.dat	MO9808SPADNFPU.002	NQ
6A-30	RIP 5.19	cat12b.rp, cat12b.btf	cat12b.btr, cat12bhs.dat	MO9808SPADNFPU.002	NQ
6A-31	RIP 5.19	cat12c.rp, cat12c.btf	cat12c.btr, cat12chs.dat	MO9808SPADNFPU.002	NQ
6A-32	RIP 5.19	cat13a.rp, cat13a.btf	cat13a.btr, cat13ahs.dat	MO9808SPADNFPU.002	NQ
6A-33	RIP 5.19	cat13b.rp, cat13b.btf	cat13b.btr, cat13bhs.dat	MO9808SPADNFPU.002	NQ
6A-34	RIP 5.19	cat13c.rp, cat13c.btf	cat13c.btr, cat13chs.dat	MO9808SPADNFPU.002	NQ
6A-35	RIP 5.19	cat15b.rp, cat15b.btf	cat15b.btr, cat15bhs.dat	MO9808SPADNFPU.002	NQ
6A-36	RIP 5.19	cat15c.rp, cat15c.btf	cat15c.btr, cat15chs.dat	MO9808SPADNFPU.002	NQ
6A-37	RIP 5.19	cat16a.rp, cat16a.btf	cat16a.btr, cat16ahs.dat	MO9808SPADNFPU.002	NQ

6A-38	RIP 5.19	cat16b.rp, cat16b.btf	cat16b.btr, cat16bhs.dat	MO9808SPADNFPU.002	NQ
6A-39	RIP 5.19	cat16c.rp, cat16c.btf	cat16c.btr, cat16chs.dat	MO9808SPADNFPU.002	NQ
6A-40	RIP 5.19	cat1b.rp - cat7b.rp	cat1b.btr - cat7b.btr cat1bhst.dat - cat7bhst.dat	MO9808SPADNFPU.002	NQ
6A-41	RIP 5.19	cat8b.rp - cat16b.rp	cat8b.btr - cat16b.btr cat8bhst.dat - cat16bhs.dat	MO9808SPADNFPU.002	NQ
6A-42	RIP 5.19	fig221.rp, fig221.btf	fig221.btr, fig221hs.dat	MO9808SPADNFPU.002	NQ
6A-43	RIP 5.19	fig222.rp, fig222.btf fig223.rp, fig223.btf	fig222.btr, fig222hs.dat fig223.btr, fig223hs.dat	MO9808SPADNFPU.002	NQ
6A-44	RIP 5.19	fig227.rp, fig227.btf cat1b.rp - cat16b.rp	fig227.btr, fig227.dat cat1b.btr - cat16b.btr cat1b.dat - cat16b.dat jcatbsm1.dat: Sum of 'b'-runs	MO9808SPADNFPU.002	NQ
6A-45	RIP 5.19	fig225.rp, fig225.btf fig311.rp, fig311.btf cat1d.rp - cat16d.rp	fig225.btr, fig225.dat fig311.btr, fig311.dat cat1d.btr - cat16d.btr jcatdsm1.dat: Sum of 'd'-runs	MO9808SPADNFPU.002	NQ
6A-46	RIP 5.19	fig228.rp, fig228.btf	fig228.btr, fig228.dat	MO9808SPADNFPU.002	NQ
6A-47	RIP 5.19	fig221.rp, fig221.btf cat1d.rp - cat16d.rp	fig221.btr, fig221.dat cat1d.btr - cat16d.btr cat1d.dat - cat16d.dat jcatdsm1.dat: Sum of 'd'-runs	MO9808SPADNFPU.002	NQ
6A-48	RIP 5.19	fig228.rp, fig228.btf cat1b.rp - cat16b.rp cat1d.rp - cat16d.rp	fig228.btr, fig228.dat cat1b.btr - cat16b.btr cat1b.dat - cat16b.dat jcatbsm1.dat: Sum of 'b'-runs cat1d.btr - cat16d.btr cat1d.dat - cat16d.dat jcatdsm1.dat: Sum of 'd'-runs	MO9808SPADNFPU.002	NQ

6A-49	RIP 5.19	fig221.rp, fig221.btf fig222.rp, fig222.btf fig223.rp, fig223.btf	fig221.btr, fig221.dat fig222.btr, fig222.dat fig223.btr, fig223.dat	MO9808SPADNFPU. 002	NQ
6A-50	RIP 5.19	fig311a.rp, fig311a.btf fig311b.rp, fig311b.btf fig311c.rp, fig311c.btf	fig311a.btr, fig311a.dat fig311b.btr, fig311b.dat fig311c.btr, fig311c.dat	MO9808SPADNFPU. 002	NQ
6A-51	RIP 5.19	fig312a.rp, fig312a.btf fig312b.rp, fig312b.btf fig312c.rp, fig312c.btf	fig312a.btr, fig312a.dat fig312b.btr, fig312b.dat fig312c.btr, fig312c.dat	MO9808SPADNFPU. 002	NQ
6A-52	RIP 5.19	fig313a.rp, fig313a.btf fig313b.rp, fig313b.btf fig313c.rp, fig313c.btf	fig313a.btr, fig313a.dat fig313b.btr, fig313b.dat fig313c.btr, fig313c.dat	MO9808SPADNFPU. 002	NQ
6A-53	RIP 5.19	cat1b.rp, cat1b.btf fig321a.rp, fig321a.btf	cat1b.btr, cat1bhst.dat fig321.btr, fig321.dat	MO9808SPADNFPU. 002	NQ
6A-54	RIP 5.19	fig225.rp, fig225.btf fig331c.rp, fig331c.btf	fig225.btr, fig225hs.dat fig331c.btr, fig331c.dat	MO9808SPADNFPU. 002	NQ
6A-55	RIP 5.19	cat1b.rp, cat1b.btf fig332c.rp, fig332c.btf	cat1b.btr, cat1bhst.dat fig332c.btr, fig332c.dat	MO9808SPADNFPU. 002	NQ
6A-56		cat1a.rp, cat1a.btf cat4b.rp, cat4b.btf cat8b.rp, cat8b.btf cat12b.rp, cat12b.btf	degrate2.csv	MO9808SPADNFPU. 002	NQ
6A-57	RIP 5.19	fig342b.rp, fig342b.btf cat9b.rp - cat9bbtf	fig342b.btr, fig342b.dat cat9b.btr, cat9bhst.dat	MO9808SPADNFPU. 002	NQ
6A-58	RIP 5.19	fig343.rp, fig343.btf cat12b.rp - cat12bbtf	fig343.btr, fig343.dat cat12b.btr, cat12bhs.dat	MO9808SPADNFPU. 002	NQ
6A-59	RIP 5.19	cat1b.rp, cat1b.btf fig351l.rp, fig351l.btf fig351h.rp, fig351h.btf	cat1b.btr, cat1hst.dat fig351l.btr, fig351l.dat fig351h.btr, fig351h.dat	MO9808SPADNFPU. 002	NQ
6A-60	RIP 5.19	fig31-2b.rp, fig31-1b.btf fig352l.rp, fig352l.btf fig352l.rp, fig352h.btf	fig31-2b.btr, fig312bt.dat fig352l.btr, fig352l.dat fig352h.btr, fig352h.dat	MO9808SPADNFPU. 002	NQ
6A-61	RIP 5.19	cat1b.rp, cat1b.btf fig353l.rp, fig353l.btf fig353m.rp, fig353m.btf fig353h.rp, fig353h.btf	cat1b.btr, cat1bhst.dat fig353l.btr, fig353l.dat fig353m.btr, fig353m.dat fig353h.btr, fig353h.dat	MO9808SPADNFPU. 002	NQ

6A-62	RIP 5.19	fig31-2b.rp, fig31-1b.btf fig354l.rp, fig354l.btf fig354m.rp, fig354m.btf fig354h.rp, fig354h.btf	fig31-2b.btr, fig312bt.dat fig354l.btr, fig354l.dat fig354m.btr, fig354m.dat fig354h.btr, fig354h.dat	MO9808SPADNFPU. 002	NQ
6A-63	RIP 5.19	cat13b.rp, cat13b.btf fig355l.rp, fig355l.btf fig355h.rp, fig355h.btf	cat13b.btr, cat13bhs.dat fig355l.btr, fig355l.dat fig355h.btr, fig355h.dat	MO9808SPADNFPU. 002	NQ
6A-64	RIP 5.19	fig361a.rp, fig361a.btf fig361c.rp, fig361c.btf	fig361a.btr, fig361a.dat fig361c.btr, fig361c.dat	MO9808SPADNFPU. 002	NQ
6A-65	RIP 5.19	fig362a.rp, fig362a.btf fig362c.rp, fig362c.btf	fig362a.btr, fig362a.dat fig362c.btr, fig362c.dat	MO9808SPADNFPU. 002	NQ
6A-66	RIP 5.19	cat13b.rp, cat13b.btf fig371a.rp, fig371a.btf fig371b.rp, fig371b.btf	cat13b.btr, cat13bhs.dat fig371a.btr, fig371a.dat fig371b.btr, fig371b.dat	MO9808SPADNFPU. 002	NQ
6A-67	RIP 5.19	cat1b.rp, cat1b.btf fig372a.rp, fig372a.btf fig372b.rp, fig372b.btf	cat1b.btr, cat1bhst.dat fig372a.btr, fig372a.dat fig372b.btr, fig372b.dat	MO9808SPADNFPU. 002	NQ
6A-68	RIP 5.19	fig225.rp, fig225.btf fig381a.rp, fig381a.btf	fig225.btr, fig225hs.dat fig381a.btr, fig381a.dat	MO9808SPADNFPU. 002	NQ
6A-69	RIP 5.19	cat1b.rp, cat1b.btf fig382.rp, fig382.btf	cat1b.btr, cat1hst.dat fig382.btr, fig382.dat	MO9808SPADNFPU. 002	NQ

Table D6-3 Data Tracking for Figures in Appendix B of Chapter 6

Figure	Code and Version	Input Filename	Btrput Filename	Data Tracking Number	Q Status
6B-3	RIP 5.19	fig41.rp, fig41.btf	fig41.btr, fig41.dat	MO9808SPADNFPU.003	NQ
6B-4	RIP 5.19	fig42.rp, fig42.btf	fig42.btr, fig42.dat	MO9808SPADNFPU.003	NQ
6B-5	RIP 5.19	fig43ac.rp, fig43ac.btf fig43b.rp, fig43b.btf	fig43ac.btr, fig43ac.dat fig43b.btr, fig43b.dat	MO9808SPADNFPU.003	NQ
6B-6	RIP 5.19	fig44.rp, fig44.btf fig43ac.rp, fig43ac.btf fig43b.rp, fig43b.btf	fig44.btr, fig44.dat fig43ab.dat (sum of total: fig43ac.dat, fig43b.dat)	MO9808SPADNFPU.003	NQ
6B-7	RIP 5.19	fig41.rp, fig41.btf fig43ac.rp, fig43ac.btf fig43b.rp, fig43b.btf	fig41.btr, fig41.dat fig43ab.dat (sum of total: fig43ac.dat, fig43b.dat)	MO9808SPADNFPU.003	NQ
6B-8	RIP 5.19	fig422ac.rp, fig422ac.btf fig422b.rp, fig422b.btf	fig422ac.btr, fig422ac.dat fig422b.btr, fig422b.dat	MO9808SPADNFPU.003	NQ
6B-9	RIP 5.19	fig42-3.rp, fig42-3.btf	fig42-3.btr, fig42-3.dat	MO9808SPADNFPU.003	NQ
6B-10	RIP 5.19	base.rp, base.btf	base.btr, bashistr.dat	MO9808SPADNFPU.003	NQ
6B-11	RIP 5.19	fig41.rp, fig41.btf fig42.rp, fig42.btf	fig41.btr, fig41.dat fig42.btr, fig42.dat	MO9808SPADNFPU.003	NQ
6B-12	RIP 5.19	fig44.rp, fig44.btf fig43ac.rp, fig43ac.btf fig43b.rp, fig43b.btf	fig44.btr, fig44.dat fig43ab.dat (sum of total: fig43ac.dat, fig43b.dat))	MO9808SPADNFPU.003	NQ
6B-13	RIP 5.19	fig42-3.rp, fig42-3.btf fig422ac.rp, fig422ac.btf fig422b.rp, fig442b.btf	fig42-3.btr, fig42-3.dat fig422ab.dat (sum of total: fig422ac.dat, fig422b.dat)	MO9808SPADNFPU.003	NQ
6B-14	RIP 5.19	fig41.rp, fig41.btf fig511l.rp, fig511l.btf fig511h.rp, fig511h.btf	fig41.btr, fig41.dat fig511l.btr, fig511l.dat fig511h.btr, fig511h.dat	MO9808SPADNFPU.003	NQ
6B-15	RIP 5.19	fig41.rp, fig41.btf fig512l.rp, fig512l.btf fig512h.rp, fig512h.btf	fig41.btr, fig41.dat fig512l.btr, fig512l.dat fig512h.btr, fig512h.dat	MO9808SPADNFPU.003	NQ
6B-16	RIP 5.19	fig422ac.rp, fig422ac.btf fig422al.rp, fig422al.btf fig422ah.rp, fig422ah.btf	fig422ac.btr, fig422ac.dat fig422al.btr, fig422al.dat fig422ah.btr, fig422ah.dat	MO9808SPADNFPU.003	NQ

6B-17	RIP 5.19	fig422ac.rp, fig422ac.btf fig513lc.rp, fig513l.btf fig513h.rp, fig513h.btf	fig422ac.btr, fig422ac.dat fig513lc.btr, fig513l.dat fig513h.btr, fig513h.dat	MO9808SPADNFPU. 003	NQ
6B-18	RIP 5.19	fig422ac.rp, fig422ac.btf fig422ag.rp, fig422ag.btf	fig422ac.btr, fig422ac.dat fig422ag.btr, fig422ag.dat	MO9808SPADNFPU. 003	NQ
6B-19	RIP 5.19	fig531ac.rp, fig531ac.btf fig531g.rp, fig531g.btf	fig531ac.btr, fig531ac.dat fig531g.btr, fig531g.dat	MO9808SPADNFPU. 003	NQ
6B-20	RIP 5.19	fig41.rp, fig41.btf fig532.rp, fig512.btf	fig41.btr, fig41.dat fig532.btr, fig532.dat	MO9808SPADNFPU. 003	NQ

Table D6-4 Data Tracking for Figures in Appendix C of Chapter 6

Figure	Code and Version	Input Filename	Output Filename	Data Tracking Number	Q Status
C6-1	Total System Model	Cas135e4* UZ Files** Cas135e6* UZ Files**	Cas135e4.btr Calc1e4.xls Cas135e6.btr Calc1e6.xls		NQ
C6-2	Total System Model + FEHM	Cas135e6* UZ Files** SZ Files (chain_B)▲	Cas135e6.btr Massrle6b.xls auz#f.d (# 1~6)		NQ
C6-3	Total System Model + FEHM	(1) Case0ee6* UZ Files** SZ Files*** (2) Cas135e6* UZ Files** SZ Files (chain_B)▲	Case0ee6.btr Cas135e6.btr Massrle6b.xls **auz#f.d (# = 1~6)**	MO9807MWDRIP00.000	NQ
C6-4	Total System Model	(1) "Activity vs time tot and main isotopes 03_03_98.xls" decay.JNB (2) Case0ee4* Case0ee5* Case0ee6* UZ File** SZ Files*** (3) Cas135e4* Cas135e5* Cas135e6* UZ Files**	 Case0ee4.btr Case0ee5.btr Case0ee6.btr Cas135e4.btr Cas135e5.btr Cas135e6.btr	MO9807MWDRIP00.000	NQ

C6-5	FEHM97 1001p RIP 5.19.01	(1)/base97/qa/ripfehm/inp1.in (2)fehmn.files (3)/base97/qa/ripfehm/ripdecay.in	(1)/base97/qa/ripfehm/out1.out (2) ripsp2.dat (3) ripsp3.dat (4) ripsp4.dat (5) ripsp5.dat (6) ripsp6.dat (7) ripsp7.dat	MO9807MWDOSEHM.000	NQ
C6-6	FEHM97 1001p	(1)/base/97/qa/ripfehm/inp1.in (2) fehmn.files	/base97/qa/ripfehm/out1.out	MO9807MWDOSEHM.000	NQ

*RIP input files. Name listed is the file name ("filename") representing the files with the following extensions:

filename.bak	filename.bpf	filename.bsr	filename.btf
filename.rp	filename.t01	filename.t02	filename.t03
filename.t04	filename.t05	filename.t06	filename.t07
filename.t08	filename.t09	filename.t10	filename.t11
filename.t12	filename.t13	filename.t14	filename.t15
filename.t16	filename.t17	filename.t18	filename.t19
filename.t20	filename.t21	filename.t22	filename.t23
filename.t24	filename.t25	filename.t26	filename.t27
filename.t28	filename.t29	filename.t30	filename.t31
filename.t32	filename.t33	filename.t34	filename.t35
filename.t36	filename.t37		

** FEHM particle tracker input files for Unsaturated-zone transport:

baserun1.dat	fehmn.files	fmQb.dpdp	fmQb.grid
fmQb.rock	fmQb.stor	fmQb.zone	fmQb.zone6
ff0100.ini	ff0300.ini	ff0500.ini	ff1100.ini
ff1300.ini	ff1500.ini	ff2100.ini	ff2300.ini
ff2500.ini	ptrk.expval (used for expected-value runs)		

*** SZ transport input files

SZ_Convolute2.dat

Breakthrough curves files used as input to the SZ_Convolute code are in the following form:

SZ0A_0B.0XXX

A= 1 through 11, represent the 9 radionuclides and the 2 irreversible Pu-239 and Pu-242 radionuclides tracked in the TSPA-VA model.

Radionuclide	Number (A)
C-14	1
I-129	2
Np-237	3
Pa-231	4
Pu-239	5
Pu-239 irreversible	6
Pu-242	7
Pu-242 irreversible	8
Se-79	9
Tc-99	10
U-234	11

B= 1 through 6 represent the six streamtubes used in the SZ transport
XXX= Used to represent the realization number
= 1 for expected-value runs
= 1 through 100 for multiple realization runs

- FEHM input files for SZ transport of decay chain B: Cm245

↓

Am241→ Np237→ U233→ Th229.

↑

Pu241

fehm.files, 1dgrid.grid, zone1.0000, trans_c_B.trac, trac_B.rxn, userc_data.dat_buz1, userc_data.dat_buz2, userc_data.dat_buz3, userc_data.dat_buz4, userc_data.dat_buz5, userc_data.dat_buz6.

Table xx Summary of computer codes that comprise the Total System Model

Computer Code	Version	Code Usage
RIP	5.19.01	Total system integrator

SFDiss	1.0	Software routine coupled to RIP code to calculate Commercial spent nuclear fuel dissolution rate
GLDiss	1.0	Software routine coupled to RIP code to calculate glass dissolution rate
EDC	1.0	Software routine coupled to RIP code to calculate effective diffusion coefficient in partially saturated medium
FEHM	1.2	Particle tracker coupled to RIP for UZ transport Reactive transport module for simulating decay chains with ingrowth used for SZ transport
SZ_CONVOLUTE	1.0	Software routine coupled to RIP code to calculate saturated-zone concentrations using saturated-zone unit breakthrough curves

Table D6-5 Data Tracking for Chapter 6 Tables

Table	Code and Version	Input Filename	Output Filename	Data Tracking Number	Q Status
6-4	NA	Ref. CRWMS M&O 97b	NA		NQ
6-5	NA	Ref. Stroup 97	NA		NQ
6-6	ORIGEN2				NQ
6-7	None		No calculations, data from Ref.		NQ
6-8	None		No calculations, data from Ref.		NQ
6-9	Lotus123, R5		Hydride2.wk4 Hydride3.wk4		NQ
6-10	Lotus123, R5		Hydride1.wk4		NQ
6-11	Lotus123, R5		Hsollim.wk4		NQ
6-12	None		No calculations, data from Ref.		NQ
6-13	Lotus123, R5		Hydride3.wk4		NQ
6-14	Lotus123, R5		Hydride3.wk4		NQ
6-15	Lotus123, R5		Zr oxide.wk4		NQ
6-16	WAPDEG				NQ
6-17	None		No calculations, data from Ref.		NQ
6-18	Lotus123, R5		Matsueo.wk4		NQ
6-19	Lotus123, R5		Strain.wk4		NQ
6-20	Lotus123, R5		He-pres.wk4		NQ
6-21	Lotus123, R5		Hydride3.wk4		NQ
6-22	Lotus123, R5				NQ
6-23	None		No calculations, data from Ref.		NQ
6-24	MathCad +, V6	BBA000000-01717-0200-00054, Rev. 01	BBA000000-01717-0200-00054, Rev. 01		NQ
6-25	MathCad +, V6	BBA000000-01717-0200-00054, Rev. 01	BBA000000-01717-0200-00054, Rev. 01		NQ
6-26	None		No calculations, data from Ref. Plotted		NQ
6-27					

6-28					
6-29					
6-30					
6-31					
6-32	NA	Ref. CRWMS M&O 95			
6-33		Ref. CRWMS M&O 98			
6-34	AREST-CT				
6-37	DRIPTESTANALYSIS V2.0 (MS Excel97)	dtanalysis5!atm103data	dtanalysis5!atm103results	TBD	NQ
6-38	DRIPTESTANALYSIS V2.0 (MS Excel97)	dtanalysis5!atm106data	dtanalysis5!atm106results	TBD	NQ
6-39	DRIPTESTANALYSIS V2.0 (MS Excel97)	dtanalysis5!atm103results; dtanalysis5!atm106results	dtanalysis5!tspacomparison	TBD	NQ
6-40	None	Ref. TSPA-VA TBD Chapter 4, Table 4.5-2		MO9807SPAAREST.000	NQ
6-41	Logkfit *	Data0.com.R22a	Datafit.txt	MO9807SPAAREST.000	NQ
6-42	Logkfit *	Data0.com.R22a and Ref. Nguyen et al. 1992	Datafit.txt	MO9807SPAAREST.000	NQ
6-43	Hand Calculation	Gray et al., 1992 Casas et al., 1994 Bruno et al., 1995 Perez et al., 1997	Notes in file	MO9807SPAAREST.000	NQ
6-44	Logkfit *	Data0.com.R22a	Datafit.txt	MO9807SPAAREST.000	NQ
6-45	RADDB CDB_R/V1.1	Self-Contained	Print-out	MO9807SPAAREST.000	NQ
6-46	Total System Model	Case0ee5	Table 6.5-1	MO9807MWDRIP00.000	NQ

* The work of fitting equilibrium constants in EQ3/6 database into polynomial functions of temperature was done at Pacific Northwest National Laboratory while Yueting Chen worked there from 1994-1997.

Table D6-6 Data Tracking for Chapter 6 Appendix A Tables

Table	Code and Version	Input Filename	Output Filename	Data Tracking Number	Q Status
A6-3					
A6-4					
A6-5					
A6-6					
A6-7					
A6-8					
A6-9					
A6-10					
A6-11					
A6-12					

Table D6-7 Data Tracking for Chapter 6 Appendix B Tables

Table	Code and Version	Input Filename	Output Filename	Data Tracking Number	Q Status
B6-1					
B6-2					
B6-3					
B6-4					

Table D6-8 Data Tracking for Chapter 6 Appendix C Tables

Table	Code and Version	Input Filename	Output Filename	Data Tracking Number	Q Status
C6-1					
C6-2					
C6-3					
C6-4					